UNIVERSIDADE FEDERAL DE MINAS GERAIS

Instituto de Ciências Biológicas

Pós-Graduação em Zoologia

Mauro Bruno da Silva Lacerda

MORPHOFUNCTIONAL EVOLUTION OF THE PELVIC GIRDLE AND HINDLIMBS OF THEROPODA (DINOSAURIA, SAURISCHIA) WITH EMPHASIS ON THE MEGALOSAUROIDEA LINEAGE

Belo Horizonte

2023

Mauro Bruno da Silva Lacerda

MORPHOFUNCTIONAL EVOLUTION OF THE PELVIC GIRDLE AND HINDLIMBS OF THEROPODA (DINOSAURIA, SAURISCHIA) WITH EMPHASIS ON THE MEGALOSAUROIDEA LINEAGE

Versão Final

Tese apresentada ao Programa de Pós-Graduação em Zoologia da Universidade Federal de Minas Gerais, como requisito parcial à obtenção do título de Doutor em Zoologia.

Orientador: Prof. Dr. Jonathas de Souza Bittencourt Rodrigues

Coorientador: Prof. Dr. Pedro Seyferth Ribeiro Romano

Belo Horizonte

2023

043 Lacerda, Mauro Bruno da Silva.
Morphofunctional evolution of the pelvic girdle and hindlimbs of Theropoda (Dinosauria, saurischia) with emphasis on the Megalosauroidea lineage [manuscrito] / Mauro Bruno da Silva Lacerda. – 2023.
189 f. : il. ; 29,5 cm.

Orientador: Prof. Dr. Jonathas de Souza Bittencourt Rodrigues. Coorientador: Prof. Dr. Pedro Seyferth Ribeiro Romano.
Tese (doutorado) – Universidade Federal de Minas Gerais, Instituto de Ciências Biológicas. Programa de Pós-Graduação em Zoologia.

1. Zoologia. 2. Macroevolução. 3. Dinossauros. 4. Anatomia. I. Rodrigues, Jonathas de Souza Bittencourt. II. Romano, Pedro Seyferth Ribeiro. III. Universidade Federal de Minas Gerais. Instituto de Ciências Biológicas. IV. Título.

CDU: 591

Ficha catalografica elaborada pela bibliotecária Fabiane C. M. Reis – CRB: 6/2680

UNIVERSIDADE FEDERAL DE MINAS GERAIS
INSTITUTO DE CIÊNCIAS BIOLÓGICAS
PÓS-GRADUAÇÃO EM ZOOLOGIA

FOLHA DE APROVAÇÃO DE TESE

Morphofunctional evolution of the pelvic girdle and hindlimbs of Theropoda (Dinosauria, Saurischia) with emphasis on the Megalosauroidea lineage

MAURO BRUNO DA SILVA LACERDA

Esta tese foi apresentada em sessão pública e submetida a avaliação em 31 de outubro de 2023, sendo aprovada pela Banca Examinadora composta pelos seguintes membros:

Prof. Dr. Alexandre Liparini Campos (Membro / UFMG)

Prof. Dr. Jonathas de Souza Bittencourt Rodrigues (Orientador / UFMG)

Prof. Dr. Martín Daniel Ezcurra (Membro / Museo Argentino de Ciencias Naturales)

Prof. Dr. Orlando Nelson Grillo (Membro / UFRJ)

Prof. Dr. Rodrigo Temp Müller (Membro / UFSM)

Documento assinado eletronicamente por **Alexandre Liparini Campos**, **Professor do Magistério Superior**, em 01/11/2023, às 16:31, conforme horário oficial de Brasília, com fundamento no art. 5º do Decreto nº 10.543, de 13 de novembro de 2020.

Documento assinado eletronicamente por **Rodrigo Temp Müller**, **Usuário Externo**, em 03/11/2023, às 09:31, conforme horário oficial de Brasília, com fundamento no art. 5º do Decreto nº 10.543, de 13 de novembro de 2020.

Documento assinado eletronicamente por **Jonathas de Souza Bittencourt Rodrigues**, **Professor do Magistério Superior**, em 03/11/2023, às 14:48, conforme horário oficial de Brasília, com fundamento no art. 5º do Decreto nº 10.543, de 13 de novembro de 2020.

Documento assinado eletronicamente por **Orlando Nelson Grillo**, **Usuário Externo**, em 04/11/2023, às 09:47, conforme horário oficial de Brasília, com fundamento no art. 5º do Decreto nº 10.543, de 13 de novembro de 2020.

Documento assinado eletronicamente por **Martin Daniel Ezcurra**, **Usuário Externo**, em 27/11/2023, às 08:49, conforme horário oficial de Brasília, com fundamento no art. 5º do Decreto nº 10.543, de 13 de novembro de 2020.

A autenticidade deste documento pode ser conferida no site https://sei.ufmg.br/sei/controlador_externo.php?acao=documento_conferir&id_orgao_acesso_externo=0, informando o código verificador **2766215** e o código CRC **5D5D3969**.

Referência: Processo nº 23072.229818/2021-05 SEI nº 2766215

ACKNOWLEDGEMENTS

I thank my advisors Jonathas Bittencourt, Pedro Romano and John Hutchinson for their dedication and discussions during my PhD. I would like to thank John for welcoming me to the Structure & Motion Laboratory (RVC) and for the activities developed under his coordination.

To my family and especially my girlfriend, Camila, for all the encouragement, emotional support and academic help over the years in different occasions. To friends Masaya Iijima, Yuting Lin, André Salvatore, Richard Torres, and Samuel Singulano for the encouragement, discussions, conversations and good times we shared on countless occasions.

To the curators who granted me access to the palaeontological collections visited, always being very kind and supportive during my stay and study of the specimens: José Carballido (Museo Paleontológico Egidio Feruglio, Argentina), Martin Ezcurra and Agustin Martinelli (Museo Argentino de Ciencias Naturales 'Bernardino Rivadavia', Argentina), Pablo Ortiz (Fundación Miguel Lillo, Universidad Nacional de Tucumán, Argentina), Eliza Howlett (Oxford University Museum of Natural History, United Kingdom), Marc Jones and Mike Day (Natural History Museum, United Kingdom).

To Orlando Grillo and Alexandre Liparini who followed the project from the beginning, actively participating in my academic training. I am grateful for the support with photogrammetry provided by Romain Pintore and François Clarac; and the teachings on surface scanning provided by Masaya Iijima. To Orlando Grillo, Alexandre Liparini, Martin Ezcurra, Rodrigo Müller, Agustin Martinelli and Fabiana Costa for agreeing to evaluate this thesis.

To the Willi Hennig Society for making TNT an open access program; MorphoSource for storing the 3D models used here (UCRC:PV170, UCRC:PV171 and UMNH:VP:7892) kindly provided by Stephanie Baumgart (University of Chicago) and Alyson Wilkins (UMNH), respectively, as well as the UCMP:V:129618 provided by University of California Museum of Paleontology; and PhyloPic for silhouettes available (under Public Domain Dedication 1.0 license or Creative Commons Attribution-NonCommercial-ShareAlike 3.0 Unported [CC BY-NC-SA 3.0]; artists: J Headden, M Martyniuk and S Hartman) that were coloured and contoured in the illustrations of this work. To Júlia d'Oliveira for the artwork of *Piatnitzkysaurus*.

To the Federal University of Minas Gerais for the opportunity to complete this doctorate, and to CAPES (Finance Code 001) for financial assistance in Brazil and CNPq (Finance Code 200203/2022-3) for financial assistance abroad. I also thank FAPEMIG for the acquisition of the Agisoft Metashape software via PGZoo (UFMG).

ABSTRACT

The Theropoda clade can be considered one of the most successful dinosaur groups, both throughout the Mesozoic Era and nowadays due to the wide diversity and variety of forms of the extant representatives of the group. One of the basic features of dinosauromorphs and the Theropoda clade is the bipedalism: a widespread locomotor adaptation that, unlike quadrupedalism, probably had a unique evolutionary origin. Among the extinct lineages, several clades are recognized as non-avian theropods; among these, the Megalosauroidea lineage stands out, which includes the oldest dinosaur ever described in the literature – *Megalosaurus bucklandii*, in addition to aberrant and large-sized species such as *Spinosaurus aegyptiacus*. The main diagnostic features of the group include: (1) presence of a prominent deltopectoral ridge on the humerus, (2) extended anterior maxillary ramus, (3) presence of separate interdental plates, among other features considered to be synapomorphic. In this thesis, I analysed the macroevolution and disparity of the morphological characters of the locomotor apparatus – pelvic girdle, stylopodium and zeugopodium – in theropod dinosaurs, with emphasis on the clade Megalosauroidea. Additionally, the musculature of part of the locomotor apparatus of the early-diverging megalosauroids *Piatnitzkysaurus floresi* and *Condorraptor currumilli* was reconstructed.

Keywords: Functional Morphology. Macroevolution. Myology. Non-Avian Theropoda. Soft tissue

RESUMO

O clado Theropoda pode ser considerado um dos grupos de dinossauros mais bem sucedidos, tanto ao longo da Era Mesozoica, quanto nos dias atuais devido a ampla diversidade e variedade de formas dos representantes viventes do grupo. Uma das características básicas dos dinossauromorfos e dos clado Theropoda é o bipedalismo: uma adaptação locomotora difundida amplamente que, ao contrário do quadrupedalismo, provavelmente teve uma origem única evolutiva. Dentre as linhagens extintas, diversos clados são reconhecidos como Theropoda não Avianos; dentre estes destaca-se a linhagem Megalosauroidea a qual inclui o dinossauro mais antigo já descrito na literatura – *Megalosaurus bucklandii*, além de espécies aberrantes e de grande porte como o *Spinosaurus aegyptiacus*. As principais características diagnósticas do grupo incluem: (1) presença de uma crista deltopeitoral proeminente no úmero, (2) ramo maxilar anterior estendido, (3) presença de placas interdentais separadas, entre outras características tidas como sinapomórficas. Nesta tese, analisei a macroevolução e disparidade dos caracteres morfológicos do aparato locomotor – cintura pélvica, estilopódio e zeugopódio – em dinossauros terópodes, com ênfase no clado Megalosauroidea. Adicionalmente foi reconstruída a musculatura de parte do aparato locomotor dos terópodes megalossauróides *Piatnitzkysaurus floresi* e *Condorraptor currumilli*.

Palavras-chave: Macroevolução. Miologia. Morfologia Funcional. Tecido mole. Theropoda Não Avianos.

LIST OF FIGURES

LIST OF TABLES

SUMMARY

INTRODUCTION

The Theropoda clade (‘beast’s feet’) was first recognized by Othniel C. Marsh as a suborder of Dinosauria, previously named by the anatomist Sir Richard Owen. The overall morphological features early noted by Marsh (1881) are related to the (1) digitigrade feet, (2) movable and prehensile claws, (3) premaxillary with teeth, (4) small forelimbs, and (5) ‘hollow’ skeletons, among others. In addition to being a taxonomically and morphologically diverse group of dinosaurs that includes strictly carnivorous and herbivorous forms as well as Neornithes, during the Mesozoic, theropods were the predominant and one of the most successful tetrapod clades that populated numerous terrestrial and coastal palaeoenvironments worldwide (Benson, 2018).

One of the basic and widespread dinosauromorph is the bipedalism, and this locomotor adaptation may have been widely disseminated as a ‘tool’ in the hunting process, and/or may be related to cursorial aspects in the dinosaur’s origin. Certainly, the bipedalism “promoted” an initial irradiation of the dinosaurs during the Triassic, as it represents a locomotor advantage and probably a plesiomorphic (Hutchinson & Gatesy, 2000). After nearly a century and a half of research with theropods, and on the eve of the 200th anniversary of the description of *Megalosaurus* (Buckland, 1824), the first theropod species to be described, in order to contribute to the topic, this thesis focuses on the analysis of morphofunctional features of the pelvis and hindlimb appendage of early theropods emphasizing the medium to large-sized bipedal predators of the Megalosauroidea clade.

Megalosauroidea includes all theropods that are more closely related to *Megalosaurus* than to either *Allosaurus* or *Tyrannosaurus* (Carrano *et al*., 2012). They can be diagnosed by the (1) extension of the posterior nasal process of the premaxilla, (2) presence of a prominent deltopectoral ridge on the humerus, and (3) an extended anterior maxillary branch; among other synapomorphic features (Holtz *et al*., 2004; Carrano *et al*., 2012). The palaeogeographic distribution of this lineage is broad, with representatives being found in South America, North America, Africa, Europe and Asia, persisting for a relatively long time-span, between the Middle Jurassic and Early Upper Cretaceous (Carrano *et al*., 2012).

The focus of this thesis is especially on the morphology and morphofunction of the pelvic girdle and hindlimbs of megalosauroid theropod dinosaurs; considering that these structures play a fundamental role in understanding the evolution of locomotor patterns, since the pelvis contains the main sites of attachment of the muscles associated with the hindlimbs (Carrano &

Hutchinson, 2002; Iijima & Kobayashi, 2014). Here I provide discussions of the key macroevolutionary trends, as well as myological reconstructions and comparisons/inferences of megalosauroid pelvis and hindlimb morphology and morphofunction in broad Theropoda evolutionary context.

The results and discussion were addressed in two distinct chapters formatted as manuscripts. The first chapter (published in the journal *Royal Society Open Science*) deals with the macroevolution of Megalosauroidea based on the analysis of morphological characters of the locomotor apparatus, providing a basic inference on possible morphofunctional adaptations. The second chapter (accepted in the *Journal of Anatomy*) focuses on the reconstruction of the locomotor musculature of the Piatnitzkysauridae clade, with a comparative evaluation within Archosauria, being the first work with this approach considering early tetanurans.

CHAPTER 1

MACROEVOLUTIONARY PATTERNS IN THE PELVIS, STYLOPODIUM AND ZEUGOPODIUM OF MEGALOSAUROID THEROPOD DINOSAURS AND THEIR IMPORTANCE FOR LOCOMOTOR FUNCTION

Abstract

During the Mesozoic, non-avian theropods represented one of the most successful clades globally distributed, with a wide diversity of forms. An example is the clade Megalosauroidea, which included medium- to large-bodied forms. Here we analyse the macroevolution of the locomotor system in early Theropoda, emphasising the Megalosauroidea. We scored the *Spinosaurus* neotype in a published taxon-character matrix and described the associated modifications in character states, mapping them onto a phylogeny and using these to study disparity. In the evolution of Megalosauroidea, there was the mosaic emergence of a low swollen ridge; enlargement of the posterior brevis fossa and emergence of a posterodorsal process on the ilium in some megalosauroids; emergence of a femoral head oriented anteromedially and medially angled, and appearance of posterolaterally oriented medial femoral condyles in spinosaurids. The greatest morphological disparity is in the ilium of megalosaurids; the ischium seems to have a high degree of homoplasy; there is a clear distinction in the femoral morphospace regarding megalosauroids and other theropods; piatnitzkysaurids show considerable disparity of zeugopodial characters. These reconstructions of osteological evolution form a stronger basis on which other studies could build, such as mapping of pelvic/appendicular musculature and/or correlating skeletal traits with changes in locomotor function.

1. INTRODUCTION

1.1. Theropod dinosaurs and bipedalism

During the Jurassic and Cretaceous Periods, non-avian theropod dinosaurs represented one of the dominant groups of tetrapods in terrestrial and coastal ecosystems distributed throughout the world. They exhibited a wide diversity and morphological disparity, presenting many body sizes, shape, locomotor and feeding specialisations acquired over more than 170 Myr of evolution (Padian, 2004; Langer *et al*., 2010; Brusatte *et al*., 2012; Foth & Rauhut, 2013). Throughout the evolutionary history of non-avian theropods, several clades independently radiated, giving rise mostly to medium-to large-sized carnivores (e.g., ceratosaurs, allosauroids, megalosauroids), as well as other clades more specialised in their morphology and ecology (e.g., coelurosaurs), including the only extant clade of theropods, Avialae (or Neornithes) (Gauthier, 1986; Padian, 2004), which have a great diversity of extant forms and ecological niches.

One of the most remarkable and widespread features in dinosauromorphs and early dinosaurs is bipedalism (Hutchinson & Gatesy, 2001; Persons & Currie, 2017). Historically, this mode of locomotion is associated with using the forelimbs for food manipulation, and the hindlimbs in cursorial specialisations; important in the origin of dinosaurs (Kubo & Kubo, 2012), considering that the retention of bipedalism occurred in several herbivorous species (Persons & Currie, 2017). As such, obligate bipedalism and an erect hindlimb posture with slightly flexed hip and knee joints are ancestral features for dinosaurs, and may have been a key factor in the initial radiation of the clade during the Late Triassic and Early Jurassic (Hutchinson & Gatesy, 2001; Langer *et al*., 2010; Cuff *et al*., 2023).

However, throughout the Mesozoic, several dinosaur lineages acquired anatomical and functional modifications of the musculoskeletal structure of the pelvic girdle and hindlimbs, associated with modifications to their limb orientation, centre of mass, muscle sizes and leverages, and morphology/positions of origins and insertions of muscles. These modifications presumably enabled diversification of locomotor modes in several theropod lineages throughout their evolution (Gatesy & Middleton, 1997; Carrano, 2000; Hutchinson 2001a,b; 2002; Carrano & Hutchinson, 2002; Hutchinson & Garcia, 2002; Grillo & Azevedo, 2011; Bates *et al*., 2012; Bishop *et al*., 2021; Rhodes *et al*., 2021; Smith, 2021; Cuff *et al*., 2023). Nevertheless, all known theropod dinosaurs retain obligate bipedalism, and unlike

quadrupedalism, this acquisition probably had a unique origin before or at Dinosauria (Hutchinson & Gatesy, 2000; Langer *et al*., 2010; Persons & Currie, 2017; Cuff *et al*., 2023).

Despite this ancestral bipedalism, hypotheses of quadrupedalism in theropod species have been raised in some more recent literature. Based on characteristics such as the robustness of the humerus and elongation of the cranium and neck of the spinosaurid *Baryonyx walkeri* Charig & Milner (1986) from the Early Cretaceous of Europe, Charig & Milner (1997) proposed that this theropod dinosaur represented a facultative quadruped. However, Ibrahim *et al*. (2014) commented that the morphology of another species closely related to *Baryonyx*, *Suchomimus tenerensis* Sereno *et al*. (1998) from the Early Cretaceous of Africa, which has a better-preserved skeleton, does not support the hypothesis raised by Charig & Milner (1997) concerning the Baryonychinae clade. In the same work, Ibrahim *et al*. (2014) described a new specimen of the enigmatic, gigantic *Spinosaurus aegyptiacus* Stromer (1915) from the first part of the Upper Cretaceous (ca. 95 Mya) of Africa. Based on some morphological features; such as the articulation between the sacral vertebrae and the ilium, and a short femur, in addition to the position of the estimated body's centre of mass; they hypothesised that this was the first (or only) theropod dinosaur which was an obligate quadruped on land. Ibrahim *et al*. (2020) and Fabbri *et al*. (2022) did not further address this issue in their description of new material along with biomechanical and morphological analyses more focused on the potential swimming abilities of *Spinosaurus* (see below). However, Sereno *et al*. (2022) produced a new 3D computer model of the centre of mass of *Spinosaurus*, estimating that it was closer to the hips than Ibrahim *et al*. (2014) reconstructed, and thus would have enabled normal bipedalism.

1.2. Megalosauroidea lineage

Megalosauroidea (senior synonym of Spinosauroidea and Torvosauroidea; Carrano *et al*., 2012) was the first major branch of the tetanuran clade to radiate (and, within the clade Orionides, is sister taxon to the lineage leading to Avetheropoda). The probable origin of megalosauroids dates back to the Early Jurassic (Toarcian), with a rapid diversification and dispersion throughout the Jurassic and Early Cretaceous (Holtz *et al*., 2004; Carrano *et al*., 2012; Rauhut *et al*., 2016). The palaeogeographic distribution of this lineage is broad, with representatives being found on almost all continents/regions, such as South America (e.g., Bonaparte (1979)), North America (e.g., Madsen (1976)), Africa (e.g., Sereno *et al*. (1998)), Europe (e.g., Buckland (1824)), and Asia (e.g., Allain *et al*. (2012)). Megalosauroids also

persisted for a relatively long time-span, between the Middle Jurassic and Early Upper Cretaceous (Holtz *et al*., 2004; Carrano *et al*., 2012; Rauhut *et al*., 2016).

Megalosauroidea includes the oldest dinosaur ever described: *Megalosaurus bucklandii* Buckland (1824), in addition to *Spinosaurus aegyptiacus* (Carrano *et al*., 2012; Hendrickx *et al*., 2015). According to Carrano *et al*. (2012), Megalosauroidea is a clade including all theropods that are more closely related to *Megalosaurus* than to either *Allosaurus* or *Tyrannosaurus*. Megalosauroids can be diagnosed by features such as extension of the posterior nasal process of the premaxilla, presence of a prominent deltopectoral ridge on the humerus, and an extended anterior maxillary branch; among other synapomorphies (Holtz *et al*., 2004; Carrano *et al*., 2012).

In general, megalosauroids represented medium- to large-sized animals, such as *Piatnitzkysaurus* and *Marshosaurus*, from the Jurassic of Patagonia (Argentina) and Morrison Formation (United States) respectively, which could reach 5–6 metres in length; megalosaurids, including *Megalosaurus* from the Jurassic of the United Kingdom (varying between 4–10 metres long); whereas in some spinosaurids from the Cretaceous of Africa, the maximum body length has been estimated at between ~14–17 metres (Dal Sasso *et al*., 2005; Therrien & Henderson, 2007; Ibrahim *et al*., 2014; Sereno *et al*., 2022). This range of body sizes makes Megalosauroidea a useful clade for studying how body size, pelvic appendicular morphology and locomotor function evolved in theropods, but these aspects have been more neglected in the literature than in other clades spanning similar size ranges (mainly allosauroids and coelurosaurs).

According to the most complete phylogeny focusing on Tetanurae, i.e., that of Carrano *et al*. (2012) and its modifies version by Rauhut *et al*. (2016), for example, three main clades compose Megalosauroidea: (i) the earliest-diverging Piatnitzkysauridae (*Piatnitzkysaurus*, *Condorraptor*, and *Marshosaurus*), (ii) Megalosauridae (*Megalosaurus*, *Torvosaurus*, *Duriavenator*, *Dubreuillosaurus*, *Afrovenator*, *Piveteasaurus*, *Leshansaurus*, *Magnosaurus*, *Wiehenvenator*, and *Poekilopleuron*), and (iii) Spinosauridae (*Spinosaurus*, *Irritator*, *Angaturama*, *Baryonyx*, and *Suchomimus*). Within Megalosauroidea, the clade Megalosauria is composed of Megalosauridae + Spinosauridae. Some taxa; e.g., *Monolophosaurus*, *Eustreptospondylus*, and *Streptospondylus*; have uncertain phylogenetic placement within Megalosauroidea, as well as *Xuanhanosaurus*, which was recovered as a piatnitzkysaurid by Rauhut *et al*. (2016) instead of a metriacanthosaurid as previously (Carrano *et al*., 2012). There recently has been an increase in the known biodiversity of Spinosauridae because some new taxa have been described, such as *Ichthyovenator* (Allain *et al*., 2012), *Vallibonavenatrix*

(Malafaia *et al*., 2020), *Ceratosuchops*, *Riparovenator* (Barker *et al*., 2021), *Iberospinus* (Mateus & Estraviz-López, 2022), and *Protathlitis* (Santos-Cubedo *et al*., 2023).

Because of their great diversity and wide palaeogeographic distribution, megalosauroids constituted important components of Mesozoic ecosystems, probably partitioning ecological niches with species from related theropod clades, such as predators of Allosauroidea since the Middle Jurassic (Benson *et al*., 2013). Throughout the Mesozoic, taxa considered as "top predators" changed since the Middle Jurassic to the Cenomanian (Benson, 2010; Carrano *et al*., 2012; Benson *et al*., 2013; Hendrickx *et al*., 2015; Rauhut *et al*., 2016). The ecosystems where megalosauroids initially dominated gradually began to be occupied by abelisauroids in Gondwana, as well as several coelurosaur lineages throughout the Upper Jurassic in Laurasia lands (Carrano *et al*., 2012; Benson *et al*., 2013). Meanwhile, the megalosauroid spinosaurids probably radiated during the Lower Cretaceous, dominating in coastal/riverine ecosystems (Amiot *et al*., 2010; Sales *et al*., 2016; Sereno *et al*., 2022), then becoming extinct during the Cenomanian, in the Upper Cretaceous (Carrano *et al*., 2012; Benson *et al*., 2013).

The palaeoecological diversification of spinosaurids is evidenced by specialisations in cranial morphology, neuroanatomy and tooth morphology (Ibrahim *et al*., 2014; Arden *et al*., 2019; Hendrickx *et al*., 2019; Schade *et al*., 2020), the postcranial skeleton (Charig & Milner, 1997; Allain *et al*., 2012; Ibrahim *et al*., 2020), the pattern of bone microstructure and compactness (Ibrahim *et al*., 2014; Fabbri *et al*., 2022), taphonomic (Sales *et al*., 2016), and isotopic features suggesting a correlation with coastal palaeoenvironments (Amiot *et al*., 2010; Hassler *et al*., 2018). Furthermore, there is direct evidence of a partially piscivorous diet, with the presence of fish scales and vertebrae found in the gut cavity and dental alveolus of the rostral region of individuals from the clade (Charig & Milner, 1997; Dal Sasso *et al*., 2005), suggest that megalosauroids inhabited environments near water.

Furthermore, Ibrahim *et al*. (2014; 2020) and Fabbri *et al*. (2022) proposed that *Spinosaurus* was the first aquatic/amphibious theropod. The purported evidence for the aquatic/amphibious hypothesis includes, among others: (1) ecomorphological adaptations to use the tail for propulsion (Ibrahim *et al*., 2020), (2) increased bone compactness and reduced buoyancy (Fabbri *et al*., 2022), (3) specialisations of the rostrum and much of the skull in spinosaurids, such as the hypertrophied premaxilla and maxilla, and tooth morphology, suggesting a more piscivorous diet or feeding on aquatic prey (e.g., Sakamoto, 2010; Hendrickx *et al*., 2016; Vullo *et al*., 2016; but see also Rayfield *et al*., 2007; Cuff & Rayfield, 2013; Souza *et al*., 2023), and, by extension (4) more than 700 footprints attributed to megalosauroids in Portugal, suggesting that animals of this clade moved to the coast, possibly in search of

resources available during low tide (Razzolini *et al*., 2016). The hypothesised aquatic/amphibious and (mainly) piscivorous adaptations of *Spinosaurus* as well as spinosaurids remain highly controversial (e.g., Hone & Holtz, 2017; 2019; 2021; Henderson, 2018; Gutara & Rahman, 2022; Sereno *et al*., 2022; Souza *et al*., 2023).

This knowledge and lingering questions about non-avian theropods – "especially megalosauroids" – morphology, locomotor modes, palaeoecology and palaeoenvironments prompts our current study. In this contribution, we analyse the evolution of morphological characters of the theropod locomotor apparatus: the pelvic girdle (i.e., ilium, pubis, and ischium) and hindlimb stylopodium and zeugopodium (i.e., femur, tibia, and fibula). Initially, to do this, we re-run the phylogenetic analysis of Carrano *et al*. (2012) using our modifications of character scorings for spinosaurids. We have four primary aims: (1) Evaluate the history of morphological characters of the locomotor system to test whether there are different homoplastic signals in different regions; (2) Reconstruct the ancestral states of the morphology of each trait, searching for correlated macroevolutionary changes of the locomotor apparatus related to hindlimb muscle attachments or other features relevant to locomotion; (3) Where feasible, infer or offer speculations on the possible functional implications of these changes (focusing, in general, on the potential associated musculature); and (4) Test whether different homoplastic signals, based on a morphospace generated by disparity analysis using morphological character states, in different regions of the locomotor apparatus are present in theropods, as well as summarise the most disparate locomotor structures. In conducting these analyses, we also present detailed illustrations and labelled photographs of key character states, which add clarity to our and future phylogenetic analyses, as well as other studies using these data.

Institutional abbreviations: AAOD, Australian Age of Dinosaur Museum of Natural History, Winton, Australia. FMNH, Field Museum of Natural History, Chicago, United States. FSAC, Faculté des Sciences Aïn Chock, University of Casablanca, Casablanca, Morocco. MACN, Museo Argentino de Ciencias Naturales 'Bernardino Rivadavia', Buenos Aires, Argentina. MB, Museum für Naturkunde Berlin, Berlin, Germany. MCNA, Museo de Ciencias Naturales y Antropológicas (J. C. Moyano) de Mendoza, Mendoza, Argentina. MDS BK Dinosaur Museum, Savannakhet, Laos. MNBH, Musée National de Boubou Hama, Niamey, Niger. MNHNUL (LHNB), Laboratório de História Natural da Batalha, Portugal. MPEF, Museo Paleontológico Egidio Feruglio, Trelew, Argentina. MUCPv, Museo de la Universidad del Comahue, Colección Chocón, Villa El Chocón, Argentina. NHMUK, Natural History Museum,

London, United Kingdom; OUMNH, Oxford University Museum of Natural History, Oxford, United Kingdom. PVL, Fundación ‘Miguel Lillo’, San Miguel de Tucumán, Argentina. PW, Paleontological Collections, Department of Mineral Resources, Bangkok, Thailand. SHN, Sociedade de História Natural, Torres Vedras, Portugal. TMM, Texas Vertebrate Paleontology Collections, The University of Texas at Austin, Texas, United States. UCMP, University of California Museum of Paleontology, California, United States. UCRC, University of Chicago Research Collection, Chicago, United States. UMNH, Natural History Museum of Utah, Utah, United States.

2. MATERIAL AND METHODS

2.1. Anatomical nomenclature

The anatomical terminology of the appendicular skeleton analysed here follows Carrano *et al*. (2012). The nomenclature and homology of the musculoskeletal system follows Hutchinson & Gatesy (2000), Hutchinson (2001a,b; 2002), and Carrano & Hutchinson (2002). All taxonomic nomenclature follows Carrano *et al*. (2012), with the exception of tetanuran "*Dilophosaurus sinensis*", which is currently considered as *Sinosaurus sinensis* (Zhang *et al*., 2023).

2.2. Taxa and character scores: inclusion and analytical procedures

Based on the *Spinosaurus* FSAC-KK 11888 neotype presented by Ibrahim *et al*. (2014), the coding of the 68 characters related to the pelvis and stylopodium and zeugopodium detailed in section 2.3 below was performed based on the phylogenetic matrix of Carrano *et al*. (2012) (see Appendix A, B, and C). Our morphological study of *Spinosaurus* was performed by accessing the 3D digital model (MorphoSource; UCRC:PV170; ark:/87602/m4/461415) recently made available by Sereno *et al*. (2022) and the brief description provided by Ibrahim *et al*. (2014). The scores are shown in Table 1 and other modifications are in Appendix C. The 3D model of *Suchomimus* (MorphoSource; UCRC:PV171; ark:/87602/m4/486547) provided by Sereno *et al*. (2022) was also used in comparative morphology.

Table 1.1. Character state scores for the pelvis, stylopodium and zeugopodium of the *Spinosaurus* neotype – morphological characters 261 to 328 (1 to 68 here) from Carrano *et al*. (2012).

Character:	0000000001	1111111111	2222222222	3333333333	4444444444	5555555555	66666666
	1234567890	1234567890	1234567890	1234567890	1234567890	1234567890	12345678
Specimen	Character scores						
FSAC-KK 11888	?001001001	1001110110	02?200?000	0200110?0?	11?01100?0	1101201000	02021101

? – missing data

As there is an ongoing debate whether some isolated material that does not overlap with the original skeleton described by Stromer (1915) should be established as *Spinosaurus aegyptiacus* (see, for example, Dal Sasso *et al*., 2005; Ibrahim *et al*., 2014; 2022, and arguments by Evers *et al*., 2015; Sales & Schultz, 2017; Lacerda *et al*., 2022), as well as because our focus

here regards the appendicular skeleton related with locomotion, we removed character scores based on isolated rostrum. In our view, the association of the pelvis and hindlimb with *Sp. aegyptiacus* (Ibrahim *et al*., 2014) is better established, since part of the material described recently was associated with dorsal and cervical vertebrae, as well as with neural spines, which in turn have some overlapping structures with the holotype (see Stromer, 1915; Smith *et al*., 2006; Ibrahim *et al*., 2014; Sereno *et al*., 2022). The pelvic girdle scoring of *Ichthyovenator* (specimen(s) MDS BK10-01 to 15) included in our analysis was primarily based on the scoring by Rauhut & Pol (2019) and the morphological description by Allain *et al*. (2012).

Although there are some important updates (e.g., Rauhut *et al*., 2016; Rauhut & Pol, 2019), the matrix by Carrano *et al*. (2012) was used in our approach because the encoding of post-cranial characters is closer to our interpretation of the studied taxa. The matrix analysed is composed of 59 taxa and 352 morphological characters (consisting of 351 taken from Carrano *et al*. (2012) and one (#352) from Rauhut & Pol (2019). Taxa *Poekilopleuron*, *Streptospondylus*, and *Xuanhanosaurus* were excluded because they acted as "wildcards" in a previous analysis (Carrano *et al*., 2012). The additional scorings/character modifications in the taxon-character matrix were performed using Mesquite version 3.6 (Maddison & Maddison, 2015). As we had changed some character scorings, we felt we needed to re-analyse the phylogeny of our study taxa to see if fundamental relationships were altered. The cladistic analysis was conducted in TNT version 1.6 (Goloboff & Morales, 2023), following similar parameters adopted by Carrano *et al*. (2012) and Hendrickx *et al*. (2020). *Eoraptor* was used as an outgroup to polarise the characters. In our heuristic search, we used the "New Technology Search" algorithms: Sectorial Searches, Ratchet (perturbation phase stopped after 20 substitutions), and Tree-fusing (5 rounds), until 100 hits of the same most parsimonious tree (MPT) were achieved using the command xmult = hits 100 rss fuse 5 ratchet 20; a final round of TBR branch swapping was performed using the bb command. The characters were analysed under equally weighted parsimony and 32 were considered as ordered, as per Rauhut & Pol (2019) (see Appendix D). Consistency (CI) and Retention (RI) indices were calculated using the stats.run script in TNT and Bremer support was calculated using suboptimal trees (up to 10 steps). Synapomorphies were mapped using WinClada version 1.61 (Nixon, 1999–2002).

2.3. Macroevolutionary history of morphological characters and reconstruction of ancestral states

In order to explore the evolutionary history of morphological characters of the locomotor apparatus in non-avian theropods, with an emphasis on megalosauroids, we used our version of the taxon-character matrix of Carrano *et al*. (2012), which focused on tetanuran theropods. Among the 352 morphological characters (see section 2.2 and Appendix A, B, and C), 68 (~19%) are related to the pelvic girdle and hindlimb stylopodium and zeugopodium (character list in Appendix B). The characters pertain to the: (1) pelvic elements (character 261); (2) ilium (characters 262–280); (3) puboischiadic plate (character 281); (4) pubis (characters 282–291); (5) ischium (characters 292–300); (6) femur (characters 301–316); (7) tibia (characters 317–324); and (8) fibula (characters 325–328) (Appendix B).

Based on the obtained topology (see Results), an analysis of the evolution of each of the aforementioned morphological characters of the locomotor apparatus was performed using Mesquite software (Maddison & Maddison, 2015). Through the maximum-likelihood method for character state reconstruction (i.e., mapping or tracing), which calculates the ancestral state that maximises the probability of the observed states to have evolved under a stochastic model (Schluter *et al*., 1997), the state of each character in the most recent common ancestor (MRCA) of each theropod clade was also estimated; however, focusing our analysis on megalosauroids. The evolutionary model assumed in the MRCA reconstructions was Mk1 (Markov k-state 1), which considers the rate of character state changes as equally probable, since this method denotes greater effectiveness when compared to the parsimony criterion (Schluter *et al*., 1997); however, when polymorphic characters were present (characters: 281, 284, 292, 301, 306, 325), the MRCA reconstructions were made using the parsimony criterion instead of likelihood calculations. Using the likelihood parameter, the proportional likelihood (pl) of each estimated MRCA is given in % values (Maddison & Maddison, 2015).

2.4. Disparity analyses

We calculated six Euclidean distance matrices based on the modified version of the taxon-character matrix from Carrano *et al*. (2012), using the aforementioned morphological characters (section 2.1, Appendix B). Each of the new matrices separately represented the elements of the locomotor apparatus studied here: (i) all characters of the pelvic girdle and hindlimb stylopodium and zeugopodium (characters 261-328); (ii) ilium (characters 262-280); (iii) pubis

(characters 282-291); (iv) ischium (characters 292-300); (v) femur (characters 301-316), and (vi) tibia/fibula (characters 317-328), which were divided to assess the influence of each of these structures on the disparity analyses (explained below).

We then removed taxa that do not have the studied pelvic and hindlimb elements preserved. Analysis (i) was conducted leaving 52 operational taxonomic units (OTU); analysis (ii) 50 OTUs; analysis (iii) 48 OTUs; analysis (iv) 43 OTUs; analysis (v) and (vi) 46 OTUs (see details in Appendix E). All polymorphic characters were treated as unknown ("?") in these analyses.

Subsequently, using the PAST v.4.01 program (Hammer *et al*., 2001), the data were sorted based on the Euclidean dissimilarity index for each of the six matrices through Principal Coordinate Analysis (PCO), in order to visualise the disparity of the morphological characters based on the distribution of the taxa in a two-dimensional morphospace of reduced dimensionality. PCO, when compared to Principal Component Analysis (PCA), is more suitable for disparity analysis of phylogenetic characters, as it better handles missing data, which are common in palaeontological studies, and are more appropriate with distance/dissimilarity matrices (Brusatte *et al*., 2011; Gower, 2014). Although there is a wide debate about corrections and adaptations to disparity methods that use discrete character states from phylogenetic matrices, as well as continuous data (e.g., Brusatte *et al*., 2011; Guillerme *et al*., 2020), in this work, we order the data in a way similar to other studies (e.g., Novas *et al*., 2015) that used the Euclidean distances among taxa posteriorly ordinated in a morphospace. All datasets used in this work can be found in (Lacerda *et al*., 2023a).

3. RESULTS AND DISCUSSION

3.1. Cladistic analysis

In the first round of analysis, 428 most parsimonious trees (MPT) were reached with 1067 steps each. Subsequent TBR application of the retained trees resulted in a total of 1800 MPTs each of 1067 steps. The strict consensus of these trees reached is shown in cladogram in Figure 1.1. Based on the consensus topology, the homoplastic index CI and RI were 0.407 and 0.677 respectively.

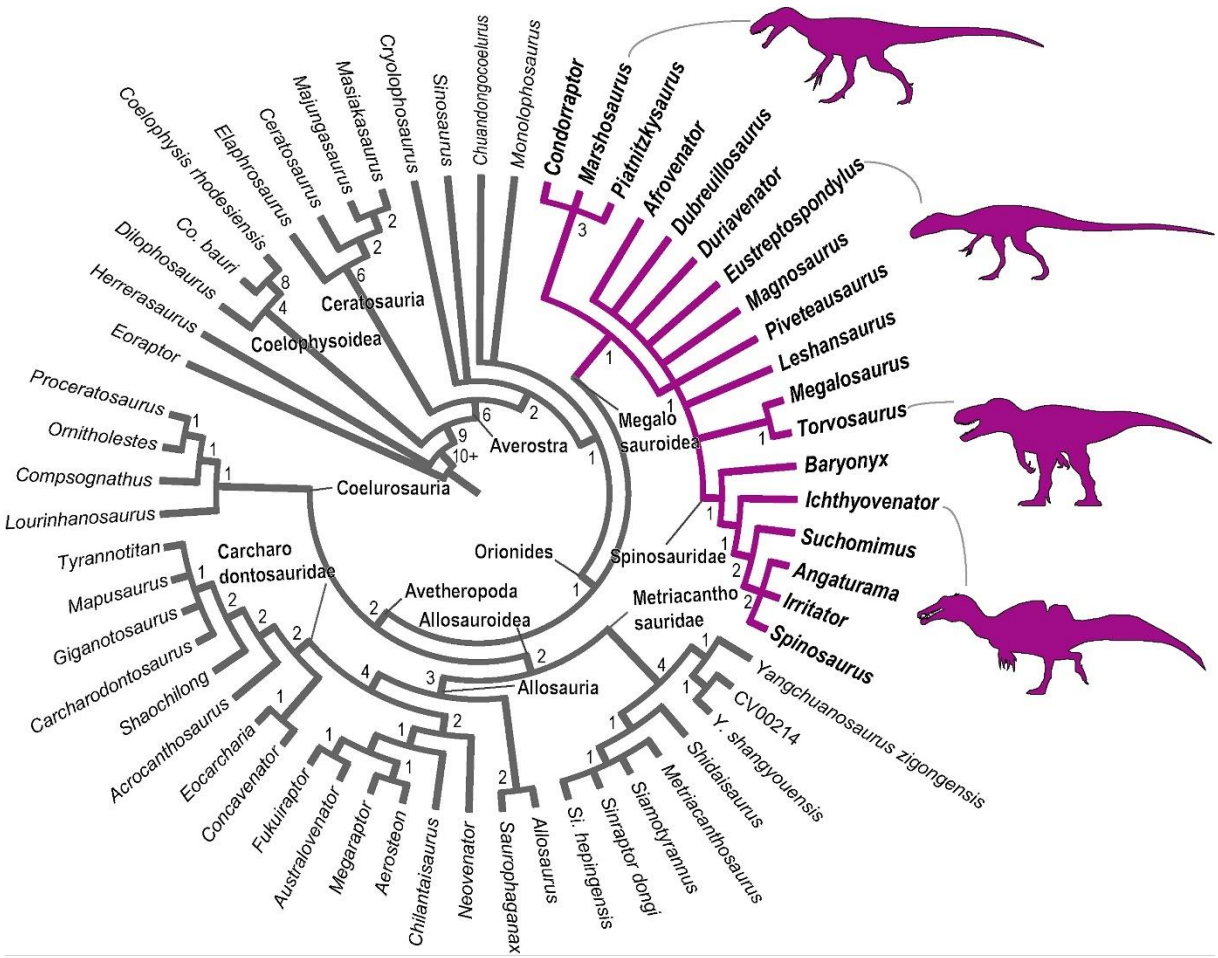

Figure 1.1. Results of phylogenetic analysis. Strict consensus cladogram of the most parsimonious trees retrieved (tree length = 1067; CI = 0.407; RI = 0.677), Bremer support is displayed below each node. The highlighted and illustrated clade represents Megalosauroidea. Silhouettes were downloaded from phylopic.org; see Acknowledgements.

In general, the topology obtained is congruent with the results of Carrano *et al*. (2012), because it recovers successive clades within Theropoda such as Coelophysoidea, Ceratosauria and the larger Tetanurae clade composed of successive taxa at its base (e.g., *Sinosaurus*,

Cryolophosaurus) as successive sister lineages of the clade Orionides, which is composed of Megalosauroidea and the larger clade Avetheropoda (Figure 1.1). Unlike a recent study (Rauhut *et al*., 2016), our analysis recovered *Dilophosaurus* within Coelophysoidea and *Monolophosaurus* as an early Tetanurae, in agreement with Carrano *et al*. (2012).

Although the large theropod clades obtained are compatible with Carrano *et al*.'s (2012) results, some clades internally lost resolution with the inclusion of the spinosaurid *Ichthyovenator* and our changes to the characters of *Spinosaurus*. In our analysis, the Megalosauroidea clade is composed of two main clades: the early-diverging clade Piatnitzkysauridae; which includes *Piatnitzkysaurus*, *Marshosaurus*, and *Condorraptor* (unresolved internal relationships); and a later-diverging clade Spinosauridae, which includes *Baryonyx*, *Ichthyovenator*, *Suchomimus*, and Spinosaurinae (*Spinosaurus*, *Irritator*, and *Angaturama*) (Figure 1.1).

The classic Megalosauridae, which includes *Eustreptospondylus* as the early-diverging species, followed by the Megalosaurinae (*Duriavenator*, *Megalosaurus*, and *Torvosaurus*) and Afrovenatorinae (*Afrovenator*, *Magnosaurus*, *Dubreuillosaurus*, *Leshansaurus*, and *Piveteasaurus*) clades (Carrano *et al*., 2012) were not recovered (however, see further discussions in topic 4.1.). Our analysis retrieved a large unresolved polytomy where the clade internally recovered is comparable with Megalosaurinae (*Megalosaurus* + *Torvosaurus*) (Figure 1.1).

Regarding Spinosauridae, *Ichthyovenator* was recovered as a non-spinosaurine spinosaurid as previously proposed (Allain *et al*., 2012; Rauhut & Pol, 2019). Indeed, in our analysis the Baryonychinae clade was not recovered, with *Baryonyx*, *Ichthyovenator*, and *Suchomimus* as a sequence of successive lineages, the latter being the outgroup of Spinosaurinae. Finally, although Spinosaurinae was recovered as a clade, similar to results obtained by Carrano *et al*. (2012), in our phylogeny the internal relationships remain unresolved (Figure 1.1). Although megalosaurids were recovered without resolution, for ease of comparison, here we presume megalosaurid monophyly (*sensu* Carrano *et al*., 2012).

3.2. Evolutionary history and ancestral states of theropod pelvic girdle and hindlimb stylopodium and zeugopodium characters

3.2.1. Pelvic elements

The articulations of the pubis, ilium and ischium (character 261) in theropods can be unfused (261[0]) or fused (261[1]) in adults. The plesiomorphic condition is observed in the sauropodomorph *Eoraptor* and most other theropods, with exceptions in coelophysoids and ceratosaurs such as *Ceratosaurus* and *Masiakasaurus*, in which the pelvic elements are fused (pelvic fusion also occurs convergently within Avialae). Throughout non-avian tetanuran evolution, the plesiomorphic condition generally persisted, including in all megalosauroids mapped. The reconstruction of this character state for the MRCA of megalosauroids suggests that it had unfused pelvic elements (pl = 99%), unlike the condition in coelophysoids, whose MRCA had a fused pelvic girdle (pl = 97%). This fusion might have biomechanical importance for the overall strength of the pelvis, but this remains untested; finite element analyses could give insights into the potential consequences.

3.2.2. Ilium

Nineteen of the studied characters (27.94%) are related to the ilium. The ilium represents a structure on which a substantial part of the locomotor musculature originates/originated in theropods (Romer, 1923a,b,c; Rowe, 1986; Gatesy, 1990; 1994; Hutchinson & Gatesy, 2002; Hutchinson, 2001b; 2002; Carrano & Hutchinson, 2002; Grillo & Azevedo, 2011; Bishop *et al*., 2021), both from the dorsal and ventral groups (e.g., *M. iliotibialis*, *M. iliotrochantericus caudalis*, *M. flexor tibialis externus*, *M. caudofemoralis brevis*).

The pneumatic foramen and the internal cavities of the ilium (character 262) of theropods may be absent (262[0]) or present (262[1]). Most of the studied species retain the plesiomorphic condition; changes are rare (*sensu* Schluter *et al*., 1997). This pneumatisation is present in carcharodontosaurs; specifically in neovenatorids; so the MRCA of neovenatorids had a pneumatic foramen and internal cavities in the ilium (pl = 98%). The pneumatisation presumably indicates expanded posterior (abdominal) air sacs (e.g., Sereno *et al*., 2008; Aureliano *et al*., 2022), although whether this had important functional ramifications is unclear.

A vertical ridge may be present on the lateral surface of the ilium, dorsal to the acetabulum (character 263). This crest is absent (263[0]) in *Eoraptor* and early theropods (e.g.,

Masiakasaurus; Figure 1.2A). A low and robust vertical ridge (263[1]) is present in early tetanurans such as *Monolophosaurus*, piatnitzkysaurids (e.g., *Piatnitzkysaurus*; Figure 1.2B), and allosaurids. A vertical ridge that represents a low and double structure (263[2]) is present only in some allosauroids, specifically in metriacanthosaurines (*Siamotyrannus* (Figure 1.2C) and *Sinraptor*). In megalosauroids, the absence of the iliac ridge is noted in *Eustreptospondylus* and *Torvosaurus*, as well as in the spinosaurids *Ichthyovenator* and *Spinosaurus*. Meanwhile, a low swollen ridge is present in *Megalosaurus*, *Afrovenator*, *Suchomimus* and the early-diverging piatnitzkysaurids. The MRCA of megalosauroids probably lacked the vertical ridge in the ilium (pl = 58%); however, the MRCA of piatnitzkysaurids probably had a robust ridge (pl = 93%) (Figure 1.2D). This ridge(s) is thought to potentially indicate clearer separation between the origins of *M. iliotrochantericus caudalis* (ITC)/*M. iliofemoralis externus* and *M. iliofibularis* (e.g., Carrano & Hutchinson, 2002).

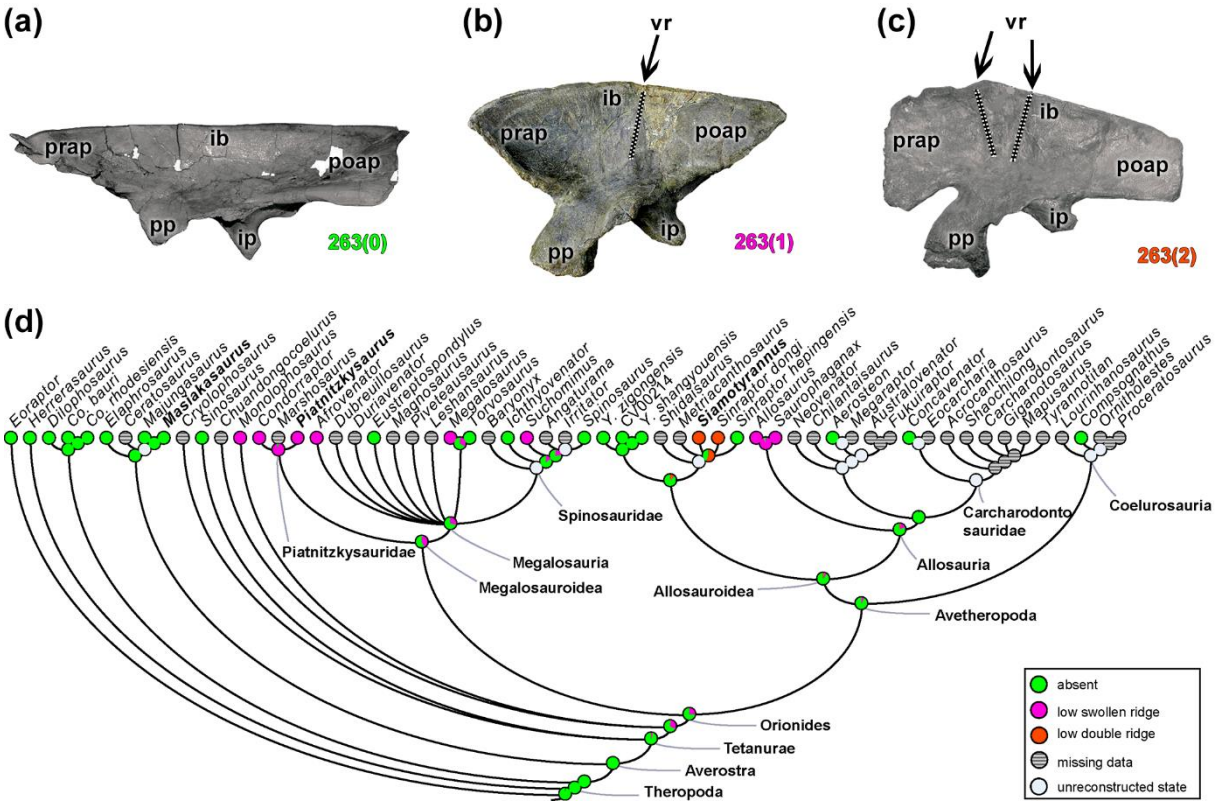

Figure 1.2. Evolutionary history of character 263 (Ilium, vertical ridge on lateral surface of blade dorsal to acetabulum) and the ancestral state reconstruction. Illustration of the left ilium in lateral view: (a) *Masiakasaurus* FMNH PR 2485; (b) *Piatnitzkysaurus* MACN-Pv-CH 895; (c) *Siamotyrannus* PW 9-1. (d) Phylogenetic tree of Tetanurae showing the reconstruction of ancestral character state for each node. (a) modified from Carrano *et al.* (2011) and (c) modified from Carrano *et al.* (2012). Not to scale. Abbreviations: ib-iliac blade, ip-ischiadic peduncle, poap-postacetabular process, pp-pubic peduncle, prap-preacetabular process, vr-vertical ridge.

The brevis or postacetabular fossa is present in the posteromedial portion of the ilium in theropods and other dinosaurs. The posterior width of this cavity (character 264), may be

approximately equal to the anterior width, with subparallel margins (264[0]), or it may have its posterior width twice the anterior width; i.e., enlarged posteriorly (264[1]) (Figure 1.3). The plesiomorphic condition exists in *Eoraptor* and *Herrerasaurus* and persists in the megalosauroids *Piatnitzkysaurus*, *Megalosaurus* (Figure 1.3A), *Torvosaurus*, and *Ichthyovenator*, but also in metriacanthosaurids and some coelurosaurs. Yet some early-diverging clades as coelophysoids and ceratosaurs, as well as allosaurs, have the brevis fossa enlarged posteriorly (264[1]). The character state in the MRCA of megalosauroids suggests the presence of a posteriorly wide brevis fossa (pl = 75%), based on the morphology of the piatnitzkysaurid *Marshosaurus*, as well as *Eustreptospondylus* (Figure 1.3B), *Baryonyx*, *Suchomimus*, and *Spinosaurus*. The same applies to both MRCAs of piatnitzkysaurids (pl = 68%) and spinosaurids (pl = 87%) (Figure 1.3C). The brevis fossa is related to the origin of the *M. caudofemoralis brevis* (CFB), similar to that in Crocodylia, and inferred for Theropoda and other dinosaurs in general (Romer, 1923a,b,c; Gatesy, 1990; Hutchinson, 2001b; Carrano & Hutchinson, 2002; Grillo & Azevedo, 2011; Bishop *et al*., 2021; Rhodes *et al*., 2021). Posterior enlargement of this fossa may indicate greater size of the CFB muscle.

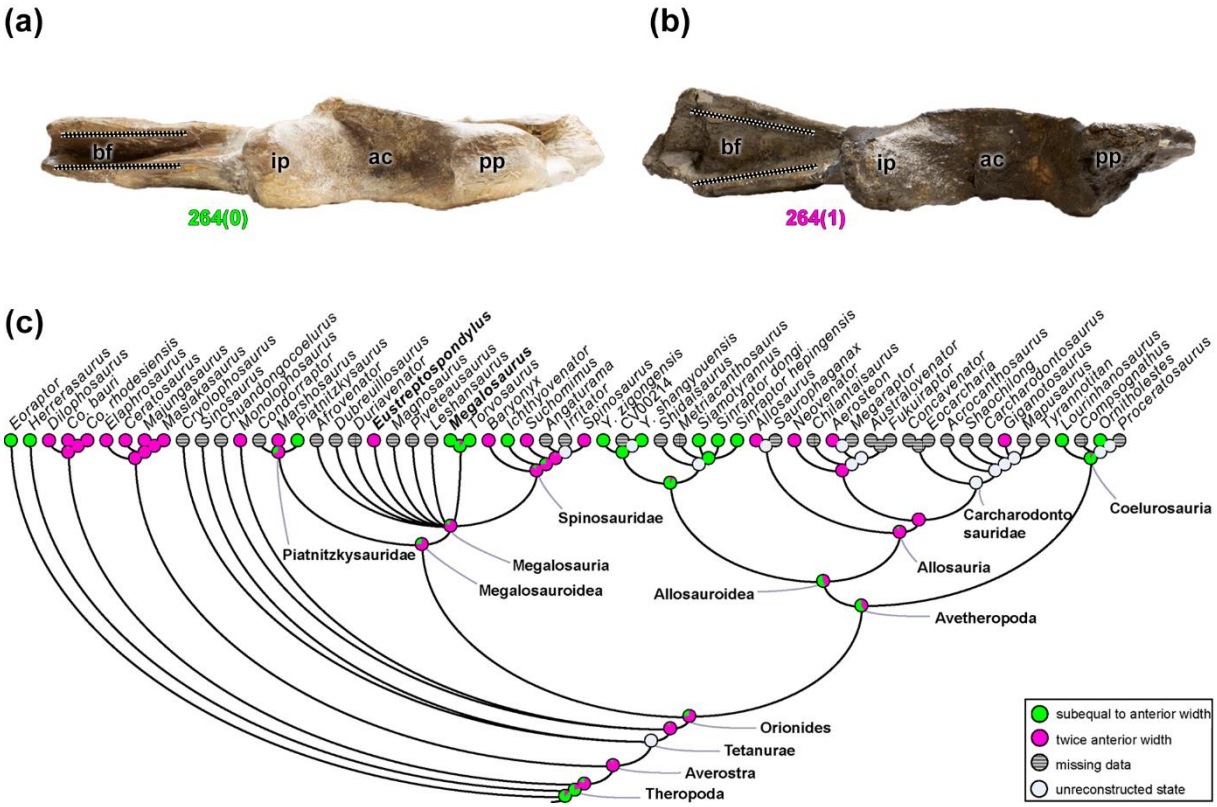

Figure 1.3. Evolutionary history of character 264 (Ilium, posterior width of brevis fossa) and the ancestral state reconstruction. Illustration of the right ilium in ventral view: (a) *Megalosaurus* OUMNH J.13560; (b) *Eustreptospondylus* OUMNH J.13558/E01. (c) Phylogenetic tree of Tetanurae showing the reconstruction of ancestral character state for each node. Not to scale. Abbreviations: ac-acetabulum, bf-brevis fossa, ip-ischiadic peduncle, pp-pubic peduncle.

By comparing the delimitations of the brevis fossa, it is evident that the height of the lateral wall relative to the medial wall (character 265) can be greater along the entire length of the brevis fossa (265[0]), as noted in coelophysoids, early-diverging tetanurans, and some avetheropods (i.e., *Shidaisaurus*, *Yangchuanosaurus*, *Concavenator*, and *Ornitholestes*). A distinct condition is evident when the most anterior portion of the lateral wall is short, exposing part of the medial wall in lateral view (265[1]); this condition is widely mapped across the phylogeny, including *Eoraptor*, *Herrerasaurus*, and many other theropods (Figure 1.4).

In megalosauroids, the ancestral condition (even if mapped as state "1"); i.e, the boundaries are shorter anteriorly; is present in several taxa (e.g., *Megalosaurus*; Figure 1.4A), except *Suchomimus* and *Spinosaurus* (Figure 1.4B). The MRCA reconstruction in megalosauroids indicates that the lateral wall was anteriorly shorter (pl = 92%) (Figure 1.4C).

Some of the morphological variations of the brevis fossa observed within megalosauroids may indicate changes of the boundaries of the CFB origin in some taxa; for example, *Megalosaurus* and *Torvosaurus* have a narrower brevis fossa than in *Eustreptospondylus* and *Spinosaurus* and thus might have had a more restricted CFB origin and smaller muscle size.

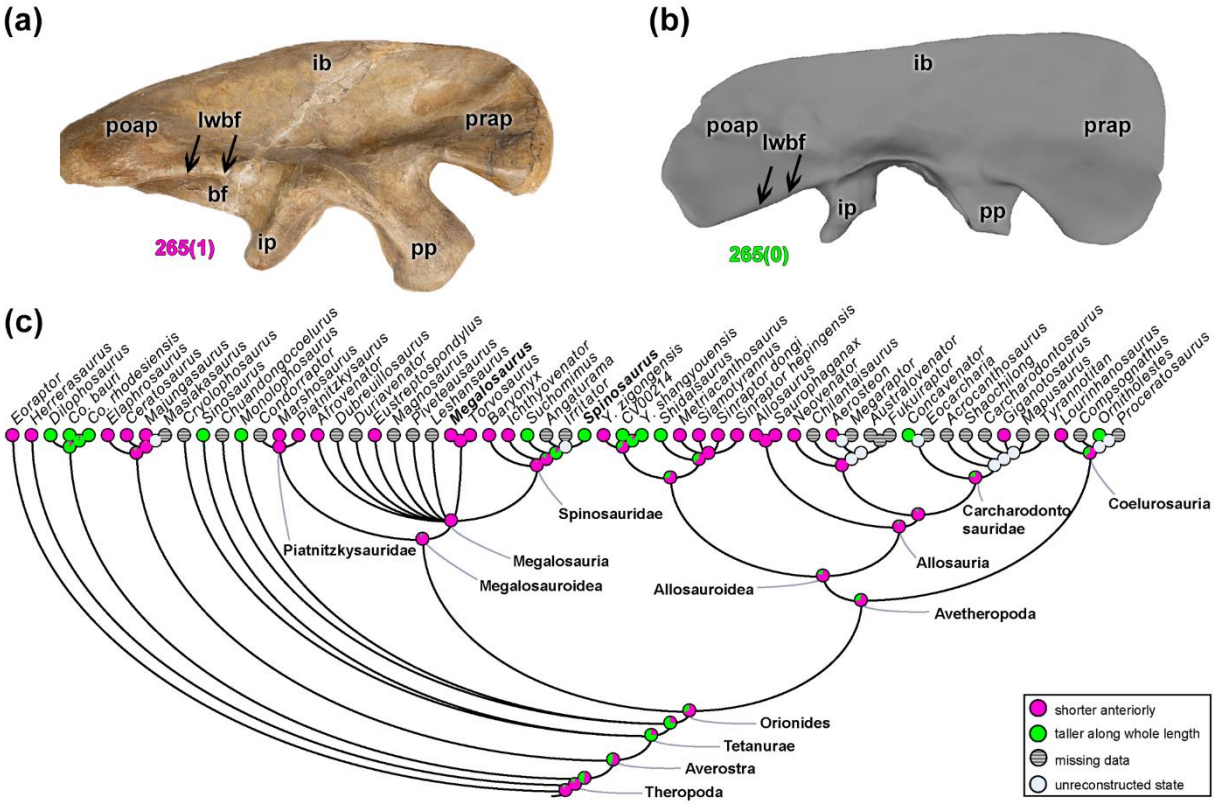

Figure 1.4. Evolutionary history of character 265 (Ilium, height of lateral wall of brevis fossa relative to medial wall) and the ancestral state reconstruction. Illustration of the right ilium in lateral view: (a) *Megalosaurus* OUMNH J.13560; (b) *Spinosaurus* FSAC-KK 11888. (c) Phylogenetic tree of Tetanurae showing the reconstruction of ancestral character state for each node. (b) based on the 3D digital model provided by Sereno *et al*. (2022). Not to scale. Abbreviations: bf-brevis fossa, lwbf-lateral wall of brevis fossa, ib-iliac blade, ip-ischiadic peduncle, poap-postacetabular process, pp-pubic peduncle, prap-preacetabular process.

The posterolateral portion of the ilium, between the supraacetabular crest and the brevis shelf (character 266), may have a “gap” (266[0]), as observed in most theropods (e.g., *Eustreptospondylus*; Figure 1.5B). A continuous ridge (266[1]) is a morphological acquisition of ceratosaurs (pl = 97% for the MRCA) (e.g., *Masiakasaurus*; Figure 1.5A), and independently in the early tetanuran *Sinosaurus* (Figure 1.5C). The development of the supraacetabular ridge of the ilium in its ventrolateral portion (character 267) may culminate in a large/suspended, or “hood”-shaped structure (267[0]), as in *Eoraptor* and non-Orionides theropods (coelophysoids [e.g., *Dilophosaurus*; Figure 1.6A,B], ceratosaurs, and early tetanurans). The supraacetabular crest of the ilium with a reduced projection (267[1]) (e.g., *Piatnitzkysaurus*; Figure 1.6C,D) is a rare change that is observed in Orionides (pl = 98% for the MRCA) (Figure 1.6E). The ventrolateral region between the supraacetabular crest and the brevis shelf may also indicate a boundary of the CFB origin (e.g., Bishop *et al*., 2021), and, based on our analysis, it represents a structure with evolutionary stability in megalosauroids. Differences between theropods in the

various states of characters related to the brevis fossa may indicate interspecific variation in where the CFB originated, or even how large it was overall.

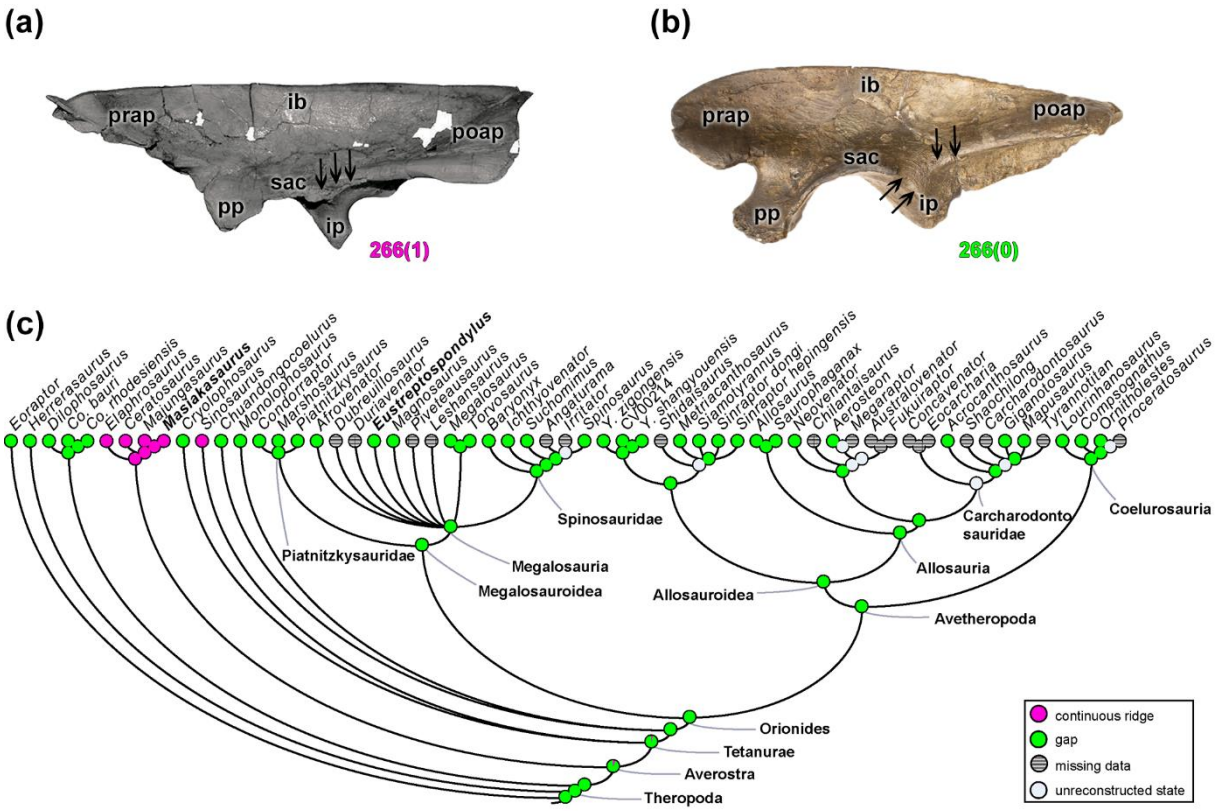

Figure 1.5. Evolutionary history of character 266 (Ilium, morphology between supraacetabular crest and brevis shelf on lateral surface) and the ancestral state reconstruction. Illustration of the left ilium in lateral view: (a) *Masiakasaurus* FMNH PR 2485; (b) *Eustreptospondylus* OUMNH J.13558/E01 (mirrored). (c) Phylogenetic tree of Tetanurae showing the reconstruction of ancestral character state for each node. (a) modified from Carrano *et al*. (2011). Not to scale. Abbreviations: ib-iliac blade, ip-ischiadic peduncle, poap-postacetabular process, pp-pubic peduncle, prap-preacetabular process, sac-supraacetabular crest.

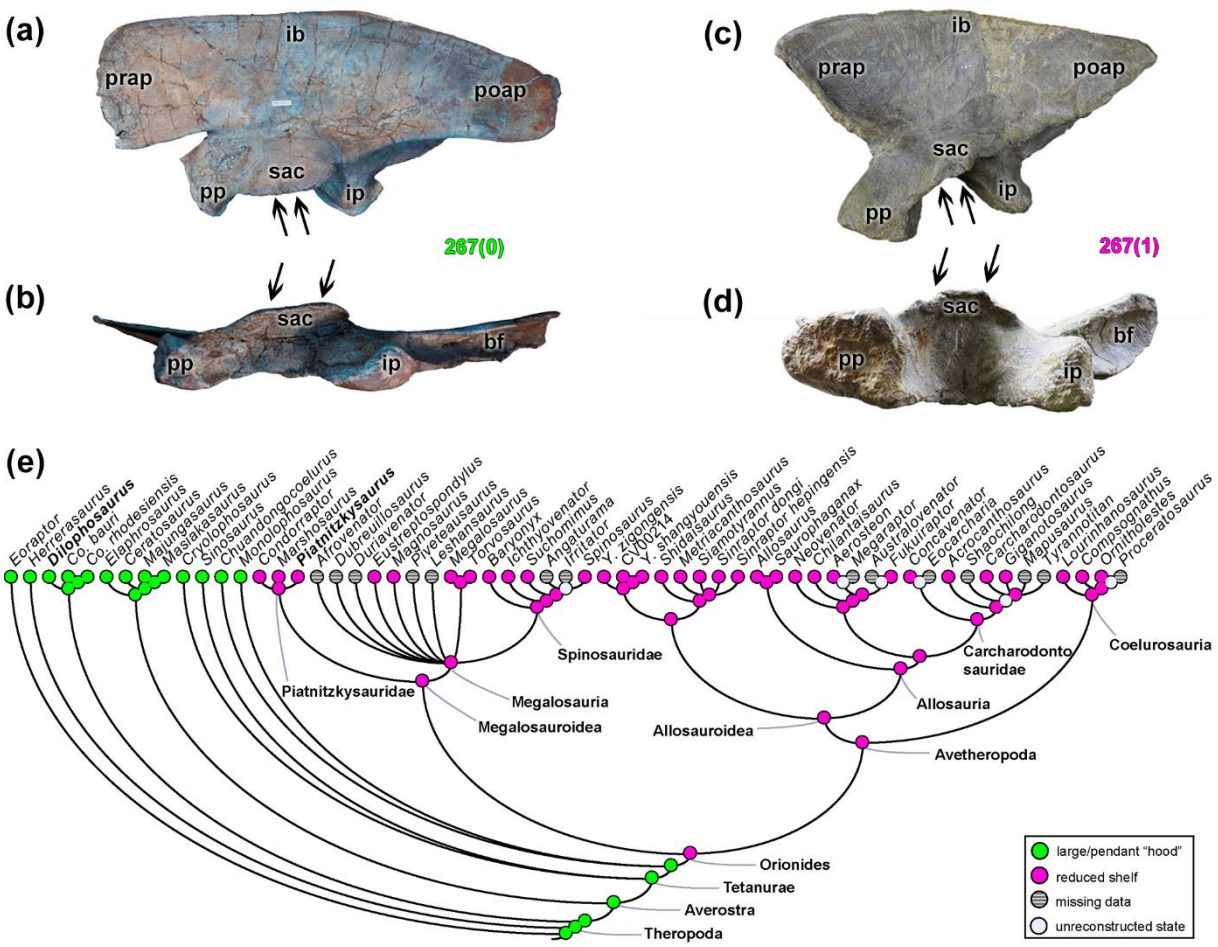

Figure 1.6. Evolutionary history of character 267 (Ilium, ventrolateral development of supraacetabular crest) and the ancestral state reconstruction. Illustration of the left ilium in lateral and ventral views: (a), (b) *Dilophosaurus* TMM 43646-1; (c), (d) *Piatnitzkysaurus* MACN-Pv-CH 895. (e) Phylogenetic tree of Tetanurae showing the reconstruction of ancestral character state for each node. (a) and (c) lateral view, (b) and (d) ventral view. (a), (b) modified from Marsh & Rowe (2020). Not to scale. Abbreviations: bf-brevis fossa, ib-iliac blade, ip-ischiadic peduncle, poap-postacetabular process, pp-pubic peduncle, prap-preacetabular process, sac-supraacetabular crest.

The orientation of the pubic peduncle in the anteroventral portion of the ilium (character 268) can be mainly in a ventral direction (268[0]), as in most theropods (e.g., *Piatnitzkysaurus*; Figure 1.7B); or in a more anteriorly located peduncle with a "double facet" projecting anteriorly and ventrally (268[1]), as present in coelophysoids (including *Dilophosaurus*; Figure 1.7A) and the early-diverging tetanurans (Figure 1.7C). Based on this, the reconstruction of the ancestral character state for the MRCA of Tetanurae suggests the apomorphic condition (pl = 96%), however, in the reconstruction for the MRCA of Orionides the ancestral orientation of the pubic peduncle was more ventral (pl = 99%), and conservative within megalosauroids. The functional implications of these orientations are obscure.

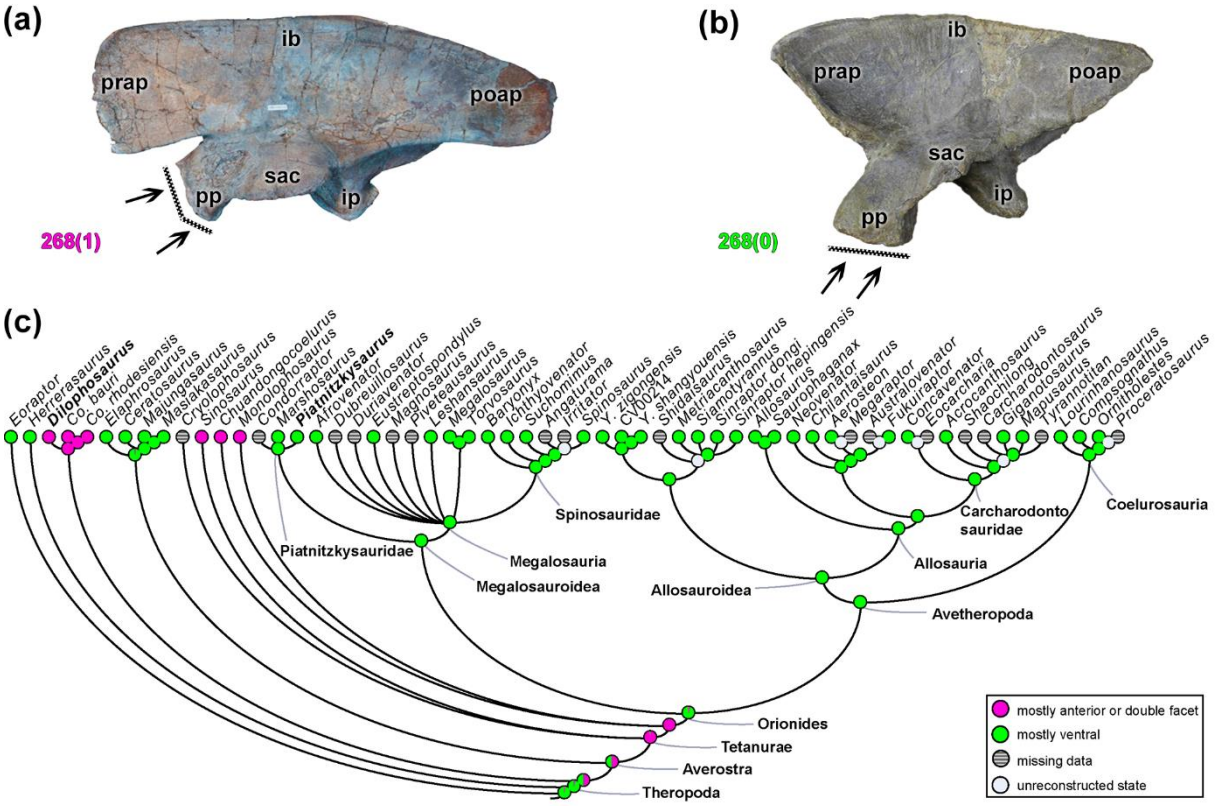

Figure 1.7. Evolutionary history of character 268 (Ilium, orientation of pubic peduncle) and the ancestral state reconstruction. Illustration of the left ilium in lateral view: (a) *Dilophosaurus* TMM 43646-1; (b) *Piatnitzkysaurus* MACN-Pv-CH 895. (c) Phylogenetic tree of Tetanurae showing the reconstruction of ancestral character state for each node. (a) modified from Marsh & Rowe (2020). Not to scale. Abbreviations: ib-iliac blade, ip-ischiadic peduncle, poap-postacetabular process, pp-pubic peduncle, prap-preacetabular process, sac-supraacetabular crest.

The pubic peduncle has its posterior margin delimited by the acetabulum. The shape of this margin (character 269) can be transversely flat or convex (269[0]), as in *Eoraptor*, *Herrerasaurus*, ceratosaurs, and avetheropods, in addition to piatnitzkysaurids (e.g., *Condorraptor*; Figure 1.8A) and *Spinosaurus*. A transversely concave posterior margin of the pubic peduncle (269[1]) is evident in coelophysoids, megalosaurids (e.g., *Megalosaurus*; Figure 1.8B), as well as independently in *Chuandongocoelurus* and *Ornitholestes* (Figure 1.8C). Considering that piatnitzkysaurids and *Spinosaurus* have the shape of the pubic peduncle transversely flat or convex, the MRCA of megalosauroids probably had the plesiomorphic condition (pl = 63%). Again, it is unclear if this variation had important functional relevance.

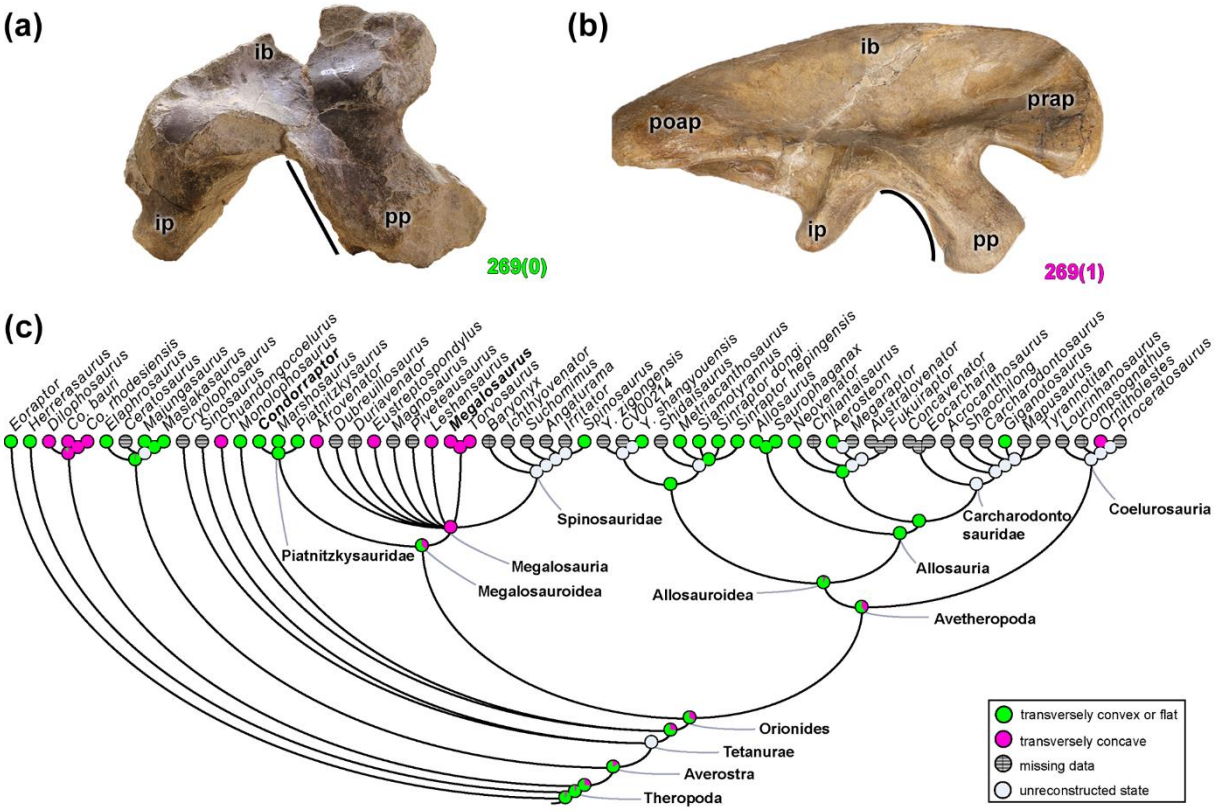

Figure 1.8. Evolutionary history of character 269 (Ilium, shape of acetabular margin of pubic peduncle) and the ancestral state reconstruction. Illustration of the left ilium in lateral view: (a) *Condorraptor* MPEF-PV 1687 (mirrored); (b) *Megalosaurus* OUMNH J.13560. (c) Phylogenetic tree of Tetanurae showing the reconstruction of ancestral character state for each node. Not to scale. Abbreviations: ib-iliac blade, ip-ischiadic peduncle, poap-postacetabular process, pp-pubic peduncle, prap-preacetabular process.

The relative sizes of the iliac articulations, the pubic and ischial joints (character 270), can be approximately equal (270[0]), as in *Eoraptor* and non-Orionides theropods. However, in the clade composed of *Chuandongocoelurus* and *Monolophosaurus* at the base and all Orionides (pl = 99% for the MRCA), the pubic joint is more robust, being ≥ 130% of the ischial articulation (270[1]). In addition to this proportionality, the morphology of the ischial peduncle (character 271) is rounded (271[0]) in the majority of theropods, being evolutionary stable. The exception is an abbreviated distalmost ischial peduncle (271[1]), which is present in the carcharodontosaurid *Concavenator*, and the coelurosaurs *Compsognathus* and *Ornitholestes*. These traits might relate to relative differences in the strengths or mobility of these joints between pelvic elements, but it is pure speculation if this is the case or if the differences would be of biologically relevant magnitudes.

The ratio between the width and length of the pubic peduncle (character 272) represents a multistate character in theropods. This ratio is ≤ 1 (272[0]) as observed in non-Orionides theropods, and independently in the megalosauroids *Eustreptospondylus*, *Suchomimus*, and *Spinosaurus*. A ratio between 1.3–1.75 (272[1]) is prevalent in tetanurans (except in *Sinosaurus*

and the aforementioned megalosauroids), in metriacanthosaurids (except *Siamotyrannus*), and independently in the coelurosaur *Ornitholestes*. In allosaurs, *Siamotyrannus* and *Ornitholestes*, the ratio is > 2 (272[2]). Although *Eustreptospondylus*, *Suchomimus*, and *Spinosaurus* have the plesiomorphic condition, the MRCA of megalosauroids had a ratio between 1.3–1.75 between the width and length of the pubic peduncle (pl = 99%). The pubic peduncle region may indicate the ventral boundary of the origin of *M. puboischiofemoralis internus 1* (PIFI1) (e.g., Carrano & Hutchinson, 2002; Bishop *et al*., 2021), so a longer peduncle might correlate with an expanded PIFI1 origin, or a partial shift of that origin from medial (as in Crocodylia) to lateral (as in Aves). As suggested by our analysis, only the proportionality of this structure relative to the ischial peduncle presents variation in megalosauroids; mainly internally in megalosaurids and spinosaurids.

In the medial region of the ilium, the portion adjacent to the preacetabular notch or "cuppedicus fossa" (related to the origin of PIFI1 and/or PIFI2; e.g., Rowe, 1986; Hutchinson & Gatesy, 2000; Hutchinson, 2001b) (character 273), may be smooth, without a crest (273[0]), as in all non-avetheropod taxa (except the coelophysoid *Coelophysis rhodesiensis* and the megalosauroid *Ichthyovenator*) and independently in *Sinraptor dongi*. In avetheropods, except *Si. dongi*, there is a crest in the portion adjacent to the "cuppedicus fossa" (273[1]); which is also the condition in *Co. rhodesiensis* and *Ichthyovenator*. In neovenatorids this crest is not only present but also is well developed, forming a projection (273[2]). With the exception of *Ichthyovenator*, the plesiomorphic condition is predominant in megalosauroids and in the MRCA (pl = 99%). The development of this fossa is widely held to relate to the shift of the PIFI1 and PIFI2 from the medial pelvis and preacetabular vertebrae to the lateral iliac surface across the lineage to Aves (see references above), with consequences for the sizes and moment arms of those muscles (e.g., Carrano, 2002; Allen *et al*., 2021).

The length of the preacetabular process in relation to the anterior edge of the pubic peduncle (character 274) was an evolutionarily stable feature in theropods. A preacetabular process with an anterior part of the pubic peduncle that projects anteriorly at the same point (274[0]) is evident only in *Eoraptor* and *Herrerasaurus*. The preacetabular process projects anteriorly well beyond the pubic peduncle (274[1]) in Neotheropoda (pl = 98% for the MRCA). The same macroevolutionary pattern exists for the depth of the preacetabular process (character 275), which is shallow (275[0]) in *Eoraptor* and *Herrerasaurus*, and is deep in Neotheropoda (275[1]) (pl = 98% for the MRCA). The most anteroventral region of the preacetabular process (character 276) may have its edges without any lobed structure (276[0]) as observed in non-Averostra theropods (e.g., *Dilophosaurus*; Figure 1.9A), *Chilantaisaurus*, and *Compsognathus*

(Figure 1.9C). Other than these exceptions, averostran taxa have an anteroventral lobe of the preacetabular process (276[1]) (e.g., *Megalosaurus*; Figure 1.9B). All mapped megalosauroids have the apomorphic condition, however the MRCA of megalosauroids cannot be reconstructed, as none of the piatnitzkysaurids have the anteriormost part of the ilium preserved. Derived states of characters 274-276 likely correlate with anterior expansion of the ITC muscle origin across Theropoda. The preacetabular process of the ilium is associated with the origin of at least three muscles of the dorsal hindlimb group: *M. iliotibialis 1* (IT1) on the lateral dorsal/anterior rim, ITC on the anteriormost lateral surface, and PIFI1 or PIFI2 muscle(s) on the preacetabular region, as noted above (e.g., Romer, 1923a,b,c; Hutchinson & Gatesy, 2000; Hutchinson, 2001b; 2002; Carrano & Hutchinson, 2002). Based on the character history, there was some conservatism in the morphology of these muscle origins within Megalosauroidea.

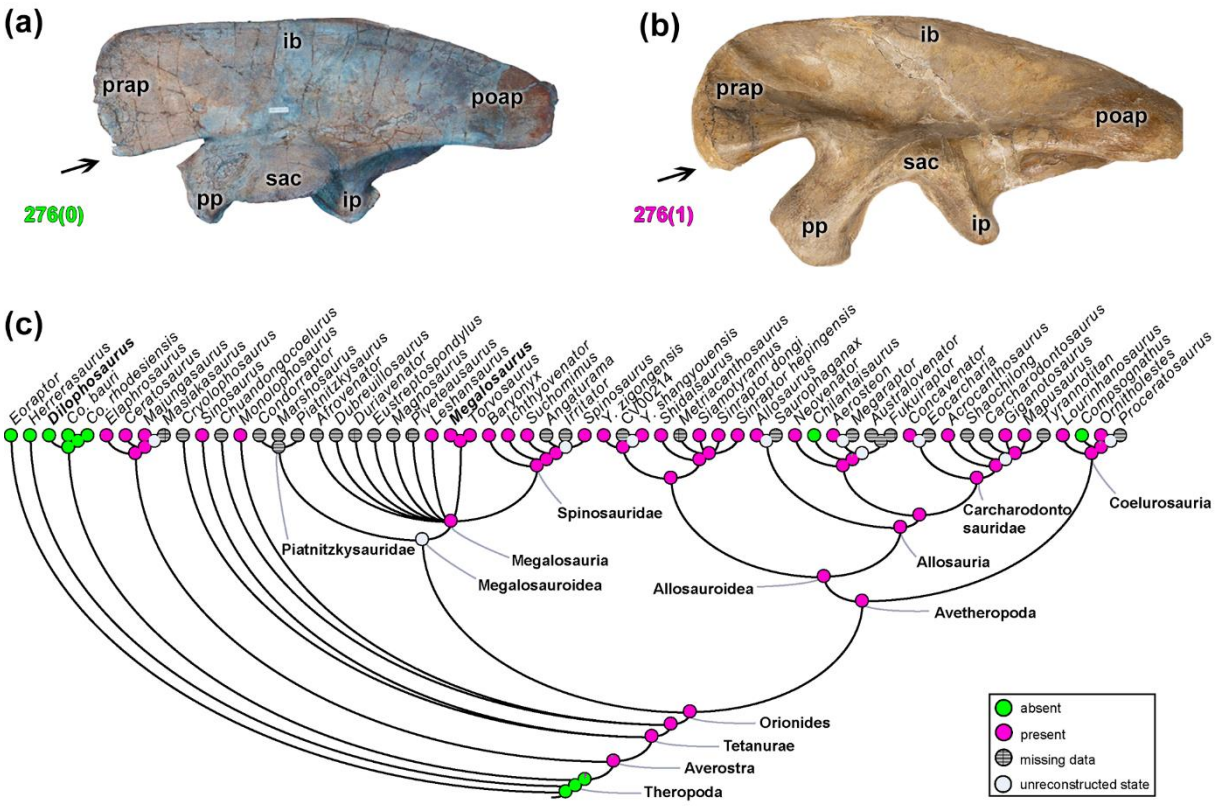

Figure 1.9. Evolutionary history of character 276 (Ilium, anteroventral lobe of preacetabular process) and the ancestral state reconstruction. Illustration of the left ilium in lateral view: (a) *Dilophosaurus* TMM 43646-1; (b) *Megalosaurus* OUMNH J.13560 (mirrored). (c) Phylogenetic tree of Tetanurae showing the reconstruction of ancestral character state for each node. (a) modified from Marsh & Rowe (2020). Not to scale. Abbreviations: ib-iliac blade, ip-ischiadic peduncle, poap-postacetabular process, pp-pubic peduncle, prap-preacetabular process, sac-supraacetabular crest.

The shape of the dorsal border of the ilium (character 277) in lateromedial view may have a convex margin (277[0]), as in most theropods including all Orionides clades (e.g.,

Eustreptospondylus; Figure 1.10B), with the exception of a straight dorsal margin morphology (277[1]), which is in coelophysids and ceratosaurs (except *Ceratosaurus*) (e.g., *Masiakasaurus*; Figure 1.10A). Interestingly, because of the plesiomorphic (state 0) character status in *Ceratosaurus*, the reconstruction of the MRCA of ceratosaurs is ambiguous (pl = 49% of state 0; and pl = 51% of state 1) (Figure 1.10C). At least two hindlimb muscles of the dorsal group have their origin from the dorsal border of the ilium other than the preacetabular process: *Mm. iliotibiales 2* and *3* (IT2, IT3; e.g., Romer, 1923b; Hutchinson, 2001b). This character would relate in some, perhaps minor, way to the extents and sizes of these muscles.

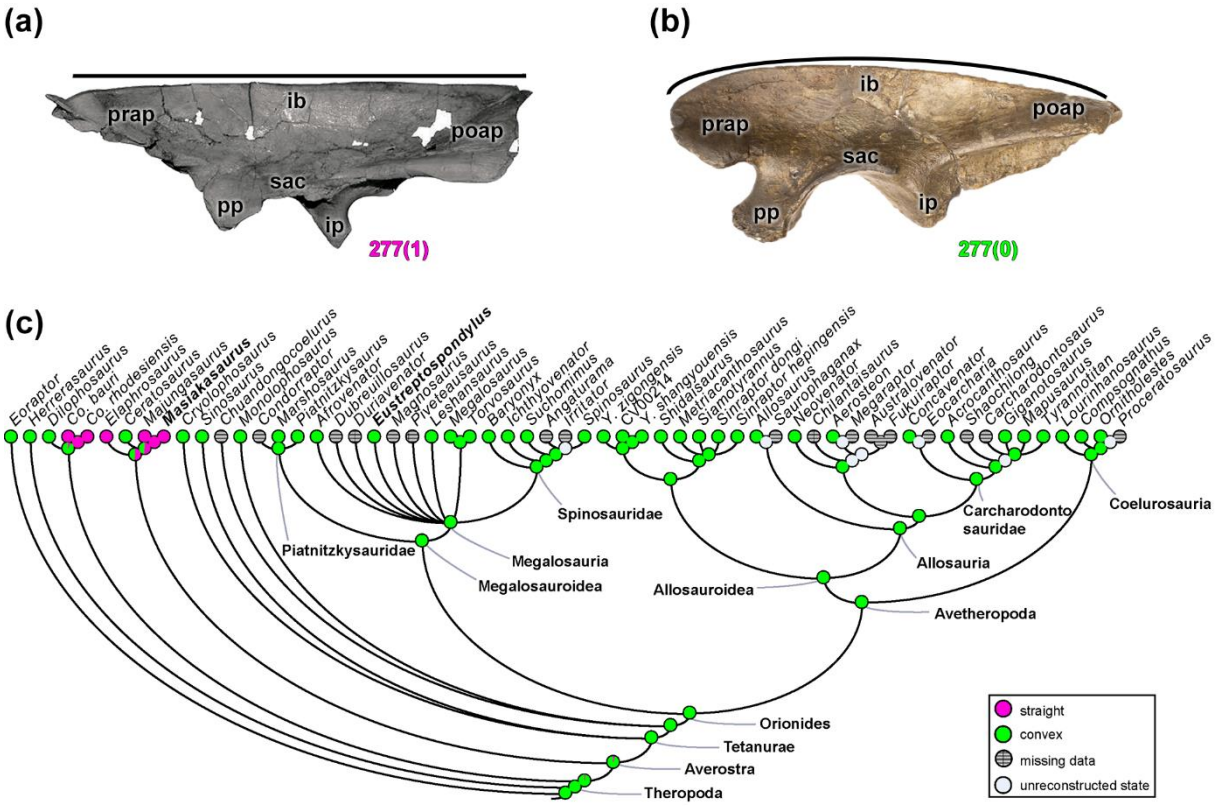

Figure 1.10. Evolutionary history of character 277 (Ilium, shape of dorsal margin) and the ancestral state reconstruction. Illustration of the left ilium in lateral view: (a) *Masiakasaurus* FMNH PR 2485; (b) *Eustreptospondylus* OUMNH J.13558/E01 (mirrored). (c) Phylogenetic tree of Tetanurae showing the reconstruction of ancestral character state for each node. (a) modified from Carrano *et al*. (2011). Not to scale. Abbreviations: ib-iliac blade, ip-ischiadic peduncle, poap-postacetabular process, pp-pubic peduncle, prap-preacetabular process, sac-supraacetabular crest.

The ratio of the width of the postacetabular process of the ilium relative to the ischial peduncle (character 278) may be less than or equal to 1 (278[0]), as per the condition in *Eoraptor* and *Herrerasaurus*. The morphology of remaining neotheropods analysed exhibits a ratio greater than 1 (278[1]) (pl = 98% for the MRCA of neotheropods). The same macroevolutionary pattern pertains to the depth of the postacetabular process (character 279),

being shallow (279[0]) in *Eoraptor* and *Herrerasaurus*, whereas in neotheropods this process is deep (279[1]) (pl = 99% on the MRCA of neotheropods). The derived state would be expected to correlate with expansion of all postacetabular iliac muscle origins (and likely sizes), to some degree; as per below.

One of the major morphological variations observed in the ilium of early theropods is related to the shape of the posterior margin of the postacetabular process (character 280) (Figure 1.11). A convex posterior margin (280[0]) is in several taxa such as *Eoraptor*, *Dilophosaurus*, the megalosauroid *Marshosaurus* and spinosaurids (e.g., *Ichthyovenator*; Figure 1.11A), in addition to avetheropods (except Metriacanthosaurine). A concave posterior margin of the postacetabular process (280[1]) is a synapomorphy of ceratosaurs (e.g., *Masiakasaurus*; Figure 1.11B); homoplastically present in coelophysids. A straight posterior margin (280[2]) exists only in the metriacanthosaurines *Siamotyrannus* (Figure 1.11C) and *Sinraptor*. In contrast, a prominent postacetabular process in the dorsal region, but with the absence of the posteroventral process (280[3]), is evident only in megalosaurids such as *Eustreptospondylus*, *Megalosaurus* (Figure 1.11D), and *Torvosaurus*. However, due to the plesiomorphic state in *Marshosaurus*, the reconstruction for the megalosauroid MRCA indicates a convex posterior margin of the ilium (pl = 98%) (Figure 1.11E). The postacetabular iliac region should have held the origins of the *M. flexor tibialis externus* (FTE) and *M. iliofibularis* (ILFB), as well as part of the posterior delimitation of the IT3 (Romer, 1923b; Carrano, 2000; Hutchinson, 2001b; 2002; Carrano & Hutchinson, 2002); based on this, the FTE, ILFB, and IT3 muscles likely varied in size/position within megalosauroids.

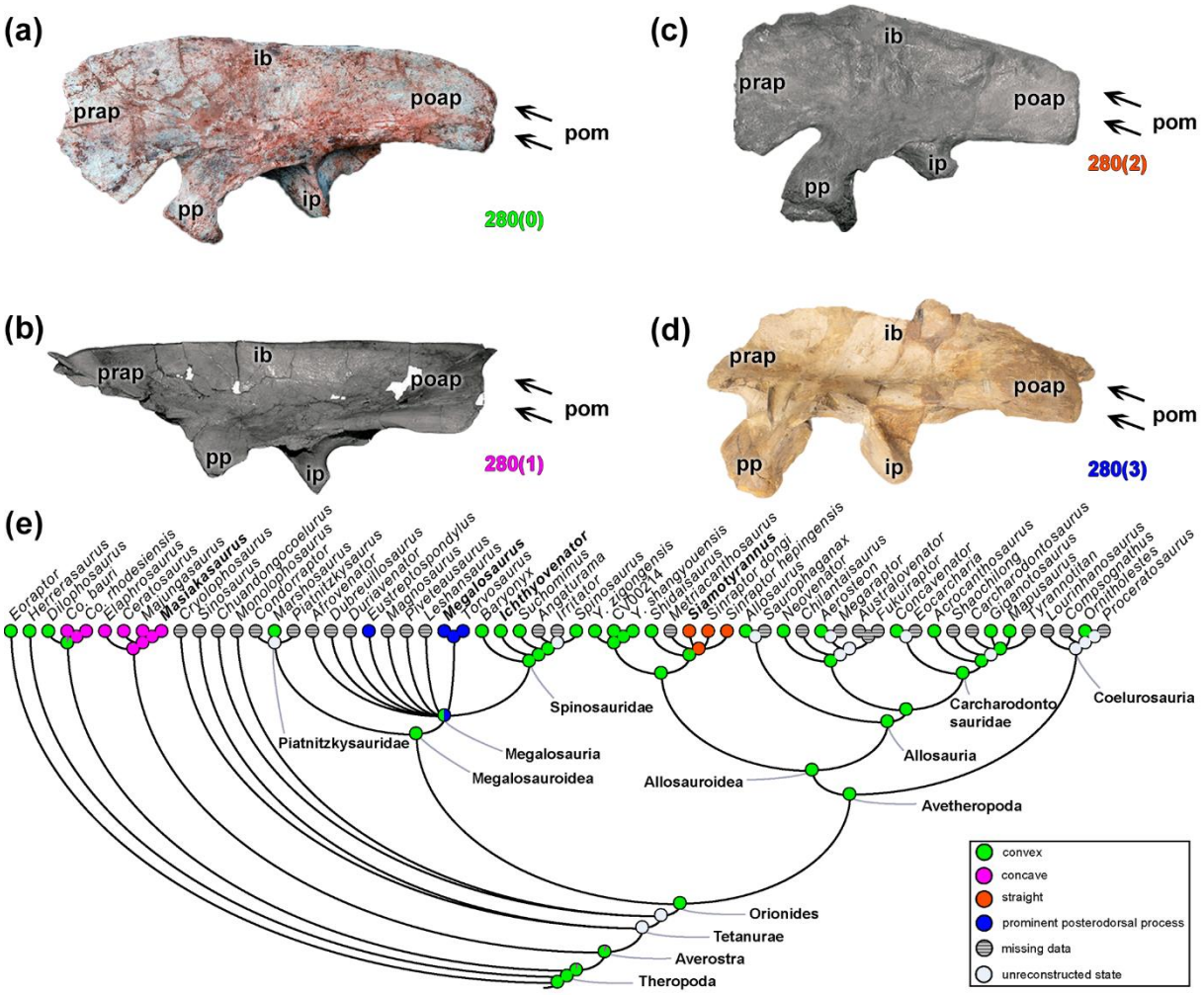

Figure 1.11. Evolutionary history of character 280 (Ilium, shape of posterior margin of postacetabular process) and the ancestral state reconstruction. Illustration of the left ilium in lateral view: (a) *Ichthyovenator* MDS BK 10-09; (b) *Masiakasaurus* FMNH PR 2485; (c) *Siamotyrannus* PW 9-1; (d) *Megalosaurus* OUMNH J.29882 (mirrored). (e) Phylogenetic tree of Tetanurae showing the reconstruction of ancestral character state for each node. (a) modified from Allain *et al*. (2012), (b) modified from Carrano *et al*. (2011), and (c) modified from Carrano *et al*. (2012). Not to scale. Abbreviations: ib-iliac blade, ip-ischiadic peduncle, poap-postacetabular process, pom-posterior margin, pp-pubic peduncle, prap-preacetabular process.

3.2.3. Puboischiadic plate

The morphology and presence/absence of foramina and notches in the puboischiadic plate (see Hutchinson, 2001b), which is the region ventral to the acetabulum (character 281), varies across Theropoda. A medially completely fused plate, with the presence of three foramina (281[0]) is in *Eoraptor*, *Herrerasaurus*, coelophysoids (although it is polymorphic in *Dilophosaurus* ((281[0,1]); see Carrano *et al*., 2012), in the early-diverging ceratosaur *Elaphrosaurus*, and non-Orionides tetanurans, as well as megalosauroids (except *Afrovenator* and *Leshansaurus*). Notably, the tetanuran *Sinosaurus* and *Baryonyx* have intraspecific/intraindividual variations in this character (281[0,1]). A puboischiadic plate

opening medially, with only the obturator foramen of the pubis, which has 1–2 notches (281[1]), is found in the early theropods *Ceratosaurus* and *Masiakasaurus*, as well as in the metriacanthosaurids *Yangchuanosaurus*. This character state also is polymorphic (281[1,2]) in the megalosaurid *Leshansaurus*, the metriacanthosaurid *Yangchuanosaurus* (CV00214) and *Si. hepingensis*, and the carcharodontosaurid *Mapusaurus*. A reinterpretation of this morphological character (e.g., with an ontogenetic perspective, if it indeed varied across ontogeny) could improve coding in taxa where the character is mapped as plesiomorphic (i.e., *Dilophosaurus*, *Sinosaurus*, *Leshansaurus*, *Baryonyx*, and *Mapusaurus*). A puboischiadic plate that is medially open, without any fenestrae, but with 1–2 notches (281[2]), is present, in addition to the aforementioned taxa, in *Afrovenator* and other avetheropods; with the exceptions noted above. Even with some variations and derived states within megalosauroids, the most parsimonious MRCA reconstruction indicates a fully closed puboischiadic plate. The puboischiadic plate region in early theropods, such as *Staurikosaurus* (Grillo & Azevedo, 2001) and *Coelophysis* (Bishop *et al*., 2021) should have provided an origin for the *M. puboischiofemoralis externus 3* (PIFE3), that plesiomorphically extended anteriorly from the ischium, ventral to the acetabulum. In contrast, for example, in the carcharodontosaurid *Acrocanthosaurus* (Bates *et al*., 2012) and in later coelurosaurs (Carrano & Hutchinson, 2002), the origin of the PIFE3 muscle seems to have been more restricted, posterior to the puboischiadic plate. In some maniraptoran taxa, the origin is positioned further ventrally on the ischium (Rhodes *et al*., 2021). These changes correlate with what may be reduction of this muscle's size (if the origin is indicative of that; e.g., Cuff *et al*., 2023) but later shifting of the origin to the medial puboischiadic membrane on the lineage to Aves (and perhaps re-expansion of the muscle).

3.2.4. Pubis

Among the analysed characters, ten of them relate to the pubis (14.7%). In Crocodylia, Aves and non-avian theropods, the pubis is the origin of *M. ambiens* (AMB) of the dorsal group, as well as PIFE1 and PIFE2 of the ventral group (Romer, 1923a,b; Hutchinson, 2002; Carrano & Hutchinson, 2002; Grillo & Azevedo, 2011; Bishop *et al*., 2021).

Generally in theropods, the orientation of the main axis of the pubis (character 282) presents a conservative morphological condition: a straight-shafted pubis (282[0]), in almost all analysed species including early theropods (e.g., *Suchomimus*; Figure 1.12A). There are a few exceptions where the pubic orientation is ventrally concave (282[1]), a trait that evolved independently in *Co. bauri*, *Masiakasaurus* (Figure 1.12B), and the megalosauroid

Marshosaurus. An autapomorphic feature is notable in *Spinosaurus*, which has a dorsally concave shaft of the pubis (282[2]) (Figure 1.12C). Even with derived states in *Marshosaurus* and *Spinosaurus*, the MRCA reconstruction of megalosauroids indicates a straight-shafted pubis (pl = 99%) (Figure 1.12D). It is conceivable that different orientations of the pubic shaft might have altered the PIFE1 and PIFE2 muscles' moment arms (Allen *et al*., 2021).

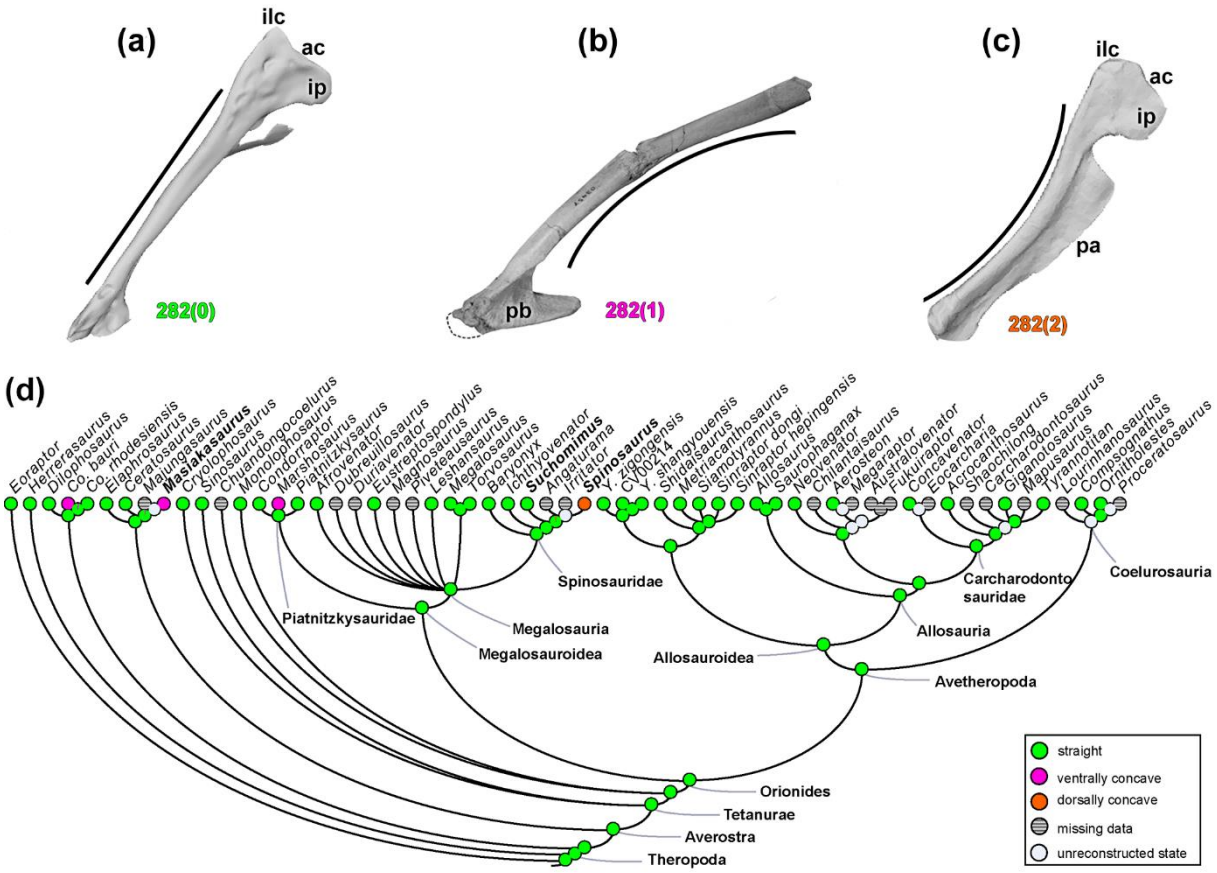

Figure 1.12. Evolutionary history of character 282 (Pubis, shaft orientation) and the ancestral state reconstruction. Illustration of the left pubis in lateral view: (a) *Suchomimus* MNBH GAD500; (b) *Masiakasaurus* FMNH PR 2470; (c) *Spinosaurus* FSAC-KK 11888. (d) Phylogenetic tree of Tetanurae showing the reconstruction of ancestral character state for each node. (a) and (c) based on the 3D digital model provided by Sereno *et al*. (2022) and (b) modified from Carrano *et al*. (2011). Not to scale. Abbreviations: ac-acetabulum, ilc-iliac contact, ip-ischiadic peduncle, pa-pubic apron, pb-pubic boot.

The pubic apical articulation (character 283) can be unfused in adult individuals (283[0]), as in early theropods (except ceratosaurs) and early tetanurans including megalosauroids (except *Afrovenator*), whereas in avetheropods only *Si. hepingensis* has this state. A fused apical articulation (283[1]) is evident in ceratosaurs, the megalosaurid *Afrovenator*, and allosauroids. Despite the apomorphic feature in *Afrovenator*, the state in the MRCA of megalosauroids has the unfused condition (pl = 95%).

The distal pubis (character 284); proximal to any fusion or distalmost contact; may have a gap between the right and left pubes (284[0]), as noted in non-averostran theropods; or have them in contact (284[1]), as unambiguously seen in *Ceratosaurus*. However, this is a polymorphic character (possibly with ontogenetic variation) in the ceratosaur *Elaphrosaurus*, in the tetanuran *Monolophosaurus*, in the megalosauroids *Megalosaurus*, *Torvosaurus*, and *Suchomimus*, as well as in the avetheropods *Shidaisaurus*, *Y. zigongensis*, and *Saurophaganax*. Even with the aforementioned variations, the predominant condition in theropods is with pubes contacting distally, but this contact forms a proximal-distal "gap" called the interpubic fenestra (284[2]) in most of the averostran species. An interpubic fenestra is predominant in *Marshosaurus*, *Piatnitzkysaurus*, *Afrovenator*, *Baryonyx*, *Ichthyovenator*, and *Spinosaurus*; and is the most parsimonious condition reconstructed for the MRCA of megalosauroids.

The distal pubis is well-known to present a structure called the pubic "boot" (i.e., posterior projection of the distal portion of the bone; e.g., Hutchinson, 2001b). The angle between the main axis of the pubis and the pubic boot (character 285) can vary between 75° and 90° (285[0]), as in most theropod species. The one exception, where the angle is less than 60° (285[1]), represents a synapomorphy of metriacanthosaurine allosauroids (Carrano *et al*., 2012). However, the state of this character is poorly characterised in early theropods such as coelophysoids and megalosauroids. The morphology of the pubic symphysis (character 286) independently observed in the early theropod *Herrerasaurus* and spinosaurids (except *Baryonyx*) represents a marginal structure (286[0]); however, all other analysed theropods have a wider pubic symphysis (286[1]); which is also the reconstructed state in the MRCA of megalosauroids (pl = 99%). As with other characters related to pelvic fusion, characters 283-285 might relate to increased rigidity or strength of the pelvis, and the boot may have provided stronger resistance to supporting body weight during sitting (as well as abdominal muscle insertions and inspiratory flow; see Carrier & Farmer, 2000).

A pubic obturator foramen (character 287) as a small subcircular structure (287[0]) is present in almost all non-avetheropods, however, the predominant condition in avetheropods is the presence of a large, oval foramen (287[1]), including also the non-avetheropod megalosauroids *Ichthyovenator* and *Suchomimus*. It is unclear what these ventral pelvic foramina might indicate in terms of soft tissues in early theropods, but the general trend across Theropoda is the appearance of these foramina and then their expansion, breaking up the formerly united puboischiadic plate (e.g., Hutchinson, 2001b). This reduction of the ventral pelvic surface area likely related to reduced muscle sizes (e.g., PIFE3) or even losses of muscles (e.g., parts of the flexor cruris ventral group).

An expansion of the anterodistal-most part of the pubis (character 288) may be absent (288[0]), as in non-allosaur theropods. Contrastingly, this expansion is present in the allosaur clade (288[1]). The maximum length of the pubic boot in relation to the length of the shaft (character 289) can be less than 30% (289[0]), as in non-avetheropod theropods (e.g., *Piatnitzkysaurus*; Figure 1.13A) and metriacanthosaurids (except *Si*. *hepingensis*); or greater than 30% (289[1]) in the metriacanthosaurid *Si*. *hepingensis,* the allosaurid *Allosaurus* (Figure 1.13B), and the coelurosaur *Compsognathus*. A pubis expansion greater than 60% (289[2]) is present in carcharodontosaurs (e.g., *Aerosteon*; Figure 1.13C).

The shape of the pubic boot from a ventral view (character 290) may be triangular (290[0]), as in most theropods analysed, except in *Herrerasaurus* and late coelurosaur *Compsognathus*, whose pubic boot is narrow with subparallel margins (290[1]). It would be interesting to ascertain if the size of this structure relates to increases of body sizes in tetanuran theropods, in light of its potential role in static weight-bearing.

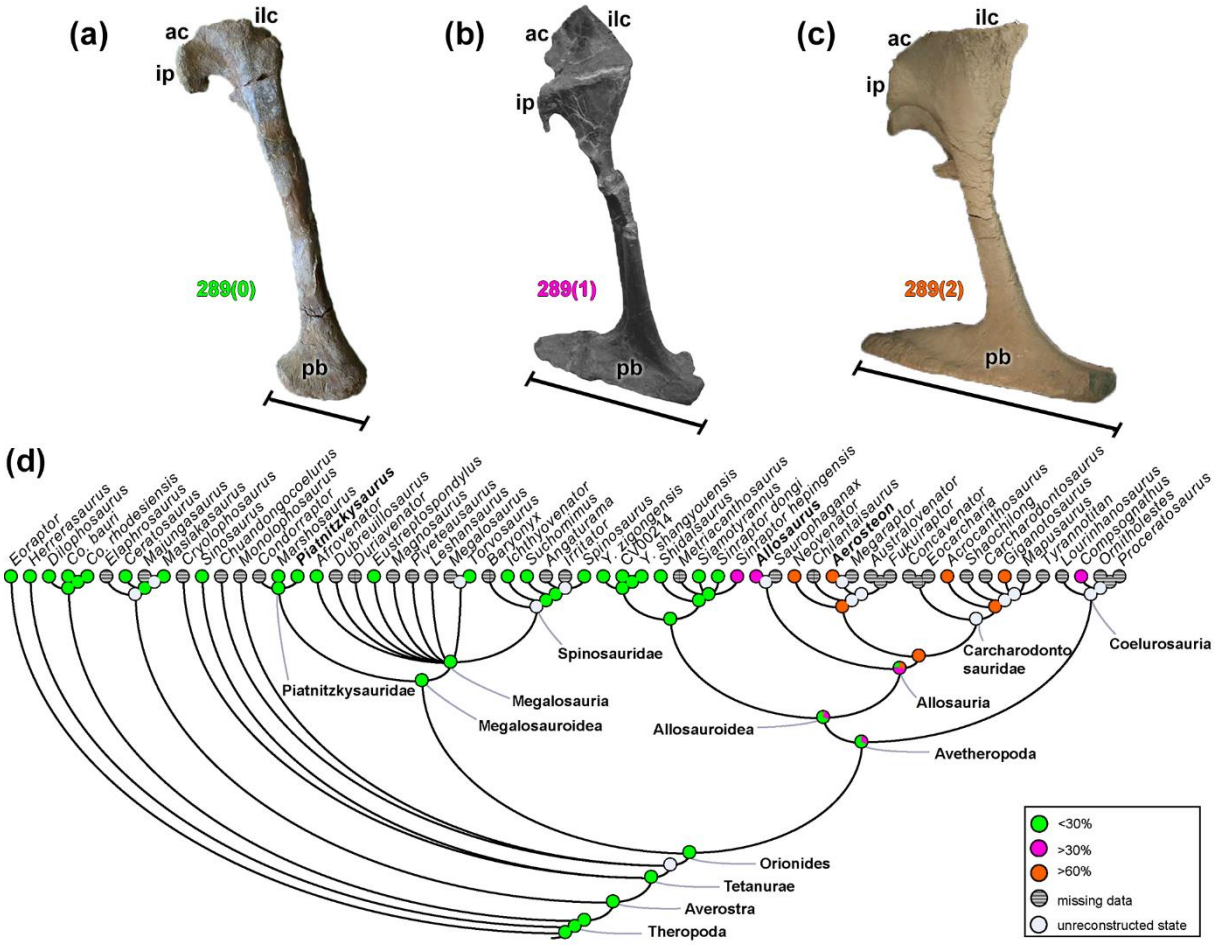

Figure 1.13. Evolutionary history of character 289 (Pubis, boot length relative to shaft length) and the ancestral state reconstruction. Illustration of the left pubis in lateral view: (a) *Piatnitzkysaurus* PVL 4073; (b) *Allosaurus* MNHNUL/AND.001/007; (c) *Aerosteon* MCNA-PV-3137 (cast; mirrored). (d) Phylogenetic tree of Tetanurae showing the reconstruction of ancestral character state for each node. (b) modified from Malafaia *et al*. (2007) and (c) modified from Sereno *et al*. (2008). Not to scale. Abbreviations: ac-acetabulum, ilc-iliac contact, ip-ischiadic peduncle, pb-pubic boot.

The shape of the iliopubic articulation (character 291) largely is conserved in theropods, being planoconcave (291[0]) in all non-ceratosaur theropods analysed. Yet the ceratosaurs *Ceratosaurus*, *Majungasaurus*, and *Masiakasaurus* have an iliopubic articulation in a ball and socket form (291[1]).

3.2.5. Ischium

The taxon-character matrix analysed here involves nine morphological characters (13.2%) related to the ischium. In the ischium of Crocodylia and non-avian theropods, some ventral hindlimb muscle groups originate(d) here, such as *M. flexor tibialis internus 1,3* (FTI1 and FTI3), in addition to the PIFE3 muscle and *M. adductor femoris* (ADD1 and ADD2) (e.g., Romer, 1923a,b; Hutchinson & Gatesy, 2000; Hutchinson, 2002; Carrano & Hutchinson, 2002).

A ratio of the length of the ischium to the pubis (character 292) between 75–80% (292[0]), independently evolved in *Eoraptor*, *Herrerasaurus*, *Co. bauri*, *Masiakasaurus*, *Monolophosaurus*, and megalosauroids (except *Torvosaurus* and *Spinosaurus*). A smaller ratio, ≤70% (292[1]), is shared between the coelophysoids *Dilophosaurus*, *Co. rhodesiensis*, *Ceratosaurus* (though polymorphic), and coelurosaurs *Ornitholestes* and *Compsognathus*. Ischia with a larger ratio, >80% (292[2]), exist in *Sinosaurus*, *Torvosaurus*, *Spinosaurus*, and allosauroids (except *Neovenator*). The most parsimonious reconstruction for the MRCA of megalosauroids suggests an ischium length relative to pubis length between 75–80% (state 0). The derived state's ratio seems to be achieved by a lengthening of the pubis; perhaps with the contribution of the enlargement of the pubic boot.

The orientation of the main axis of the ischium (character 293) is straight (293[0]) in *Eoraptor* and several analysed theropods (e.g., *Ichthyovenator*; Figure 1.14A). A ventrally curved main ischial axis (293[1]) evolved repeatedly in some theropod clades such as coelophysids, the megalosaurids *Afrovenator*, *Eustreptospondylus*, *Megalosaurus* (Figure 1.14B), metriacanthosaurine allosauroids, and *Compsognathus*. Although the megalosauroid MRCA probably had a straight ischium (pl = 93%), at least three aforementioned megalosaurids had the derived condition (i.e., ventrally curved ischial shaft) (Figure 1.14C). These shape differences would at least slightly alter the moment arms of muscles with ischial origins (e.g., Allen *et al*., 2021).

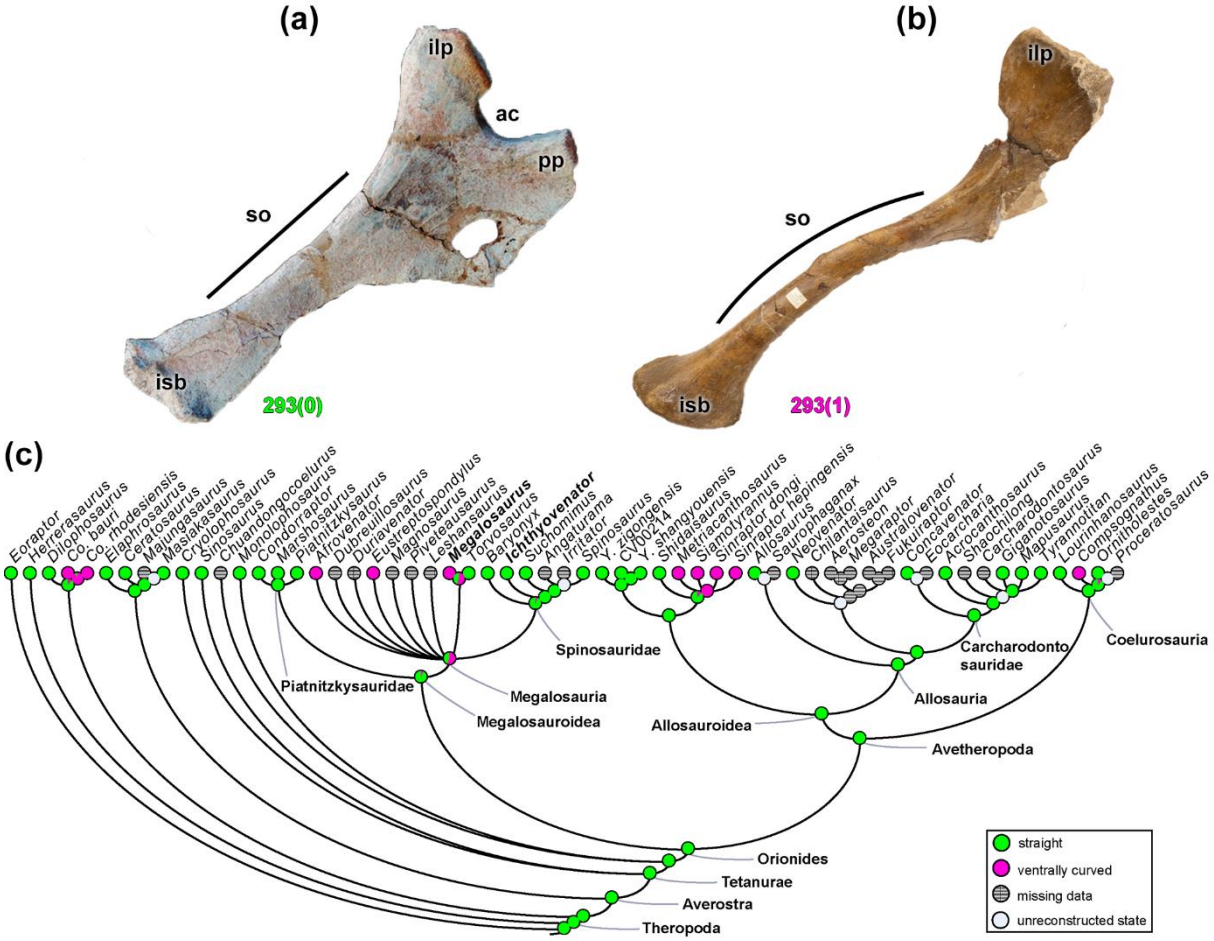

Figure 1.14. Evolutionary history of character 293 (Ischium, shaft orientation) and the ancestral state reconstruction. Illustration of the left ischium in lateral view: (a) *Ichthyovenator* MDS BK 10-13; (b) *Megalosaurus* OUMNH J.13565 (mirrored). (c) Phylogenetic tree of Tetanurae showing the reconstruction of ancestral character state for each node. (a) modified from Allain *et al*. (2012). Not to scale. Abbreviations: ac-acetabulum, ilp-iliac peduncle, isb-ischial boot, pp-pubic peduncle, so-shaft orientation.

The ilioischiadic articulation (character 294) has two forms in theropods: a concave plane (294[0]), present in most clades, the exceptions being *Co. rhodesiensis*, *Majungasaurus*, and *Masiakasaurus*, *Ichthyovenator*, and Carcharodontosauridae, which have a ball and socket articulation (294[1]). Although the spinosaurid *Ichthyovenator* presents the apomorphic condition, the MRCA of megalosauroids had a plano-concave articulation (pl = 99%).

The ischial antitrochanter (character 295) is a large, notch-shaped structure (295[0]) in non-tetanuran theropods and in *Ichthyovenator*. In all other taxa, the ischial antitrochanter is reduced (295[1]), which likely was the state in the MRCA of Megalosauroidea (pl = 99%). The functional significance of various acetabular "antitrochanter" structures around the ilium and ischium remains unclear, but is thought to relate to differences in hip joint function, and deserves deeper investigation (see Hutchinson & Allen, 2009).

A notch (character 296) ventral to the ischial obturator process may be absent (296[0]), as in many theropods including *Herrerasaurus* and some tetanurans (e.g., *Ichthyovenator*;

Figure 1.15A). This notch is present (296[1]) in *Dilophosaurus* and *Ceratosaurus*, and unites Tetanurae (pl = 79%) (e.g., *Condorraptor*; Figure 1.15B). Three megalosauroids (*Eustreptospondylus*, *Torvosaurus*, and *Ichthyovenator* [Figure 1.15A]) have a reversal of this character, but the MRCA of megalosauroids probably had the apomorphic state (296[1]; pl = 66%) (Figure 1.15C). The PIFE3 and ADD1 muscle origins associated with this ischial region (e.g., Romer, 1923a; Carrano & Hutchinson, 2002; Hutchinson, 2002; Grillo & Azevedo, 2011) may be reduced in size in taxa with the derived state.

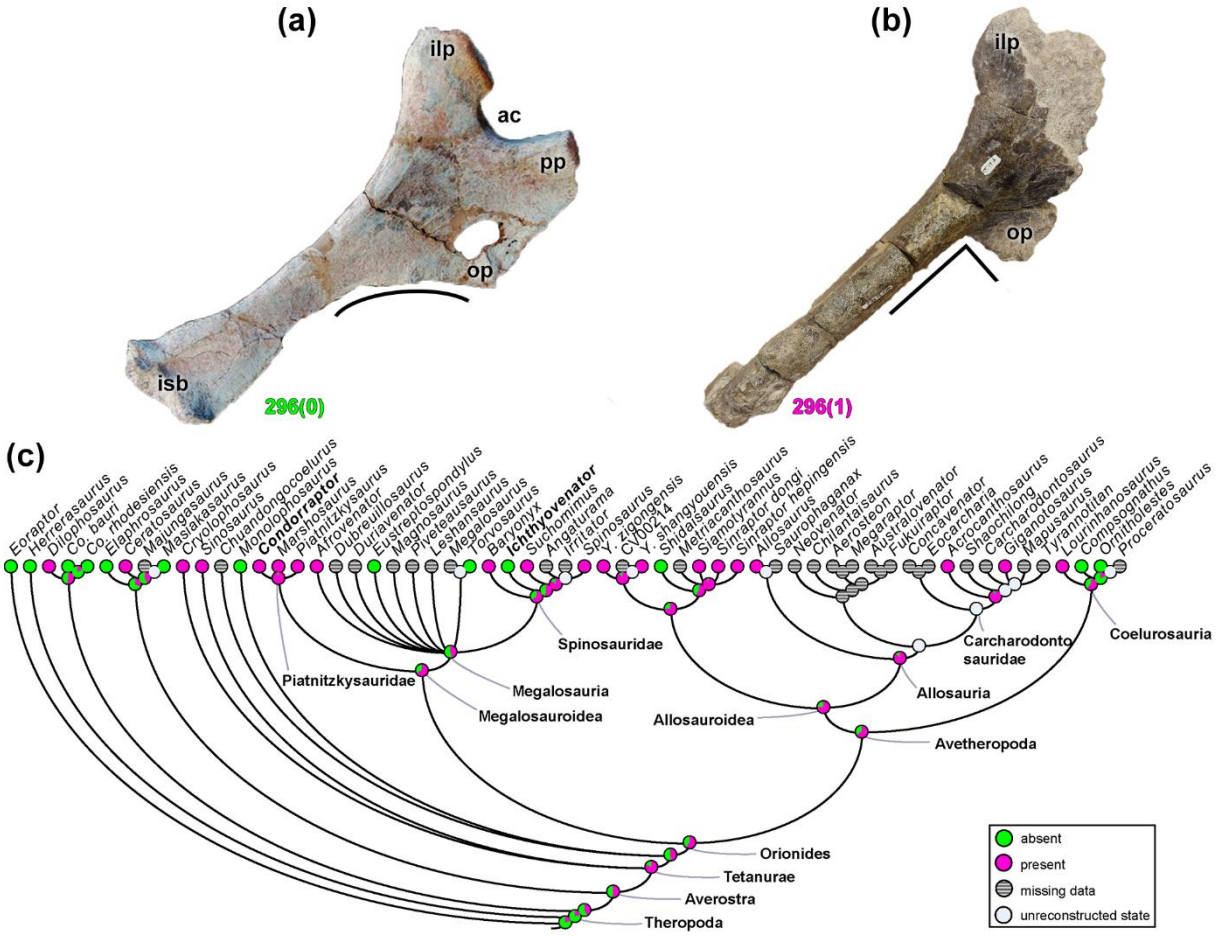

Figure 1.15. Evolutionary history of character 296 (Ischium, notch ventral to obturator process) and the ancestral state reconstruction. Illustration of the left ischium in lateral view: (a) *Ichthyovenator* MDS BK 10-13; (b) *Condorraptor* MPEF-PV 1689 (mirrored). (c) Phylogenetic tree of Tetanurae showing the reconstruction of ancestral character state for each node. (a) modified from Allain *et al.* (2012). Not to scale. Abbreviations: ac-acetabulum, ilp-iliac peduncle, isb-ischial boot, pp-pubic peduncle, op-obturator process.

An unexpanded ischial symphysis (297[0]) exists several theropod clades as in *Eoraptor*, coelophysids, ceratosaurs (except *Masiakasaurus*), early tetanurans, megalosauroids (except *Marshosaurus*, megalosaurids, and *Ichthyovenator*), as well as allosaurs. An ischial symphysis expanded as an apron (297[1]) appeared independently in *Masiakasaurus* and the allosaur clade. Additionally, the state is variable in megalosauroids because *Marshosaurus*,

megalosaurids, and *Ichthyovenator* have the derived condition (i.e., expanded ischial symphysis). An unexpanded ischial symphysis is a plausible condition for the megalosauroid MRCA (pl = 72%); however, the MRCA of spinosaurids have an ambiguous reconstruction (pl = ~50% for each state). An apron-like expansion could correlate with enlarged muscle origins such as for ADD1 and PIFE3.

The cross-sectional shape of the middle axes of the articulated ischia (character 298) commonly is oval (298[0]) in theropods. In some clades such as coelophysids and metriacanthosaurids, however, the cross-section is heart-shaped, with the medial portions protruding posteriorly (298[1]).

The distal portion of the ischium (character 299) has a rounded tip (299[0]) in most of the analysed theropods (e.g., *Megalosaurus*; Figure 1.16A). An ischium with a triangularly expanded distal end (299[1]) is observed in ceratosaurs (e.g., *Elaphrosaurus*; Figure 1.16B), *Cryolophosaurus*, and *Sinosaurus*, *Yangchuanosaurus*, *Si. hepingensis*, *Neovenator*, and *Concavenator*. Ischia with rounded ends are probable for the MRCA of Neotheropoda (pl = 85%); however, the averostran MRCA seemingly was triangular (pl = 81%). Finally, the Megalosauroidea MRCA had the plesiomorphic condition (pl = 95%) that remained conservative within the clade (Figure 1.16C). As with the pubic boot (see above), this expansion must relate in some obscure way to static weight support as well as abdominal/caudal muscle attachments.

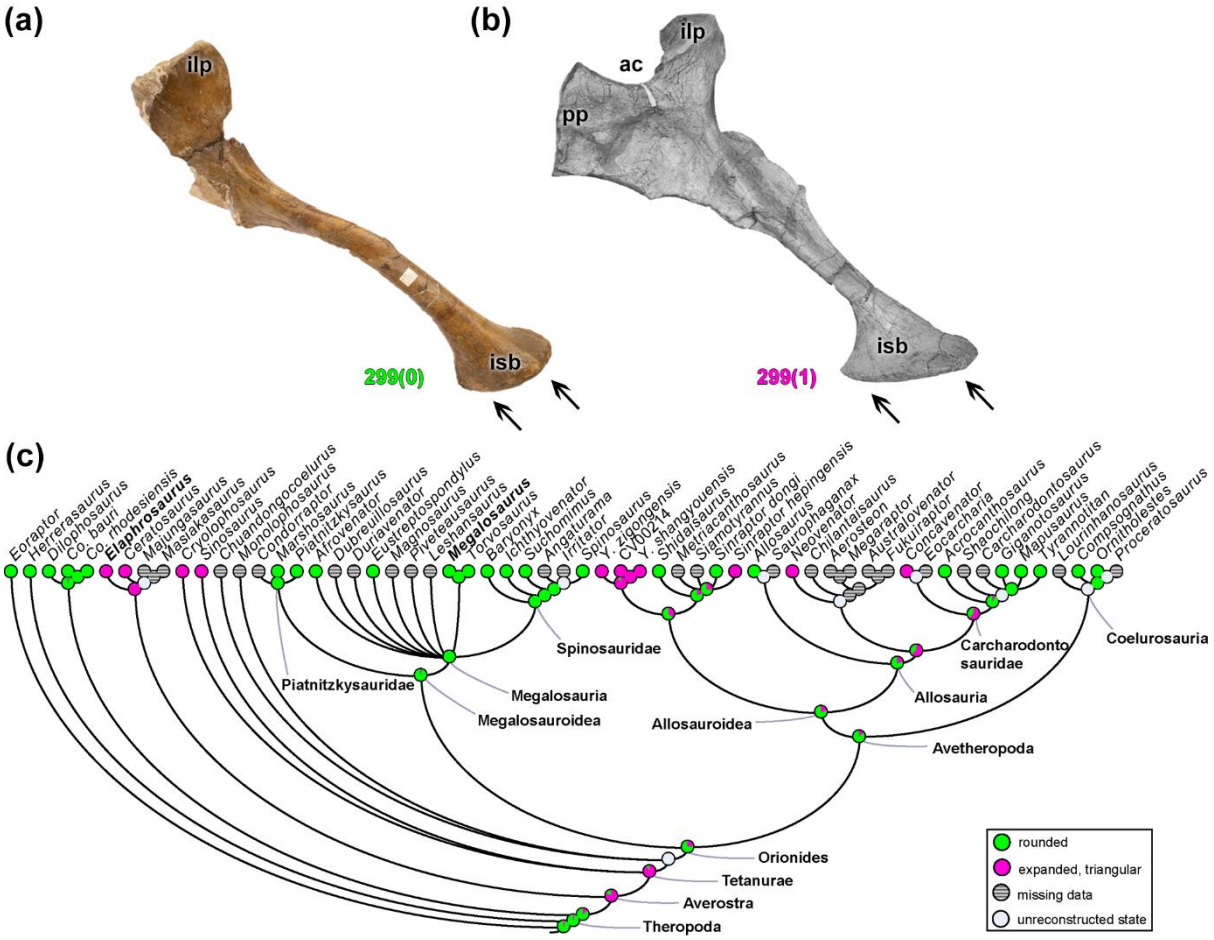

Figure 1.16. Evolutionary history of character 299 (Ischium, morphology of distal end) and the ancestral state reconstruction. Illustration of the left ischium in lateral view: (a) *Megalosaurus* OUMNH J.13565; (b) *Elaphrosaurus* MB R 4960. (c) Phylogenetic tree of Tetanurae showing the reconstruction of ancestral character state for each node. (b) modified from Rauhut & Carrano (2016). Not to scale. Abbreviations: ac-acetabulum, ilp-iliac peduncle, isb-ischial boot, pp-pubic peduncle.

The distalmost ischia (character 300), may remain unfused in adult individuals (300[0]) as in most theropods. Distal ischial fusion in adults (300[1]) occurs in *Dilophosaurus*, ceratosaurs, early tetanurans and *Sinosaurus*, in metriacanthosaurids (except *Si. hepingensis*), and *Neovenator*. Again, this fusion-related trait might vary ontogenetically.

3.2.6. Stylopodium (femur)

Sixteen morphological characters (23.5%) in this study relate to the femur. Several of the muscles that originate from the pelvic girdle and (post cervical) vertebrae insert on the femur. In Crocodylia and non-avian theropods (as well as Aves), the proximal region of the femur is the insertion site of the PIFI1-2, PIFE1-3, ITC, and *iliofemoralis externus* (IFE) muscles or their homologs (Romer, 1923a,b,c; Rowe, 1986; Hutchinson, 2001a; Carrano & Hutchinson, 2002;

Hutchinson, 2002; Grillo & Azevedo, 2011; Bishop *et al*., 2021). A large portion of the posterior diaphysis of the femur has the *Mm. caudofemorales* (CFB and CFL) attached and, distally, the *Mm. adductores femores 1* and *2* (ADD1 and ADD2). However, the femoral diaphysis also predominantly is/was the area of origin of some dorsal *Triceps femoris* group muscles. Furthermore, the metaphyseal region is the origin for several lower limb muscles (e.g., *M. gastrocnemius externus*/*lateralis* (GE); *M. flexor halluces longus* (FHL); *M. extensor digitorum longus* (EDL)) that ultimately inserted onto the tarsals, metatarsus or phalanges and unguals (Carrano & Hutchinson, 2002; Hutchinson, 2002; Bishop *et al*., 2021; Hattori & Tsuihiji, 2021).

The femoral head's orientation varies in two ways, more anteriorly and medially versus more dorsoventrally and medially, so it is scored as two characters. The femoral head is oriented (character 301) 45° anteromedially (301[0]) in most early theropods including coelophysoids (e.g., *Co. bauri*; Figure 1.17A) and ceratosaurs. An intermediate condition, which varies between 10° and 30° anteromedially (301[1]), is the morphological feature in megalosauroids (e.g., *Eustreptospondylus*; Figure 1.17B), metriacanthosaurids, and the coelurosaur *Lourinhanosaurus*. A medially oriented femoral head (301[2]) is a synapomorphy of allosauroids (e.g., *Allosaurus*; Figure 1.17C), and independently evolved in *Compsognathus* and *Ornitholestes*. Notably, two states (301[0,1]) exist in the megalosaurid *Leshansaurus* and in *Allosaurus* (301[1,2]). An intermediate condition (i.e., femoral head orientation between 10–30°) is the most parsimonious state for the megalosauroid MRCA (Figure 1.17D). A more medially oriented femoral head should have contributed to a more parasagittal gait and support (e.g., Carrano, 2000; Hutchinson & Gatesy, 2000; Egawa *et al*., 2022; Pintore *et al*., 2022).

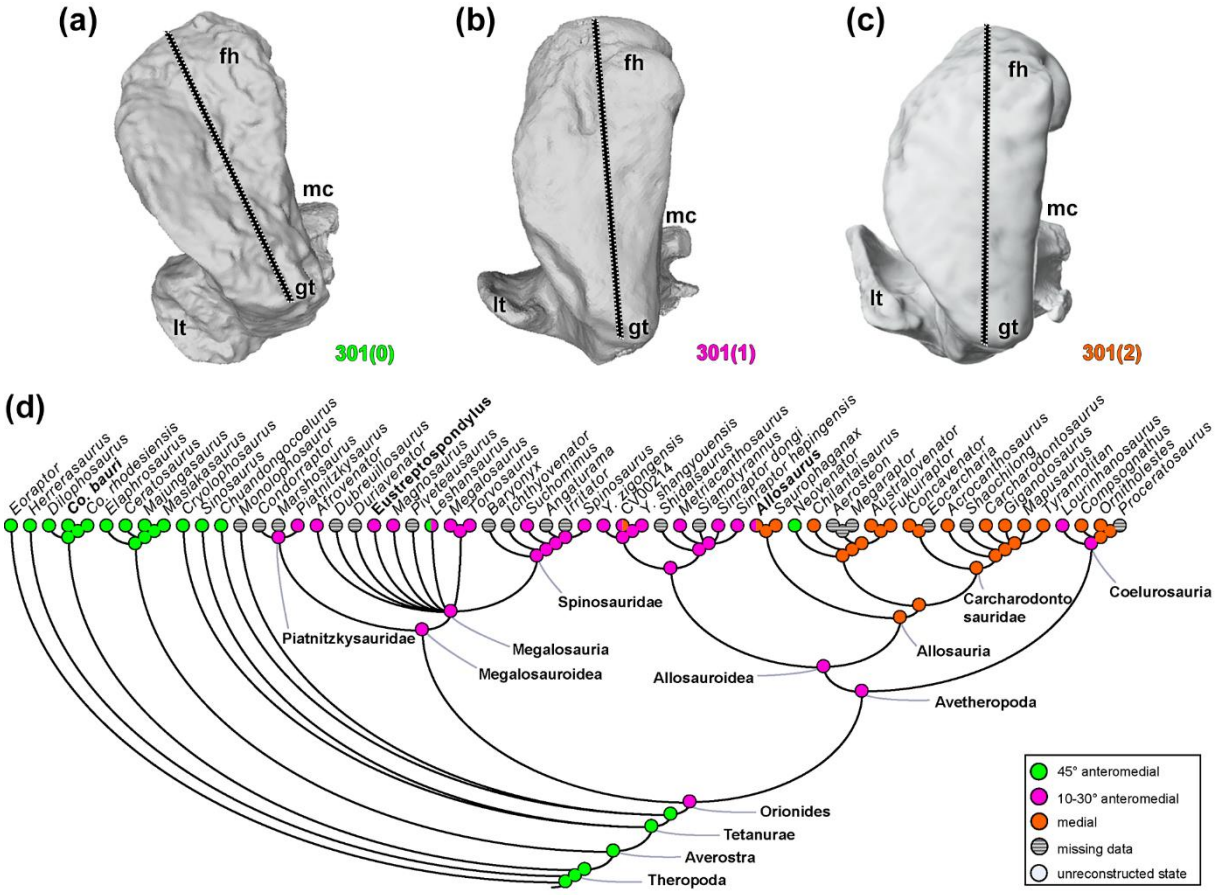

Figure 1.17. Evolutionary history of character 301 (Femur, head orientation) and the ancestral state reconstruction. Illustration of the left femur in proximal view: (a) *Coelophysis* UCMP 129618 (mirrored); (b) *Eustreptospondylus* OUMNH J.13558/F02; (c) *Allosaurus* UMNH VP 7892. (d) Phylogenetic tree of Tetanurae showing the reconstruction of ancestral character state for each node. (a) Based on the 3D model provided by University of California Museum of Paleontology (MorphoSource; UCMP:V:129618) and (c) based on the 3D digital model provided by Natural History Museum of Utah (MorphoSource; UMNHVP:7892; ark:/87602/m4/509051). Not to scale. Abbreviations: fh-femoral head, gt-greater trochanter, lt-lesser trochanter, mc-medial condyle.

The orientation of the femoral head (character 302) is ventromedial (302[0]), again in most early theropods (e.g., *Ceratosaurus*; Figure 1.18A). As a transitional state, however, the head of the femur is horizontal (medial) (302[1]) in megalosauroids (e.g., *Eustreptospondylus*; Figure 1.18B), metriacanthosaurids, allosaurids, in the neovenatorid *Fukuiraptor*, and coelurosaurs; a feature evolved in the MRCA of Orionides (pl = 97%). A dorsomedially inclined femoral head (302[2]) is a feature widespread in carcharodontosaurs (e.g., *Giganotosaurus*; Figure 1.18C), except *Fukuiraptor*. These differences in orientation should have implications for biomechanical loading of the proximal femur (e.g., Bates *et al*., 2012; Bishop *et al*., 2018).

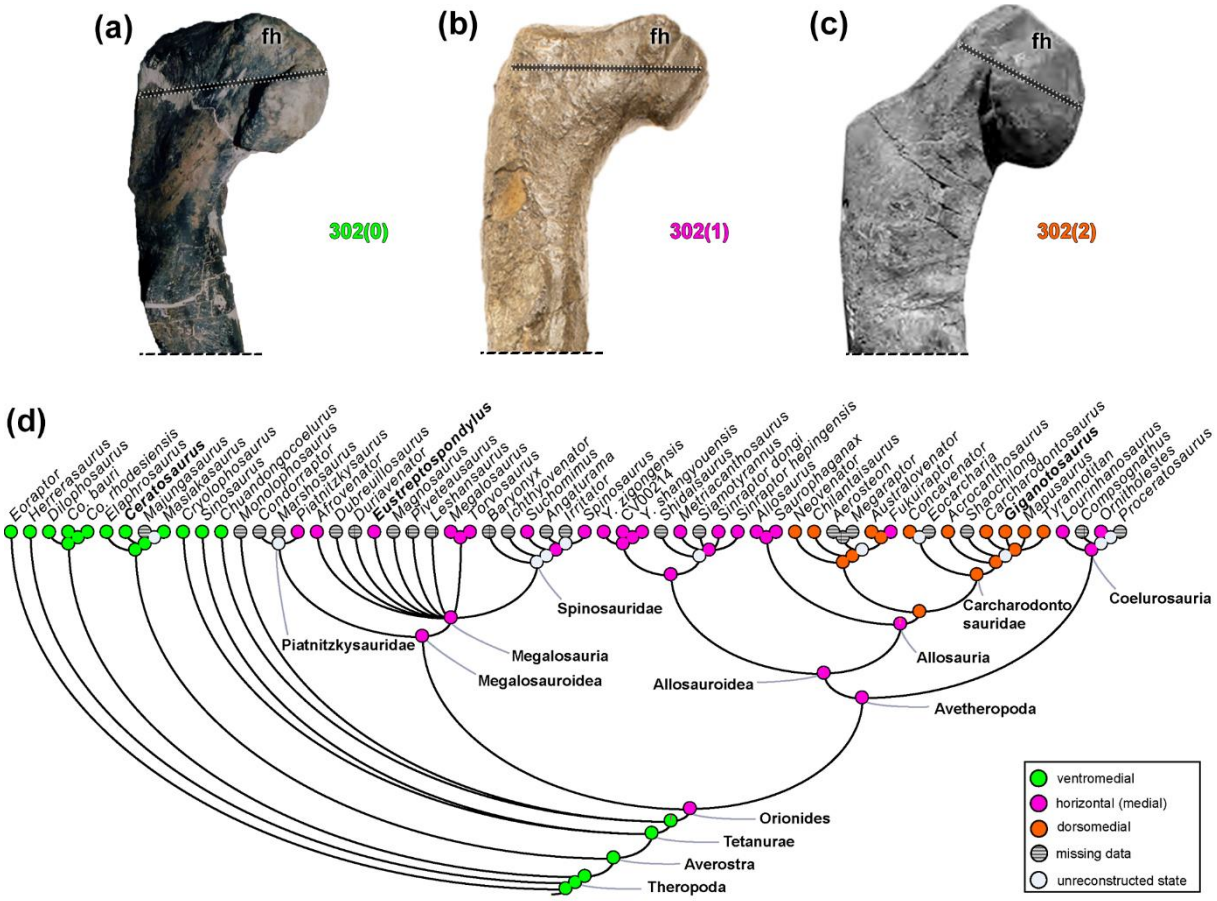

Figure 1.18. Evolutionary history of character 302 (Femur, head angle) and the ancestral state reconstruction. Illustration of the left femur in posterior view: (a) *Ceratosaurus* UMNH 5278; (b) *Eustreptospondylus* OUMNH J.13558/F02; (c) *Giganotosaurus* MUCPv-Ch 1 (mirrored). (d) Phylogenetic tree of Tetanurae showing the reconstruction of ancestral character state for each node. (c) modified from Cuesta *et al*. (2018). Not to scale. Abbreviation: fh-femoral head.

An articular groove (or fovea capitis, e.g., Novas, 1996; Tsai *et al*., 2018) that is oriented obliquely along the main axis of the femoral head's proximal surface (character 303) may be absent (303[0]) in theropods as in *Eoraptor* and all analysed avetheropods; or present (303[1]) as in many early theropods including megalosauroids. The groove of the oblique ligament on the surface of the posterior portion of the femoral head (character 304) is shallow, with its bordering lip not projecting beyond the posterior surface of the femoral head (304[0]) only in megalosauroids, specifically the *Afrovenator*, *Megalosaurus*, *Torvosaurus*, and *Spinosaurus*. Although this character is unknown in *Eoraptor* and *Herrerasaurus*, all neotheropods (MRCA pl = 99%) studied have a deep groove of the oblique ligament (considered as derived feature [31]), with medial delimitation by the posterior lip of the well-developed groove (304[1]). Although the aforementioned megalosauroids have a shallow groove, the MRCA is reconstructed with the derived condition (state 1; pl = 98%), suggesting a reversion within this clade.

The position of the lesser trochanter (also called anterior trochanter) in relation to the femoral head (character 305) does not reach the ventral/distal margin (305[0]), as in early theropods (except *Co. rhodesiensis* and *Sinosaurus*), and the metriacanthosaurid *Yangchuanosaurus* (*Y. shangyouensis* + CV00214) (also *Dilophosaurus*; Figure 1.19A). In most studied theropods of the Orionides clade, however, the lesser trochanter projects proximal to the ventral margin of the femoral head (305[1]), including megalosauroids (e.g., *Eustreptospondylus*; Figure 1.19B) and averostrans. The carcharodontosaurs *Australovenator* (Figure 1.19C) and *Fukuiraptor*, and the coelurosaur *Ornitholestes*, on the other hand, have a lesser trochanter reaching the proximal surface of the femoral head (305[2]). Although a more distally restricted lesser trochanter relative to the femoral head is widely seen in early theropods, a lesser trochanter projecting beyond the ventral margin of the femoral head is the plausible condition for the MRCA of Orionides (pl = 94%) (Figure 1.19D).

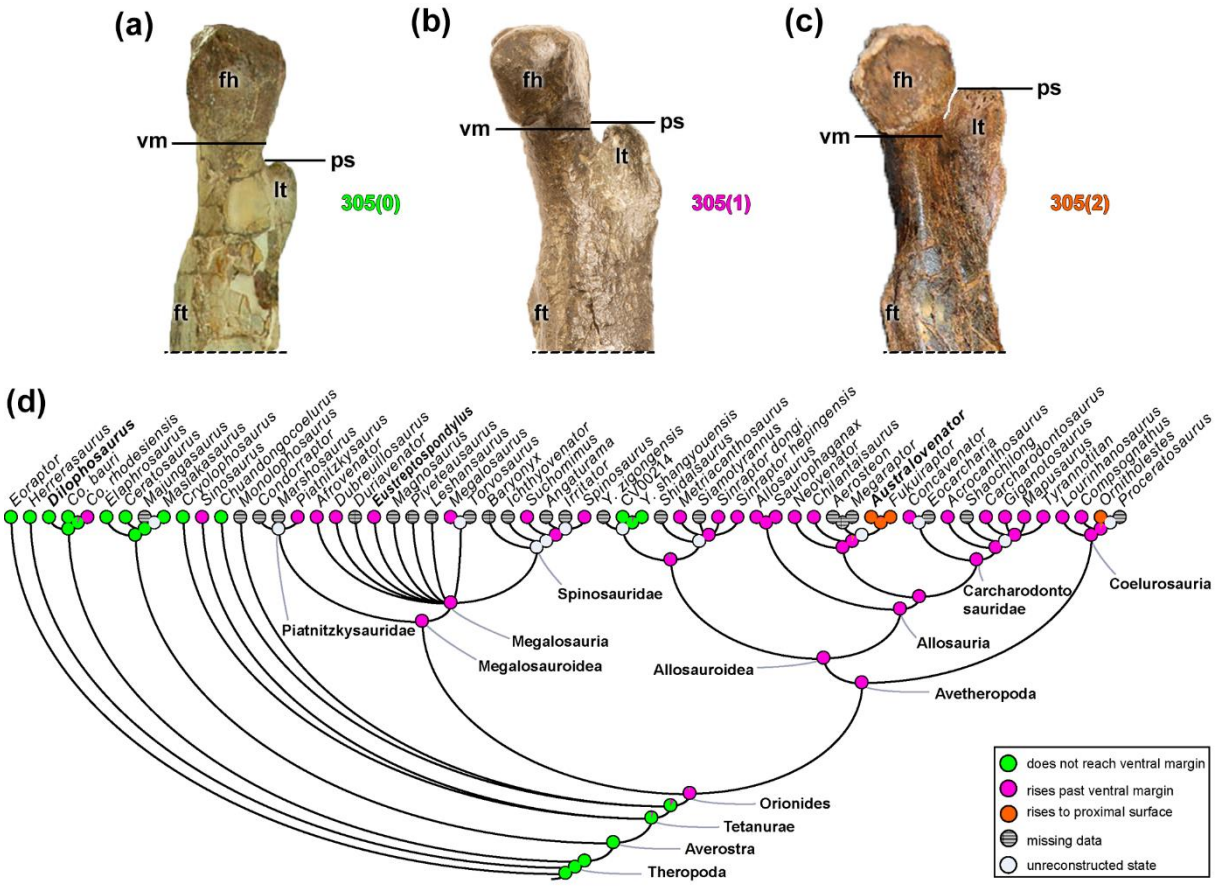

Figure 1.19. Evolutionary history of character 305 (Femur, placement of lesser trochanter relative to femoral head) and the ancestral state reconstruction. Illustration of the left femur in medial view: (a) *Dilophosaurus* UCMP 37302; (b) *Eustreptospondylus* OUMNH J.13558/F02; (c) *Australovenator* AODF604 (mirrored). (d) Phylogenetic tree of Tetanurae showing the reconstruction of ancestral character state for each node. (a) modified from Marsh & Rowe (2020) and (c) modified from White *et al.* (2013). Not to scale. Abbreviations: fh-femoral head, ft-fourth trochanter, lt-lesser trochanter, ps-proximal surface, vm-ventral margin.

The morphology of the insertion sites of the anterolateral muscles of the thigh, on the proximal portion of the femur (character 306; e.g., Hutchinson, 2001a) may represent a continuous lesser trochanter shelf (306[0]), as in *Eoraptor* and *Herrerasaurus*, as well as polymorphic in coelophysoids and *Ceratosaurus* (306[0,1]). Other theropod species, including all Tetanurae (see Hutchinson, 2001a), except the early-diverging *Sinosaurus* and the ceratosaurs *Majungasaurus* and *Masiakasaurus*, have a distinct insertion site of the lesser trochanter (discrete rugosity) (306[1]) on the proximal region of the femur. The most parsimonious condition in MRCA of megalosauroids is a distinct lesser trochanter and trochanteric shelf reduced to a bulge (state 1). These features probably relate to the *ischiotrochantericus* (ISTR), IFE and ITC muscles (e.g., Hutchinson, 2001a; Carrano & Sampson, 2008; Grillo & Azevedo, 2011; Bishop *et al*., 2021), with the ITC moving proximally and anteriorly with the lesser trochanter (altering its moment arms; Allen *et al*., 2021), while the IFE and ISTR maintained conservative positions.

A predominant theropod (and other diapsid reptile) feature is the presence of a fourth trochanter of the femur (character 307), which is the attachment site of the powerful CFL and CFB musculature (Romer, 1923a; 1956; Gatesy, 1990; Hutchinson, 2001a; Carrano & Hutchinson, 2002). A fourth trochanter as a laterally prominent semioval projection (307[0]) is the predominant condition in theropods. Exceptions are shown by the unnamed allosauroid (CV00214) and *Chilantaisaurus*, as well as by the coelurosaurs *Compsognathus* and *Ornitholestes*, which have a fourth trochanter that is poorly developed or even absent (307[1]). Gatesy (1990) outlined how reduction of the fourth trochanter (and tail, and CFL muscle) indicates a gradual shift in locomotor function from more hip-driven to more knee-driven across the lineage to Aves.

A distinct anterodistal projection of the lesser trochanter, the accessory trochanter (character 308; e.g., Hutchinson, 2001a), may be a poorly developed structure that only forms a thickened distal margin of the lesser trochanter (308[0]) as in all non-avetheropods (except *Suchomimus*; Figure 1.20A) analysed, including megalosauroids (e.g., *Spinosaurus*; Figure 1.20B). Within avetheropods, the accessory trochanter represents a lateralised triangular projection (308[1]) except the carcharodontosaurid *Concavenator* which presents the plesiomorphic condition. Although *Suchomimus* has the apomorphic condition of a triangular projection, the MRCA of megalosauroids was plesiomorphic (pl = 99%), whereas the MRCA of Averostra had the derived state (pl = 94%) (Figure 1.20C). PIFI2 is thought to have inserted here (Hutchinson, 2001a; Carrano & Hutchinson, 2002), so the more derived states suggest at least slight alterations in PIFI2 muscle actions (Carrano, 2000; Allen *et al*., 2021).

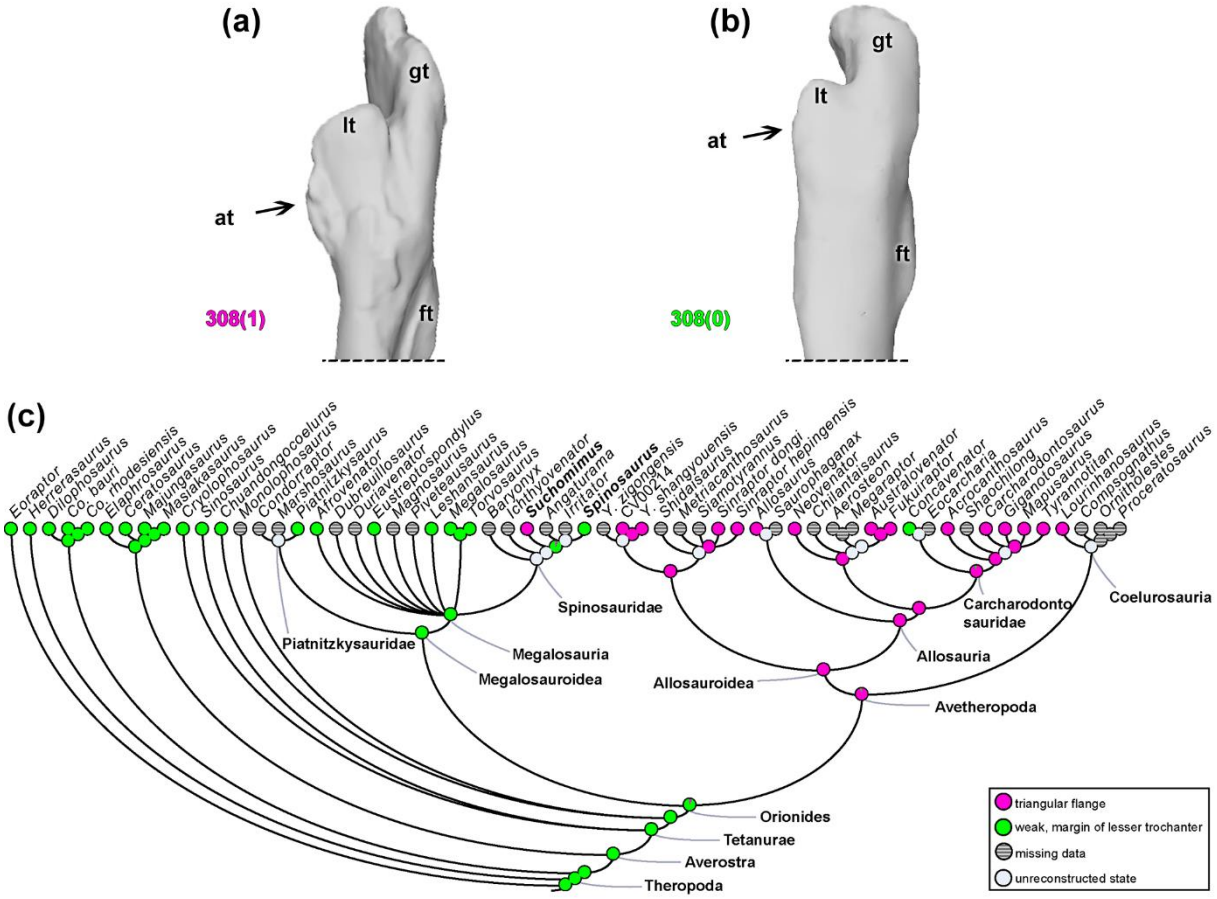

Figure 1.20. Evolutionary history of character 308 (Femur, distinctly projecting accessory trochanter [derived from lesser trochanter]) and the ancestral state reconstruction. Illustration of the left femur in lateral view: (a) *Suchomimus* MNBH GAD500; (b) *Spinosaurus* FSAC-KK 11888. (c) Phylogenetic tree of Tetanurae showing the reconstruction of ancestral character state for each node. (a) and (b) based on the 3D digital model provided by Sereno *et al*. (2022). Not to scale. Abbreviations: at-accessory trochanter, ft-fourth trochanter, gt-greater trochanter, lt-lesser trochanter.

On the anterodistal surface of the femur, on the medial side of the *M. femorotibialis externus* (FMTE; e.g., Romer, 1923b; Hutchinson, 2001a) origin (character 309), the scar is small and rough (309[0]) in *Dilophosaurus* and early tetanurans including Megalosauroidea (Carrano *et al*., 2012). In other theropods, including ceratosaurs and averostrans, this part of the origin of the FMTE is marked by a rough and pronounced oval depression, which extends distally (309[1]). Megalosauroids have the plesiomorphic condition (Carrano *et al*., 2012), being the feature at the MRCA (pl = 96%), whereas derived Orionides such as allosaurs have the apomorphic condition (state 1 in the MRCA; pl = 93%). This is an interesting, persistent trait that likely has some implications for the biomechanics of the FMTE muscle; perhaps at least its size.

Distally, the medial epicondyle of the femur (character 310) may be rounded in shape (310[0]), as in most early theropods (except ceratosaurs; Carrano & Sampson, 2008) including megalosauroids. Yet this character varies widely, because in *Co. rhodesiensis*, ceratosaurs, early tetanurans, and allosauroids (except *Saurophaganax*), the medial epicondyle is a bony crest (310[1]). This character's state is ambiguous for the MRCA of Orionides (pl = 52% for state 0), although the MRCA of megalosauroids had the plesiomorphic condition (pl = 95%).

The distal end of the femur, on the anterior surface dividing the medial and lateral condyles, may have a distal extensor groove (character 311), which is correlated with *triceps femoris* muscle paths (Hutchinson, 2001a). This groove may be absent (311[0]), such as in non-Orionides theropods (e.g., *Elaphrosaurus*; Figure 1.21A) and the megalosauroid *Dubreuillosaurus*. All other Orionides have the extensor groove (311[1]) (e.g., *Piatnitzkysaurus*; Figure 1.21B). This character represents a rare change; the MRCA of Orionides had the distal extensor sulcus (pl = 97%) (Figure 1.21C).

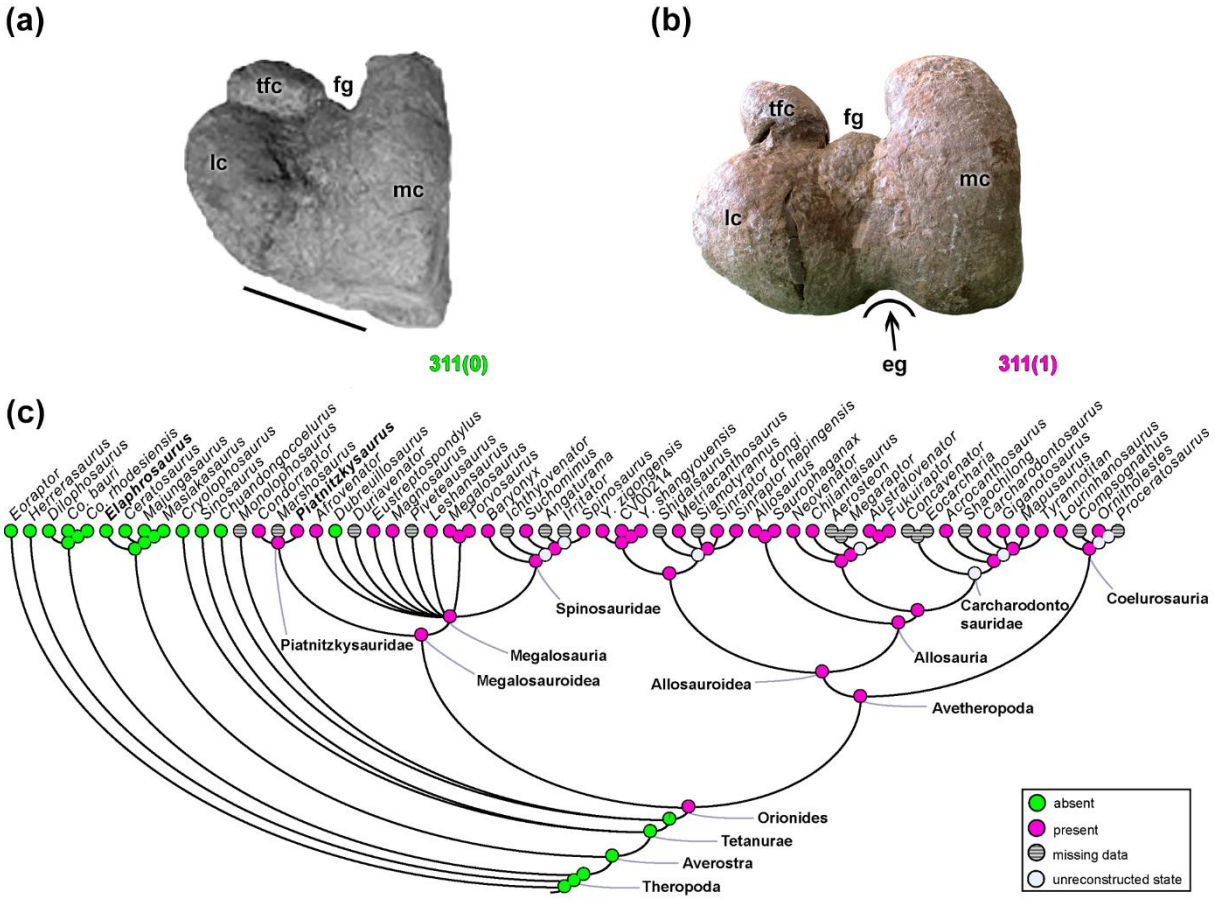

Figure 1.21. Evolutionary history of character 311 (Femur, distal extensor groove) and the ancestral state reconstruction. Illustration of the left femur in distal view: (a) *Elaphrosaurus* MB R 4960; (b) *Piatnitzkysaurus* PVL 4073. (c) Phylogenetic tree of Tetanurae showing the reconstruction of ancestral character state for each node. (b) modified from Rauhut & Carrano (2016). Not to scale. Abbreviations: eg-extensor groove, fg-flexor groove, lc-lateral condyle, mc-medial condyle, tfc-tibiofibular crest.

The tibiofibular crest (or crista tibiofibularis; Benson, 2010) of the femur (character 312) may represent an enlarged structure (312[0]), as in several taxa including *Eoraptor*, *Herrerasaurus*, *Dilophosaurus*, piatnitzkysaurids (e.g., *Piatnitzkysaurus*; Figure 1.22A), and avetheropods (except *Metriacanthosaurus* and *Lourinhanosaurus*). In early-diverging tetanurans, megalosauroids (except piatnitzkysaurids) and aforementioned avetheropods, the tibiofibular crest is narrow and longitudinally oriented (312[1]) (e.g., *Eustreptospondylus*; Figure 1.22C). In non-tetanurans such as *Co. rhodesiensis* and ceratosaurs (e.g., *Ceratosaurus*; Figure 1.22B), this crest is a lobular ridge that is obliquely oriented (312[2]). Piatnitzkysaurids have a broad tibiofibular crest whereas other megalosauroids have a narrow and longitudinal crest. Consequently, the MRCA of megalosauroids may have had a broad crest (pl = 78%), whereas the MRCA of megalosaurids + spinosaurids had a narrow, longitudinal tibiofibular crest (pl = 99%) (Figure 1.22D).

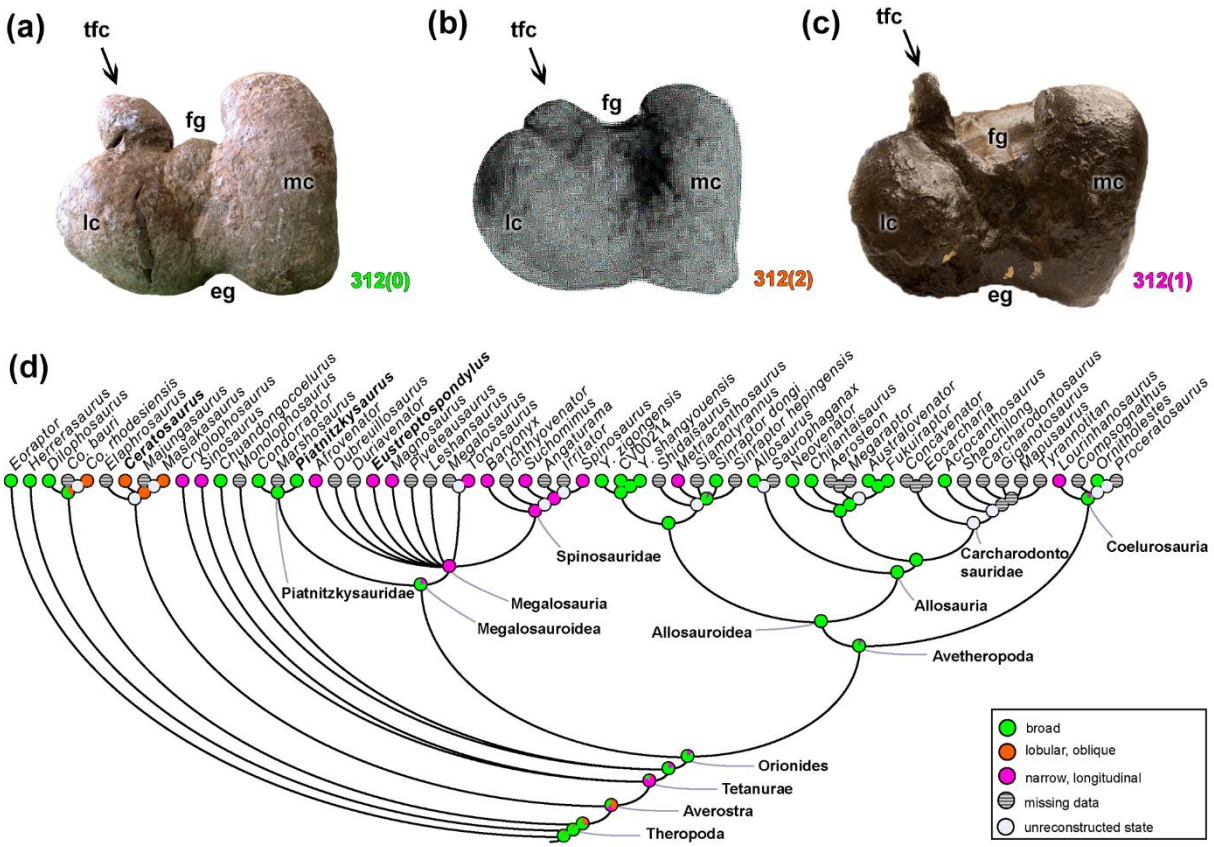

Figure 1.22. Evolutionary history of character 312 (Femur, morphology and orientation of tibiofibularis crest) and the ancestral state reconstruction. Illustration of the left femur in distal view: (a) *Piatnitzkysaurus* PVL 4073; (b) *Ceratosaurus* SHN(JJS)-65/1; (c) *Eustreptospondylus* OUMNH J.13558/F02. (d) Phylogenetic tree of Tetanurae showing the reconstruction of ancestral character state for each node. (b) modified from Malafaia *et al*. (2016). Not to scale. Abbreviations: eg-extensor groove, fg-flexor groove, lc-lateral condyle, mc-medial condyle, tfc-tibiofibular crest.

A connection between the distal part of the medial femoral condyle and the tibiofibular crest, the infrapopliteal crest (character 313; e.g., Tykoski, 2005), may be absent (313[0]), as in all non-ceratosaur theropods, or present (313[1]) in ceratosaurs. The orientation of the main axis of the medial femoral condyle (character 314) can be arranged anteroposteriorly (314[0]), as observed conservatively in almost all theropod clades (e.g., *Megalosaurus*; Figure 1.23A). The exception is spinosaurid taxa (e.g., *Spinosaurus*; Figure 1.23B), in which the orientation of the medial condyle is in the posterolateral direction (314[1]), being the condition in the MRCA (pl = 98%) (Figure 1.23C).

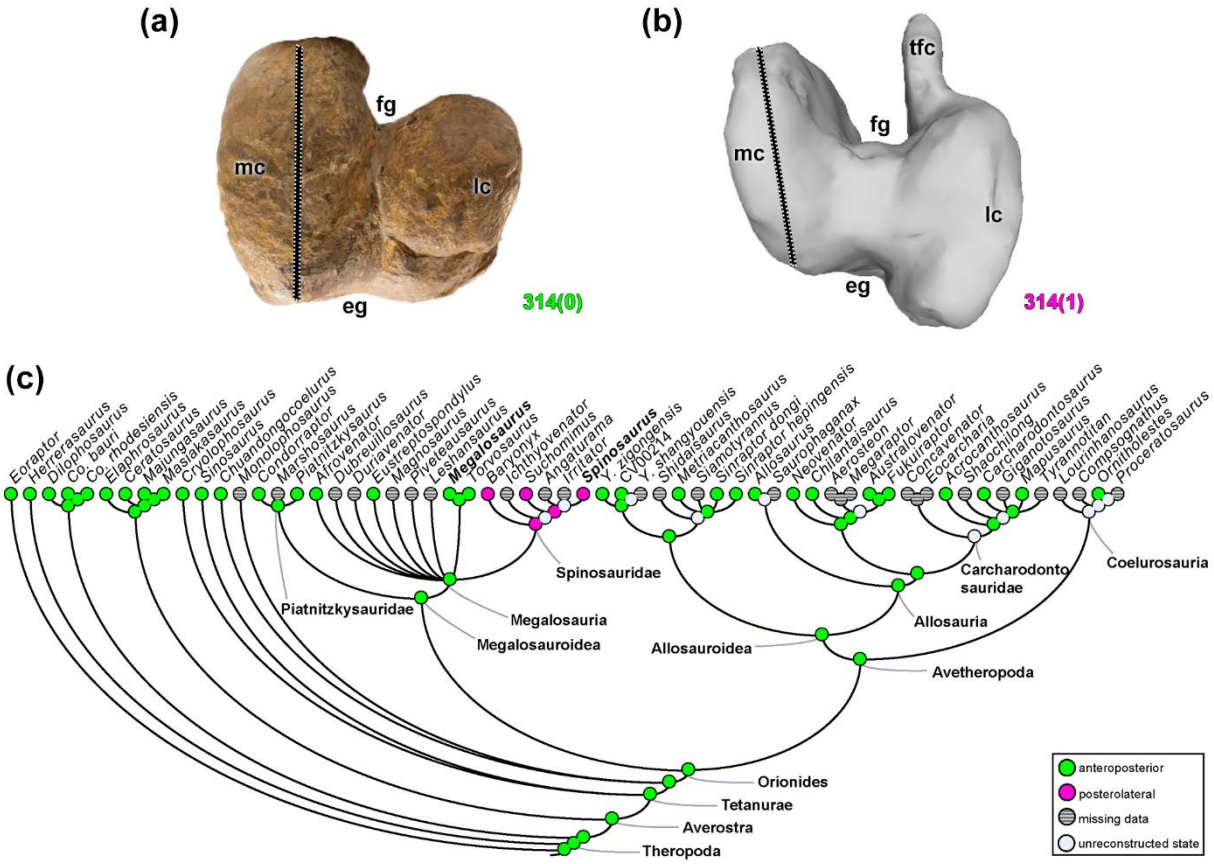

Figure 1.23. Evolutionary history of character 314 (Femur, orientation of long axis of medial condyle in distal view) and the ancestral state reconstruction. Illustration of the right femur in distal view: (a) *Megalosaurus* OUMNH J.13561; (b) *Spinosaurus* FSAC-KK 11888. (c) Phylogenetic tree of Tetanurae showing the reconstruction of ancestral character state for each node. (b) based on the 3D digital model provided by Sereno *et al*. (2022). Not to scale. Abbreviations: eg-extensor groove, fg-flexor groove, lc-lateral condyle, mc-medial condyle, tfc-tibiofibular crest.

The medial and lateral condyles of the femur may have their projection (character 315) approximately equal (315[0]), as seen in most theropods (e.g., *Megalosaurus*; Figure 1.24A). A lateral condyle that projects beyond the medial condyle, with the distal surface of the medial condyle slightly flattened (315[1]), is a feature independently evolved in the megalosauroid

Leshansaurus, neovenatorids (e.g., *Australovenator*; Figure 1.24C), and *Carcharodontosaurus*. A medial condyle that projects distinctly further than the lateral (315[2]) exists only in *Suchomimus* and *Spinosaurus* (Figure 1.24B). Even with some internal variations, the MRCA of megalosauroids (pl = 99%) and spinosaurids (pl = 96%) had condyles that projected equally (Figure 1.24D).

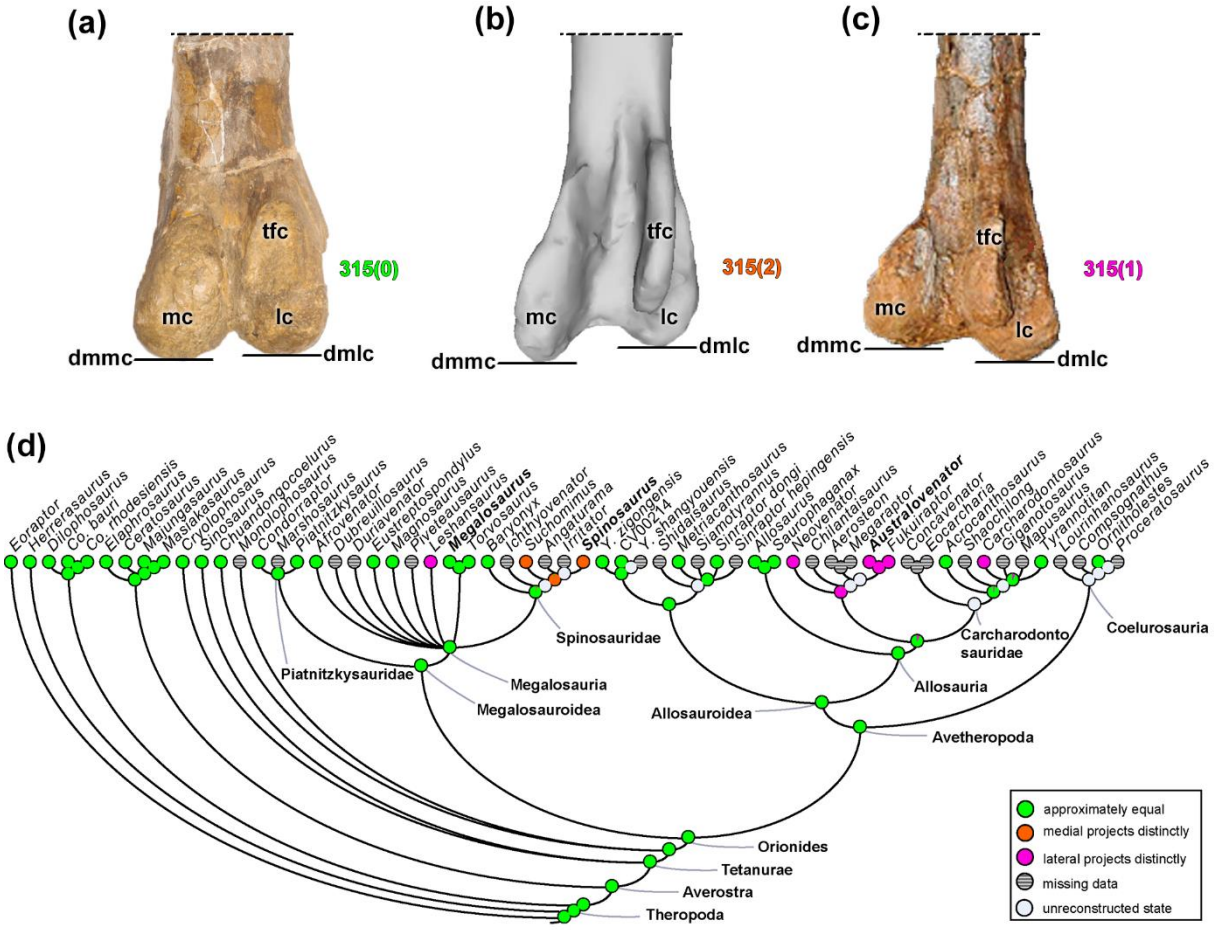

Figure 1.24. Evolutionary history of character 315 (Femur, projection of lateral and medial distal condyles) and the ancestral state reconstruction. Illustration of the right femur in posterior view: (a) *Megalosaurus* OUMNH J.13561; (b) *Spinosaurus* FSAC-KK 11888; (c) *Australovenator* AODF604. (d) Phylogenetic tree of Tetanurae showing the reconstruction of ancestral character state for each node. (b) based on the 3D digital model provided by Sereno et al. (2022) and (c) modified from White *et al*. (2013). Not to scale. Abbreviations: dmlc-distal margin of lateral condyle, dmmc-distal margin of medial condyle, lc-lateral condyle, mc-medial condyle, tfc-tibiofibular crest.

The distal end of the femur (character 316) may present a centralized posterior depression, which is connected to the tibiofibular crest by a narrow groove (316[0]), as in non-avetheropod taxa. Within avetheropods (except *Y. zigongensis*), the depression separating the lateral and medial convexities is shallow and anteroposteriorly oriented (316[1]).

These changes of the morphology of the distal femur (characters 310–316) pertain to the femorotibial and femorofibular joints (i.e., knee), and surely would influence the kinematics of

those articulations (e.g., Pintore *et al*., 2022). Some may also relate to ligaments connecting the three long bones involved in the knee. More investigation of knee form and function in theropods (e.g., Manafzadeh *et al*., 2021) is needed to understand such traits.

3.2.7. Zeugopodium (tibia)

Eight morphological characters (11.76%) relate to the tibia. The proximal tibia in theropods and crocodylians is where several muscles of the thigh such as IT1– 3, AMB, FMT, FTI3 and FTE or their homologs are/were attach(ed); as well as the origin of EDL and *M. gastrocnemius pars medialis* (GM) (e.g., Romer, 1923a,b; Carrano & Hutchinson, 2002; Grillo & Azevedo, 2011; Bishop *et al*., 2021; Hattori & Tsuihiji, 2021).

The lateral malleolus of the distal tibia (character 317) can be positioned posterior to the astragalus (317[0]), as in early theropods. The overall feature of averostran theropods (except *Cryolophosaurus*) is a lateral malleolus that overlaps the calcaneum (317[1]). The shape of the lateral malleolus's edge (character 318) is conservative, being smoothly curved (318[0]) in all non-coelophysoid theropods, whereas coelophysoids present a tubular notch (318[1]). Perhaps characters 317 and 318 indicate reduced mobility of the tibiotarsal joints with derived states.

The cnemial process or cnemial crest (e.g., [101]) on the proximal tibia of theropods has its distalmost morphology (character 319) rounded (319[0]) in all non-ceratosaurid theropods analysed (e.g., *Piatnitzkysaurus*; Figure 1.25B). The feature in ceratosaurids (e.g., *Majungasaurus*; Figure 1.25A) is a proximodistally expanded cnemial crest (319[1]). This derived expansion suggests an expanded set of tendinous insertions of the *triceps femoris* knee extensor muscles (IT1-3, AMB, *Mm. femorotibiales*).

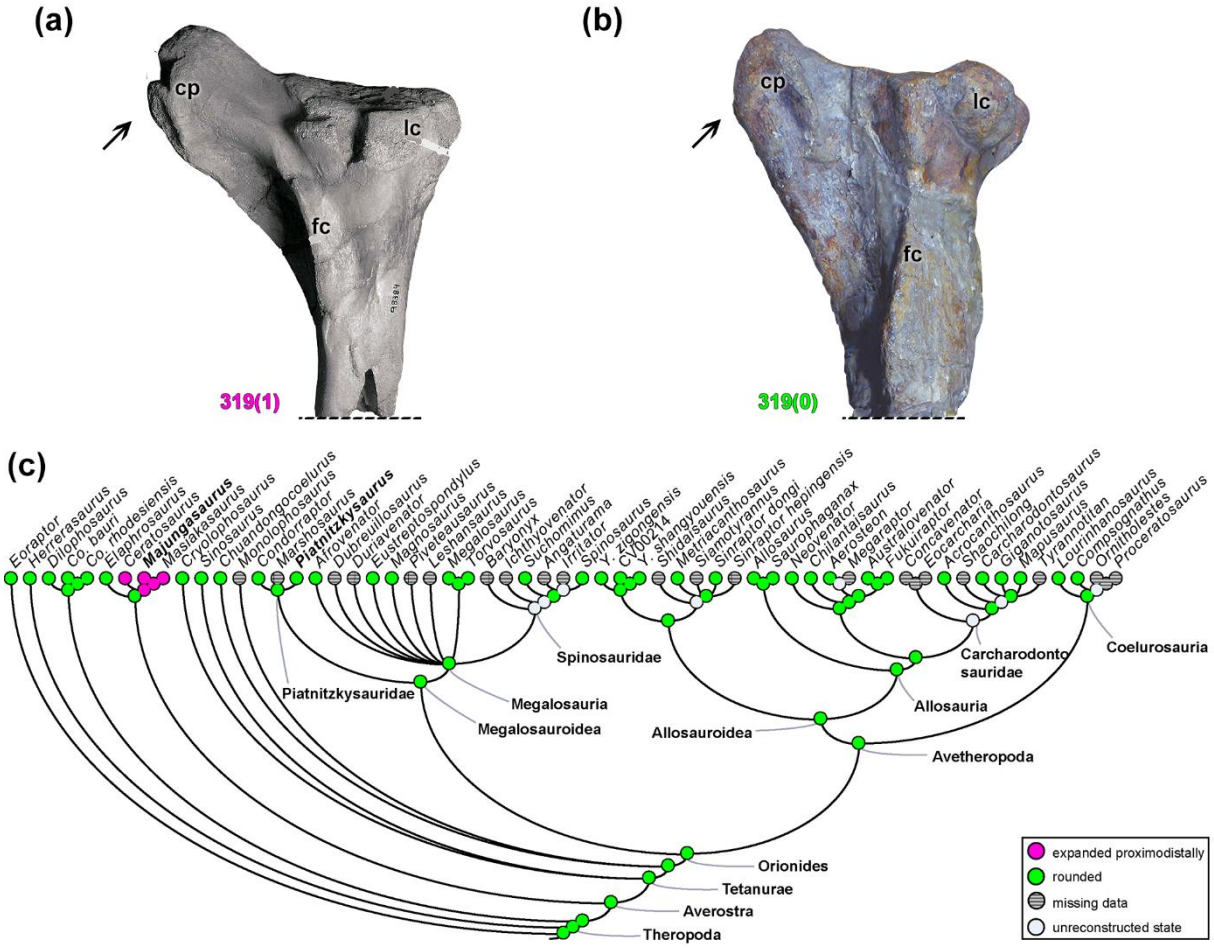

Figure 1.25. Evolutionary history of character 319 (Tibia, morphology of distal cnemial process) and the ancestral state reconstruction. Illustration of the left tibia in lateral view: (a) *Majungasaurus* FMNH PR 2424; (b) *Piatnitzkysaurus* MACN-Pv-CH 895. (c) Phylogenetic tree of Tetanurae showing the reconstruction of ancestral character state for each node. (a) modified from Carrano (2007). Not to scale. Abbreviations: cp-cnemial process, fc-fibular crest, lc-lateral condyle.

The lateral condyle/cotyle of the tibia (or fibular condyle; Novas, 1996) (character 320) may be large (320[0]) as in all non-avetheropods (except *Suchomimus*), or small and lobular (320[1]), as in avetheropods (except *Sinraptor*) and *Suchomimus*. The derived condition present in *Suchomimus* represents a secondary acquisition, because the MRCA of megalosauroids had a large lateral condyle of the tibia (pl = 99%). An anterolateral process of the lateral tibial condyle/cotyle (character 321) may be absent or represent a horizontal projection (321[0]), as in all non-neovenatorid theropods. A prominent and ventrally curved process (321[1]) is a synapomorphy of neovenatorids. While suggestive of changes in knee joint function, it is difficult to even speculate on what those changes might be, as the function of the tibiofibular side of the knee joint in archosaurs is even more poorly understood than that of the femoral side.

In the distal tibia, the anteromedial buttress for the astragalus (supraastragalar buttress) (character 322) is absent (322[0]) in *Herrerasaurus*. A ventrally positioned anteromedial buttress (322[1]) exists in coelophysids. In most theropods analysed including ceratosaurs, early tetanurans, megalosauroids (except *Suchomimus*), and non-carcharodontosaurian avetheropods, the anteromedial buttress is a marked oblique step-like ridge (322[2]). In carcharodontosaurids and *Neovenator*, the anteromedial buttress is a reduced oblique ridge (322[3]). Meanwhile, neovenatorids (except *Neovenator*), and the spinosaurid *Suchomimus* have the bluntly rounded vertical ridge on the medial side of the anteromedial buttress (322[4]). Despite the derived state in *Suchomimus*, the MRCA of megalosauroids had a marked oblique step-like ridge related to the anteromedial tibial buttress (pl = 99%). Like characters 317 and 318, this character may signal reduction of mobility.

On the proximal tibia, the morphology of the fibular crest, or crista fibularis (character 323), is narrow (323[0]) in most of the analysed theropods (e.g., *Majungasaurus*; Figure 1.26A). Exceptions are when the crista fibularis becomes a bulbous structure (323[1]), as in *Sinosaurus*, *Piatnitzkysaurus* (Figure 1.26B), *Megalosaurus*, and some metriacanthosaurids. Even with the derived state of a bulbous crest in *Piatnitzkysaurus* and *Megalosaurus*, the MRCA of megalosauroids had a narrow structure (pl = 99%) (Figure 1.26C).

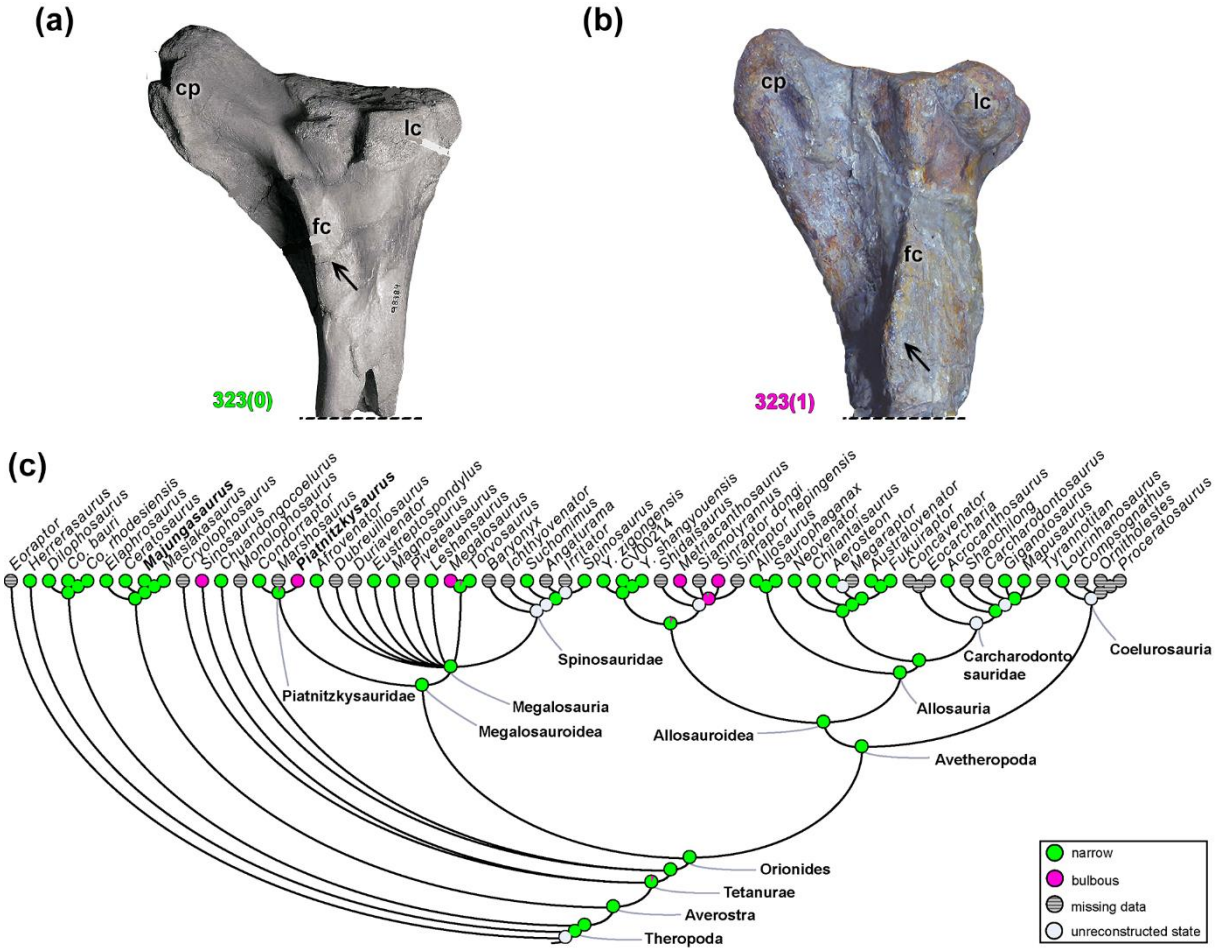

Figure 1.26. Evolutionary history of character 323 (Tibia, morphology of fibular crest) and the ancestral state reconstruction. Illustration of the left tibia in lateral view: (a) *Majungasaurus* FMNH PR 2424; (b) *Piatnitzkysaurus* MACN-Pv-CH 895. (c) Phylogenetic tree of Tetanurae showing the reconstruction of ancestral character state for each node. (a) modified from Carrano (2007). Not to scale. Abbreviations: cp-cnemial process, fc-fibular crest, lc-lateral condyle.

The fibular crest development (character 324) in some early theropods such as coelophysoids and ceratosaurs (e.g., *Majungasaurus*; Figure 1.27A) is proximally high, extending to the proximal end of the tibia (324[0]). In megalosauroids (except *Torvosaurus* and spinosaurids) and metriacanthosaurids, the fibular crest extends to the proximal end of tibia as a low ridge (324[1]) (e.g., *Piatnitzkysaurus*; Figure 1.27B). Non-metriacanthosaurid averostrans and *Torvosaurus* + spinosaurids have a fibular crest that does not extend to the proximal end of tibia (324[2]) (e.g., *Australovenator*; Figure 1.27C). Because most of the megalosauroids have a low ridge fibular crest, the MRCA had this state (pl = 94%) (Figure 1.27D). The crista tibiofibularis is considered to indicate strengthening of the attachment between the two zeugopodial bones, enhanced action of the ILFB, and perhaps more (reviewed in Hutchinson, 2002).

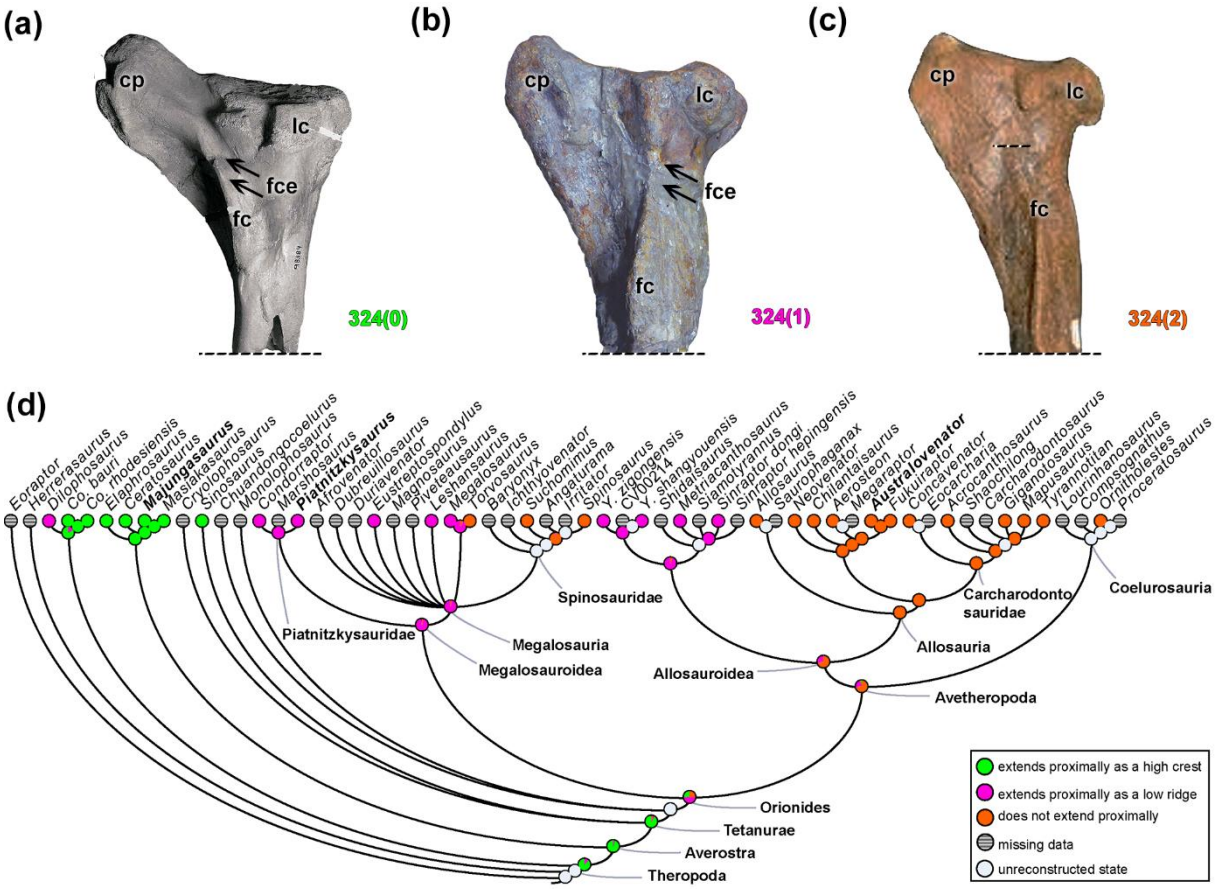

Figure 1.27. Evolutionary history of character 324 (Tibia, development of fibular crest) and the ancestral state reconstruction. Illustration of the left tibia in lateral view: (a) *Majungasaurus* FMNH PR 2424; (b) *Piatnitzkysaurus* MACN-Pv-CH 895; (c) *Australovenator* AODF604. (d) Phylogenetic tree of Tetanurae showing the reconstruction of ancestral character state for each node. (a) modified from Carrano (2007) and (c) modified from White *et al*. (2013). Not to scale. Abbreviations: cp-cnemial process, fc-fibular crest, fce-fibular crest extension, lc-lateral condyle.

3.2.8. Zeugopodium (fibula)

At least four morphological characters (5.88%) relate to the fibula. Some muscles such as *M. fibularis longus* (FL), *M. fibularis brevis* (FB), and *M. extensor hallucis longus* (EHL) are shared among crocodylians, Aves and non-avian theropods and originate(d) from the fibula; whereas the ILFB inserts here (Carrano & Hutchinson, 2002; Hutchinson, 2002; Grillo & Azevedo, 2011; Bishop *et al*., 2021).

The depth of the fibular fossa on the medial fibula (character 325) may be a groove (325[0]) as in coelophysoids and *Sinosaurus*; or a shallow fossa (325[1]) that is present only in spinosaurids and megalosaurids. Therefore, a deep fossa (325[2]) is acquired independently in ceratosaurs, *Chuandongocoelurus*, piatnitzkysaurids, and averostran theropods. Although a shallow fossa is a widespread feature among megalosauroids (most parsimonious for the MRCA of Megalosauria), the most parsimonious condition for the MRCA of megalosauroids

is the presence of a deep fossa. The fibular fossa on the fibula can be positioned (character 326) posteriorly (326[0]), as in coelophysoids, or centrally (326[1]), as seen widely in neotheropods. This fossa might be a more concentrated origin of part of the digital flexors, or part of the "popliteus"/interosseous cruris/pronator profundus (see Hutchinson, 2002; Hattori & Tsuihiji, 2021).

The shape of the iliofibularis tubercle (character 327) that is widespread within tetanuran theropods is a faint scar (327[0]) (e.g., *Piatnitzkysaurus*; Figure 1.28C). In ceratosaurs (except *Elaphrosaurus*), the tubercle is a large structure (327[1]) (e.g., *Majungasaurus*; Figure 1.28B); and the morphology in coelophysoids (e.g., *Dilophosaurus*; Figure 1.28A), *Elaphrosaurus*, and *Chuandongocoelurus* is an anterolaterally curved flange (327[2]).

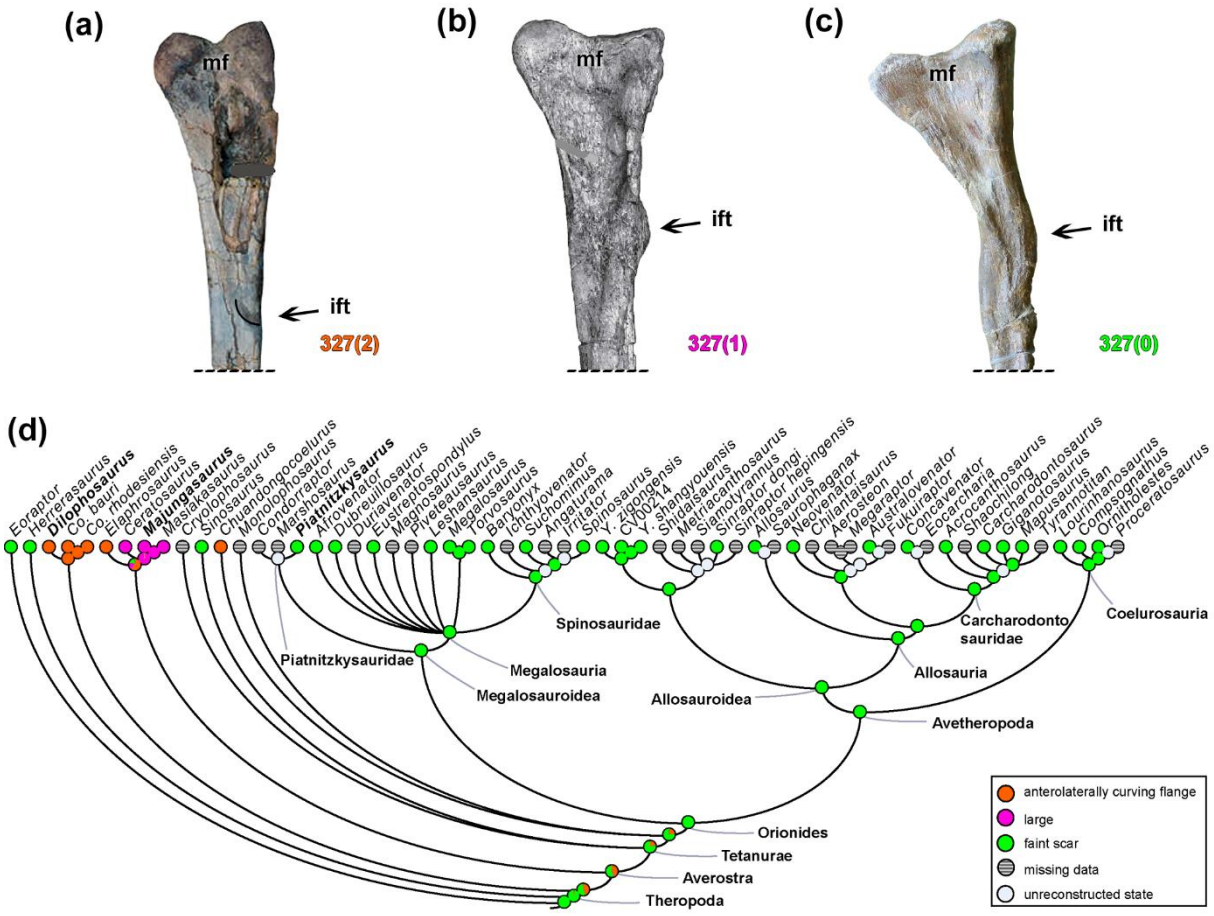

Figure 1.28. Evolutionary history of character 327 (Fibula, size of iliofibularis tubercle) and the ancestral state reconstruction. Illustration of the left fibula in medial view: (a) *Dilophosaurus* TMM 43646-1; (b) *Majungasaurus* FMNH PR 2424; (c) *Piatnitzkysaurus* PVL 4073. (d) Phylogenetic tree of Tetanurae showing the reconstruction of ancestral character state for each node. (a) modified from Marsh & Rowe (2020) and (b) modified from Carrano (2007). Not to scale. Abbreviations: ift- iliofibularis tubercle, mf-medial fossa.

The size of the proximal fibula relative to the width of the proximal tibia (character 328) is <75% (328[0]) only in *Eoraptor*; all theropods analysed here have this proportion ≥75%

(328[1]). This difference may indicate the enlarged tibia (and knee extensor insertions) in early theropods; along with part of the protracted trend of reduction of the fibula along the lineage to Aves.

3.3. Morphological disparity

3.3.1. Pelvic girdle and hindlimb stylopodium and zeugopodium

In the morphological disparity analysis considering all the characters related to the pelvic girdle and stylopodium/zeugopodium, the morphospace with the highest variance accumulates 75.3% of the data dissimilarity. The PCO1 vs. PCO2 (Figure 1.29A) reveals the overlap of several theropod lineages: *Eoraptor*, *Herrerasaurus*, coelophysoids, ceratosaurs, and most of the early-diverging tetanurans occupy positive PCO1 and negative PCO2 scores. As expected, non-Orionides occupy different positions in morphospace when compared with Orionides, indicating more dissimilarity (also confirmed in box plots, e.g., *Coelophysis*; Figure 1.29B). A biplot (Figure 1.29A) indicates that the Orionides clade is distributed in a similar way in the morphospace, since there is a high degree of overlap of several groups including megalosauroids, allosauroids and coelurosaurs; however, with the main groups distributed along five main axes with a high degree of overlap between piatnitzkysaurids, megalosaurids, and a moderate overlap with spinosaurids. Considering the PCO2 axis, the clades that occupy the largest area in morphospace are the neovenatorids, metriacanthosaurids, megalosaurids, and carcharodontosaurids, with a high to moderate degree of overlap between clades. Megalosauroidea are distributed in a similar way as other Orionides clades in the biplot, however, megalosaurids, based on the convex hulls, have a larger occupation of the morphospace (influenced most by the negatively scored taxa, *Dubreuillosaurus* and *Magnosaurus*).

3.3.2. Ilium

In the biplot focusing on the morphological characters of the ilium (PCO1 vs. PCO2 = 80.6% of variance; Figure 1.29C), the taxon distribution is nearly similar to the complete dataset analysis (i.e., pelvis + stylopodium/zeugopodium; Figure 1.29A). At the most positive scores of PCO1, *Eoraptor* and *Herrerasaurus* completely overlap, and the morphospace is gradually occupied along the PCO1 (to negative scores) by coelophysoids, ceratosaurs, and early-

diverging tetanurans (which occupy a large morphospace area), indicating more dissimilarity to Orionides (Figure 1.29C,D). More negative scores of PCO1 have a similar distribution of the major Orionides clades distributed along a main axis with the overlap of several clades. The early-diverging tetanurans, carcharodontosaurids, megalosaurids, and neovenatorids cover a great area of the morphospace. Considering the PCO2 axis, megalosauroids expanded their morphospace distribution compared with the complete dataset analysis. The Orionides clade have a broad distribution along the PCO2 axis; however, this clade is almost restricted to negative scores along PCO1. Our analysis considering the morphological characters of the ilium shows that they have a strong influence on the disparity metrics quantified by the complete dataset analysis (pelvis + stylopodium/zeugopodium), because they contain many studied characters (27.94%) and both biplots present a similar pattern.

3.3.3. Pubis

When we consider only the pubis, *Eoraptor* and coelophysoids retain extreme negative scores for PCO2 and positive scores for PCO1 in the morphospace (PCO1 vs. PCO2 = 66.7% of variance; Figure 1.29E). On the other hand, averostran taxa are differently distributed in the morphospace, mainly due to the influence of the PCO2 axis that segregates these taxa from non-averostrans, and distributes them approximately across five main axes according to the clade-based delimitations of the convex hulls (Figure 1.29E). The most positive scores along PCO1 reached by ceratosaurs are influenced by *Masiakasaurus* and *Ceratosaurus* distribution; but the clade has a nearly homogeneous distribution along the PCO2 axis. Spinosaurids, piatnitzkysaurids and early-diverging tetanurans have similar patterns for their morphospace distributions, with spinosaurids being more positively scored along both axes. Allosauria, including carcharodontosaurids, neovenatorids, and allosaurids, reaches the most positive scores in the PCO2 in similar pattern, but distributed differently when compared with ceratosaurs and early tetanurans. The clades occupying larger areas in the morphospace are megalosaurids, which are restricted to negative scores of PCO1; and metriacanthosaurids, which overlap with several other clades such as coelurosaurs, spinosaurids, and ceratosaurs.

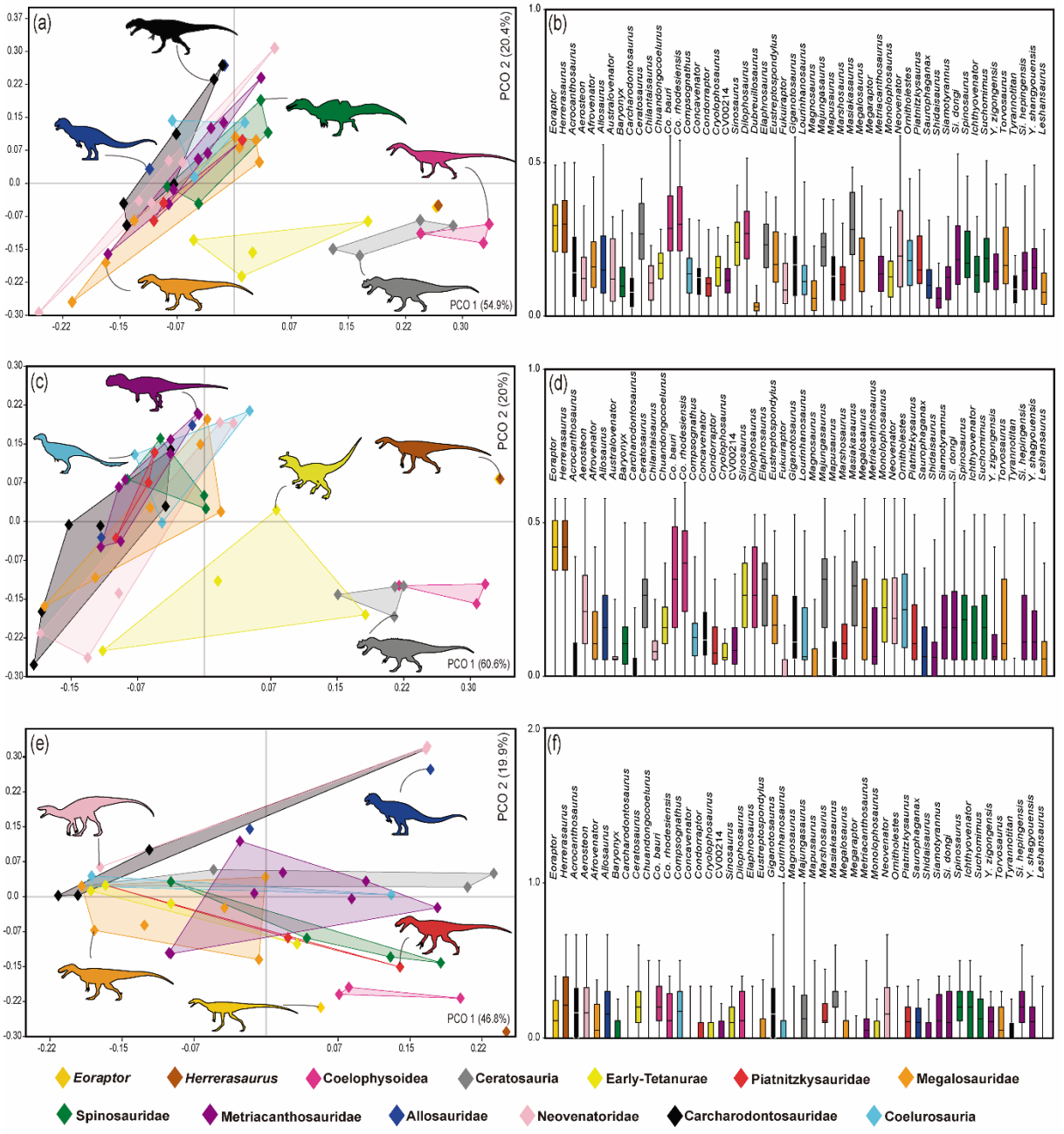

Figure 1.29. Two-dimensional morphospace and box plot diagrams based on Euclidean taxon-taxon distance related to morphological characters of the theropod locomotor system. (a) PCO1 vs. PCO2 biplot (75.3% of variance) and (b) Box plot diagram of pelvic girdle and hindlimb's stylopodium and zeugopodium (characters 261–328). (c) PCO1 vs. PCO2 biplot (80.6% of variance) and (d) Box plot diagram of ilium (characters 262–280). (e) PCO1 vs. PCO2 biplot (66.7% of variance) and (f) Box plot diagram of pubis (characters 282–291). Silhouettes were download from phylopic.org; see Acknowledgements.

3.3.4. Ischium

In our analysis of the ischium, for the morphospace with greatest morphological variance (PCO1 vs. PCO2 = 58%; Figure 1.30A), the coelophysoid clade retains the most positive scores for the PCO1; influenced by *Coelophysis* (confirmed in box plot; Figure 1.30B).

The remaining taxa are distributed along five main axes, with a high degree of overlap. Ceratosaurs, early tetanurans, metriacanthosaurids, carcharodontosaurids and spinosaurids occupy large areas of the morphospace; with ceratosaurs, metriacanthosaurids and early tetanurans retaining negative PCO2 scores, and remaining clades having more positive scores (Figure 1.30A). Compared with our previous analyses above, there is a large relative increase of the morphospace area occupied by several groups, for example, metriacanthosaurids, early tetanurans, ceratosaurs, carcharodontosaurids, piatnitzkysaurids and spinosaurids.

3.3.5. Stylopodium

By analysing only the influence of the femur on the morphospace (PCO1 vs. PCO2 = 68.7% of variance; Figure 1.30C), we find that the non-Orionides taxa *Herrerasaurus*, coelophysoids, ceratosaurs, and early tetanurans occupy positive scores for PCO1, close together. Meanwhile, Orionides has mainly negative scores for PCO1, although some megalosauroids (e.g., *Torvosaurus*, *Piatnitzkysaurus*, *Spinosaurus*) have slightly positive scores along this axis. There is great overlap between avetheropods for the most negative PCO1 scores; by coelurosaurs, allosaurs, metriacanthosaurids, and carcharodontosaurids. In this analysis, the distribution in morphospace is consistent with the phylogeny of theropods, with the delimited clades occupying different areas: non-Orionides (*Herrerasaurus*, coelophysoids, ceratosaurs, and early tetanurans) retaining positive scores for PCO1 and close to the average or slightly negative for PCO2; megalosauroids (piatnitzkysaurids, megalosaurids, and spinosaurids) retaining near average to slightly negative PCO1 scores and from positive to near average PCO2 scores; and avetheropods retaining negative PCO1 scores and ranging from positive to negative PCO2 scores, with the neovenatorid theropods being the most negatively positioned along PCO2 (Figure 1.30C,D).

3.3.6. Zeugopodium

In our analysis of the zeugopodium, for the morphospace with greatest morphological variance (PCO1 vs. PCO2 = 71.3%; Figure 1.30E), almost all non-Orionides taxa retain positive PCO1 scores, with coelophysoids isolated to extreme positive values (and consequently larger box plots; Figure 1.30F), followed by ceratosaurs. Regarding tetanurans, five main distribution axes are evident based on the divisions of clades: piatnitzkysaurids, the majority of megalosaurids, and metriacanthosaurids converge in the morphospace, as well as

carcharodontosaurids, coelurosaurs, and neovenatorids that are distributed close together, however neovenatorids reach extreme PCO2 scores that seem influenced by *Australovenator* and *Neovenator* (Figure 1.30F,E). Both megalosaurids and metriacanthosaurids occupy a large area in the morphospace. Spinosaurids occupy a distinct and large morphospace area, influenced by *Suchomimus*.

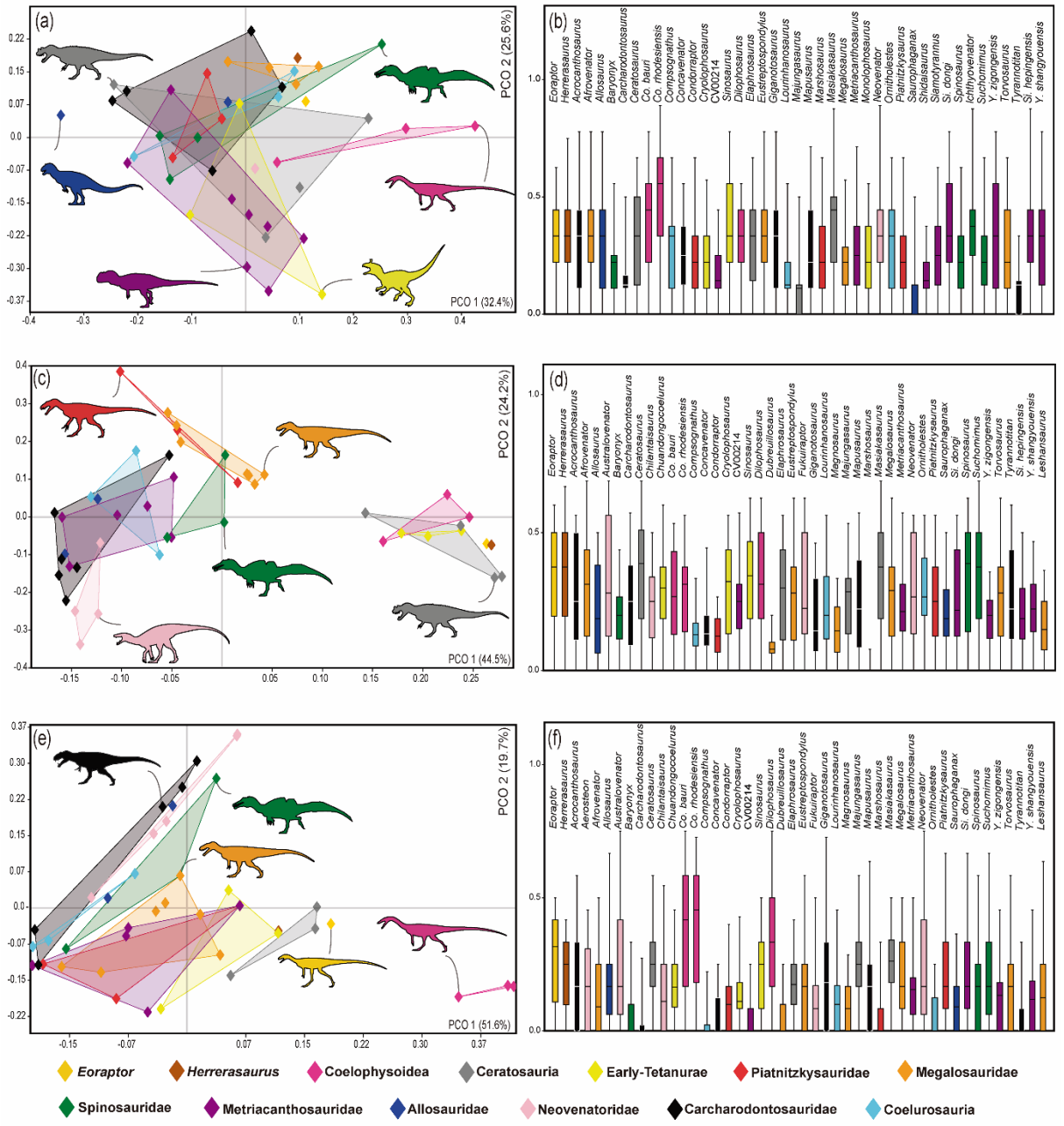

Figure 1.30. Two-dimensional morphospace and box plot diagrams based on Euclidean taxon-taxon distance related to morphological characters of the theropod locomotor system. (a) PCO1 vs. PCO2 biplot (58% of variance) and (b) Box plot diagram of ischium (characters 292–300). (c) PCO1 vs. PCO2 biplot (68.7% of variance) and (d) Box plot diagram of stylopodium (characters 301–316). (e) PCO1 vs. PCO2 biplot (71.3% of variance) and (f) Box plot diagram of zeugopodium (tibia and fibula) (characters 317–328). Silhouettes were downloaded from phylopic.org; see Acknowledgements.

3.4. Alternative phylogenies and the potential validity of the Carnosauria

Some recent phylogenies have recovered Carnosauria (i.e., Megalosauroidea + Allosauroidea; *sensu* Rauhut & Pol, 2019) as a clade (e.g., Rauhut & Pol, 2019; Barker *et al*., 2021; Schade *et al*., 2023), which would have important implications for the early evolution of tetanurans. Carnosauria is defined as a clade that includes all theropods that are more closely related to *Allosaurus* and to *Megalosaurus* than to Neornithes (Rauhut & Pol, 2019). Previously, most analyses recovered three distinct clades: Megalosauroidea, Allosauroidea and Coelurosauria, with the latter two traditionally recovered a sister group (Avetheropoda clade); and Megalosauroidea being rootward to Avetheropoda (e.g., Benson, 2010; Allain *et al*., 2012; Carrano *et al*., 2012; Rauhut *et al*., 2016; Samathi *et al*., 2021; this Chapter). In the analysis of Rauhut & Pol (2019, Spinosauridae was the first group of tetanurans to diverge, followed by Megalosauridae and Piatnitzkysauridae (the latter being allocated in Allosauroidea), thus with Megalosauridae as the sister group of Allosauroidea. Barker *et al*. (2021) obtained similar results, but Allosauroidea (+ Piatnitzkysauridae) species generally formed only a polytomy. However, in contrast with Rauhut & Pol (2019), the clade composed of Megalosauridae and Spinosauridae (i.e., Megalosauria) was recovered. Schade *et al*. (2023) also found a monophyletic Carnosauria, but in contrast to the previous hypotheses, the taxa classically considered as Megalosauridae formed a grade outside of Spinosauridae, and Piatnitzkysauridae was placed as an Allosauroidea clade. These studies' main implications (in terms of evolution of pelvic and appendage characters) contrasting with our results are as follows.

(1) Character 263; Ilium, vertical ridge on the lateral surface of blade dorsal to acetabulum: In our results, the presence of a low swollen ridge (263[1]) converges between some megalosauroids (including Piatnitzkysauridae) and Allosauridae. Considering Carnosauria, the presence of a low swollen ridge could have arisen in the MRCA of Allosauroidea (and homoplastically in the megalosauroids *Afrovenator*, *Megalosaurus*, and *Suchomimus*), and later having been lost (263[0]) or expanded (263[2]) in late allosauroids.

(2) Character 269; Ilium, shape of acetabular margin of pubic peduncle: Although it is a relatively homoplastic character, in our results an acetabular margin convex or flat (269[0]) was a feature of Piatnitzkysauridae that would potentially be present in the MRCA of megalosauroids. In the Carnosauria hypothesis, in which Piatnitzkysauridae is a member of Allosauroidea, this condition would have been independently acquired in *Eoraptor*, *Herrerasaurus*, ceratosaurs, *Spinosaurus*, and predominant in Allosauroidea.

(3) Character 281; Puboischiadic plate, morphology and foramina/notches: Although with some variations (mainly in *Yangchuanosaurus*), in our results, the presence of an open midline without fenestrae and 1–2 notches (281[2]) is predominant and the condition for the MRCA of Avetheropoda; also present homoplastically in *Afrovenator*. In the Carnosauria hypothesis, this condition (i.e., 281[2]) was present in the MRCA of Tetanurae, considering what is observed in Coelurosauria, and later in Megalosauria reverted to the condition of being fully closed along midline with 3 fenestrae (281[0]) (except *Afrovenator* and *Leshansaurus*); also independently in Piatnitzkysauridae.

(4) Character 292; Ischium, length relative to pubis length: Contrary to our results, in the Carnosauria hypothesis, the acquisition of the ischium length relative to the pubis >80% (292[2]) would be characteristic of the clade formed by Metriacanthosauridae + Carcharodontosauria (except *Neovenator*) and independently acquired in *Sinosaurus*, *Torvosaurus*, and *Spinosaurus*; rather than an acquisition of the MRCA from Allosauroidea, because Piatnizkysauridae presents the plesiomorphic condition of this character (i.e., 75–80%; (292[0])).

(5) Character 297; Ischium, morphology of symphysis: Although this character is homoplastic, we hypothesise that the presence of unexpanded symphysis (297[0]) in Piatnitzkysauridae (except *Marshosaurus*) was present in the MRCA of Megalosauroidea, modified in Megalosauria (to an expanded apron (297[1])) and later reversed in Spinosauridae (except *Ichthyovenator*). In the Carnosauria hypothesis, the plesiomorphic condition observed in Piatnitzkysauridae would potentially be shared between this group and Metriacanthosauridae (both at the base of Allosauroidea outside of Allosauria).

(6) Character 303; Femur, groove on proximal surface of head-oriented oblique to long axis of head (articular groove or fovea capitis): In our results, a clear step in the acquisition of the articular groove or fovea capitis (303[1]) is noted in the MRCA of neotheropods, having been reversed (303[0]) in the MRCA of avetheropods. In the Carnosauria hypothesis, this scenario would be more complicated, and the loss of this structure would converge between Coelurosauria and non-Piatnitzkysauridae allosauroids.

(7) Character 308; Femur, distinctly projecting accessory trochanter (derived from lesser trochanter): Based on our results, the presence of an accessory trochanter such as a triangular flange (308[1]) is a shared condition among avetheropods (reversed in *Concavenator* and acquired independently in *Suchomimus*). In the Carnosauria hypothesis, Coelurosauria and non-Piatnitzkysauridae allosauroids (and *Suchomimus*) would converge in the acquisition of the triangular flange; whereas Piatnitzkysauridae (as early allosauroids) would diverge from

other allosauroids due to their weak and slightly thickened margin of the lesser trochanter (308[0]).

(8) Character 309; Femur, *M. femorotibialis externus* origin medially on anterodistal surface: In our results, megalosauroids converge with *Dilophosaurus*, *Sinosaurus*, and *Chuandongocoelurus* in the presence of a faint, small rugose patch (309[0]), whereas Allosauroidea (including the MRCA) have a pronounced rugose depression that extends to the distal femur (309[1]). Considering the Carnosauria hypothesis, the placement of Piatnitzkysauridae at the base of Allosauroidea would suggest this represented the plesiomorphic allosauroid condition for this character, later modified in non-Piatnitzkysauridae allosauroids.

(9) Character 310; Femur, development of medial epicondyle: Our results find the presence of a ridge (310[1]) as convergent between *Coelophysis*, ceratosaurs, early tetanurans, and allosauroids (except *Saurophaganax*). In the Carnosauria hypothesis, not all allosauroids would have this condition, because Piatnitzkysauridae has a rounded medial epicondyle (310[0]).

(10) Character 316; Femur, morphology of distal end: Our results indicate that the acquisition of an anteroposteriorly oriented shallow trough separating the medial and lateral convexities on the distal end of the femur (316[1]) evolved in the MRCA of avetheropods (except *Yangchuanosaurus*). In the Carnosauria hypothesis, this scenario becomes more complex: this feature (i.e., 316[1]) would have arisen independently in Coelurosauria and non-Piatnitzkysauridae allosauroids.

(11) Character 325; Fibula, depth of fibular fossa on medial aspect: Although there is some homoplasy in our results, a deep fossa (325[2]) was present in Tetanurae (except Megalosauria, which presents a shallow fossa (325[1])). Even in the Carnosauria hypothesis, the interpretation is similar, because Piatnitzkysauridae shares the same condition (i.e., 325[2]) with Allosauroidea and Coelurosauria.

3.5. Summary of results

First, our phylogeny recovers piatnitzkysaurids as the first clade to diverge among megalosauroids, then a succession of taxa represented by a polytomy among megalosaurids, but with *Megalosaurus* and *Torvosaurus* being closely related, and then spinosaurids having *Baryonyx* as the first branch of divergence and *Suchomimus* as the outgroup of Spinosaurinae.

Second, we reveal key morphological transitions within/at Megalosauroidea. During the evolution of megalosauroids, there was (i) the mosaic emergence of a low swollen ridge on the ilium (in piatnitzkysaurids, *Afrovenator*, *Megalosaurus*, and *Suchomimus*); (ii) enlargement of the posterior portion of the brevis fossa (in *Marshosaurus*, *Eustreptospondylus*, and spinosaurids except *Ichthyovenator*); (iii) the anterior wall of the brevis fossa became taller along its whole length in *Suchomimus* and *Spinosaurus*; (iv) emergence of a prominent posterodorsal process on the ilium in some megalosaurids; (v) changes in the orientation of the pubis shaft, becoming ventrally concave in *Marshosaurus* and dorsally concave in *Spinosaurus*; (vi) the ischial shafts became ventrally curved in some megalosaurids; (vii) origin of a femoral head that is anteromedially oriented and medially angulated; (viii) a narrow and longitudinal tibiofibularis crest in non-piatnitzkysaurid megalosauroids; (ix) appearance of a posterolaterally oriented medial condyle of the femur in spinosaurids, and (x) medial and lateral condyles that project distally in *Suchomimus* and *Spinosaurus*. The posterior width of brevis fossa and the morphology of ischial symphysis seems to be the most homoplastic features in megalosauroids. These and other traits have some functional relevance (as well as some unclear relevance) detailed above, and further considered below.

Third, we characterise how pelvic and hindlimb characters occupy different (or similar) regions of morphospace in Theropoda. The greatest dissimilarity in the ilium was in megalosaurids based on the large morphospace area – a high degree of homoplasy is suggested for this structure in Orionides. For the pubis, the greatest morphological variation occurs in piatnitzkysaurids and spinosaurids, and there is a distinction among coelophysoids, carcharodontosaurs and others theropods – the overlap between non-carcharodontosaur tetanurans suggests a moderate amount of pubic homoplasy. The largest ischial morphospace area is occupied by spinosaurids and ceratosaurs – we find a weak phylogenetic signal, suggesting abundant homoplasy. We uncover a clear distinction in the femoral morphospace distribution pattern regarding megalosauroids and other theropods, such as avetheropods and non-tetanurans (suggesting a strong phylogenetic signal). Finally, piatnitzkysaurids show the greatest dissimilarity of zeugopodial characters: a distinction in the morphospace is evident for carcharodontosaurs, ceratosaurs and coelophysoids, whereas overlaps occur mainly among megalosaurids, piatnitzkysaurids and neovenatorids, suggesting some homoplasy.

4. CONCLUSIONS

4.1. Phylogenetic inference

Our phylogenetic analysis conducted after inclusion of extra spinosaurid specimens, and reinterpretation of a few characters related to the locomotor system (Carrano *et al*., 2012), recovered a monophyletic Megalosauroidea clade (Figure 1.1) based on at least 11 synapomorphies (ambiguous and unambiguous) related to cranial and axial skeleton structures (Figure 1.31). Similar to previous analyses (e.g., Carrano *et al*., 2012; Evers *et al*., 2015; Rauhut *et al*., 2016; Sales & Schultz, 2017; Malafaia *et al*., 2020), our phylogenetic inference includes taxa from the clades Piatnitzkysauridae, Megalosauridae, and Spinosauridae in Megalosauroidea (however, see below).

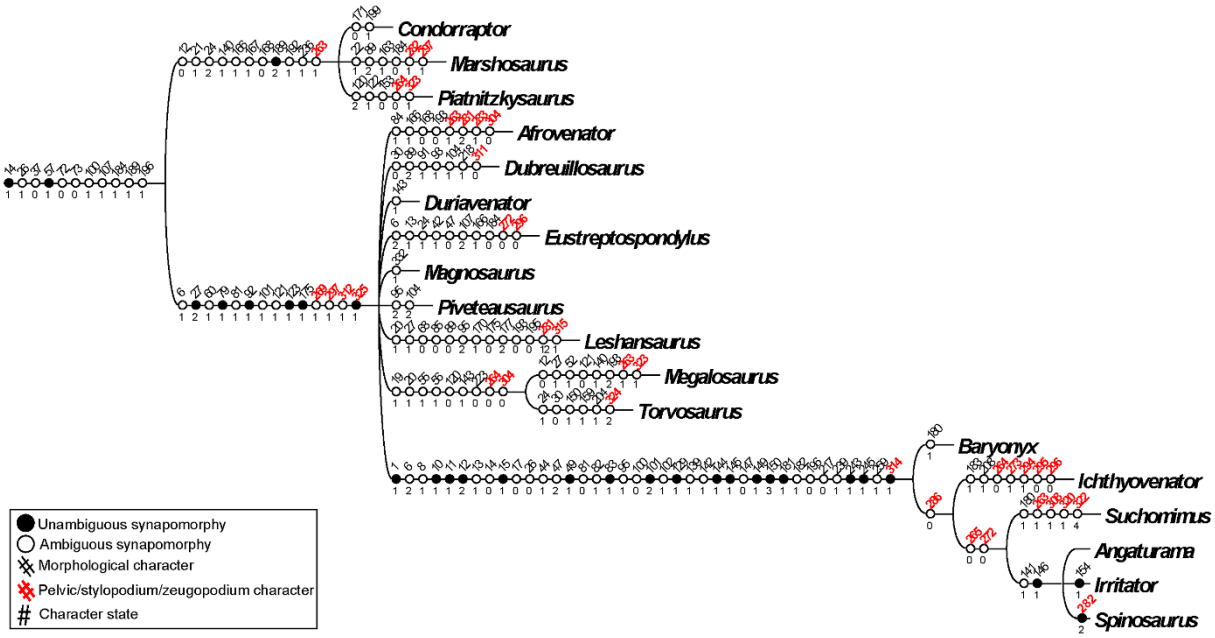

Figure 1.31. Mapped synapomorphies (unambiguous changes) for Megalosauroidea based on results retrieved from our phylogenetic analysis.

Within Megalosauroidea, the first branch of divergence is the medium-sized species of the Piatnitzkysauridae clade (*Condorraptor*, *Marshosaurus*, and *Piatnitzkysaurus*) (Figure 1.1), which also have 11 synapomorphic features related to cranial structures and the axial and appendicular skeleton (Figure 1.31), in addition to a synapomorphy of the locomotor system, which is the presence of a low swollen ridge on the lateral surface of the ilium (263[1]; Figure 1.2, Figure 1.31). Our analysis recovers Piatnitzkysauridae as a polytomy for the three species of the clade, differing from previous analyses that usually recovered the North American

Jurassic taxon *Marshosaurus* as an early-diverging species, followed by a clade formed by the South American Jurassic forms *Condorraptor* + *Piatnitzkysaurus* (e.g., Carrano *et al*., 2012; Rauhut & Pol, 2019). However, in other approaches (e.g., Benson, 2010; Rauhut *et al*., 2016), the Middle Chinese Jurassic taxon *Xuanhanosaurus* is recovered at the base of Piatnitzkysauridae. Instead, Carrano *et al*. (2012) recovered *Xuanhanosaurus* within the avetheropod clade Metriacathosauridae, and considered it as a wildcard, so we did not include this taxon in our search. Even though our analysis is inconclusive about the internal evolutionary relationships of Piatnitzkysauridae, our inference supports that this clade represents the early Megalosauroidea clade, which in turn represents the first group of Tetanurae to diversify.

Our analysis recovered Megalosauria as a sister clade of Piatnitzkysauridae. Megalosauria is composed of the species traditionally placed in Megalosauridae and Spinosauridae. Megalosauria is supported by at least 14 synapomorphies (Figure 1.31), four of which (three ambiguous and one unambiguous) related to the locomotor system: 1) transversely concave shape of acetabular margin of the ilium (269[1]; Figure 1.8); 2) morphology of the ischial symphysis expanded as apron (297[1]); 3) narrow and longitudinal tibiofibularis crest of the femur (312[1]; Figure 1.22); and the unambiguous 4) shallow fossa on the medial position of the fibula (325[1]).

Our search failed to retrieve Megalosauridae as a clade as previously defined (Carrano *et al*., 2012); instead, in our consensus topology the Jurassic species traditionally allocated in Megalosauridae represent a grade, with successive taxa representing outgroups to Spinosauridae (Figure 1.1). Megalosauridae represented by a polytomy is not new in the literature (e.g., Charig & Milner, 1997; Holtz, 1998; Sales & Schultz, 2017; but see Carrano *et al*., 2012), however, the group is based on previous diagnoses, based on cranial, axial and appendicular skeletal synapomorphies (Holtz *et al*., 2004; Carrano *et al*., 2012). Nevertheless, when we adopt the Majority Rules Consensus tree, considering 85% of the "required frequency of clades", we recover Megalosauridae as a clade (Figure 1.32a); considering 80% of frequency, the Megalosaurinae clade is also recovered with the presence of *Duriavenator* at the base (Figure 1.32b); and in the last approach, considering 60% of frequency, we recovered both monophyletic Megalosauridae, as well as Megalosaurinae and Afrovenatorinae (Figure 1.32c) – similar to the results of Carrano *et al*., 2012). One of the synapomorphies of Megalosauridae hypothesised by Carrano *et al*. (2012), related to the locomotor system, is the presence of a shallow groove on the posterior surface of the femur that demarcates the presence of the oblique ligament (304[0]). However, in our results this condition seems to represent an independent

acquisition in *Afrovenator* and in the clade composed by *Megalosaurus* + *Torvosaurus* (Figure 1.31). Finally, although we failed to recover Megalosauridae, a clade composed by *Megalosaurus* + *Torvosaurus* is recovered (Figure 1.1), somewhat equivalent with the clade Megalosaurinae (*sensu* Carrano *et al*., 2012), however without *Dubreuillosaurus*. This clade is supported by 9 synapomorphies, two of which are related to the locomotor apparatus: 304[0] above, in addition to the presence of a brevis fossa whose posterior width is subequal to the anterior 264[0] (Figure 1.3; Figure 1.31). A close evolutionary relation between *Megalosaurus* and *Torvosaurus* was corroborated by several approaches (e.g., Benson, 2010; Carrano *et al*., 2012; Samathi *et al*., 2021). If the polytomy represented by Megalosauridae recovered here and in previous studies (e.g., Sales & Schultz, 2017) represents a soft or a hard polytomy, future efforts to re-study and describe new materials (which have been developed in recent decades; e.g., Sereno *et al*., 1994; Benson, 2008; 2010; Sadleir *et al*., 2008; Carrano *et al*., 2012; Rauhut *et al*., 2016; Malafaia *et al*., 2017) should clarify this issue.

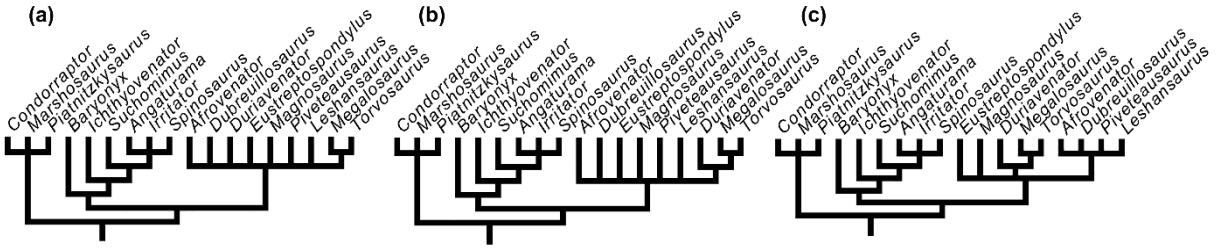

Figure 1.32. Majority Rules Consensus Tree of Megalosauroidea considering the "required frequency of clades": (a) 85%; (b) 80%; (c) 60%.

We recovered the Spinosauridae clade based on several synapomorphies (Figure 1.31), among them the posterolateral orientation of the long axis of the medial condyle of the femur in distal view (314[1]; Figure 1.23), representing an unambiguous synapomorphy. Internally, *Baryonyx* represents the first species to diverge, representing the outgroup of a larger clade containing *Ichthyovenator*, *Suchomimus*, and the more deeply nested clade Spinosaurinae; that larger clade has a marginal pubic symphysis morphology (286[0]) as a synapomorphy. *Ichthyovenator* in turn is the outgroup of a smaller clade containing *Suchomimus* and Spinosaurinae, being supported by two synapomorphies of the locomotor apparatus: lateral wall of brevis fossa of the ilium in relation to the medial wall taller along whole length (265[0]; Figure 1.4) and length to width ratio of the pubic peduncle </= 1 (272[0]). Finally, the Spinosaurinae clade presents two unambiguous synapomorphies (Figure 1.31) related to dentition, however there is no internal resolution for this clade. The dichotomy between Baryonychinae and Spinosaurinae has been recently questioned (Evers *et al*., 2015; Sales &

Schultz, 2017), however most of the recent phylogenetic approaches, even with low support, recover Baryonychinae as a natural group (e.g., Rauhut *et al*., 2016; Malafaia *et al*., 2020; Barker *et al*., 2021; Lacerda *et al*., 2022; Rauhut & Pol, 2019; see a summary in Lacerda *et al*., 2023b). Our results do not recover a monophyletic Baryonychinae (Figure 1.1), but rather taxa considered "Baryonychinae" in a succession of outgroups of Spinosaurinae, as proposed by Sales & Schultz (2017). However, it is noteworthy that other species that are not based on the appendicular skeleton, or that are only poorly preserved, were not considered here (e.g., Malafaia *et al*., 2020; Barker *et al*., 2021; Mateus & Estraviz-López, 2022), so more integrative approaches combined with new discoveries can shed light on this subject.

4.2. Numerical sampling of the characters evaluated

The characters we studied here, which include the pelvis and the hindlimb stylopodium and zeugopodium, are about 19.3% of the characters in the original taxon-character matrix of Carrano *et al*. (2012). If we consider all of the bony elements of the pelvic girdle and hindlimbs (i.e., metatarsals and pedal digits), the total percentage is 24.5% of the total of the morphological characters. According to Cashmore & Butler (2019), the bones of the pelvis and hindlimbs (including the elements of the feet), on average, have the highest numerical representation in theropods (35.75%). Thus, there is no numerical congruence between the proportional mean of the elements of the locomotor apparatus and the total of characters used in this study. Therefore, in general, more revisions and eventual inclusions of new morphological characters from the locomotor system are needed. However, a balance between the number of characters and the degree of information must be considered in order not to decrease the quality of the character matrices (Yu *et al*., 2021).

The completeness of the fossil record in different groups of theropods is influenced by factors such as climate dynamics, research history and transport energy, for example. Additional possible biases are linked to the depositional environment (ecology), but not to body size (Cashmore & Butler, 2019). Regardless of these factors, the correlation between proportional mean of skeletal elements versus mean percentage of characters of skeletal elements does not seem to be influenced by preservational aspects, but by historical focus in the research on certain skeletal elements (e.g., cranial characters versus postcranial characters).

Finally, the greatest representation of characters from the locomotor apparatus (used here, derived from Carrano *et al*. 2012) is from the ilium (27.94%) and femur (23.52%), followed by pubis (14.7%) and ischium (13.2%), whereas the tibia (11.76%) and fibula (5.88%) are the

structures with the fewest morphological characters used. Revisions of morphological characters, especially of the zeugopodium, may improve understanding of the osteological evolution of the locomotor system in theropod dinosaurs.

4.3. Locomotor apparatus morphology and main morphological changes throughout theropod evolution

Functional aspects related to bipedalism and gait gradually changed over macroevolutionary time in the lineage of theropod dinosaurs, which consequently gave rise to the most diverse locomotor mechanisms observed in birds (Gatesy, 1990; Carrano, 2000; Hutchinson & Gatesy, 2000; Hutchinson & Allen, 2009; Allen *et al*., 2021; Cuff *et al*., 2023). However, such morphofunctional adaptations present a continuous series, or stepwise functional evolution (Hutchinson, 2001a; 2002; Hutchinson & Allen, 2009). As an example of this "gradual evolution" in the avian lineage, features such as hip flexion and knee articulation, among others, stand out (Gatesy, 1990; Hutchinson, 2002). Early-diverging tetanurans, as noted by Carrano *et al*. (2012), represent a prime example of this transition from an ancestral dinosaurian locomotor morphology to a derived or "bird-like" morphology present in coelurosaurs. Many morphological acquisitions related to the evolution of the locomotor system in dinosaurs occurred in parallel more than once throughout the evolution of the clade (Carrano, 2000), among them more expanded iliac processes, changes of the morphology of the head of the femur and the lesser trochanter, many of which contributed to altered biomechanical functions in locomotion (Carrano, 2000; Hutchinson, 2001a,b; 2002; Hutchinson & Allen, 2009; Allen *et al*., 2021).

Carrano *et al*. (2012) highlighted that even though there were variations in the locomotor morphology of early tetanurans throughout their evolution, such characteristics seem to have occurred to a lesser extent when compared to other theropod clades (e.g., ceratosaurs and coelurosaurs). Thus, early tetanurans had a relatively generalised locomotor morphology for early theropods. However, morphological variations, especially in megalosauroids (summarised in section 3.4), suggest distinctions in functions of parts of the locomotor apparatus.

Based on our analysis, we summarise the following evolutionary aspects and their potential morphofunctional implications in megalosauroids:

Pelvis. A low swollen ridge on the lateral surface of the ilium is present in Piatnitzkysauridae and other species such as Afrovenator, Megalosaurus, and Suchomimus

(Figure 2); this ridge potentially indicates a strong separation between the origins of the ITC/IFE and ILFB muscles (e.g., Carrano & Hutchinson, 2002). The brevis fossa with a posterior width greater than the anterior one is the condition in *Marshosaurus*, *Eustreptospondylus*, and spinosaurids (except *Ichthyovenator*) (Figure 1.3); furthermore, in the spinosaurids *Suchomimus* and *Spinosaurus* the height of the lateral wall of the brevis fossa relative to the medial one is taller along the whole length (differing from other megalosauroids) (Figure 1.4). Both latter conditions of the brevis fossa suggest a greater size of the CFB muscle (with the posterior enlargement) and might indicate a more restricted CFB origin and smaller muscle size anteriorly in *Suchomimus* and *Spinosaurus*. In general, the pubic peduncle length to width ratio in megalosauroids is between 1.3–1.75; however, in *Eustreptospondylus* and the spinosaurids *Suchomimus* and *Spinosaurus*, the plesiomorphic condition of the ratio ≤1 may indicate a more restricted origin of PIFI1 in these taxa. The presence of a ridge on the medial surface of the ilium adjacent to the preacetabular notch is a feature noted in *Ichthyovenator*; this condition combined with a larger peduncle may suggest an expanded PIFI1 origin. The posterior margin of the postacetabular blade of the ilium in megalosauroids is generally convex, however in *Eustreptospondylus*, *Megalosaurus*, and *Torvosaurus* (Figure 1.11) the presence of a prominent posterodorsal process may indicate a greater extent of the origin of IT3 and somewhat a more restricted origin of the IFE at the posterior margin of the ilium.

The pubic shaft in almost all megalosauroids studied is straight, the exceptions being *Marshosaurus* with a ventrally concave shaft and *Spinosaurus* with a dorsally concave pubic shaft (Figure 1.12). Such differences may not influence the area of origin or the size of the PIFE1–2 muscles; however, the moment arms of the associated musculature might have had at least slight changes with this disparate morphology. The shape of the pubic symphysis in non-spinosaurid megalosauroids is broad, whereas in spinosaurids (except *Baryonyx*) the morphology of the symphysis is marginal. This feature associated with other pelvic fusion conditions might be relate to increased rigidity/strength of this structure, and the pubic boot may have provided stronger resistance to supporting body weight during sitting (as well as enlarged abdominal muscle insertions and improved inspiratory flow, as previously suggested (e.g., Carrier & Farmer, 2000). In spinosaurids (based on *Ichthyovenator* and *Suchomimus*), there is an increase in the size of the obturator foramen, which may reflect the reduction of the pelvic surface area and hence reduction of the associated musculature size (e.g., PIFE3) or even losses of muscles (e.g., parts of the *flexor cruris* ventral group).

The relative size of the ischium to the pubis in megalosauroids generally ranges from 75–80% (although this relationship is poorly understood in megalosaurids). A relatively larger

ischium, >80% of the pubis, is characteristic of *Torvosaurus* and *Spinosaurus*; such taxa may have had an increased area of origin of the associated musculature (e.g., PIFE3, ADD2, ISTR). The shaft of the ischium in piatnitzkysaurids and spinosaurids is straight, whereas in megalosaurids (except *Torvosaurus*) the shaft is ventrally curved (Figure 1.14); these shape differences would at least slightly alter the moment arms (e.g., Allen *et al*., 2021) of muscles with ischial origins. Most megalosauroids have a reduced ischial antitrochanter, except for the spinosaurid *Ichthyovenator*, which has a large and notched antitrochanter. The latter feature may have limited abduction of the hindlimb as well as perhaps reduce stresses, similar to how the antitrochanter is assumed to function in Aves (Hertel & Campbell, 2007); however, more quantitative, biomechanical research is needed in this regard, as antitrochanter function remains obscure. In the region ventral to the obturator process, a notch is present in piatnitzkysaurids, *Afrovenator*, and spinosaurids (except *Ichthyovenator*) (Figure 1.15), suggesting that in these taxa the PIFE3 and ADD1 origins may have been reduced in size. The opposite is evident for the expanded apron morphology of the ischial symphysis observed in *Marshosaurus*, *Eustreptospondylus*, *Megalosaurus*, *Torvosaurus*, and *Ichthyovenator*; which could be correlated with an enlargement of muscle origins, such as for ADD1 and PIFE3.

Appendage. In the proximal part of the femur, the groove for the oblique ligament in the posterior region of the head is shallow in *Afrovenator*, *Megalosaurus*, *Torvosaurus*, and *Spinosaurus*, which differs from the deep groove noted in other theropods. However, it is not clear whether this ligament and groove depth provided any special constraints to mobility, being a feature that is variable in Dinosauriformes (Tsai *et al*., 2018). In megalosauroids, the presence of an accessory trochanter that derives from the lesser trochanter in general represents a weak structure that forms only a slightly thickened margin. However, in *Suchomimus* the accessory trochanter is represented by a triangular flange (Figure 1.20), and this structure is associated with the insertion of PIFI2, which suggests at least slight alterations in PIFI2 muscle actions in this species. On the distal part of the femur, the tibiofibularis crest in piatnitzkysaurids is broad, but in other megalosauroids this crest is narrow and longitudinal (Figure 1.22); it is not clear how these differences might have altered the biomechanics of the knee joint. Two other features of the distal femur that may have altered locomotor biomechanics are the orientation of the medial condyle axis, which is posterolateral only in spinosaurids (Figure 1.23); and the distal projection of the lateral and medial condyles, which is approximately equal in several megalosauroids, with a distally projection of the lateral condyle in *Leshansaurus*, and distally projection of the medial condyle in *Suchomimus* and *Spinosaurus* (Figure 1.24), but further biomechanical studies are needed to unravel any implications of these structures. Finally, a

shallow fibular fossa is the main feature of megalosauroids; except piatnitzkysaurids, which have a deep medial fossa on the fibula; this fossa might be a more concentrated origin of part of the digital flexor's muscles, or part of the "popliteus"/interosseous cruris/pronator profundus, which suggests greater robustness of this musculature in piatnitzkysaurids.

Together, these possible changes of muscle positions and sizes (reductions and expansions), and alterations of joint morphology, hint at widespread, complex changes of musculoskeletal function across Megalosauroidea. As these features sometimes are subtle or simply qualitatively described here, they deserve more rigorous quantitative characterisation. Although there has been progress in studies of the evolution of the locomotor system in theropods (e.g., Carrano & Hutchinson, 2002; Hutchinson, 2002; Grillo & Azevedo, 2011; Bates *et al*., 2012; Rhodes *et al*., 2020; Allen *et al*., 2021; Bishop *et al*., 2021; Smith *et al*., 2021; Cuff *et al*., 2023), focus on groups such as the Megalosauroidea has been almost non-existent. Armed with the basic insights on morphological evolution presented here, future studies could, for example, map the appendicular musculature in Megalosauroidea and use such data to conduct quantitative biomechanical analyses of the functional impact of morphological traits (e.g., Grillo & Azevedo, 2011; Bates *et al*., 2012; Bishop *et al*., 2018; 2021), contextualising Megalosauroidea with other theropods.

4.4. Morphological disparity of the locomotor apparatus in early theropods (especially Megalosauroidea)

Based on our disparity analyses focusing in megalosauroids, the greatest disparity calculated for the ilium is among megalosaurids; for the pubis it is in both piatnitzkysaurids and spinosaurids; for the ischium it is in spinosaurids; there is a clear distinction in femoral morphospace distribution for megalosauroids and other theropods; and piatnitzkysaurids show the greatest disparity of zeugopodium characters (Figure 1.29; Figure 1.30). Based on our interpretations, the most homoplastic structures are: (1) the ilium in Orionides; (2) the pubis, to a lesser extent, among non-carcharodontosaur averostrans; (3) the ischium among most species; and (4) fibula/tibia, to a lesser extent, between non-spinosaurid megalosauroids and neovenatorids.

Using morphological data and taxa different from those used here, an approach carried out by Novas *et al*. (2015) evaluated key aspects of morphological disparity in theropod dinosaurs. Considering all morphological characters of the skeleton, Novas *et al*. (2015) found that the clade that occupies the largest area in morphospace is Coelurosauria, which is expected

given the wide variety of forms found in this clade; including Aves (Foth & Rauhut, 2013; Novas *et al*., 2015). Similarly, Brusatte *et al*. (2012) found, based on cranial morphology and palaeoecology, that non-carnivorous theropods have greater morphological disparity than carnivorous theropods; in a second taxonomically-based approach, they showed that the greatest disparities are in ceratosaurs and in coelurosaurian oviraptorosaurs, interestingly noting that non-carnivorous taxa are included in both clades. Both studies (Brusatte *et al*., 2012; Novas *et al*., 2015) suggest that theropod skulls have broad disparity, probably relating to disparate feeding mechanisms and ecologies.

Considering postcranial elements, Novas *et al*. (2015) divided their analyses into several structures. They obtained the following results for the locomotor apparatus: 1) Pelvic girdle. Three distinct morphospaces, occupied by non-neotheropods, non-megalosauroids tetanurans, and coelurosaurs; a large area occupied by coelurosaurs could in part be explained by the retroverted pubis, absence of the supraacetabular crest, and the presence of a transversely enlarged ischial peduncle noted in some taxa; 2) Hindlimb stylopodium and zeugopodium. Four distinct morphospaces, occupied by non-neotheropods, non-averostrans, ceratosaurs, and tetanurans. Again, coelurosaurs occupied a large area, especially with the influence of the greatest variance component (i.e., PCoA1).

In our complete analysis (Figure 1.29A), the distribution of megalosaurids in the morphospace can be explained by the puboischiadic plate, morphology of the femoral condyles, and the morphology/development of the fibular crest of the tibia. Considering the pubis (Figure 1.29E), megalosaurids occupy a large area in morphospace influenced by PCO2, which can be explained by both proximal and distal pubic articulations. In the analysis of the ischium (Figure 1.30A), the distribution of megalosaurids, influenced by PCO1, seems to be explained by the relative length of the pubis/ischium, the orientation of the ischial shaft, and the ventral notch of the obturator process. Analysing only the femur (Figure 1.30C), a clearly distinction among Orionides and non-Orionides theropods are noted. Considering the zeugopodium (Figure 1.30E), the great overlap area is shared among the megalosauroid piatnitzkysaurids, megalosaurids and the allosauroid metriacanthosaurids. The distribution of the megalosaurids is influenced by the morphology of the fibular crest of the tibia. As final remarks, throughout the macroevolution of tetanuran theropod dinosaurs, the ilium, ischium and the femur seem to play a role in the differentiation of several taxa, appearing to be the most disparate structures of the locomotor system. Meanwhile, the femur in megalosauroids causes the group to be segregated in the morphospace between non-Orionides and Avetheropods. New approaches

revising the characters used here and complementing them with autapomorphic proposals for some species (e.g., Ibrahim *et al*., 2014) may increase our understanding of this dinosaur clade.

5. REFERENCES

Allain R, Xaisanavong T, Richir P, Khentavong B. 2012. The first definitive Asian spinosaurid (Dinosauria: Theropoda) from the early cretaceous of Laos. **Naturwissenschaften**, 99(5):369–377.

Allen VR, Kilbourne BM, Hutchinson JR. 2021. The evolution of pelvic limb muscle moment arms in bird-line archosaurs. **Science Advances**, 7(12):eabe2778.

Amiot R, Buffetaut E, Lécuyer C, Wang X, Boudad L, Ding Z, Fourel F, Hutt S, Martineau F, Medeiros MA, Mo J, Simon L, Suteethorn V, Sweetman S, Tong H, Zhang F, Zhou Z. 2010. Oxygen isotope evidence for semi-aquatic habits among spinosaurid theropods. **Geology**, 38(2):139–142.

Arden TMS, Klein CG, Zouhri S, Longrich NR. 2019. Aquatic adaptation in the skull of carnivorous dinosaurs (Theropoda: Spinosauridae) and the evolution of aquatic habits in spinosaurs. **Cretaceous Research**, 93:275–284.

Aureliano T, Ghilardi AM, Müller RT, Kerber L, Pretto FA, Fernandes MA, Ricardi-Branco F, Wedel MJ. 2022. The absence of an invasive air sac system in the earliest dinosaurs suggests multiple origins of vertebral pneumaticity. **Scientific Reports**, 12(1):20844.

Barker CT, Hone DW, Naish D, Cau A, Lockwood JA, Foster B, Clarkin CE, Schneider P, Gostling NJ. 2021. New spinosaurids from the Wessex Formation (Early Cretaceous, UK) and the European origins of Spinosauridae. **Scientific Reports**, 11:19340.

Bates KT, Benson RBJ, Falkingham. 2012. A computational analysis of locomotor anatomy and body mass evolution in Allosauroidea (Dinosauria, Theropoda). **Paleobiology**, 38(3):486–507.

Benson RB. 2008. A redescription of '*Megalosaurus*' *hesperis* (Dinosauria, Theropoda) from the Inferior Oolite (Bajocian, Middle Jurassic) of Dorset, United Kingdom. **Zootaxa**, 1931(1):57–67.

Benson RBJ. 2010. A description of *Megalosaurus bucklandii* (Dinosauria: Theropoda) from the Bathonian of the UK and the relationships of Middle Jurassic theropods. **Zoological Journal of the Linnean Society**, 158:882–935.

Benson RBJ, Mannion PD, Butler RJ, Upchurch P, Goswami A, Evans SE. 2013. Cretaceous tetrapod fossil record sampling and faunal turnover: implications for biogeography and the rise of modern clades. **Palaeogeography, Palaeoclimatology, Palaeoecology**, 372:88-107.

Bishop PJ, Cuff AR, Hutchinson JR. 2021. How to build a dinosaur: Musculoskeletal modeling and simulation of locomotor biomechanics in extinct animals. **Paleobiology**, 47(1):1–38.

Bishop PJ, Hocknull SA, Clemente CJ, Hutchinson JR, Farke AA, Beck BR, Barret RS, Lloyd DG. 2018. Cancellous bone and theropod dinosaur locomotion. Part I—an examination of cancellous bone architecture in the hindlimb bones of theropods. **PeerJ**, 6:e5778.

Bonaparte JF. 1979. Dinosaurs: A Jurassic Assemblage from Patagonia. **Science**, 205(4413):1377–1379.

Brusatte SL, Montanari S, Yi H, Norell MA. 2011. Phylogenetic corrections for morphological disparity analysis: new methodology and case studies. **Paleobiology**, 37(1):1–22.

Brusatte SL, Sakamoto M, Montanari S, Harcourt Smith WEH. 2012. The evolution of cranial form and function in theropod dinosaurs: insights from geometric morphometrics. **Journal of Evolutionary Biology**, 25(2):365–377.

Buckland W. 1824. XXI.—Notice on the *Megalosaurus* or great Fossil Lizard of Stonesfield. **Transactions of the Geological Society of London**, 1(2):390–396.

Carrano MT. 2000. Homoplasy and the evolution of dinosaur locomotion. **Paleobiology**, 26(3):489–512.

Carrano MT. 2007. The appendicular skeleton of *Majungasaurus crenatissimus* (Theropoda: Abelisauridae) from the Late Cretaceous of Madagascar. **Journal of Vertebrate Paleontology**, 27(S2):163–179.

Carrano MT, Hutchinson JR. 2002. Pelvic and hindlimb musculature of *Tyrannosaurus rex* (Dinosauria: Theropoda). **Journal of Morphology**, 253:207–228.

Carrano MT, Sampson SD. 2008. The phylogeny of Ceratosauria (Dinosauria: Theropoda). **Journal of Systematic Palaeontology**, 6(2):183–236.

Carrano MT, Benson RBJ, Sampson SD. 2012. The phylogeny of Tetanurae (Dinosauria; Theropoda). **Journal of Systematic Palaeontology**, 10(2):211–300.

Carrano MT, Loewen MA, Sertich JJ. 2011. New materials of *Masiakasaurus knopfleri* Sampson, Carrano, and Forster, 2001, and implications for the morphology of the Noasauridae (Theropoda: Ceratosauria). **Smithsonian Contributions to Paleobiology**, 95:53 p.

Carrier DR, Farmer CG. 2000. The evolution of pelvic aspiration in archosaurs. **Paleobiology** 26(2):271-293.

Cashmore DD, Butler RJ. 2019. Skeletal completeness of the non-avian theropod dinosaur fossil record. **Palaeontology**, 62(6):951–981.

Charig AJ, Milner AC. 1986. *Baryonyx*, a remarkable new theropod dinosaur. **Nature**, 324(27):359–361.

Charig AJ, Milner AC. 1997. *Baryonyx walkeri*, a fish-eating dinosaur from the Wealden of Surrey. **Bulletin of the Natural History Museum: Geology Series**, 53(1):11–70.

Cuesta E, Ortega F, Sanz JL. 2018. Appendicular osteology of *Concavenator corcovatus* (Theropoda: Carcharodontosauridae) from the Lower Cretaceous of Spain. **Journal of Vertebrate Paleontology**, 38(4):1–24.

Cuff AR, Demuth OE, Michel K, Otero A, Pintore R, Polet DT, Wiseman ALA, Hutchinson JR. 2023. Walking—and Running and Jumping—with Dinosaurs and their Cousins, Viewed Through the Lens of Evolutionary Biomechanics. **Integrative and Comparative Biology**, 62(5):1281–1305.

Cuff AR, Rayfield EJ. 2013. Feeding mechanics in spinosaurid theropods and extant crocodilians. **PLoS One**, 8(5), e65295.

Dal Sasso C, Maganuco S, Buffetaut E, Mendez MA. 2005. New information on the skull of the enigmatic theropod *Spinosaurus*, with remarks on its size and affinities. **Journal of Vertebrate Paleontology**, 25(4):888–896.

Egawa S, Griffin CT, Bishop PJ, Pintore R, Tsai HP, Botelho JF, Smith-Paredes D, Kuratani S, Norell MA, Nesbitt SJ, Hutchinson JR, Bhullar BAS. 2022. The dinosaurian femoral head experienced a morphogenetic shift from torsion to growth along the avian stem. **Proceedings of the Royal Society B: Biological Sciences**, 289(1984):20220740.

Evers SW, Rauhut OW, Milner AC, McFeeters B, Allain R. 2015. A reappraisal of the morphology and systematic position of the theropod dinosaur *Sigilmassasaurus* from the "middle" Cretaceous of Morocco. **PeerJ**, 3:e1323.

Fabbri M, Navalón G, Benson RB, Pol D, O'Connor J, Bhullar BAS, Erickson GM, Norell MA, Orkney A, Lamanna MC, Zouhri S, Becker J, Emke A, Dal Sasso C, Bindellini G, Maganuco S, Auditore M, Ibrahim N. 2022. Subaqueous foraging among carnivorous dinosaurs. **Nature**, 603(7903):852–857.

Foth C, Rauhut OWM. 2013. Macroevolutionary and morphofunctional patterns in theropod skulls: a morphometric approach. **Acta Palaeontologica Polonica**, 58(1):1–16.

Gatesy SM. 1990. Caudofemoral musculature and the evolution of theropod locomotion. **Paleobiology**, 16(2):170–186.

Gatesy SM. 1994. Neuromuscular diversity in archosaur deep dorsal thigh muscles. **Brain, Behavior and Evolution**, 43(1):1–14.

Gatesy SM, Middleton KM. 1997. Bipedalism, flight, and the evolution of theropod locomotor diversity. **Journal of Vertebrate Paleontology**, 17(2):308–329.

Gauthier J. 1986. Saurischian monophyly and the origin of birds. **Memoirs of the Californian Academy of Sciences**, 8:1–55.

Goloboff PA, Morales ME. 2023. TNT version 1.6, with a graphical interface for MacOS and Linux, including new routines in parallel. **Cladistics**, 39:144–153.

Gower JC. 2014. Principal coordinates analysis. Wiley StatsRef: Statistics Reference Online, 1–7.

Grillo ON, Azevedo SAK. 2011. Pelvic and hind limb musculature of *Staurikosaurus pricei* (Dinosauria: Saurischia). **Anais da Academia Brasileira de Ciências**, 83(1):73–98.

Guillerme T, Cooper N, Brusatte SL, Davis KE, Jackson AL, Gerber S, Goswami A, Healy K, Hopkins MJ, Jones MEH, Lloyd GT, O'Reilly JE, Pate A, Puttick MN, Rayfield EJ, Saupe EE, Sherratt E, Slater GJ, Weisbecker V, Thomas GH, Donoghue PC. 2020. Disparities in the analysis of morphological disparity. **Biology Letters**, 16(7):20200199.

Gutarra S, Rahman IA. 2022. The locomotion of extinct secondarily aquatic tetrapods. **Biological Reviews**, 97(1):67–98.

Hammer Ø, Harper DAT, Ryan PD. 2001. PAST: Paleontological statistics software package for education and data analysis. **Palaeontologia Electronica**, 4(1):1–9.

Hassler A, Martin JE, Amiot R, Tacail T, Godet FA, Allain R, Balter V. 2018. Calcium isotopes offer clues on resource partitioning among Cretaceous predatory dinosaurs. **Proceedings of the Royal Society B: Biological Sciences**, 285(1876):20180197.

Hattori S, Tsuihiji T. 2021. Homology and osteological correlates of pedal muscles among extant sauropsids. **Journal of Anatomy**, 238(2):365–399.

Henderson DM. 2018. A buoyancy, balance and stability challenge to the hypothesis of a semi-aquatic *Spinosaurus* Stromer, 1915 (Dinosauria: Theropoda). **PeerJ**, 6:e5409.

Hendrickx C, Hartman SA, Mateus O. 2015. An overview of non-avian theropod discoveries and classification. **Palarch's Journal of Vertebrate Palaeontology**, 12(1):1–73.

Hendrickx C, Mateus O, Araújo R. 2019. The distribution of dental features in non-avian theropod dinosaurs: taxonomic potential, degree of homoplasy, and major evolutionary trends. **Palaeontologia Electronica**, 22(3):1–10.

Hendrickx C, Mateus O, Buffetaut E. 2016. Morphofunctional analysis of the quadrate of Spinosauridae (Dinosauria: Theropoda) and the presence of *Spinosaurus* and a second spinosaurine taxon in the Cenomanian of North Africa. **PLoS One**, 11(1):e0144695.

Hendrickx C, Tschopp E, Ezcurra MD. 2020. Taxonomic identification of isolated theropod teeth: the case of the shed tooth crown associated with *Aerosteon* (Theropoda: Megaraptora) and the dentition of Abelisauridae. **Cretaceous Research**, 108:104312.

Hertel F, Campbell Jr KE. 2007. The antitrochanter of birds: Form and function in balance. **The Auk**, 124(3):789–805.

Holtz Jr TR. 1998. A new phylogeny of the carnivorous dinosaurs. **GAIA: revista de Geociências**, 15:5–61.

Holtz Jr TR, Molnar RE, Currie PJ. 2004. Basal Tetanurae. In The Dinosauria (eds DB Weishampel, P Dodson, H Osmólska), pp. 71–110. University of California Press, Berkeley, Florida.

Hone DWE, Holtz Jr TR. 2017. A century of spinosaurs - A review and revision of the Spinosauridae with comments on their ecology. **Acta Geologica Sinica**, 91(3):1120–1132.

Hone DWE, Holtz Jr TR. 2019. Comment on: Aquatic adaptation in the skull of carnivorous dinosaurs (Theropoda: Spinosauridae) and the evolution of aquatic habits in spinosaurids. 93: 275–284. **Cretaceous Research**, 134:104152.

Hone DW, Holtz Jr TR. 2021. Evaluating the ecology of *Spinosaurus*: Shoreline generalist or aquatic pursuit specialist?. **Palaeontologia Electronica**, 24(1):a03.

Hutchinson JR. 2001a. The evolution of femoral osteology and soft tissues on the line to extant birds (Neornithes). **Zoological Journal of the Linnean Society**, 131(2):169–197.

Hutchinson JR. 2001b. The evolution of pelvic osteology and soft tissues on the line to extant birds (Neornithes). **Zoological Journal of the Linnean Society**, 131(2):123–168.

Hutchinson JR. 2002. The evolution of hindlimb tendons and muscles on the line to crown-group birds. **Comparative Biochemistry & Physiology. Part A: Molecular and Integrative Physiology**, 133(4):1051–1086.

Hutchinson JR, Allen V. 2009. The evolutionary continuum of limb function from early theropods to birds. **Naturwissenschaften**, 96:423–448.

Hutchinson JR, Garcia M. 2002. *Tyrannosaurus* was not a fast runner. **Nature**, 415(6875):1018–1021.

Hutchinson JR, Gatesy SM. 2000. Adductors, abductors, and the evolution of archosaur locomotion. **Paleobiology**, 26(4):734–751.

Ibrahim N, Maganuco S, Dal Sasso C, Fabbri M, Auditore M, Bindellini G, Martill DM, Zouhri S, Mattarelli DA, Unwin DM, Wiemann J, Bonadonna D, Amane A, Jakubczak J, Joger U, Lauder GV, Pierce SE. 2020. Tail-propelled aquatic locomotion in a theropod dinosaur. **Nature**, 51(7806):67–70.

Ibrahim N, Sereno PC, Dal Sasso C, Maganuco S, Fabbri M, Martill DM, Zouhri S, Myhrvold N, Iurono D A. 2014. Semiaquatic adaptations in a giant predatory dinosaur. **Science**, 345(6204):1613-1616.

Kubo T, Kubo MO. 2012. Associated evolution of bipedality and cursoriality among Triassic archosaurs: a phylogenetically controlled evaluation. **Paleobiology**, 38(3):474–485.

Lacerda MBS, Bittencourt JS, Hutchinson JR. 2023a. Macroevolutionary patterns in the pelvis, stylopodium and zeugopodium of non-avian megalosauroid theropod dinosaurs and their importance for locomotor function. figshare. Dataset. (doi:10.6084/m9.figshare.22325662)

Lacerda MBS, Aragão PRL, Vieira FS, Sales MAF, Liparini A. 2023b. On the first Baryonychinae (Theropoda, Spinosauridae) teeth from South America. **Zootaxa**, 5264(4):526–544.

Lacerda MBS, Grillo ON, Romano PS. 2022. Rostral morphology of Spinosauridae (Theropoda, Megalosauroidea): premaxilla shape variation and a new phylogenetic inference. **Historical Biology**, 34(11):2089–2109.

Langer MC, Ezcurra MD, Bittencourt JS, Novas FE. 2010. The origin and early evolution of dinosaurs. **Biological Reviews**, 85(1):55–110.

Maddison WP, Maddison DR. 2015. Mesquite: a modular system for evolutionary analysis. Version 3.61. Available in http://www.mesquiteproject.org.

Madsen JH. 1976. A second new theropod dinosaur from the Late Jurassic of east central Utah. **Utah Geology**, 3:51–60.

Malafaia E, Dantas P, Ortega F, Escaso F. 2007. Nuevos restos de *Allosaurus fragilis* (Theropoda: Carnosauria) del yacimiento de Andrés (Jurásico Superior; centro-oeste de Portugal). **Cantera Paleontológica**, 1:255–271.

Malafaia E, Gasulla JM, Escaso F, Narvaéz I, Sanz JL, Ortega F. 2020. A new spinosaurid theropod (Dinosauria: Megalosauroidea) from the upper Barremian of Vallibona, Spain: implications for spinosaurid diversity in the Early Cretaceous of the Iberian Peninsula. **Cretaceous Research**, 106:104221.

Malafaia E, Mocho P, Escaso F, Ortega F. 2017. New data on the anatomy of *Torvosaurus* and other remains of megalosauroid (Dinosauria, Theropoda) from the Upper Jurassic of Portugal. **Journal of Iberian Geology**, 43:33–59.

Malafaia E, Ortega F, Escaso F, Silva B. 2015. New evidence of *Ceratosaurus* (Dinosauria: Theropoda) from the Late Jurassic of the Lusitanian Basin, Portugal. **Historical Biology**, 27(7):938–946.

Manafzadeh AR, Kambic RE, Gatesy SM. 2021. A new role for joint mobility in reconstructing vertebrate locomotor evolution. **Proceedings of the National Academy of Sciences**, 118(7):e2023513118.

Marsh AD, Rowe TB. 2020. A comprehensive anatomical and phylogenetic evaluation of *Dilophosaurus wetherilli* (Dinosauria, Theropoda) with descriptions of new specimens from the Kayenta Formation of northern Arizona. **Journal of Paleontology**, 94.S78:1–103.

Mateus O, Estraviz-López D. 2022. A new theropod dinosaur from the early Cretaceous (Barremian) of Cabo Espichel, Portugal: Implications for spinosaurid evolution. **PLoS ONE**, 17(2):e0262614.

Nixon KC. 1999-2002. WinClada ver. 1.0000. Ithaca (NY, USA): Published by the author.

Novas FE. 1996. Dinosaur monophyly. **Journal of Vertebrate Paleontology**, 16(4):723–741.

Novas FE, Salgado L, Suárez M, Agnolín FL, Ezcurra MD, Chimento NR, de la Cruz R, Isasi MP, Vargas AO, Rubilar-Rogers D. 2015. An enigmatic plant-eating theropod from the Late Jurassic period of Chile. **Nature**, 522(7556):331–334.

Padian K. 2004. Basal Avialae. In: The Dinosauria (eds DB Weishampel, P Dodson, H Osmólska), pp. 210–231. University of California Press, Berkeley, Florida.

Persons WS, Currie PJ. 2017. The functional origin of dinosaur bipedalism: Cumulative evidence from bipedally inclined reptiles and disinclined mammals. **Journal of Theoretical Biology**, 420:1–7.

Pintore R, Houssaye A, Nesbitt SJ, Hutchinson JR. 2022. Femoral specializations to locomotor habits in early archosauriforms. **Journal of Anatomy**, 240(5):867–892.

Rauhut OWM, Carrano MT. 2016. The theropod dinosaur *Elaphrosaurus bambergi* Janensch, 1920, from the Late Jurassic of Tendaguru, Tanzania. **Zoological Journal of the Linnean Society**, 178(3):546–610.

Rauhut OWM, Pol D. 2019. Probable basal allosauroid from the early Middle Jurassic Cañadón Asfalto Formation of Argentina highlights phylogenetic uncertainty in tetanuran theropod dinosaurs. **Scientific Reports**, 9:18826.

Rauhut OWM, Hübner TR, Lanser K-P. 2016. A new Megalosaurid theropod dinosaur from the late Middle Jurassic (Callovian) of north-western Germany: Implications for theropod evolution and faunal turnover in the Jurassic. **Palaeontologia Electronica**, 19(2):1–65.

Rayfield EJ, Milner AC, Xuan VB, Young PG. 2007. Functional morphology of spinosaur 'crocodile-mimic' dinosaurs. **Journal of Vertebrate Paleontology**, 27(4):892–901.

Razzolini NL, Oms O, Castanera D, Vila B, dos Santos VF, Galobart A. 2016. Ichnological evidence of Megalosaurid Dinosaurs Crossing Middle Jurassic Tidal Flats. **Scientific Reports**, 6(1):1–15.

Rhodes MM, Henderson DM, Currie PJ. 2021. Maniraptoran pelvic musculature highlights evolutionary patterns in theropod locomotion on the line to birds. **PeerJ**:e10855.

Romer AS. 1923a. Crocodilian pelvic muscles and their avian and reptilian homologues. **Bulletin of the American Museum of Natural History**, 48:533–552.

Romer AS. 1923b. The pelvic musculature of saurischian dinosaurs. **Bulletin of the American Museum of Natural History,** 48:605–617.

Romer AS. 1923c. The ilium in dinosaurs and birds. **Bulletin of the American Museum of Natural History**, 48, 141–145.

Romer AS. 1956. Osteology of the Reptiles. Chicago: University of Chicago Press.

Rowe T. 1986. Homology and evolution of the deep dorsal thigh musculature in birds and other Reptilia. **Journal of Morphology**, 189(3):327–346.

Sadleir R, Barret PM, Powell HP. 2008. The anatomy and systematics of *Eustreptospondylus oxoniensis*, a theropod dinosaur from the Middle Jurassic of Oxfordshire, England. **Monograph of the Palaeontographical Society**, 160(627):1–82.

Sakamoto M. 2010. Jaw biomechanics and the evolution of biting performance in theropod dinosaurs. **Proceedings of the Royal Society B: Biological Sciences**, 277(1698):3327–3333.

Sales MA, Schultz CL. 2017. Spinosaur taxonomy and evolution of craniodental features: Evidence from Brazil. **PLoS One**, 12(11):e0187070.

Sales MAF, Lacerda MB, Horn BLD, Oliveira IAP, Schultz CL. 2016. The "X" of the matter: Testing the relationships between paleoenvironments and the three theropod clades. **Plos ONE**, 11(2):1–25.

Samathi A, Sander PM, Chanthasit P. 2021. A spinosaurid from Thailand (Sao Khua Formation, Early Cretaceous) and a reassessment of *Camarillasaurus cirugedae* from the Early Cretaceous of Spain. **Historical Biology**, 33(12):3480–3494.

Santos-Cubedo A, de Santisteban C, Poza B, Meseguer S. 2023. A new spinosaurid dinosaur species from the Early Cretaceous of Cinctorres (Spain). **Scientific Reports**, 13(1):6471.

Schade M, Rauhut OWM, Evers SW. 2020. Neuroanatomy of the spinosaurid *Irritator challengeri* (Dinosauria: Theropoda) indicates potential adaptations for piscivory. **Scientific Reports**, 10:9259.

Schade M, Rauhut OW, Foth C, Moleman O, Evers SW. 2023. A reappraisal of the cranial and mandibular osteology of the spinosaurid *Irritator challengeri* (Dinosauria: Theropoda). **Palaeontologia Electronica**, 26(2), 1–116.

Sereno PC, Beck AL, Dutheil DB, Gado B, Larsson HCE, Lyon GH, Marcot JD, Rauhut OWM, Sadleir RW, Sidor CA, Varricchio DD, Wilson GP, Wilson JA. 1998. A Long-Snouted Predatory Dinosaur from Africa and the Evolution of Spinosaurids. **Science**, 282:1298–1302.

Sereno PC, Martinez RN, Wilson JA, Varricchio DJ, Alcober OA, Larsson HC. 2008. Evidence for avian intrathoracic air sacs in a new predatory dinosaur from Argentina. **PLoS ONE**, 3(9):e3303.

Sereno PC, Myhrvold N, Henderson DM, Fish FE, Vidal D, Baumgart SL, Keillor TM, Formoso KK, Conroy LL. 2022. *Spinosaurus* is not an aquatic dinosaur. **eLife**, 11:e80092.

Sereno PC, Wilson JA, Larsson HC, Dutheil DB, Sues H.D. 1994. Early Cretaceous dinosaurs from the Sahara. **Science**, 266(5183):267–271.

Schluter D, Price T, Mooers AØ, Ludwig D. 1997. Likelihood of ancestor states in adaptative radiation. **Evolution**, 51(6):1699–1711.

Smith DK. 2021. Hind limb muscle reconstruction in the incipiently opisthopubic large therizinosaur *Nothronychus* (Theropoda; Maniraptora). **Journal of Anatomy**, 238(6):1404–1424.

Smith JB, Lamanna MC, Mayr H, Lacovara KJ. 2006. New information regarding the holotype of *Spinosaurus aegyptiacus* Stromer, 1915. **Journal of Paleontology**, 80(2):400–406.

Souza LG, Pêgas RV, Lacerda MBS, Riff D. 2023. Tales of long faces: piscivorous Archosauriformes and the evolutionary ways to form a fisher. In **Ruling Reptiles: Crocodylian Biology and Archosaur Paleobiology** (eds HN Woodward, JO Farlow). Bloomington: Indiana University Press, Indiana. p.215–239.

Stromer E. 1915. Ergebnisse der Forschugsreisen Prof. E. Stromers in den Wüsten Ägyptens. II. Wirbeltier-Reste der Baharîje-Stufe (untertes Cenoman). III. Das Original des Theropoden *Spinosaurus aegyptiacus* nov. gen., nov. spec. **Abh Königlichen Bayerischen Akad Wiss, Math-Phys Kl**. 22:1–79.

Therrien F, Henderson DM. 2007. My theropod is bigger than yours… or not: estimating body size from skull length in theropods. **Journal of Vertebrate Paleontology**, 27(1):108–115.

Tsai HP, Middleton KM, Hutchinson JR, Holliday CM. 2018. Hip joint articular soft tissues of non-dinosaurian Dinosauromorpha and early Dinosauria: evolutionary and biomechanical implications for Saurischia. **Journal of Vertebrate Paleontology**, 38(1):e1427593.

Tykoski RS. 2005. Anatomy, ontogeny, and phylogeny of coelophysoid theropods. (Ph.D. Dissertation, The University of Texas, Austin), 553 pp.

Vullo R, Allain R, Cavin L. 2016. Convergent evolution of jaws between spinosaurid dinosaurs and pike conger eels. **Acta Palaeontologica Polonica**, 61(4):825–828.

White MA, Benson RBJ, Tischler TR, Hocknull SA, Cook AG, Barnes DG, Poropat SF, Wooldridge SJ, Sloan T, Sinapius GHK, Elliot DA. 2013. New *Australovenator* Hind Limb Elements Pertaining to the Holotype Reveal the Most Complete Neovenatorid Leg. **PLoS ONE**, 8(7):e68649.

Yu C, Jiangzuo Q, Tschopp E, Wang H, Norell M. 2021. Information in morphological characters. **Ecology and Evolution**, 11(17):11689–11699.

Zhang Z-C, Wang T, You H. 2023. A new specimen of *Sinosaurus triassicus* (Dinosauria: Theropoda) from the Early Jurassic of Lufeng, Yunnan, China. **Historical Biology**, 1 – 15. (doi:10.1080/08912963.2023.2190760)

APPENDIX A - Clades/species list

SAUROPODOMORPHA; *Eoraptor lunensis*, THEROPODA; Herrerasauridae, *Herrerasaurus ischigualastensis*, NEOTHEROPODA; Coelophysoidea, *Dilophosaurus wetherilli*, Coelophysidae, *Coelophysis bauri*, *Co*. *rhodesiensis*, AVEROSTRA; Ceratosauria, *Elaphrosaurus bambergi*, *Ceratosaurus nasicornis*, Abelisauroidea, *Masiakasaurus knopleri*, *Majungasaurus crenatissimus*, TETANURAE; *Sinosaurus sinensis*, *Cryolophosaurus ellioti*, *Monolophosaurus jiangi*, *Chuandongocoelurus primitivus*, ORIONIDES; Megalosauroidea, Piatnitzkysauridae, *Condorraptor currumili*, *Marshosaurus bicentesimus*, *Piatnitzkysaurus floresi*, Megalosauria, *Eustreptospondylus oxoniensis*, Spinosauridae, *Angaturama limai*, *Baryonyx walkeri*, *Ichthyovenator laosensis*, *Irritator challengeri*, *Spinosaurus aegyptiacus*, *Suchomimus tenerensis*, Megalosauridae, *Afrovenator abakensis*, *Dubreuillosaurus valesdunensis*, *Leshansaurus qianweiensis*, *Magnosaurus nethercombensis*, *Piveteasaurus divesensis*, *Duriavenator hesperis*, *Megalosaurus bucklandii*, *Torvosaurus tanneri*, AVETHEROPODA; Allosauroidea, Metriacanthosauridae, *Yangchuanosaurus shangyouensis*, *Y. zigongensis*, *Metriacanthosaurus parkeri*, *Shidaisaurus jinae*, *Siamotyrannus isanensis*, *Sinraptor hepingensis*, *Si. dongi*, Allosauria, Allosauridae, *Allosaurus europaeus*, *Al. fragilis*, *Al. jimmadseni*, *Saurophaganax maximus*, Carcharodontosauria, Neovenatoridae, *Neovenator salerii*, *Chilantaisaurus tashuikouensis*, Megaraptora, *Aerosteon riocoloradensis*, *Australovenator wintonensis*, *Fukuiaraptor kitadaniensis*, *Megaraptor namunhuaiquii*, Carcharodontosauridae, *Acrocanthosaurus atokensis*, *Concavenator corcovatus*, *Eocarcharia dinops*, *Shaochilong maortuensis*, *Carcharodontosaurus iguidensis*, *Ca*. *saharicus*, *Giganotosaurus carolinii*, *Mapusaurus roseae*, *Tyrannotitan chubutensis*, COELUROSAURIA; *Lourinhanosaurus antunesi*, *Compsogntahus longipes*, *Ornitholestes hermanni*, *Proceratosaurus bradleyi*.

APPENDIX B – list of morphological characters

The entire morphological character list can be accessed in Carrano *et al*. (2012), here is presented the list of characters mapped in this work:

261. Pelvic elements, articulations in adults: separate (0), fused (1).

262. Ilium, large external pneumatic foramina and internal spaces: absent (0), present (1).

263. Ilium, vertical ridge on lateral surface of blade dorsal to acetabulum: absent (0), low swollen ridge (1), low double ridge (2).

264. Ilium, posterior width of brevis fossa: subequal to anterior width, fossa margins subparallel (0), twice anterior width, fossa widens posteriorly (1).

265. Ilium, height of lateral wall of brevis fossa relative to medial wall: taller along whole length (0), shorter anteriorly, exposing medial wall in lateral view (1).

266. Ilium, morphology between supraacetabular crest and brevis shelf on lateral surface: gap (0), continuous ridge (1).

267. Ilium, ventrolateral development of supraacetabular crest: large/pendant ‘hood’ (0), reduced shelf (1).

268. Ilium, orientation of pubic peduncle: mostly ventral (0), mostly anterior or ‘kinked’ double facet with anterior and ventral components (1).

269. Ilium, shape of acetabular margin of pubic peduncle: transversely convex or flat (0); transversely concave (1).

270. Ilium, relative sizes of pubic and ischial articulations: subequal (0), pubic articulation ≥ 130% of iliac articulation (1).

271. Ilium, morphology of ischial peduncle: rounded (0), acuminate (1).

272. Ilium, pubic peduncle length to width ratio: ≤ 1 (0), 1.3–1.75 (1), > 2 (2). Ordered.

273. Ilium, ridge on medial surface adjacent to preacetabular notch: absent (0), present (1), strongly developed, forming a shelf (2). Ordered.

274. Ilium, preacetabulum length relative to anterior edge of pubic peduncle: reaches anteriorly to same point as (‘brachyiliac’) (0), or well past (‘dolichoiliac’) (1).

275. Ilium, depth of preacetabular process: shallow (0), deep (1).

276. Ilium, anteroventral lobe of preacetabular process: absent (0), present (1).

277. Ilium, shape of dorsal margin: convex (0), straight (1).

278. Ilium, postacetabulum length relative to ischial peduncle length: ≤ (0), > (1).

279. Ilium, depth of postacetabular process: shallow (0), deep (1).

280. Ilium, shape of posterior margin of postacetabular process: convex (0), concave (1), straight (2), with prominent posterodorsal process but lacking posteroventral process (3).

281. Puboischiadic plate, morphology and foramina/notches: fully closed along midline, 3 fenestrae (0), open along midline, 1 fenestra (obturator foramen of pubis) and 1–2 notches (1), open along midline, 0 fenestrae, 1–2 notches (2).

282. Pubis, shaft orientation: straight (0), ventrally concave (1); dorsally concave (2).

283. Pubis, articulation between apices in adults: unfused (0); fused (1).

284. Pubis, contact between distal portions: separate distally (0), contacting (1), contacting with slit-like opening proximal to distal expansion (interpubic fenestra) (2).

285. Pubis, angle between long axes of shaft and boot: 75–90° (0), < 60° (1).

286. Pubis, morphology of symphysis: marginal (0), broad (1).

287. Pubis, morphology of obturator foramen: small and subcircular (0), large and oval (1).

288. Pubis, anterior expansion of distal end: absent (0), present (1).

289. Pubis, boot length relative to shaft length: < (0), > 30% (1), > 60% (2). Ordered.

290. Pubis, shape of boot in ventral view: broadly triangular (0), narrow, with subparallel margins (1).

291. Pubis, articulation with ilium: planoconcave (0), peg-and-socket (1).

292. Ischium, length relative to pubis length: 75–80% (0), ≤ 70% (1), > 80% (2).

293. Ischium, shaft orientation: straight (0), ventrally curved (1).

294. Ischium, articulation with ilium: planoconcave (0), peg-and-socket (1).

295. Ischium, morphology of antitrochanter: large and notched (0), reduced (1).

296. Ischium, notch ventral to obturator process: absent (0), present (1).

297. Ischium, morphology of symphysis: unexpanded (0), expanded as apron (1).

298. Ischium, cross-sectional shape of paired midshafts: oval (0), heart-shaped, medial portions of shafts extend posteriorly as midline flange (1).

299. Ischium, morphology of distal end: rounded (0), expanded, triangular (1).

300. Ischium, articulation at distal end in adults: separate (0), fused (1).

301. Femur, head orientation: 45° anteromedial (0), 10–30° anteromedial (1), medial (2). Ordered.

302. Femur, head angle: ventromedial (0), horizontal (medial) (1), dorsomedial (2). Ordered.

303. Femur, groove on proximal surface of head-oriented oblique to long axis of head (‘articular groove’ or fovea capitis): absent (0), present (1).

304. Femur, oblique ligament groove on posterior surface of head: shallow, groove bounding lip does not extend past posterior surface of head (0), deep, bound medially by well-developed posterior lip (1).

305. Femur, placement of lesser trochanter relative to femoral head: does not reach ventral margin (0), rises past ventral margin (1), rises to proximal surface (2). Ordered.

306. Femur, morphology of anterolateral muscle attachments at proximal end: continuous trochanteric shelf (0), distinct lesser trochanter and attachment bulge (1).

307. Femur, development of fourth trochanter: prominent semioval flange (0), very weak or absent (1).

308. Femur, distinctly projecting accessory trochanter (derived from lesser trochanter): weak, forms slightly thickened margin of lesser trochanter (0), present as triangular flange (1).

309. Femur, M. femorotibialis externus origin medially on anterodistal surface: faint, small rugose patch (0), pronounced rugose depression that extends to distal femur (1).

310. Femur, development of medial epicondyle: rounded (0), ridge (1).

311. Femur, distal extensor groove: absent (0), present (1).

312. Femur, morphology and orientation of tibiofibularis crest: broad (0), narrow, longitudinal (1), lobular, oblique (2).

313. Femur, infrapopliteal ridge connecting medial distal condyle and crista tibiofibularis: absent (0), present (1).

314. Femur, orientation of long axis of medial condyle in distal view: anteroposterior (0), posterolateral (1).

315. Femur, projection of lateral and medial distal condyles: approximately equal (0), lateral projects distinctly further than medial, distal surface of medial is gently flattened (1), medial projects distinctly further than lateral (2).

316. Femur, morphology of distal end: central depression connected to crista tibiofibularis by a narrow groove (0), anteroposteriorly oriented shallow trough separating medial and lateral convexities (1).

317. Tibia, lateral malleolus: backs astragalus (0), overlaps calcaneum (1).

318. Tibia, shape of edge of lateral malleolus: smoothly curved (0), tabular notch (1).

319. Tibia, morphology of distal cnemial process: rounded (0), expanded proximodistally (1).

320. Tibia, morphology of lateral (fibular) condyle: large (0), small and lobular (1).

321. Tibia, anterolateral process of lateral condyle: absent or horizontal projection (0), prominent, curves ventrally (1).

322. Tibia, anteromedial buttress for astragalus: absent (0), ventral (1), marked oblique step-like ridge (2), reduced oblique ridge (3), bluntly rounded vertical ridge on medial side (4).
323. Tibia, morphology of fibular crest: narrow (0), bulbous (1).
324. Tibia, development of fibular crest: extends to proximal end of tibia as high crest (0), extends to proximal end of tibia as low ridge (1), does not extend to proximal end of tibia (2). Ordered.
325. Fibula, depth of fibular fossa on medial aspect: groove (0), shallow fossa (1), deep fossa (2).
326. Fibula, position of fibular fossa on medial aspect: posterior edge (0), central (1).
327. Fibula, size of iliofibularis tubercle: faint scar (0), large (1), anterolaterally curving flange (2).
328. Fibula, size of proximal end relative to width of proximal tibia: < 75% (0), ≥ 75% (1).

APPENDIX C - Remarks on character/scoring

264. Ilium, posterior width of brevis fossa: subequal to anterior width, fossa margins subparallel (0), twice anterior width, fossa widens posteriorly (1).

Remarks: State "?" in *Piatnitzkysaurus* (Carrano *et al*., 2012) modified to state "0". State "?" in *Ichthyovenator* (Rauhut & Pol, 2019) modified to state "1".

265. Ilium, height of lateral wall of brevis fossa relative to medial wall: taller along whole length (0), shorter anteriorly, exposing medial wall in lateral view (1).

Remarks: State "?" in *Suchomimus* (Carrano *et al*., 2012) modified to state "0". State "?" in *Ichthyovenator* (Rauhut & Pol, 2019) modified to state "1".

271. Ilium, morphology of ischial peduncle: rounded (0), acuminate (1).

Remarks: State "1" in *Ichthyovenator* (Rauhut & Pol, 2019) modified to "0".

277. Ilium, shape of dorsal margin: convex (0), straight (1).

Remarks: State "1" in *Ichthyovenator* (Rauhut & Pol, 2019) modified to "0".

278. Ilium, postacetabulum length relative to ischial peduncle length: ≤ (0), > (1), 2x (2).

Remarks: State (2) removed.

282. Pubis, shaft orientation: straight (0), ventrally concave (1); dorsally concave (2).

Remarks: State (1) changed from "ventrally curved" (Carrano *et al*., 2012) to "ventrally concave"; state (2) dorsally concave added.

286. Pubis, morphology of symphysis: marginal (0), broad (1).

Remarks: State "1" in *Ichthyovenator* (Rauhut & Pol, 2019) modified to "0".

287. Pubis, morphology of obturator foramen: small and subcircular (0), large and oval (1).

Remarks: State "1" in *Ichthyovenator* (Rauhut & Pol, 2019) modified to "0".

290. Pubis, shape of boot in ventral view: broadly triangular (0), narrow, with subparallel margins (1).

Remarks: State "?" in *Suchomimus* (Carrano *et al*., 2012) modified to state "0".

297. Ischium, morphology of symphysis: unexpanded (0), expanded as apron (1).

Remarks: State "?" in *Suchomimus* (Carrano *et al*., 2012) modified to state "0".

299. Ischium, morphology of distal end: rounded (0), expanded, triangular (1).

Remarks: State "?" in *Ichthyovenator* (Rauhut & Pol, 2019) modified to "0".

303. Femur, groove on proximal surface of head-oriented oblique to long axis of head ('articular groove' or fovea capitis): absent (0), present (1).

Remarks: State "?" in *Baryonyx* and *Piatnitzkysaurus* (Carrano *et al*., 2012) modified to state "1"; Inclusion of fovea capitis as the character description, since this groove refers to the

pubofemoral and ischiofemoral ligaments that form the ligamentum captis femoris, which is inserted onto the fovea capitis on the proximal femoral head (see Tsai *et al*., 2018).

304. Femur, oblique ligament groove on posterior surface of head: shallow, groove bounding lip does not extend past posterior surface of head (0), deep, bound medially by well-developed posterior lip (1).

Remarks: State "?" in *Suchomimus* (Carrano *et al*., 2012) modified to state "1".

306. Femur, morphology of anterolateral muscle attachments at proximal end: continuous trochanteric shelf (0), distinct lesser trochanter and attachment bulge (1).

Remarks: State "1" in *Irritator* (Carrano *et al*., 2012) modified to state "?".

315. Femur, projection of lateral and medial distal condyles: approximately equal (0), lateral projects distinctly further than medial, distal surface of medial is gently flattened (1), medial projects distinctly further than lateral (2).

Remarks: State (2) medial projects distinctly further than lateral added; state "0" in *Suchomimus* (Carrano *et al*., 2012) modified to state "2".

320. Tibia, morphology of lateral (fibular) condyle: large (0), small and lobular (1).

Remarks: State "?" in *Suchomimus* (Carrano *et al*., 2012) modified to state "1".

321. Tibia, anterolateral process of lateral condyle: absent or horizontal projection (0), prominent, curves ventrally (1).

Remarks: State "?" in *Suchomimus* (Carrano *et al*., 2012) modified to state "0".

APPENDIX D - List of ordered characters'

Following Rauhut & Pol, 2019: 2, 4, 6, 12, 24, 47, 74, 96, 129, 150, 152–153, 156, 172, 180, 189, 193, 197, 223, 231, 233, 249, 272–273, 281, 289, 301–302, 305, 324, 335, and 341.

APPENDIX E – disparity analyses

Taxa that do not have the studied pelvic and hindlimb elements preserved and were removed from the disparity analyses. The taxa removed in analysis (i) and remaining analyses were *Angaturama*, *Duriavenator*, *Eocarcharia*, *Irritator*, *Piveteasaurus*, *Proceratosaurus*, and *Shaochilong*. For the analysis (ii) we removed *Dubreuillosaurus* and *Megaraptor*. For the analysis (iii) we removed *Australovenator*, *Chilantaisaurus*, *Dubreuillosaurus*, and *Fukuiraptor*. For the analysis (iv) we removed *Aerosteon*, *Australovenator*, *Chilantaisaurus*, *Chuandongocoelurus*, *Dubreuillosaurus*, *Fukuiraptor*, *Magnosaurus*, *Megaraptor*, and *Leshansaurus*. For the analysis (v) we removed *Aerosteon*, *Ichthyovenator*, *Megaraptor*, *Monolophosaurus*, *Shidaisaurus*, and *Siamotyrannus*. For the analysis (vi) we removed *Ichthyovenator*, *Megaraptor*, *Monolophosaurus*, *Shidaisaurus*, *Siamotyrannus*, and *Si. hepingensis*.

CHAPTER 2

RECONSTRUCTION OF THE PELVIC GIRDLE AND HINDLIMB MUSCULATURE OF THE EARLY TETANURANS PIATNITZKYSAURIDAE (THEROPODA, MEGALOSAUROIDEA)

Abstract

Piatnitzkysauridae were Jurassic theropods that represented the earliest diverging branch of Megalosauroidea, being one of the earliest lineages to have evolved moderate body size. This clade's size and some unusual anatomical features raise questions about locomotor function to aid in body support. Biomechanical models can illuminate how extinct animals may have moved, but require anatomical data as inputs. With a phylogenetic context, osteological evidence, and neontological data on anatomy, it is possible to infer the musculature of extinct taxa. Here, we reconstructed the hindlimb musculature of Piatnitzkysauridae. We chose this clade for future usage in biomechanics, for comparisons with myological reconstructions of other theropods, and for the evolutionary implications of our reconstructions. We considered 32 muscles, for *Piatnitzkysaurus*, the attachments of 29 muscles could be inferred based on the osteological correlates; meanwhile, in *Condorraptor* and *Marshosaurus*, we respectively inferred 21 and 12 muscles. We find a great anatomical similarity within Piatnitzkysauridae, but differences such as the origin of *M. ambiens* and size of *M. caudofemoralis brevis* are present. Similarities were evident with Aves, such as the division of the *M. iliofemoralis externus* and *M. iliotrochantericus caudalis* and the broad depression of origin of *M. gastrocnemius pars medialis* in the cnemial crest. Nevertheless, plesiomorphic features such as the origin of *M. puboischiofemoralis 1* around the "cuppedicus" fossa and the *M. ischiotrochantericus* medially positioned on the ischium are inferred. As the first attempt to reconstruct muscles in early tetanurans, our study allows a more complete understanding of myological evolution in theropod pelvic appendages.

1. INTRODUCTION

1.1. Piatnitzkysauridae clade

Piatnitzkysauridae is a clade of medium-sized (~4 to 6 meters long; ~200 kg body mass) tetanuran theropods within Megalosauroidea (sensu Carrano *et al*., 2012), known from the Jurassic of South America and North America (Madsen, 1976; Bonaparte, 1979; Rauhut, 2005). Currently, at least three species constitute Piatnitzkysauridae: *Piatnitzkysaurus floresi* Bonaparte, 1979 and *Condorraptor currumili* Rauhut, 2005, from the Aalenian–Callovian (Middle Jurassic) assemblages of the Cañadón Asfalto Formation in Patagonia, Argentina; and *Marshosaurus bicentesimus* Madsen, 1976, from the Kimmeridgian (Upper Jurassic) assemblages of the Morrison Formation in the United States (Utah, possibly Colorado). A phylogenetic definition of the clade was present by Carrano *et al*. (2012) as all megalosauroid theropods that are more closely related to *Piatnitzkysaurus* than to *Spinosaurus* or *Megalosaurus*. However, in some phylogenetic studies/hypotheses (e.g., Benson, 2010; Dai *et al*., 2020), the poorly preserved Middle Jurassic taxon *Xuanhanosaurus* from China falls within piatnitzkysaurids as an early diverging species. However, this taxon also has also been recovered as an early tetanuran (Holtz *et al*., 2004) or an allosauroid (Carrano *et al*., 2012); and therefore, is considered a "wildcard" taxon (Carrano *et al*., 2012).

Condorraptor and *Piatnitzkysaurus* are taxa of great importance, both geographically and temporally, as they are some of the few known Middle Jurassic theropods with a relatively well-preserved skeleton, especially from South America (Bonaparte, 1979; Rauhut, 2003; 2004; 2005; 2007; Carrano *et al*., 2012). They also provide important phylogenetic clues about the evolution of early theropod dinosaurs (Rauhut, 2003; Carrano *et al*., 2012). Concerning the skull, the North American taxon *Marshosaurus* is better known than both *Condorraptor* and *Piatnitzkysaurus* (Madsen, 1976; Chure *et al*., 1997; Carrano *et al*., 2012), also preserving a rare case of osteopathological evidence (Chure *et al*., 1997). Additional skeletal elements (e.g., Chure *et al*., 1997) are yet undescribed. The two Argentinean taxa are also known from decent skeletal material: both skeletons of *Piatnitzkysaurus* are relatively well-preserved including a sizeable portion of the appendicular skeleton and braincase, for example; and *Condorraptor*, although more fragmentary, has numerous postcranial elements (e.g., Bonaparte, 1986; Rauhut, 2004; 2005; 2007; Paulina-Carabajal, 2015). The Piatnitzkysauridae is a key clade for understanding the evolution of tetanuran theropods, because they are the earliest and oldest known tetanurans (Carrano *et al*., 2012; Rauhut *et al*., 2016). The main distinctions between

the three species are based on characters present in the dentaries and the axial skeleton (Madsen, 1976; Bonaparte, 1986; Rauhut, 2005; Carrano *et al*., 2012); however, additional dissimilarities in pelvic bones and zeugopodial elements are also recognisable (Chapter 1). Furthermore, the Middle Jurassic was an important time for the diversification of tetanuran theropods, which soon populated all continents, although these main evolutionary patterns remain poorly known (e.g., Sereno, 1999; Rauhut, 2004; 2005).

Piatnitzkysaurid species can be diagnosed, for example, by the following morphological features: (1) short or absent anterior maxillary ramus, (2) presence of two parallel rows of foramina on the maxilla, (3) vertically striated paradental plates, and (4) anteriorly inclined neural spines of the posterior dorsal vertebrae (Carrano *et al*., 2012). The first cladistic studies that phylogenetically positioned and characterised these species as a clade were Benson (2010) and Carrano *et al*. (2012), who included the piatnitzkysaurids within the clade Megalosauroidea, differing from other approaches. Historical classifications generally had assigned *Marshosaurus* and *Piatnitzkysaurus* as members of allosaurids or megalosaurids (e.g., Bonaparte, 1979; 1986; Russel, 1984; for a summary see Carrano *et al*., 2012).

Marshosaurus and *Piatnitzkysaurus* are known from skeletons of adult individuals (Madsen, 1976; Bonaparte, 1986), whereas *Condorraptor* is known from a probably subadult specimen (Rauhut, 2005). The estimated typical body length of the three species is 4.5 metres, with a body mass of about 200 kg for *Marshosaurus* and *Condorraptor*; whereas the body mass of *Piatnitzkysaurus* was estimated as 275 kg (Paul, 1988; 2016). Hendrickx *et al*. (2015) estimated longer body lengths, between 5–6 metres, and Foster (2020) estimated a slightly greater body mass for *Marshosaurus* (250 kg). Nevertheless, an estimate of body mass, based on femoral morphometrics, suggests that the Argentinean taxa *Condorraptor* and *Piatnitzkysaurus* could have reached ~360 kg and 750 kg in mass, respectively; exemplifying the origin of medium-sized tetanurans during the Jurassic, thus suggesting an increase in theropod macropredatory habits (Benson *et al*., 2014).

1.2. Muscle reconstruction in extinct vertebrates

Reconstruction of muscles and estimation of their architecture and functions is an important approach in palaeobiology (e.g., Witmer, 1995; Bates & Falkingham, 2018; Bishop *et al*., 2021; Cuff *et al*., 2023a). Even with intrinsic limitations to these reconstructions for fossil organisms, biomechanical models and simulations, among useful methods, have been developed with the aid of computational techniques (e.g., Hutchinson, 2012). Advances in

morphofunctional and ecomorphological studies in extinct vertebrates, together with advances in evolutionary biomechanics applied to locomotion, for example, are essential for understanding broader macroevolutionary aspects such as paleoecology and potential selective pressures (e.g., Jones *et al*., 2021).

Over a century of studies has focused on the variations in pelvic and hindlimb functional morphology in extinct and extant archosaur species, and its implications for muscle architecture and locomotor biomechanics. These studies have provided broad datasets, a solid background, and general inferences that have led to a greater understanding of comparative myology and biomechanical evolution of locomotion at different levels (e.g., Gregory & Camp, 1918; Romer, 1923a,b,c; 1927; Russel, 1972; Tarsitano, 1983; Rowe, 1986; Gatesy, 1990; Farlow *et al*., 1995; 2000; Gatesy & Middleton, 1997; Hutchinson, 2001a,b; 2004a,b; 2012; Carrano & Hutchinson, 2002; Hutchinson & Garcia, 2002; Langer, 2003; Hutchinson *et al*., 2005; Hutchinson & Allen, 2009; Mallison, 2010; Grillo & Azevedo, 2011; Maidment & Barret, 2011; Schachner *et al*., 2011; Zinoviev, 2001; Bates *et al*., 2012a,b; Liparini & Schultz, 2013; Costa *et al*., 2014; Bishop *et al*., 2018a,b; 2021; Piechowski & Tałanda, 2020; Allen *et al*., 2021; Smith 2021; 2023; Cuff *et al*. 2023a,b).

However, how can these reconstructions be accurately performed for extinct vertebrates? In general, soft tissues (e.g., muscles/tendons) are not normally preserved in fossils. Yet there are rare exceptions where favourable geochemical conditions for preservation occurred during fossil diagenesis provided rare preservation. These exceptions include muscle fibres or tendons, partial musculature and internal organs (e.g., Kellner, 1996; Dal Sasso & Signore, 1998; Surmik *et al*., 2023), as well as integumentary structures (e.g., Barbi *et al*., 2019) in dinosaurs. With few exceptions, almost all vertebrate fossils consist of some degree of biomineralization (e.g., bones, teeth, ossified ligaments/tendons). However, some bony structures (e.g., muscle origin/insertions) leave discernible anatomical traces on fossils; thus, this muscle–bone interface allows reconstruction of unpreserved locomotor musculature based on a reliable osteological set of features (e.g., Romer, 1923b,c; 1927; Gatesy, 1990; Dilkes, 2000; Hutchinson, 2001a,b; Carrano & Hutchinson, 2002; Grillo & Azevedo, 2011; Maidment & Barret, 2011; Bishop *et al*., 2021; Rhodes *et al*., 2021; Smith 2021).

A methodology that has been widely used in recent decades is the Extant Phylogenetic Bracket (EPB), formalized by Witmer (1995). The EPB is based on the phylogenetic relationships of the extinct clade under study, with at least two evolutionarily outgroups having extant representatives. The EPB method represents a rigorously explicit method that aims to minimise speculations in muscle reconstruction, allowing tissue reconstitution to be performed

and then judged through inference levels (see Methods below). Additionally, the inclusion of fossil taxa facilitates interpretations about muscular homology and evolution, because extinct relatives of the study taxon may present evidence for transitional character states or even novel states; either being absent in extant taxa (Dilkes, 2000; Hutchinson, 2001a,b; 2002; Maidment & Barret, 2011; Bishop *et al*., 2021).

The EPB has been particularly popular for studying locomotor form and function in archosaurs (e.g., Hutchinson, 2001a,b; Carrano & Hutchinson, 2002; Langer, 2003; Grillo & Azevedo, 2011; Liparini & Schultz, 2013; Bishop *et al*., 2018a,b; 2021; Rhodes *et al*., 2021; Smith 2021). As many extinct organisms do not currently have analogous taxa (Costa *et al*., 2014; Bishop *et al*., 2021), muscle reconstructions can provide different a posteriori interpretations and revisions of previously raised hypotheses (e.g., for *Tyrannosaurus rex*, pelvic muscle reconstructions by Romer, 1923b vs. Carrano & Hutchinson, 2002; and running abilities by Paul, 1988 vs. Hutchinson & Garcia, 2002).

1.3. Why study musculature in non-avian theropods?

Hutchinson & Allen (2009) listed at least four questions considered fundamental for the understanding of macroevolution and morphofunctional adaptations that support and motivate researchers to reconstruct the musculature and locomotor aspects in theropod dinosaurs: (1) understand how the bipedal stance and gait of birds evolved; (2) what myological/locomotor traits are novel for birds; (3) how far down the tree is it possible to trace ancestral traits in theropods (or other archosaurs), and what are the plesiomorphic traits? and (4) how did novelties such as bipedalism and flight arise and/or were modified, or even how did the performance of terrestrial/aerial locomotion change over evolutionary time?

To answer some of these questions, there are growing efforts in the study of muscle, especially the locomotor apparatus in dinosaurs (e.g., Dilkes, 2000; Langer, 2003; Mallison, 2010; Maidment & Barret, 2011). Considering Theropoda, among the myological reconstructions and modelling carried out so far, in addition to pioneering work (e.g., Romer, 1923a,b; 1927; Gatesy, 1990; Russel, 1972; Tarsitano, 1983; Gatesy & Middleton, 1997; Farlow *et al*., 2000), the results presented for one of the earliest theropods, the herrerasaurid *Staurikosaurus* (Grillo & Azevedo, 2011), is worth highlighting, in addition to the reconstruction of the coelophysoid *Coelophysis* (Bishop *et al*., 2021). Regarding ceratosaurs, Persons IV & Currie (2011) did not fully reconstruct the locomotor musculature, but explored the caudal musculature in the abelisauroid *Carnotaurus*. Concerning early tetanuran theropods,

the only efforts to date relate to the allosauroids *Allosaurus* and *Acrocanthosaurus*, not only on the basis of musculature (e.g., Cau & Serventi, 2017), but also, body mass estimation and biomechanical analysis (Bates *et al*., 2012a). Other muscle reconstructions generally have been carried out for lineages that are more closely related to Aves, with great effort spent on Coelurosauria; for example, the tyrannosauroid *Tyrannosaurus* (Carrano & Hutchinson, 2002), Ornithomimidae (Russel, 1972), and maniraptoran species (Hutchinson *et al*., 2008; Rhodes *et al*., 2021; Smith 2021; 2023).

In addition to the studies cited above, there is an ongoing effort to understand the main evolutionary features related to bipedalism in theropod dinosaurs (e.g., Bishop *et al*., 2018a,b; Allen *et al*. 2021; Cuff *et al*. 2023a). However, the earliest tetanuran clades studied generally include only allosauroids; whereas there have not been detailed studies of Megalosauroidea, the earliest-diverging branch of tetanuran evolution. In the Chapter 1, we mapped the evolution and reconstructed the ancestral states of the morphological characters of the pelvic appendage, characterising potential variations related to muscle insertions; and tested whether different homoplastic signals in different regions of the locomotor system are present in theropods. Thus, providing a stronger basis for the muscle reconstruction performed here (see below).

Although piatnitzkysaurids are important representatives for understanding theropod evolution (Rauhut, 2003; Carrano *et al*., 2012), as well as megalosauroid diversity and the acquisition of larger body size in terms of locomotor function and body support, little is known about these palaeobiological issues (Chapter 1). Our aim here is to begin addressing these deficiencies by reconstructing the hindlimb muscles (origins and insertions) of the three piatnitzkysaurid species (*Condorraptor*, *Marshosaurus*, and *Piatnitzkysaurus*), and to compare our findings with the myological reconstructions of other extinct and extant archosaurs. We chose these taxa not only for (1) future usage in biomechanical models, and (2) comparisons with existing myological reconstructions of other theropods and resulting evolutionary implications, but also (3) addressing how similar their musculature might have been, (4) determining if any show unusual apomorphies, and (5) assessing how differential taphonomic preservation affects these inferences. We considered a total of 32 muscles, focusing on the major muscles (not the many, small, complex pedal muscles).

Institutional abbreviations: MACN, Museo Argentino de Ciencias Naturales ‘Bernardino Rivadavia’, Buenos Aires, Argentina. MPEF, Museo Paleontológico Egidio Feruglio, Trelew, Argentina. PVL, Fundación ‘Miguel Lillo’, San Miguel de Tucumán, Argentina. UMNH, Natural History Museum of Utah, Utah, United States.

2. MATERIAL AND METHODS

2.1 Species and specimens

For *Piatnitzkysaurus*, we personally examined the holotype PVL 4073, housed at Fundación Miguel Lillo (Universidad Nacional de Tucumán, Argentina), and the partial skeleton (hypodigm MACN-Pv-CH 895), housed at Museo Argentino de Ciencias Naturales 'Bernardino Rivadavia' (Argentina). For *Condorraptor*, directly inspected the holotype MPEF-PV 1672, as well as the hypodigm specimens (MPEF-PV 1676–1683, MPEF-PV 1686–1688, MPEF-PV 1690–1693, MPEF-PV 1696–1697, MPEF-PV 1700–1702, MPEF-PV 1704–1705), deposited in the Museo Paleontológico Egidio Feruglio (Argentina). For *Marshosaurus*, although one of us (JRH) personally examined known specimens (UMNH VP 6372 [= UUVP 1845], UMNH VP 6374 [= UUVP 2742], UMNH VP 6380 [= UUVP 2878], UMNH VP 6384 [= UUVP 40-295], UMNH VP 6387 [= UUVP 4736]) deposited in the Natural History Museum of Utah (United States), the myological inferences presented here are based upon photographs, notes, and the original description provided by Madsen (1976). More detailed information is focused only on the South American taxa, for which we have the best image quality and have been studied recently.

2.2 Myological reconstruction, homology and character mapping

We used the EPB method (Witmer 1995) for our reconstructions (Figure 2.1A). Three levels of inference are established by EPB to characterise the confidence in reconstructing a particular soft tissue for an extinct species: (I) represents an unequivocal structure of a particular feature, that is, when the two (or more) extant taxa have the homologous soft tissue and its osteological correlate; (II) represents an equivocal reconstruction, when the ancestral condition for two or more taxa is ambiguous, such as the presence of a particular soft tissue and the osteological correlate only in one of the extant taxa; (III) represents an unequivocal absence of a particular feature, that is, when the ancestral condition favoured by the EPB involves not having the soft tissue and its osteological evidence (i.e., inferring an absent feature; with no or contrary evidence). In addition, if soft tissue inferences lack conclusive data from their osteological correlates, they are qualified as level I', II', and III' inferences (Witmer, 1995). Using the EPB, our comparisons mainly were based on Crocodylia and Aves, but not restricted to these groups; Lepidosauria and Testudines were also considered (Hutchinson, 2002; Bishop

et al., 2021). The pelvic and thigh musculature of extant taxa was evaluated from the following literature Crocodylia (e.g., Romer, 1923a; Otero *et al*., 2010; Suzuki *et al*., 2011; Hattori & Tsuihiji, 2020), Avialae (e.g., Romer, 1923c; Hudson *et al*., 1959; Rowe, 1986; McKitrick, 1991; Patak & Baldwin, 1998; Picasso, 2010; Suzuki *et al*., 2014; Clifton *et al*., 2018; Hattori & Tsuihiji, 2020), and other Tetrapoda/Reptilia (e.g., Gregory & Camp, 1918; Romer, 1942; Dick & Clemente, 2016; Hattori & Tsuihiji, 2020). Dissection of one *Crocodylus niloticus* and one *Numida meleagris* specimen during this study further enhanced our comparisons and delineations of muscle positioning.

The phylogenetic framework adopted here was provided by Carrano *et al*. (2012), where Piatnitzkysauridae is an early Megalosauroidea clade composed of *Marshosaurus* as the earliest piatnitzkysaurid taxon to diverge, being sister taxon of a subclade composed of *Piatnitzkysaurus* and *Condorraptor* (Figure 2.1B).

The nomenclature and homology of the musculoskeletal system here follows the propositions of Hutchinson & Gatesy (2000), Hutchinson (2001a,b; 2002), Carrano & Hutchinson (2002), and Hattori & Tsuihiji 2020 (adaptations summarised in the Table 2.1), which built on earlier work by Romer (1923a; 1942) and Rowe (1986). The work of Baumel & Witmer (1993) is followed in the description and nomenclature of osteological correlates and muscle scars.

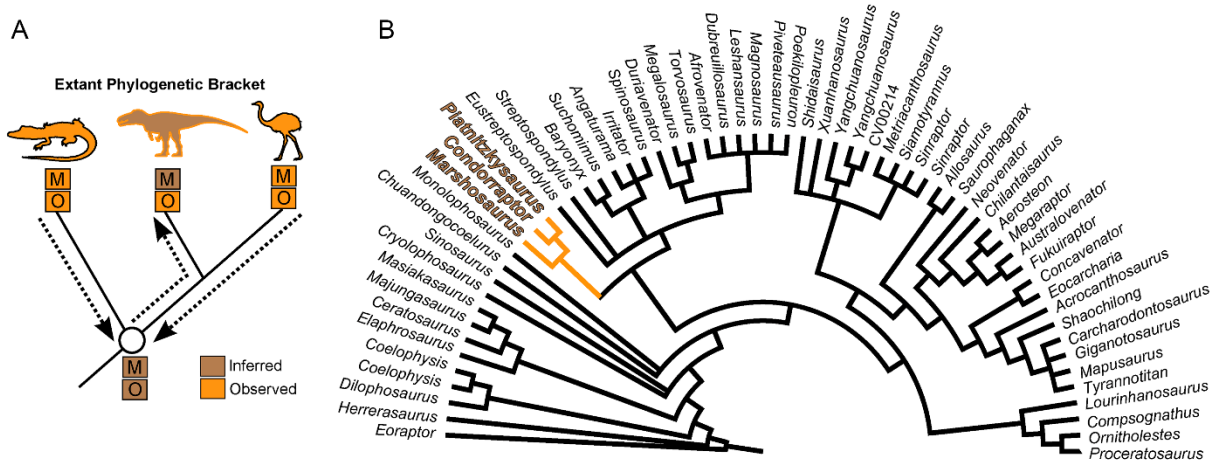

Figure 2.1. A, Simplified example of Extant Phylogenetic Bracket (EPB) application in Theropoda. B, Theropod phylogeny (up to Coelurosauria) highlighting the phylogenetic position of Piatnitzkysauridae. A, adapted from Grillo & Azevedo (2011); B, adapted from Carrano *et al*. (2012). Abbreviations: M, muscle; O, osteological correlate. Silhouettes are from phylopic.org; see Acknowledgements.

Table 2.1. Muscular homologies in extant archosaurs, considering the musculature of the pelvic girdle and hindlimb (modified from Carrano & Hutchinson, 2002). The EPB uses the state in each most recent common ancestor of Crocodylia and of Aves as its bracket, informed by further data from outgroups Lepidosauria and Testudines (not shown here; see Hutchinson, 2002).

Muscles (Crocodylia)	**Muscles (Aves)**
DORSAL GROUP	
Triceps femoris	
M. iliotibialis 1 (IT1)	*M. iliotibialis cranialis* (IC)
Mm. iliotibialis 2, 3 (IT2, IT3)	*M. iliotibialis lateralis* (2 main parts) (IL)
M. ambiens (AMB)	*M. ambiens* (AMB)
M. femorotibialis externus (FMTE)	*M. femorotibialis lateralis* (FMTL)
M. femorotibialis internus (FMTI)	*M. femorotibialis intermedius* (FMTIM) & *M. femorotibialis medialis* (FMTM)
M. iliofibularis (ILFB)	*M. iliofibularis* (ILFB)
Deep dorsal	
M. iliofemoralis (IF)	*M. iliofemoralis externus* (IFE) & *M. iliotrochantericus caudalis* (ITC)
M. puboischiofemoralis internus 1 (PIFI1)	*M. iliofemoralis internus* (IFI)
M. puboischiofemoralis internus 2 (PIFI2)	*M. iliotrochantericus cranialis* (ITCR) & *M. iliotrochantericus medius* (ITM)
VENTRAL GROUP	
Flexor cruris	
M. puboischiotibialis (PIT)	[absent]
M. flexor tibialis internus 1 (FTI1)	[absent]
M. flexor tibialis internus 2 (FTI2)	[absent]
M. flexor tibialis internus 3 (FTI3)	*M. flexor cruris medialis* (FCM)
M. flexor tibialis internus 4 (FTI4)	[absent]
M. flexor tibialis externus (FTE)	*M. flexor cruris lateralis pars pelvica* (FCLP and *accessoria* FCLA)
Mm. adductores femores	
M. adductor femoris 1 (ADD1)	*M. puboischiofemoralis pars medialis* (PIFM)
M. adductor femoris 2 (ADD2)	*M. puboischiofemoralis pars lateralis* (PIFL)
Mm. puboischiofemorales externi	
M. puboischiofemoralis externus 1 (PIFE1)	*M. obturatorius lateralis* (OL)
M. puboischiofemoralis externus 2 (PIFE2)	*M. obturatorius medialis* (OM)
M. puboischiofemoralis externus 3 (PIFE3)	[absent]
M. ischiotrochantericus (ISTR)	*M. ischiofemoralis* (ISF)
Mm. caudofemorales	
M. caudofemoralis brevis (CFB)	*M. caudofemoralis pars pelvica* (CFP)

Muscles (Crocodylia)	**Muscles (Aves)**
M. caudofemoralis longus (CFL)	*M. caudofemoralis pars caudalis* (CFC)
DIGITAL EXTENSOR GROUP	
M. extensor digitorum longus (EDL)	*M. extensor digitorum longus* (EDL)
M. extensor digitorum brevis (EDB)	[absent]
M. extensor hallucis longus (EHL)	*M. extensor hallucis longus* (EHL)
M. tibialis anterior (TA)	*M. tibialis cranialis* (TC)
Mm. gastrocnemii	
M. gastrocnemius externus (GE)	*M. gastrocnemius pars lateralis* (GL) *et intermedia* (GIM)
M. gastrocnemius internus (GI)	*M. gastrocnemius pars medialis* (GM)
LOWER LEG MUSCLES	
M. fibularis longus (FL)	*M. fibularis longus* (FL)
M. fibularis brevis (FB)	*M. fibularis brevis* (FB)

Piatnitzkysaurus was scored for character states of 86 characters (character ranges 1–71, 78–88, and 97–100; see Appendix A), to replace the "basal Tetanurae" lineage (which previously was a rough composite of transitional character states from this and other lineages) from Hutchinson (2001a,b; 2002) and Bishop *et al*. (2021) in a modified taxon-character matrix. As usual for the EPB, we used the maximum parsimony criterion for our reconstructions, similar to previous studies (e.g., Witmer, 1995; Molnar *et al*., 2018; Bishop *et al*., 2021). By doing so, we refine character scoring for early Tetanurae in general, which will be useful for future studies. We only scored *Piatnitzkysaurus*, as it has more osteological correlates preserved than the other taxa do, and consequently a greater number of muscles could be inferred for this species (see Results and Discussion). However, we sought to test if any muscles reconstructed differed in any details across the three taxa. To score and trace evolutionary changes in locomotor muscles, as well as to assess the most parsimonious states in our reconstructions, we used Mesquite software version 3.6 (Maddison & Maddison, 2015) considering an informal composite "consensus" tree of Reptilia based on the recent phylogenetic framework used by Bishop *et al*. (2021) and references in therein. The dataset used in this analysis can be found in Lacerda *et al*. (2023).

3. RESULTS AND DISCUSSION

3.1 Myological reconstruction

3.1.1 Triceps Femoris

Mm. iliotibiales (IT1, IT2, and IT3). In Aves and Crocodylia, the *Mm. iliotibiales* is a large and superficial sheet that generally is composed by three heads over the dorsal and anteroposterior rim of the ilium, superficially positioned in relation to the other pelvic and thigh muscles (Romer, 1923a; Hudson *et al*., 1959; Patak & Baldwin, 1998; Hutchinson, 2001b; 2002; Otero *et al*., 2010; Picasso, 2010; Clifton *et al*., 2018). In other reptiles, the homologous muscle presents one or two weakly separated heads (Romer, 1942; Hutchinson, 2002; Dick & Clemente, 2016). The IT1–3 muscles attach to the dorsal rim of the ilium and are dorsally delimited by the *crista dorsolateralis ilii* (Baumel & Witmer, 1993), marking the border between the dorsal and lateral surfaces of the supraacetabular iliac blade.

In the *Piatnitzkysaurus* ilium MACN-Pv-CH 895, the anteriormost margin of the preacetabular process is not preserved, so the anterior limits/extension of the IT1 are not possible to infer; however, a great part of the supraacetabular rim is preserved. On the anteriormost part of the preacetabular blade, an expanded area is evident. This area is posteriorly delimited by an invagination present over the dorsalmost part of the supraacetabular rim (Figure 2.2A,B). Furthermore, immediately ventral to the dorsal rim of the ilium, there is a rough osteological delimitation, which posteriorly becomes more dorsally positioned (Figure 2.3A). Because these osteological correlates are topologically compatible with the positions (and similar osteological correlates) noted in extant archosaurs (e.g., Romer, 1923a; Hudson *et al*., 1959; Carrano & Hutchinson, 2002; Otero *et al*., 2010; Picasso, 2010), the rough delimitation and the dorsal invagination seem to be the posterior edge of the IT1 (level I), as well as the anterior demarcation of the IT2 (Figure 2.2A, Figure 2.3A). Concerning the IT2, we infer the anterior limits to be at the same position of the main axis of the pubic peduncle, on a dorsal invagination of the dorsal rim of the preacetabular blade (level I) (Figure 2.2A), as aforementioned. Although not clearly preserved, the posterior limits of this muscle head seem to be demarcated by a small protuberance that is located on the dorsal postacetabular blade (Figure 2.2A), which is posterior to the posterior facet of the ischial peduncle. This protuberance also probably delimited the anterior origin of the IT3; the attachment area of the IT3 is on the posterior dorsal rim of the postacetabular blade of the ilium. A rough scar which

becomes posteriorly large is on the ilium of MACN-Pv-CH 895, seeming to be dorsally delimited by the *crista dorsolateralis ilii*. This area of the IT3 is delimited by a faint osteological protuberance (level I). Most of the origination region of the IT1–3 muscles are not preserved in *Condorraptor* – the supraacetabular crest is highly damaged anterior and dorsal to the acetabulum in the only preserved ilium MPEF-PV 1687 of this taxon (Figure 2.2C,D). The *Condorraptor* ilium only preserves a small portion of the dorsal margin of the supraacetabular crest, being part of the posterior portion of the preacetabular blade. This small part is ventral to the boundaries of the IT2 origin (Figure 2.2C,D).

Although fragmentary, this region has an osteological correlate indicating that the anterior boundaries of the IT2 origin were from an invagination preserved at the same axis of the pubic peduncle (level I). However, as a consequence of this fragmentation of the *Condorraptor* ilium, the reconstruction of the origin of IT1 and IT3, as well as the extent of IT2, are uncertain, although these origins should have been similar to those reconstructed for *Piatnitzkysaurus*. In the studied ilia of *Marshosaurus* (UMNH VP 6372 and UMNH VP 6374) and in the holotype UMNH VP 6373 [= UUVP 2826] specimen (Madsen, 1976), the best-preserved part is the postacetabular process of the ilium. Although the subdivisions of the IT heads are not as discernible as in *Piatnitzkysaurus*, the origin of the IT3 in both UMNH VP 6372 and UMNH VP 6373 is clearly discernible by several scars on the dorsal edge of the postacetabular blade and the presence of the *crista dorsolateralis ilii* (level I) (Figure 2.2E,F, Figure 2.3B).

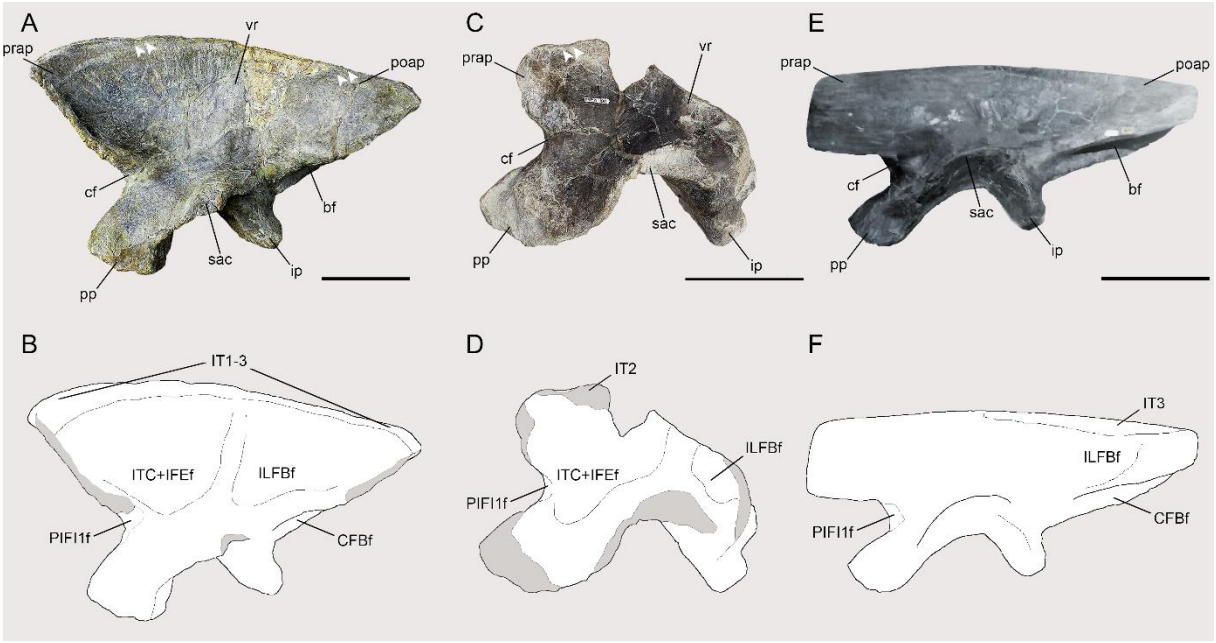

Figure 2.2. Osteological correlates observed in the ilia of Piatnitzkysauridae (left ilia, lateral view). A–B, *Piatnitzkysaurus* (MACN-Pv-CH 895). C–D, *Condorraptor* (MPEF-PV 1687). *Marshosaurus* (UMNH VP 6372). Anatomical/muscular abbreviations: bf, brevis fossa; cf, "cuppedicus" fossa; CFBf, *M. caudofemoralis brevis* origin fossa; IFEf, *M. iliofemoralis externus* origin fossa; ILFBf, *M. iliofibularis* origin fossa; ip, ischiadic peduncle; IT1–3, *Mm. iliotibiales 1–3* origin scars; PIFI1, *M. puboischiofemoralis 1* origin fossa; pp, pubic peduncle; poap, postacetabular process; prap, preacetabular process; sac, supraacetabular crest; vr, vertical ridge. Arrows indicates potential subdivision of IT heads. Scale bar = 100mm.

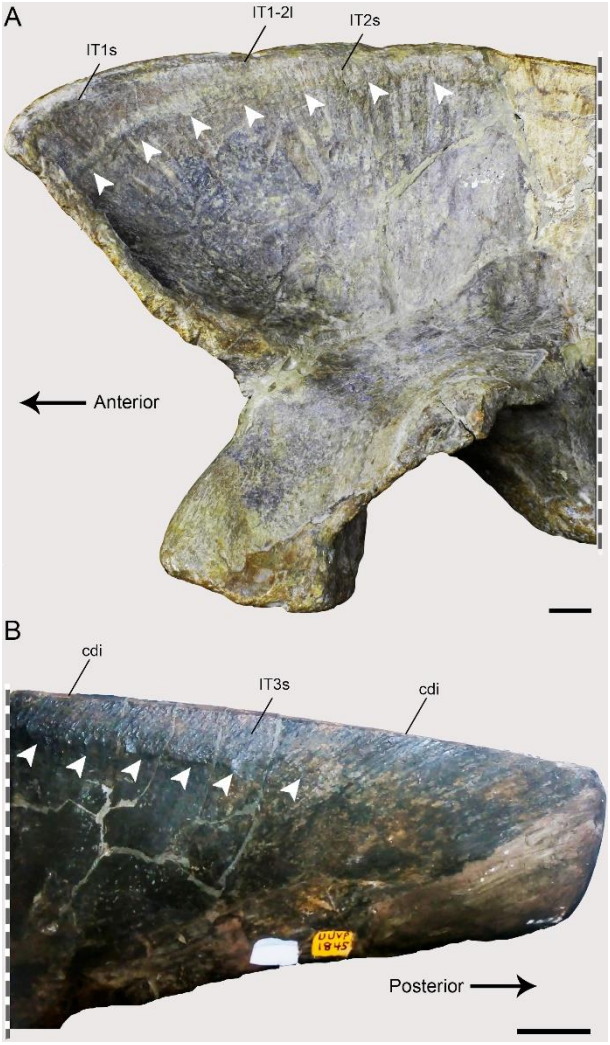

Figure 2.3. Osteological correlates of *M. iliotibiales 1–3* observed in the ilia of Piatnitzkysauridae (left ilia, lateral view). A, *Piatnitzkysaurus* (MACN-Pv-CH 895). B, *Marshosaurus* (UMNH VP 6372). Anatomical/muscular abbreviations: cdi, *crista dorsolateralis ilii*; IT1–3s, *Mm. iliotibiales* scars; IT1–2l, *M. iliotibialis 1* and *2* limits. Arrows indicates muscle scars. Scale bar = 20mm.

As in Crocodylia, Aves and other reptiles, those three heads of *Mm. iliotibiales* converge with *M. ambiens*, and *Mm. femorotibiales* into at least one extensor tendon and fascial sheet, which inserts on the tibial cnemial crest or *crista cnemialis cranialis* (Baumer & Witmer, 1993) of the proximal metaphysis of the tibia (Gregory & Camp, 1918; Romer, 1923a,b; 1942; Patak & Baldwin, 1998; Hutchinson, 2002; Otero *et al*., 2010; Dick & Clemente, 2016).

The tibiae of both *Piatnitzkysaurus* specimens, MACN-Pv-CH 895 and PVL 4073 (Figure 2.4A,B), have an expanded and rough area on the tibial cnemial crest with an anterior protuberance that is distal to the cnemial crest. On this basis, we infer the same condition that is observed in extant archosaurs, with the cnemial crest as the osteological correlate for the insertion of IT1–3 (and the remainder of the *triceps femoris*: AMB and FMTE, FMTI) (level I) (Figure 2.4A,B). In the *Condorraptor* holotype MPEF-PV 1672, the cnemial crest is rounded

and presents a small crest (Figure 2.4C,D) when compared with *Piatnitzkysaurus*, and similar with other archosaurs, this is probably the same attachment area for the main tendon(s) of IT1–3 and other *triceps femoris* muscles (level I) (Figure 2.4C,D). No tibia associated with *Marshosaurus* has been formally described so far, to our knowledge.

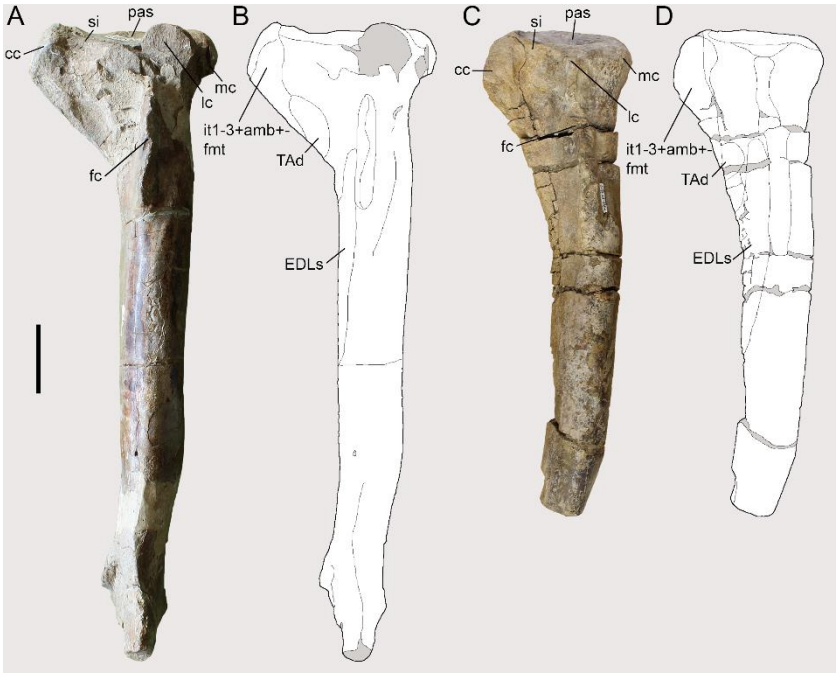

Figure 2.4. Osteological correlates of the *triceps femoris* insertion and origins of lower leg muscles from the tibiae of Piatnitzkysauridae (left tibia, lateral view). A–B, *Piatnitzkysaurus* (PVL 4073). C–D, *Condorraptor* (MPEF-PV 1672). Anatomical/muscular abbreviations: cc, cnemial crest; EDLs, *M. extensor digitorum longus* scar; fc, fibular crest; it1–3+amb+fmt, insertion of the tendon composed of the *iliotibiales+ambiens+femorotibiales* muscles; lc, lateral condyle; mc, medial condyle; pas, proximal articular surface; si, sulcus intercnemialis; TAd, *M. tibialis* anterior depression. Scale bar = 50mm.

M. ambiens (AMB). The AMB in extant Reptilia typically takes its origin from the pubic tubercle or tuberculum preacetabulare (Romer, 1923a,b; 1942; Hutchinson, 2001b; 2002; Picasso, 2010), also termed the pectineal process (Hudson *et al*., 1959; Suzuki *et al*., 2014), preacetabular tubercle (Hutchinson, 2002), or ambiens process (Langer, 2003). As noted by Hutchinson (2001b), the pubic tubercle is small or even absent in Crocodylia which have a derived feature, relative to other Reptilia, related with having mobile pubes and two heads of AMB (Gregory & Camp, 1918; Romer, 1923a,b; Hutchinson, 2001b; Suzuki *et al*., 2011). In most Aves, as is ancestral for other Reptilia, the AMB has a single head (Hutchinson, 2001b; Picasso, 2010).

The pubes of both *Piatnitzkysaurus* individuals (left and right in MACN-Pv-CH 895 and left in PVL 4073) have a pubic tubercle that is well-developed (Figure 2.5A–D), as in Aves and other theropods (Gregory & Camp, 1918; Romer, 1923b; Hudson *et al*., 1959; Hutchinson,

2001b; Carrano & Hutchinson, 2002; Grillo & Azevedo, 2011). However, this tubercle slightly differs from other piatnitzkysaurid species in position – being more laterally and distally positioned instead of anterior as in *Condorraptor*, and more distally positioned than the condition in *Marshosaurus* (Madsen, 1976) (Figure 2.5). Nonetheless, the pubic tubercle is an osteological correlate of the presence and origin of the single head of the AMB in *Piatnitzkysaurus* (level I), as previously noted by Bonaparte (1986). The pubic tubercle in *Condorraptor* is remarkably large (Figure 2.5E–H); this strongly pronounced tubercle generally is not seen in other tetanuran theropods (Rauhut, 2005). It thus is plausible, based on the osteological correlate of the right pubis MPEF-PV 1696 and a small fragment of the left pubis MPEF-PV 1688, that the AMB had a robust attachment to the pelvic girdle of *Condorraptor* (level I). The best-preserved pubis of *Marshosaurus* (right pubis UMNH VP 6387) also osteologically concurs with the single head of the AMB; as previously noted, the anterolateral part of the proximal portion of the pubis presents a visibly rough area (Madsen, 1976) topographically equivalent to the AMB origin (level I) (Figure 2.5I–J).

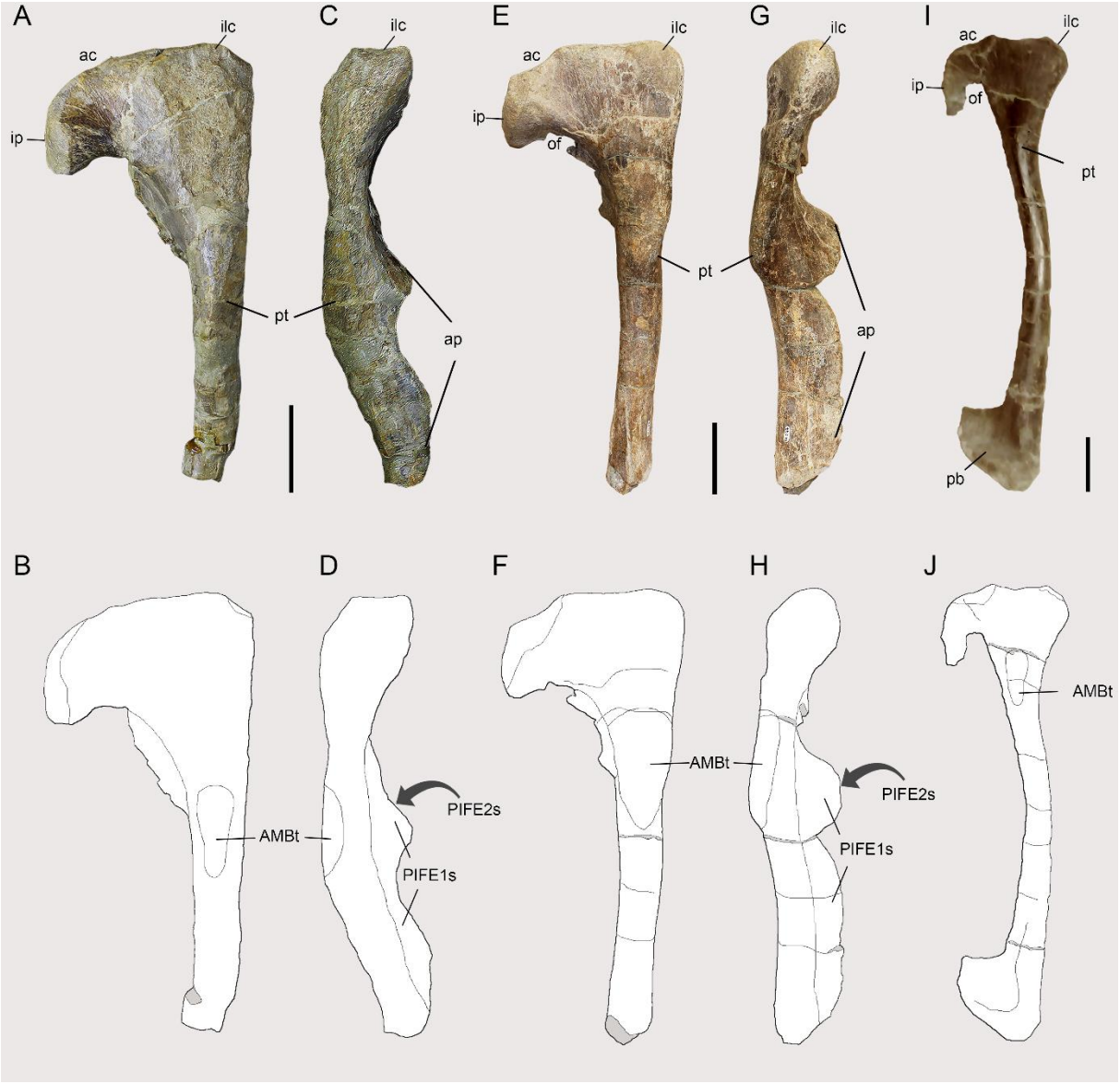

Figure 2.5. Osteological correlates observed on the pubes of Piatnitzkysauridae (right pubes, lateral and anterior views). A–D, *Piatnitzkysaurus* (MACN-Pv-CH 895). E–H, *Condorraptor* (MPEF-PV 1696). I–J, *Marshosaurus* (UMNH VP 6387). Anatomical/muscular abbreviations: ac, acetabulum; AMBt, *M. ambiens* tubercle; ap, apron; ilc, iliac peduncle; ip, ischial peduncle; of, obturator foramen; pb, pubic boot; PIFE1s, *M. puboischiofemoralis externus 1* scar; PIFE2s, *M. puboischiofemoralis externus 2* scar; pt, pubic tubercle. A, B, E, F, I, J in lateral view; C, D, G, H in anterior view. Scale bar = 50mm.

The insertion of AMB converges on the tibial cnemial crest with the rest of the *triceps femoris* muscle group (Romer, 1923a,b; Hutchinson, 2001b; 2002; Suzuki *et al*., 2014). Furthermore, as noted by Romer (1923a,b), McKitrick (1991), and Hutchinson (2002), the AMB muscle has a secondary tendon which perforates the extensor tendon and merges with the origin of *M. gastrocnemius externus*/l*ateralis* near the proximal fibula. While this shared tendon might be had been present in early tetanurans such as piatnitzkysaurids, as is ancestral for Archosauria, there is no evidence of it (Level I').

Thus, as previously described, the insertion of the AMB in *Piatnitzkysaurus* and *Condorraptor* occurred in a shared tendon attached to the cnemial crest (level I) (Figure 2.4). As there is no formally described tibia for *Marshosaurus*, the insertion of this muscle is not reconstructed here.

Mm. femorotibiales (FMTE and FMTI). The *Mm*. *femorotibiales* of Crocodylia has two heads (i.e., *M*. *femorotibialis externus* – FMTE and *M*. *femorotibialis internus* – FMTI), whereas in Aves, there are three heads (i.e., *M*. *femorotibialis medialis* – FMTM, *M*. *femorotibialis intermedius* – FMTIM, and *M*. *femorotibialis lateralis* – FMTL) (Romer, 1923a; Hudson *et al*., 1959; McKitrick, 1991; Hutchinson, 2001a; 2002; Otero *et al*., 2010; Picasso, 2010; Suzuki *et al*., 2011; Zinoviev, 2011; Clifton *et al*., 2018); here we use the names from Crocodylia as per other studies of non-avian theropods (e.g., Carrano & Hutchinson, 2002; Grillo & Azevedo, 2011; Bishop *et al*., 2021). The origins of FMTE and FMTI are located between the trochanteric (proximal) and the condylar (distal) regions across a great portion of the femoral shaft (Romer, 1923a,b; McKitrick, 1991; Hutchinson, 2001a; 2002; Carrano & Hutchinson, 2002; Picasso, 2010; Grillo & Azevedo, 2011; also see Cuff *et al*., 2023b). On the femoral shaft, the FMTE and FMTI origins are delimited by three ridges, namely: *linea intermuscularis cranialis* (*lia*), *linea intermuscularis caudalis* (*lip*) and *linea aspera* (= adductor ridge, *la*) (Baumer & Witmer, 1993; Hutchinson, 2001a). However, these structures are variable throughout ontogeny in both extant and extinct archosaurs (Griffin, 2018). The FMTE origin has boundaries delimited by the *lia* and *lip* (on the lateral femoral shaft), whereas the FMTI origin is delimited by the *lia* and *la* (on the anteromedial femoral shaft) (Hutchinson, 2001a; 2002; Griffin, 2018), also there seems to have been the participation of the craniomedial distal crest (cdc) in those subdivisions in some extinct archosaurs (Hutchinson, 2001a).

The three femora of the two *Piatnitzkysaurus* skeletons lack well-preserved shaft surfaces. Regardless, the left femur of PVL 4073 preserves the most distal parts of both *la* and *lip* on the posterior shaft of the femur, and lia on the distal femur, arising medially and becoming anteriorly positioned along to the proximal shaft of the femur (Figure 2.6C–D). Furthermore, the right femur of PVL 4073 preserves the distal base of the *la* (Figure 2.6G–H). Although not entirely preserved, the presence of the *la*, *lia* and *lip* allows inference of the FMTE and FMTI origins without precise boundaries (Figure 2.6). The FMTE and FMTI in *Piatnitzkysaurus*, as well as in other theropods (e.g., *Staurikosaurus* – Grillo & Azevedo, 2011; *Coelophysis* – Bishop *et al*., 2021; allosauroids – Bates *et al*., 2012a; *Tyrannosaurus* – Carrano & Hutchinson, 2002; *Nothronychus* – Smith 2021) have the same origins from the lateral and the anteromedial

surfaces of the femoral shaft, respectively (level I). In *Condorraptor*, both femora are quite fragmentary, lacking the proximal portions. The right femur MPEF-PV 1690 is better preserved, with a great portion of the femoral shaft (Figure 2.7); however, the three longitudinal ridges/lineae (*lia*, *lip* and *la*) are not completely preserved. It remains possible to reconstruct the FMTE and FMTI origins in positions similar to our *Piatnitzkysaurus* reconstruction (level I), but their proximal extent remains indeterminate. Rauhut (2005) noted the presence of the cdc in both *Condorraptor* femora (Figure 2.7E–H); this being a structure related with the distal divisions between the FMTE and FMTI origins (Hutchinson, 2001a). *Marshosaurus* has no preserved femur, preventing any inferences about these muscles.

The FMTE and FMTI heads converge into a main tendon and fascia inserting onto the tibial cnemial crest deep to IT1–3 and AMB (level I) (Figure 2.4), as noted above.

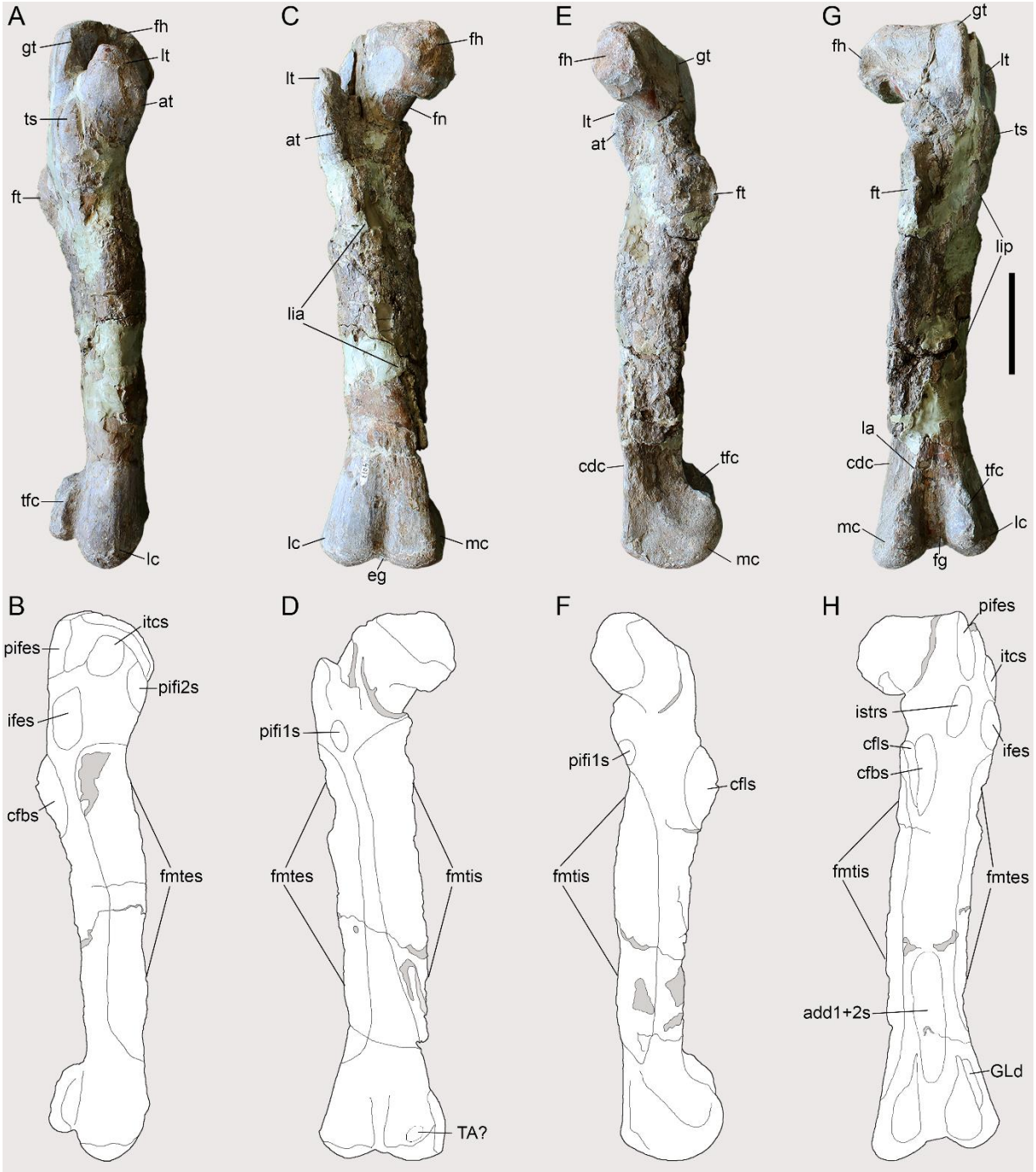

Figure 2.6. Osteological correlates observed on the femur of *Piatnitzkysaurus* (right femur, PVL 4073). A–B, lateral view; C–D, anterior view; E–F, medial view; G–H, posterior view. Anatomical/muscular abbreviations: add1+2s, *Mm. adductores femores* insertion scar; at, anterior trochanter; cdc, craniomedial distal crest; cfbs, *M. caudofemoralis brevis* insertion scar; cfls, *M. caudofemoralis longus* insertion scar; eg, extensor groove; fh, femoral head; fg, flexor groove; fmtes, *M. femorotibialis externus* scar; fmtis, *M. femorotibialis internus* scar; fn, femoral neck; ft, fourth trochanter; GLd, *M. gastrocnemius pars lateralis* depression; gt, greater trochanter; ifes, *M. iliofemoralis externus* insertion scar; istrs, *M. ischiotrochantericus* insertion scar; itcs, *M. iliotrochantericus caudalis* insertion scar; *la*, *linea aspera*; lc, lateral condyle; *lia*, *linea intermuscularis cranialis*; *lip*, *linea intermuscularis caudalis*; lt, lesser trochanter; mc, medial condyle; pifes, *Mm. puboischiofemorales externi* insertion scar; pifi1s, *M. puboischiofemoralis 1* insertion scar; pifi2, *M. puboischiofemoralis 2* insertion scar; TA?, *M. tibialis anterior*?; tfc, tibiofibular crest; ts, trochanteric shelf. Scale bar = 100mm.

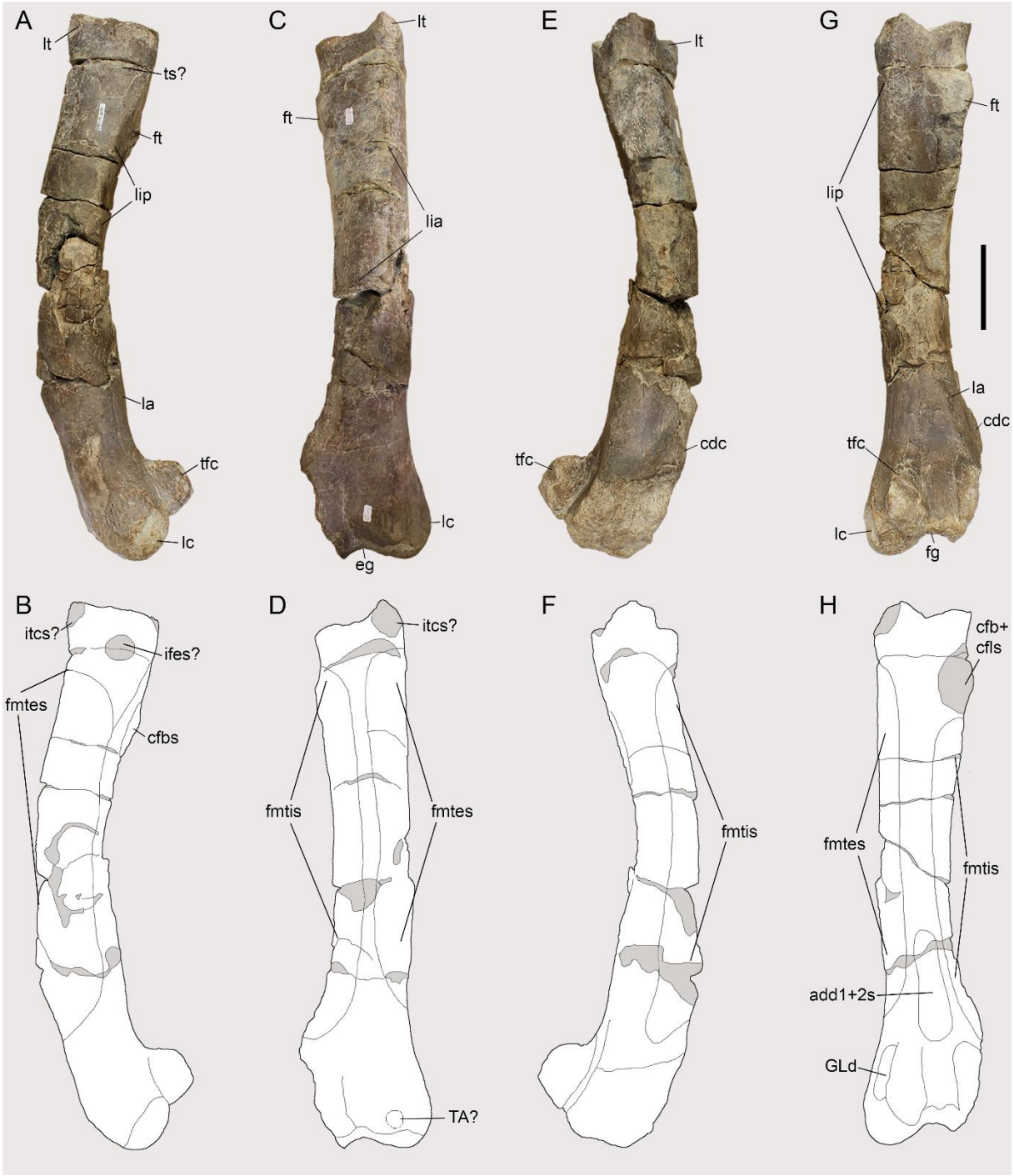

Figure 2.7. Osteological correlates observed on the femur of *Condorraptor* (left femur, MPEF-PV 1690). A–B, lateral view; C–D, anterior view; E–F, medial view; G–H, posterior view. Anatomical/muscular abbreviations: add1+2s, *Mm. adductores femores* insertion scar; cdc, craniomedial distal crest; cfb+cfls, *Mm. caudofemorales* insertion scar; cfbs, *M. caudofemoralis brevis* insertion scar; eg, extensor groove; fg, flexor groove; fmtes, *M. femorotibialis externus* scar; fmtis, *M. femorotibialis internus* scar; ft, fourth trochanter; GLd, *M. gastrocnemius pars lateralis* depression; ifes?, *M. iliofemoralis externus* insertion scar?; itcs?, *M. iliotrochantericus caudalis* insertion scar?; *la*, *linea aspera*; lc, lateral condyle; *lia*, *linea intermuscularis cranialis*; *lip*, *linea intermuscularis caudalis*; lt, lesser trochanter; TA?, *M. tibialis anterior*?; tfc, tibiofibular crest; ts?, trochanteric shelf?. Scale bar = 100mm.

M. iliofibularis (ILFB). In Reptilia and extant archosaurs, the ILFB originates from the lateral surface of the ilium in the postacetabular blade, positioned posterior to the IFE (IF in Crocodylia), anterior to the FTE (FCLA and FCLP in Aves), and ventral to the IT. ILFB is a large, fusiform and superficial muscle of the thigh (Gregory & Camp, 1918; Romer, 1923a,b; 1942; McKitrick, 1991; Hutchinson, 2001a,b; 2002; Picasso, 2010; Suzuki *et al*., 2011; Dick & Clemente, 2016; Clifton *et al*., 2018), more expanded in the ilium of dinosaurs (Hutchinson, 2002).

As previously noted by Bonaparte (1986), the lateral surface of iliac blade in *Piatnitzkysaurus* has a large and deep depression. This lateral depression is subdivided by a swollen vertical ridge, positioned just above the acetabulum (Carrano *et al*., 2012; Chapter 1). This ridge has been suggested as the anterior limit of the ILFB (Hutchinson, 2001b; Carrano & Hutchinson, 2002). Anterior to the vertical ridge and anterodorsal to the acetabulum, the lateral depression is large and deep; whereas the posterior depression is shallow and positioned just above the ischial peduncle (Figure 2.2A,B). Topographically, this posterior concavity is equivalent to the ILFB origin, as in other extinct theropods and extant archosaurs (Hutchinson, 2001a; Carrano & Hutchinson, 2002; Otero *et al*., 2010; Picasso, 2010; Grillo & Azevedo, 2011). The ventral limit of the ILFB origin is indicated by the brevis shelf, and its anterior limits seem to be related to the vertical iliac ridge (Hutchinson, 2001a), whereas the posterodorsal limits appear to have been demarcated by a semi-circular scar just below the IT3 origin (level I). In *Condorraptor*, although the supraacetabular crest is fragmentary, the left ilium MPEF-PV 1687 bears a small and shallow concavity dorsal to the ischiadic peduncle and posterior to the supraacetabular vertical ridge, on the postacetabular blade (Figure 2.2C,D), which may have been the osteological correlate for the anterior limits of the ILFB origin. As noted by Carrano & Hutchinson (2002), the scars made by ILFB are difficult to discern; however, a well-developed iliac ridge lies just above the acetabulum in most megalosauroids (Carrano *et al*., 2012; Chapter 1), indicating the anterior edge of the ILFB origin and the posterior edge of the *M. iliofemoralis externus*. Ventrally, the concavity related to the ILFB origin is delimited by the brevis shelf. Although the anterior, posterior and ventral limits of the ILFB origin are discernible (level I), the dorsal limit of this muscle origin is unclear, because the supraacetabular rim is not preserved in the only known ilium of *Condorraptor*. The ilia of *Marshosaurus* seem to lack the supraacetabular vertical ridge, or at least taphonomic issues preclude scoring this character in this taxon (Carrano *et al*., 2012; Chapter 1); however, the dorsal, ventral and posterior boundaries of the ILFB origin can be inferred in this species based on the presence of a concavity and its posterior, dorsal and ventral delimitations (level I) (Figure 2.2E,F).

The insertion of the ILFB in Reptilia is located on the fibular tubercle, a scarred or rounded and prominent structure on the proximal region of the fibular shaft; typically most prominent in archosaurs. Furthermore, a secondary tendon is present in extant taxa (in Aves, constrained by a loop termed *ansa m. iliofibularis* – Baumel & Witmer, 1993; also see Hutchinson, 2001a), which inserts onto *M. gastrocnemius internus*/*lateralis* near its origin (Romer, 1923a; Hutchinson, 2001a; 2002; Carrano & Hutchinson, 2002; Otero *et al*., 2010; Picasso, 2010; Dick & Clemente, 2016; Clifton *et al*., 2018).

The right fibula of *Piatnitzkysaurus* PVL 4073 preserves the fibular tubercle (Chapter 1), which also presents small scar (Figure 2.8), as sometimes seen in other archosaurs. As in other theropods (e.g., *Tyrannosaurus* – Carrano & Hutchinson, 2002), there is no osteological evidence for a secondary tendon in early tetanurans based on *Piatnitzkysaurus*, although this structure is predicted to have been present (level I'). The fibula is not preserved in *Condorraptor* and *Marshosaurus*.

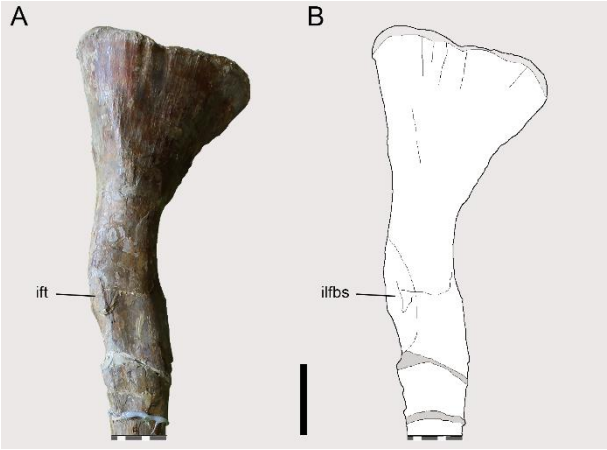

Figure 2.8. Osteological correlate observed on the left fibula of *Piatnitzkysaurus* (PVL 4073). A–B, lateral view. Anatomical/muscular abbreviations: ift, iliofibularis (fibular) tubercle; ilfbs, *M. iliofibularis* insertion scar. Scale bar = 50mm.

3.1.2 Deep Dorsal Group

M. iliofemoralis* or *M. iliofemoralis externus (IFE)* and *M. iliotrochantericus caudalis (ITC). The *M. iliofemoralis* in Crocodylia is a single muscle, not divided, with an origin located just above the acetabular aperture and deep to IT2, on the lateral surface of the ilium (Gregory & Camp, 1918; Romer, 1923a,b; Hutchinson, 2002; Otero *et al*., 2010). In Aves, the "*M. iliofemoralis*" is split into two muscles (i.e., *M. iliofemoralis externus* – IFE and *M. iliotrochantericus caudalis* – ITC; Hudson *et al*., 1959; Rowe, 1986; Hutchinson, 2001a; 2002; Picasso, 2010; Clifton *et al*., 2018) which are located above the acetabular aperture (IFE) and

on the anteriormost surface of the preacetabular blade (ITC)(Rowe, 1986; Hutchinson, 2002; Suzuki *et al*., 2014). The subdivision of the *M. iliofemoralis* in extant Aves might be evidenced by an insertion area on the proximal femur (Hutchinson, 2001a). Dinosauromorpha in general have a protuberance (lesser/anterior trochanter) on the proximolateral femur (e.g., Müller & Garcia, 2023), homologous with the ITC insertion area in Aves; Dinosauriformes also have a more posterodistal scarred ridge or lump (trochanteric shelf; Novas, 1996) that might correspond to the IFE insertion, suggesting that the *M. iliofemoralis* was subdivided in ancestral Dinosauriformes (Hutchinson & Gatesy, 2000; Hutchinson, 2001a; Carrano & Hutchinson, 2002; Grillo & Azevedo, 2011). As per below, *Piatnitzkysaurus* and *Condorraptor* show evidence of this subdivision, too.

Nonetheless, the area of origin of *M. iliofemoralis* does not present scars indicating these subdivisions between the IFE and ITC (Hutchinson, 2001a; Carrano & Hutchinson, 2002). We consider the semi-circular concavity of the *Piatnitzkysaurus* preacetabular ilium (MACN-Pv-CH 895; Bonaparte, 1986) anterior to the iliac ridge as the origin of both of these muscular divisions (level I) (Figure 2.2A,B). The dorsal limits of both muscle origins are quite visible, indicated by striations located just ventral to the origins of the IT1–3 (Figure 2.2, Figure 2.3). The anterior limits of the ITC are undefined in this specimen due the lack of the anteriormost and anteroventralmost preacetabular blade (Bonaparte, 1986). Following avian myology, the ITC origin presumably would be anterior to the IFE head (level II'). Even though the dorsal rim of the iliac blade is not preserved in *Condorraptor*, a large, deep, almost circular concavity is anterodorsal to the acetabulum (Figure 2.2C,D); again suggesting the origins of the IFE and ITC (level I). Otherwise, due to the fragmentary nature of the specimen, it is not possible to delimit the boundaries of these muscle origins in this taxon; only to suggest relative general positions. Although the ITC and IFE origins in *Marshosaurus* must have been in a similar pattern, it is not possible to reconstruct this musculature because the anterior part of the ilium is not preserved and the figured ilium (Figure 2.2E,F) represents a plaster reconstruction of the preacetabular process.

As commented by Bonaparte (1986), the femur of *Piatnitzkysaurus* has a well-developed lesser trochanter in the shape of a proximodorsally positioned blade (Figure 2.6A–D, Figure 2.9); as in other megalosauroids, it rises past the ventral margin of the femoral head (Carrano *et al*., 2012; Chapter 1). A rough area on the trochanteric shelf is not discernible; however, this structure is quite elevated and distinct (Figure 2.9), being posterodistal to the lesser trochanter and anterodistal to the greater trochanter of the femur. It is thus possible to infer the subdivision of *M. iliofemoralis* in this taxon; IFE should have inserted onto the femoral trochanteric shelf

(level II) and ITC onto the lesser/anterior trochanter (level II) (Figure 2.6, Figure 2.9). The left femur of *Condorraptor* MPEF-PV 1690 has the base of the lesser trochanter anterolaterally located, also indicating a quite well-developed lesser trochanter in *Condorraptor* (and perhaps a fragment of the trochanteric shelf) and IFE and ITC muscle subdivisions (level II) (Figure 2.7). The femur of *Marshosaurus* is not preserved.

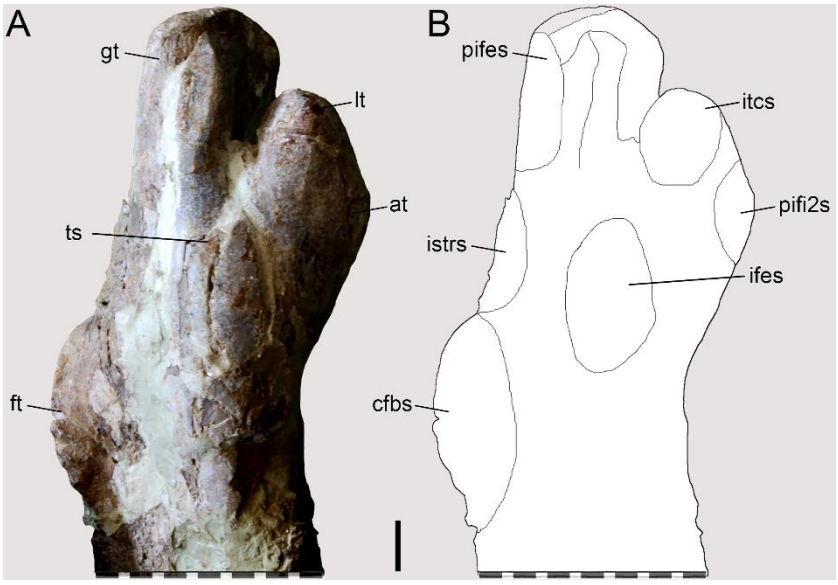

Figure 2.9. Osteological correlates observed on the femur of *Piatnitzkysaurus* (right femur, PVL 4073). A–B, lateral view. Anatomical/muscular abbreviations: at, acessory trochanter; cfbs, *M. caudofemoralis brevis* insertion scar; ft, fourth trochanter; gt, greater trochanter; ifes, *M. iliofemoralis externus* insertion scar; istrs, *M. ischiotrochantericus* insertion scar; itcs, *M. iliotrochantericus caudalis* insertion scar; lt, lesser trochanter; pifes, *Mm. puboischiofemorales externi* insertion scar; pifi2, *M. puboischiofemoralis 2* insertion scars; ts, trochanteric shelf. Scale bar = 20mm.

M. pubo-ischio-femoralis internus 1 (PIFI1). The PIFI1 in Crocodylia (or *M. iliofemoralis internus* – IFI or *M.* "*cuppedicus*" in Aves; Rowe, 1986) is considered to be homologous to the muscles PIFI1 and PIFI2 in Reptilia (Romer, 1923b; Rowe, 1986; Patak & Baldwin, 1999; Hutchinson, 2002; Suzuki *et al*., 2011). The PIFI1 origin in Crocodylia is located on the medioventral surface of the ilium, as well as on the proximal ischium, being a short and thick muscle (Romer, 1923a,b; Hutchinson, 2001a; 2002; Otero *et al*., 2010). The IFI origin in Aves is on the lateral surface of the ilium, between the anterodorsal region of the pubic peduncle and the posteroventral extremity of the preacetabular blade (Romer, 1923a; Rowe, 1986; Hudson *et al*., 1959; Hutchinson, 2002; Picasso, 2010; Suzuki *et al*., 2014). In many extinct theropods, there is evidence of the muscle origin (in a state intermediate between the ancestral reptilian and derived avian condition) from a preacetabular "cuppedicus" fossa (Hutchinson, 2002 [or preacetabular notch – Carrano *et al*., 2012; Chapter 1]) in that same region, suggesting a shift of the muscle origin from the medial to lateral pelvis (Romer, 1923a;

Rowe, 1986; Hutchinson, 2002; Carrano & Hutchinson, 2002). This inference is complicated by the fact that homologues of the PIFI2 in Crocodylia also originate from a similar area in Aves, so there is some ambiguity about which PIFI1 or 2 muscle(s) may have shifted into this fossa and when (Hutchinson, 2001b; 2002; Carrano & Hutchinson, 2002).

In *Piatnitzkysaurus*, even though the anterior margin of the preacetabular iliac blade is not entirely preserved on the specimen MACN-Pv-CH 895, the "cuppedicus" fossa/preacetabular notch is evident in the ventromedial surface of the iliac blade (Figure 2.2A,B), being dorsally delimited by the preacetabular ridge, suggesting the PIFI1 origin (level I). In *Condorraptor* and *Marshosaurus* (Madsen, 1976), despite the fragmentary nature of the ilium of MPEF-PV 1687 (Figure 2.2C,D) and UMNH VP 6372 (Figure 2.2E,F), respectively, the same preacetabular notch is evident and inferred as the PIFI1 origin (level I).

The PIFI1/IFI insertion in extant archosaurs is located on the anteromedial surface of the femoral shaft. In Crocodylia, the insertion is on a keel that separates the site of insertion of PIFI2 laterally; and the origin of FMTI; laterally, anteromedial to the fourth trochanter (Romer, 1923a; Hutchinson, 2001b; 2002; Otero *et al*., 2010). In Aves, IFI inserts onto a rounded mark on the proximomedial portion of the femur (Hudson *et al*., 1959; Hutchinson, 2001b; 2002; Suzuki *et al*., 2014).

The femoral surface in *Piatnitzkysaurus* is not well-preserved, however, a rounded and small tubercle is positioned distal to the anterior trochanter in both femora PVL 4073, that corresponds to the PIFI1 insertion (level II) (Figure 2.6D,F). This bump is not discernible on the *Condorraptor* femora MPEF-PV 1690–1691 (level I').

M. pubo-ischio-femoralis internus 2 (PIFI2)* or *M. iliotrochantericus cranialis (ITCR)* and *M. iliotrochantericus medius (ITM). The PIFI2 muscle in Crocodylia is considered to be the homologous to the PIFI3 in non-archosaurian Reptilia instead of the homonymous muscle; however, it is uncertain whether, in the avian lineage, PIFI2 was completely lost (in this hypothesis IF split into four muscles: IFE, ITC, ITCR, and ITM) or whether PIFI2 split into ITCR and ITM in Aves (Romer, 1923a; Rowe, 1986; Carrano & Hutchinson, 2002; Hutchinson, 2002). Even with these uncertainties, the second hypothesis (PIFI2 = ITCR+ITM) is considered better supported, as it requires fewer transformations (Rowe, 1986; Grillo & Azevedo, 2011). Based on this, although with variations, most recent theropod reconstructions (e.g., Grillo & Azevedo, 2011; Bishop *et al*., 2021; Rhodes *et al*., 2021; Smith, 2023) have adopted the second hypothesis, which is also followed here. In Crocodylia the PIFI2 is a triangular and broad "fan-shaped" muscle that originates from the centra of the last 6-7 dorsal vertebrae and their

transverse processes (Romer, 1923a; Otero *et al*., 2010; Suzuki *et al*., 2011). In Aves, the homologous ITCR and ITM are small muscles that originate from the anteroventralmost part of the lateral portion of the preacetabular iliac blade (Rowe, 1986; Patak & Baldwin, 1999; Picasso, 2010). As above, this evident evolutionary shift of muscle origins is related to the expansion of the preacetabular blade and the origin of the preacetabular notch (Romer, 1923a; Hutchinson, 2001b; 2002).

The last dorsal vertebrae in *Piatnitzkysaurus* possess well-developed vertebral centra (Bonaparte, 1986) lacking pleurocoels. A large and shallow concavity located bellow the parapophyseal region is well-demarcated on some vertebrae (e.g., 19th and 20th; Figure 2.10) and could be part of the PIFI2 origin (level II) as in Crocodylia, which also potentially originated near the PIFI1 on the ilium (level I'). Only two posteriormost presacral vertebra are preserved in *Condorraptor* (MPEF-PV 1680 and 1700) with massive vertebral centra (Rauhut, 2005), being similar to those of *Piatnitzkysaurus* and also possessing a wide and well-demarcated shallow concavity that could have been part of the PIFI2 origin (level I). No vertebrae associated with *Marshosaurus* were studied, so no inference was made here.

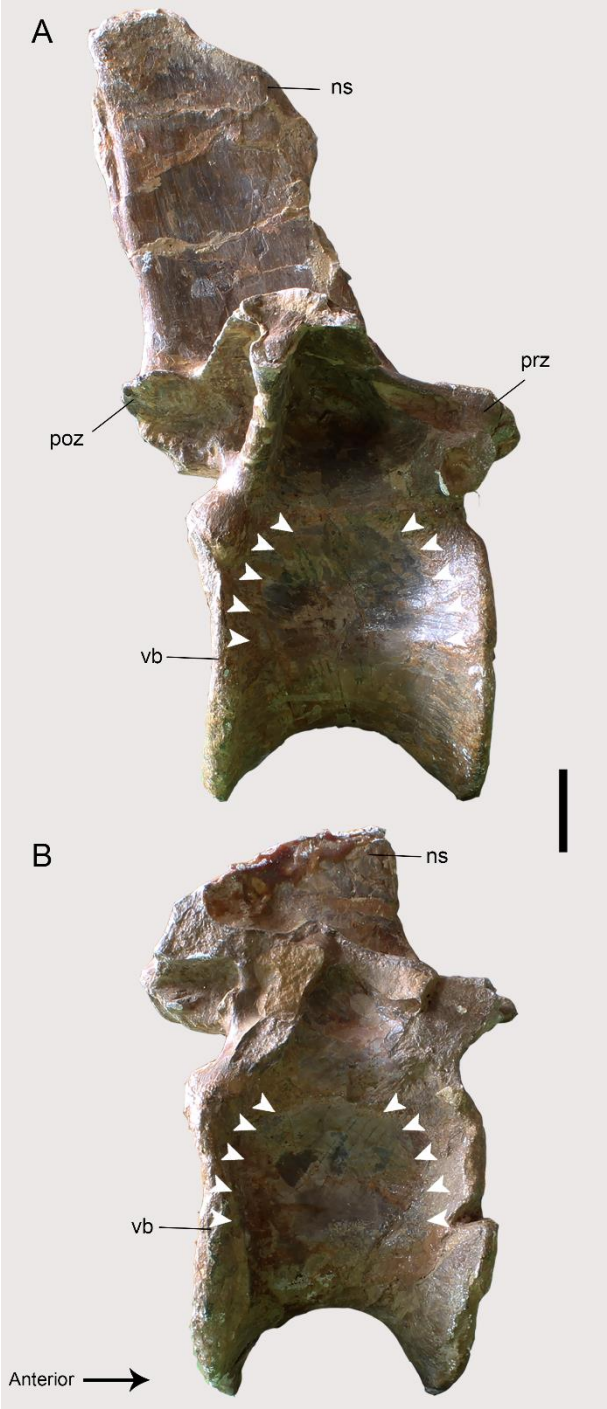

Figure 2.10. Osteological correlates observed on the vertebrae of *Piatnitzkysaurus* (PVL 4073). A, 19th dorsal vertebra. B, 20th dorsal vertebra. Anatomical/muscular abbreviations: ns, neural spine; poz, postzygapophyses; prz, prezygapophysis; vb, vertebral body. Arrows indicates muscle scars. Scale bar = 20mm.

The PIFI2 insertion in Crocodylia occurs via a tendon on the proximolateral femur near the fourth trochanter, on an anteromedial keel at two distinct points separated by the proximal FMTE origin (Romer, 1923a; Hutchinson, 2001a; Otero *et al*., 2010; Suzuki *et al*., 2011). In Aves, the homologous muscles insert onto the distal end of the trochanteric crest, marked by small scars (Patak & Baldwin, 1999; Hutchinson, 2001a; 2002). Avetheropoda (Allosauroidea

+ Coelurosauria; Paul, 1988) evolved a large accessory trochanter, as a "blade-like" structure; however, this structure, although small, is also present in early Tetanurae (Hutchinson, 2001a; Carrano *et al*., 2012; Chapter 1). The accessory trochanter is topologically equivalent to the PIFI2 insertion (Hutchinson, 2001a; 2002).

The right femur of *Piatnitzkysaurus* PVL 4073 preserves a well-developed blade-shaped lesser trochanter (Bonaparte, 1986) with a clear anterolateral and distal projection: the accessory trochanter, which is the insertion of the PIFI2 muscle (level I) (Figure 2.6A–F, Figure 2.9). In *Condorraptor*, although the best-preserved femur MPEF-PV 1690 has the base of a prominent lesser trochanter, the most proximal part of it is not preserved and the accessory trochanter is not discernible, so the PIFI2 insertion cannot directly be reconstructed.

3.1.3 Flexor Cruris

M. flexor tibialis internus 1 (FTI1). In Aves, the FTI1 muscle is absent (Hutchinson, 2002), whereas in Crocodylia it is a thin and long muscle originating from the distal portion of the ischium, on the posterodorsal surface (Gregory & Camp, 1918; Romer, 1923a,b; Otero *et al*., 2010; Suzuki *et al*., 2011). Other Reptilia lack an obvious FTI1, so homologies are unclear (for example PIT in Romer, 1942 or FTI (D) in Dick & Clemente, 2016); originating from the posterior ischium (Dick & Clemente, 2016). Many theropod dinosaurs have a distal ischial tubercle on the posterolateral ischial shaft (e.g., Carrano & Hutchinson, 2002; Hutchinson, 2001b; 2002), which is topographically equivalent to the approximate FT1 origin in Crocodylia.

Bonaparte (1986) speculated that the ischial tubercle might be the origin of the "*M. ischiofemoralis*" (or homologous *M. ischiotrochantericus*, ISTR). However, we interpret the ischial tubercle on the distal ischial shaft of the PVL 4073 left ischium as the origin for the FTI1 in *Piatnitzkysaurus*, as a level II inference (Figure 2.11A–B) (see below for rationale for the ISTR origin). The distalmost portion of the ischial shaft in the ischium of *Condorraptor* MPEF-PV 1689 is not well-preserved, with no sign of the ischial tubercle; thus, we made no inference of the FTI1 origin in this taxon. In the left ischium of *Marshosaurus* UMNH VP 6380, although not as discernible as in *Piatnitzkysaurus*, the ischial tubercle appears to be positioned on the medial shaft of the ischium (Figure 2.11D–E), similar in position to *Piatnitzkysaurus* and topographically equivalent to the FTI1 origin (level II).

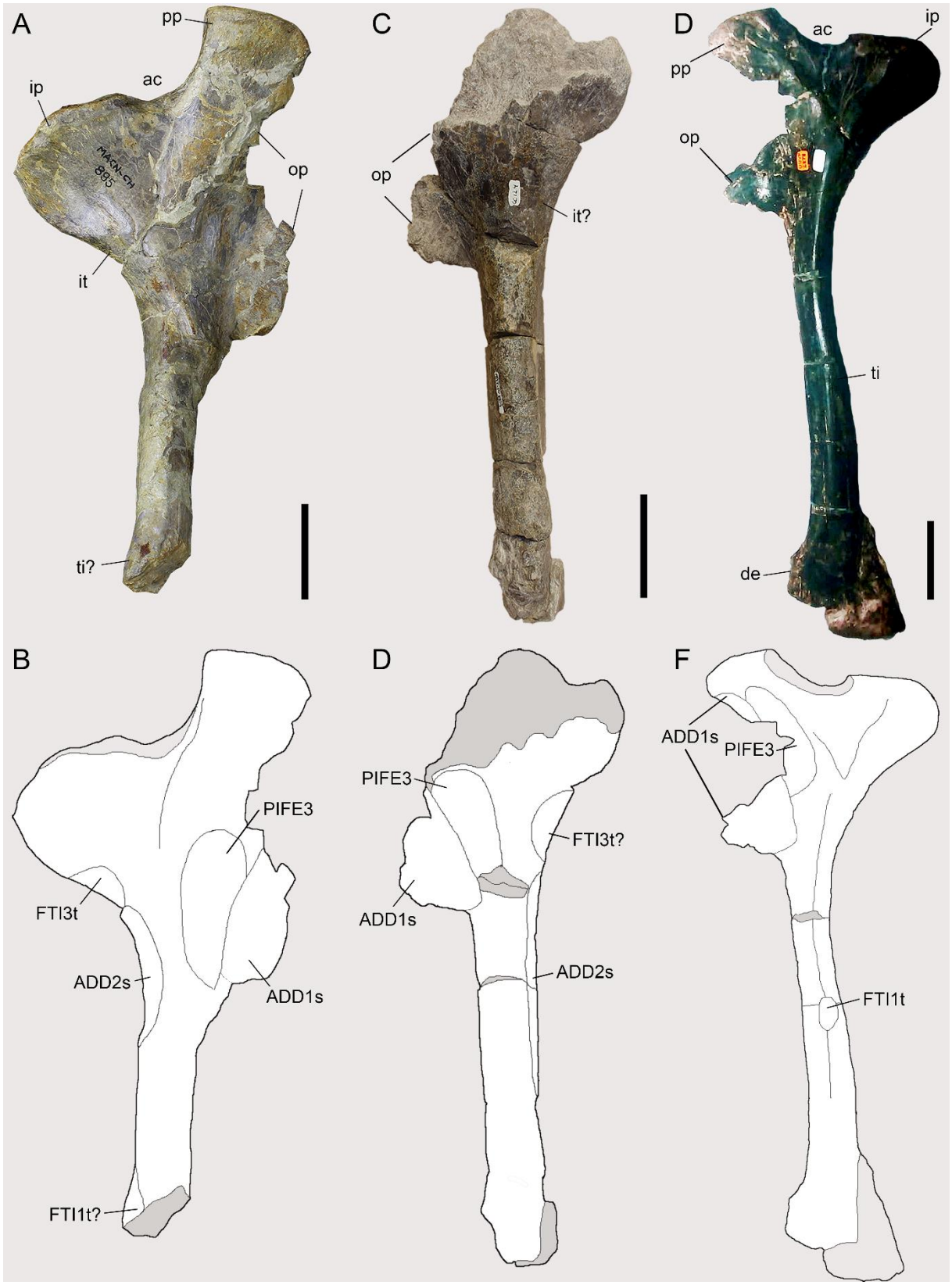

Figure 2.11. Osteological correlates observed on the ischia of Piatnitzkysauridae. A–B, *Piatnitzkysaurus* (right ischium, MACN-Pv-CH 895). C–D, *Condorraptor* (left ischium, MPEF-PV 1696). D–F, *Marshosaurus* (left ischium, UMNH VP 6387). Anatomical/muscular abbreviations: ac, acetabulum; ADD1s, *M. adductor femoris 1* scar; ADD2s, *M. adductor femoris 2* scars; de, distal expansion; FTI1t, *M. flexor tibialis internus 1* tubercle; FTI3t, *M. flexor tibialis internus 3* tubercle; ip, iliac peduncle; it, ischial tuberosity; op, obturator process; pp, pubic peduncle; PIFE3, *M. puboischiofemoralis externus 3*; ti, ischiadic tubercle. Scale bar = 50mm.

In Crocodylia, the FTI1 insertion is onto the medial (Otero *et al*., 2010; Suzuki *et al*., 2011) or posterior portion of the proximal tibial metaphysis (Carrano & Hutchinson, 2002), whereas it inserts onto the lateral surface of the tibia in other Reptilia (Dick & Clemente, 2016).

The posteromedial surface of the proximal region of the tibia in *Piatnitzkysaurus* has a broad depression below the medial condyle (Figure 2.12A–D), mainly visible in the PVL 4073 specimen (Figure 2.12A). We interpret this depression as the FTI1 insertion (level II). In *Condorraptor*, a topologically similar depression is also noticeable (Figure 2.12E), and here considered the FTI1 insertion (level II).

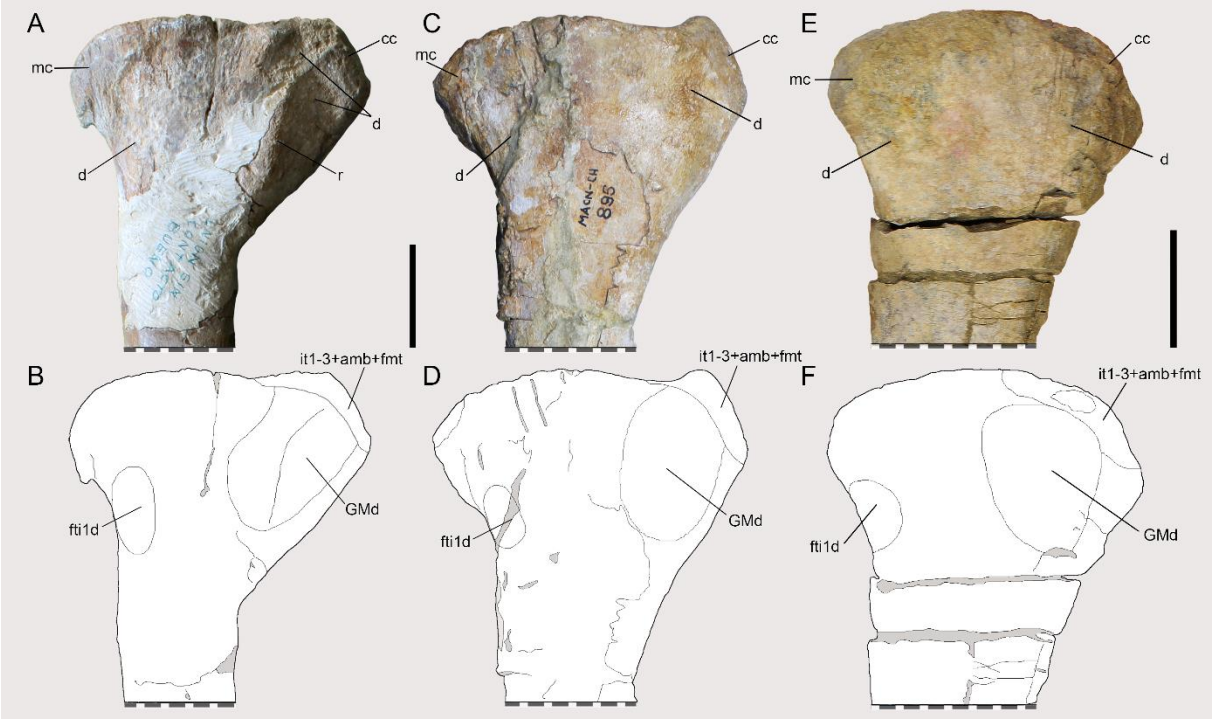

Figure 2.12. Osteological correlates observed on the tibiae of Piatnitzkysauridae (left tibiae, medial view). A–B, *Piatnitzkysaurus* (PVL 4073). C–D, *Piatnitzkysaurus* (MACN-Pv-CH 895). E–F, *Condorraptor* (MPEF-PV 1672). Anatomical/muscular abbreviations: cc, cnemial crest; d, depression; fti1d, *M. flexor tibialis internus 1* depression; GMd, *M. gastrocnemius pars medialis* depression; it1–3+amb+fmt, insertion of the tendons of the *iliotibiales+ambiens+femorotibiales* muscles; mc, medial condyle; r, ridge. Scale bar = 50mm.

M. flexor tibialis internus 2 (FTI2). In Crocodylia, the FTI2 originates from the lateral ilium, on the postacetabular iliac process just ventral to the origin of FTE (see below); it inserts together with FTI1 and M. puboischiotibialis onto the posteromedial proximal tibia (Romer, 1923a,b; Otero *et al*., 2010; Hutchinson, 2002). In Aves, the FTI2 appears to be absent (Hutchinson, 2002). Similar to other theropod dinosaurs such as *Staurikosaurus* (Grillo & Azevedo, 2011), *Coelophysis* (Bishop *et al*., 2021), and *Tyrannosaurus* (Carrano & Hutchinson, 2002), there are no scars suggesting the presence of FTI2 in *Piatnitzkysaurus* and

Marshosaurus, so it is ambiguous if this muscle was present or not (Level II'); the postacetabular blade is not well-preserved in *Condorraptor*, preventing infer anything about this muscle. The latter studies generally considered the FTI2 to more likely be a Crocodylia autapomorphy or a trait lost at some early point in Avemetatarsalia–Dinosauromorpha (e.g., Hutchinson, 2002; Allen *et al*., 2021).

M. flexor tibialis internus 3 (FTI3). In Crocodylia, the FTI3 (= *M. flexor cruris medialis*, FCM in Aves; Hutchinson, 2001b) has its origin on the lateral surface of the ischial tuberosity, on the proximolateral portion of the ischium (Romer, 1923a; Otero *et al*., 2010; Suzuki *et al*., 2011), which tends to be a scarred area in most non-avian archosaurs (Hutchinson, 2001b). In Aves, the homologous muscle, FCM, originates from a similar position, although more distally positioned and shifted closer to the ilium via rotation of the ischia (Patak & Baldwin, 1999; Hutchinson, 2002; Picasso, 2010; Suzuki *et al*., 2014). In other reptiles, the FTI has only two heads, i.e., FTI1 and FTI2 (Gregory & Camp, 1918; Romer, 1942; Russel & Bauer, 1988; Hutchinson, 2002). In non-avian theropods, the origin of the FTI3 is thought to have been from the prominent ischial tuberosity (Romer, 1923a,b; Carrano & Hutchinson, 2002; Grillo & Azevedo, 2011; Smith, 2021), which gradually shifted its relative position distally to merge with the ilium within stem-birds (Hutchinson, 2001b).

On the ischium of *Piatnitzkysaurus* MACN-PV-CH 895, which is better preserved proximally, a prominent ischial tuberosity that is triangular in shape is present near the proximoposterior edge of the ischium, ventral to the ischial peduncle; we infer this location as the FTI3 origin (level II) (Figure 2.11A–B). The delimitation of the FTI3 origin in *Condorraptor* is less evident than in *Piatnitzkysaurus*, but is similarly positioned (level II) (Figure 2.11C–D). In *Marshosaurus* is not possible to determine the FTI3 origin due to lack of osteological correlates (level II'), so the muscle origin was not reconstructed in any detail, but it should have been in the same location.

The FTI3 muscular head in extant archosaurs inserts onto the posterior surface of the proximal portion of the tibia together with the FTE and other FTI head(s), which may form a slightly roughened and rounded structure made by the tibiocalcaneal tendon or ligament (Romer, 1923a; Otero *et al*., 2010; Suzuki *et al*., 2011).

A region topologically related to the FTI3 insertion in *Piatnitzkysaurus* is positioned on the posteromedial surface of the proximal tibia, just below the medial and lateral cotyles, and some scarring is proximally located here (level II). Again, in *Condorraptor* there is no scar (level II').

M. flexor tibialis internus 4 (FTI4). The *M. flexor tibialis internus* division called FTI4 is only present in the Crocodylia clade (though it may have been lost in *Caiman*; Otero *et al*., 2010), being the division equivalent to the superficial portion of FTI2 of other reptiles (Romer, 1942). It is a small and thin muscle that originates from the fascia around the posteroventral ilium and posterodorsal ischium (Romer, 1923a,b; Suzuki *et al*., 2011). Since this muscle leaves no evident scars and is absent in Aves (Carrano & Hutchinson, 2002; Hutchinson, 2002), the presence in *Piatnitzkysaurus* and *Marshosaurus* is equivocal (level II') so we do not infer this muscle here. The condition is even more ambiguous in *Condorraptor*, as the posterior portion of the ilium is not well-preserved. Following prior studies, we assume that the FTI4 is a crocodylian autapomorphy, absent in theropods.

M. flexor tibialis externus (FTE). The FTE muscle (= *M. flexor cruris lateralis pars pelvica*, FCLP in Aves) in extant archosaurs is a large muscle and originating from the posterolateral surface of the ilium, just posterior to the origins of ILFB and IFE, and dorsal to *M. caudofemoralis brevis* on the postacetabular blade (Gregory & Camp, 1918; Romer, 1923a,b; Hutchinson, 2002; Otero *et al*., 2010; Picasso, 2010; Suzuki *et al*., 2014). In other Reptilia, the FTE also originates from the posterior ilium and ilioischiadic ligament (e.g., Romer, 1942; Dick & Clemente, 2016).

On the posterior region of the *Piatnitzkysaurus* ilium MACN-Pv-CH 895, above the brevis shelf and below the IT3 origin, there are some linear scars topographically equivalent to the position of the FTE origin in extant archosaurs (Figure 2.2A–B). We thus infer that the FTE origin is located here (level I), as in other dinosaurs (e.g., Russell, 1972; Carrano & Hutchinson, 2002; Langer, 2003; Grillo & Azevedo, 2011; Bishop *et al*., 2021; Smith, 2021). Yet as noted by Bonaparte (1986), the posterior edge of the postacetabular blade of the *Piatnitzkysaurus* ilium is not entirely preserved, thus, the posterior limits of the FTE origin remain unclear. In *Marshosaurus* left ilium UMNH VP 6372, it is also possible to infer the FTE origin due to some anterior delimitations located posterior to the ILFB (level I) (Figure 2.3B). Because the postacetabular blade of *Condorraptor* is not preserved, is not possible to directly infer the FTE origin.

As the FTE inserts very close to the FTI3, or sharing a common tendon in extant archosaurs (e.g., Romer, 1923a,b; Otero *et al*., 2010), this applies to *Piatnitzkysaurus* (level I), but more is equivocal in *Condorraptor* (level I') and not possible to infer in *Marshosaurus*.

3.1.3.1 Mm. adductores femores

M. adductor femoris 1 (ADD1). In extant archosaurs, the ADD1 (= *M. puboischiofemoralis pars medialis*, PIFM in Aves; Hutchinson, 2001a,b) has its origin from in the anterolateroventral surface of the ischium, located on equivalent of the obturator process (ischial apron/anteroventralmost ischial shaft) (Romer, 1923a; Hudson, 1959; McKitrick, 1991; Hutchinson, 2001a,b; 2002; Picasso, 2010; Suzuki *et al*., 2011; 2014). However, no clear osteological correlate for this origin is evident on the ischial surface (Carrano & Hutchinson, 2022). Only one head of the *adductor femoris* is present in non-archosaur Reptilia, originating from the puboischiadic ligament (Romer, 1942; Dick & Clemente, 2016).

The incomplete obturator process in *Piatnitzkysaurus* extends proximally, almost to the anterior line of the pubic peduncle (Bonaparte, 1986). Some scars are visible on the most anterodorsal portion of the ischial apron (mainly in the PVL 4073 specimen), which could be related to the puboischiadic membrane (Hutchinson, 2002). Based on relative positions, the ADD1 in *Piatnitzkysaurus* probably originated from the anteroventral obturator process of the ischium in the ventral portion of the ischial apron (level I') (Figure 2.10A–B). In *Condorraptor* MPEF-PV 1689, the obturator process is damaged, making it difficult to determine its anterior contact with the pubis. However, even in its broken state it obviously is a developed structure (Rauhut, 2005) (Figure 2.10C–D), and the same is noted in *Marshosaurus* UMNH VP 6380 (Madsen, 1976) (Figure 2.10D–E). A few scars are evident in the obturator process of the ischium; thus, this region probably was the site of origin of the ADD1 (level I').

The ADD1 in extant archosaurs has small, somewhat tendinous insertion located on the posterior shaft of the distalmost femur (Romer, 1923a; Hutchinson, 2001a; Otero *et al*., 2010; Picasso, 2010; Suzuki *et al*., 2014); medial to the ADD2, with both insertions located between the *la* and *lip* (Hutchinson, 2001a).

Although there is no osteological correlate for the ADD1 insertion discernible in *Piatnitzkysaurus*, some delimitations are on the *Condorraptor* left femur MPEF-PV 1690, in a location topologically equivalent to that in archosaur fossils (e.g., Russell, 1972; Dilkes, 2000; Carrano & Hutchinson, 2002; Hutchinson, 2001a; 2002; Grillo & Azevedo, 2011; Bishop *et al*., 2021; Smith, 2021; 2023) (level I' for *Piatnitzkysaurus* and level I for *Condorraptor*; Figure 2.6, Figure 2.7), however, see comments below.

M. adductor femoris 2 (ADD2). The ADD2 (= *M. puboischiofemoralis pars lateralis*, PIFL in Aves; Hutchinson, 2001a,b) originates from a fleshy attachment on the posterior

portion of the ischium on the edge distal to the FTI3 and the ischial tuberosity in Crocodylia, although in Aves this origin is more anteroventral (Hudson *et al*., 1959; McKitrick, 1991; Patak & Baldwin, 1999; Hutchinson, 2001b; Otero *et al*., 2010; Picasso, 2010; Suzuki *et al*., 2011; 2014).

A small depression is evident on the posterodorsal rim of the right ischium of *Piatnitzkysaurus* MACN-Pv-CH 895, distally delimited by a bump. This position is topographically equivalent to the inferred ADD2 origin in other theropods (e.g., Carrano & Hutchinson, 2002; Grillo & Azevedo, 2011; Bishop *et al*., 2021; Smith, 2021). Although no roughened scars are discernible, this depression is interpreted as the origin of ADD2 (level II) (Figure 2.11A–B). The osteological correlate of the ADD2 origin on the ischium of *Condorraptor* is less evident, but can be delimited in position similar to that of *Piatnitzkysaurus*, but extending further distally (level II) (Figure 2.11C–D). In *Marshosaurus*, the ADD2 boundaries were not observed, therefore this muscle's origin was not reconstructed.

The ADD2 insertion in extant archosaurs is located on the posterior shaft of the femur, lateral to the ADD1 (Romer, 1923a,b; Hutchinson, 2001a; Otero *et al*., 2010; Picasso, 2010; Suzuki *et al*., 2014); as above.

Again, we infer an insertion in the same relative position as in other extinct archosaurs (e.g., Romer, 1923b; Russell, 1972; Dilkes, 2000; Carrano & Hutchinson, 2002; Hutchinson, 2001a; 2002; Grillo & Azevedo, 2011; Bishop *et al*., 2021; Smith, 2021; 2023). No scars are noted in the posterior shaft of the femoral diaphysis in *Piatnitzkysaurus* (level I'), but discernible marks can be noted in *Condorraptor* (level I) (Figure 2.6, Figure 2.7). As these scars in both studied species are not distinct, we conservatively reconstructed both insertions, i.e., ADD1+2, in a single region (Figure 2.6, Figure 2.7). However, based on the right femur (MPEF-PV 1691) of *Condorraptor*, some scars might indicate where these muscles inserted separately (Figure 2.13), although we are cautious to interpret it this way, as these potential ADD1+2 boundaries are more distally positioned than observed in other theropods (Carrano & Hutchinson, 2002).

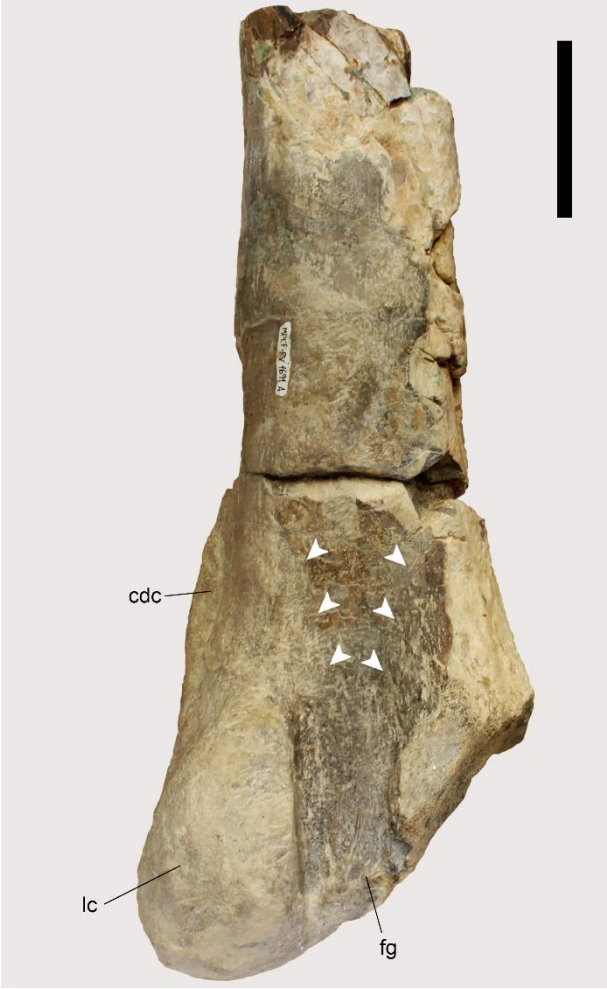

Figure 2.13. Possible *Mm. adductores femores* division on the *Condorraptor* right femur (MPEF-PV 1691, posterior view). Anatomical abbreviations: cdc, craniomedial distal crest, fg, flexor groove; lc, lateral condyle. Scale bar = 50mm.

3.1.3.2 Mm. puboischiofemorales externi

M. puboischiofemoralis externus 1 (PIFE1). In Crocodylia, the PIFE1 originates from the anteromedial surface of the pubic apron and epipubic cartilage (Romer, 1923a,b; Otero *et al*., 2010; Suzuki *et al*., 2011). The later structure corresponds to an anteromedially expanded surface of the pubic symphysis (Hutchinson, 2001b). In Aves, a pubic symphysis is absent; thus, the origin of PIFE1 homologue (i.e., the small *M. obturatorius lateralis*; Hutchinson, 2001b) is from the proximolateral surface of the pubis, close to the acetabulum (Patak & Baldwin, 1999; Hutchinson & Gatesy, 2000; Hutchinson, 2002; Picasso 2010; Suzuki *et al*., 2014). Only one head (or weak subdivision) of PIFE is present in other Reptilia (Romer, 1942; Hutchinson, 2002).

Even though the distal regions of the pubes in *Piatnitzkysaurus* MACN-Pv-CH 895 are lacking due to the taphonomy of this specimen, an expanded pubic apron is on the anteromedial

pubis, confirmed in PVL 4073 specimen (Figure 2.5A–D), and similar to the condition in other non-avian theropods (e.g., Hutchinson, 2001b; Carrano & Hutchinson, 2002; Grillo & Azevedo, 2011; Bishop *et al*., 2021; Rhodes *et al*., 2021). As in Crocodylia, in *Piatnitzkysaurus* this likely is the PIFE1 origin on the anterior surface of the pubes (level II) (Figure 2.5C–D). Similarly, the pubic aprons of *Condorraptor* and *Marshosaurus* are well-developed but is not entirely preserved, and consistent with the same PIFE1 origin (level II) (Figure 2.5G–H).

The PIFE1–3 in extant archosaurs have a common tendon of insertion that attaches onto the proximolateral femur on the greater trochanter (Romer, 1923a; Hutchinson, 2001a; 2002; Otero *et al*., 2010).

The greater trochanter in *Piatnitzkysaurus* has a straight angle to the femoral long axis (Bonaparte, 1986) and we infer it to represent the PIFE1 insertion (level I) (Figure 2.6, Figure 2.9). This structure is not preserved in *Condorraptor*.

M. puboischiofemoralis externus 2 (PIFE2). In Crocodylia, the PIFE2 (= *M. obturaturious medialis*, OM in Aves; Hutchinson, 2001b) is a fan-shaped muscle, originating from the posterior surface of the pubic apron, on the posterolateral pubis (Romer, 1923a,b; Otero *et al*., 2010; Suzuki *et al*., 2011). Contrastingly in Aves, the large homologous muscle, OM, is more posteriorly positioned (via pubic retroversion) and originates medially from the puboischiadic membrane (Patak & Baldwin, 1999; Hutchinson, 2001b, 2002; Suzuki *et al*., 2014).

Considering the well-developed pubic apron in the piatnitzkysaurids studied here, a level II inference allows us to infer that these taxa had a PIFE2 origin from the posterior portion of the pubic apron (Figure 2.5). The insertion with PIFE1–3 is described above (Figure 2.6, Figure 2.9).

M. puboischiofemoralis externus 3 (PIFE3). The PIFE3 in Crocodylia has a large fleshy origin from the anterolateral surface of the ischium, on the obturator process between the origins of ADD1+2, and anterodorsally delimited by the ischial ridge (Romer, 1923a,b; Hutchinson, 2001b; 2002; Otero *et al*., 2010; Suzuki *et al*., 2011). In Aves, the obturator process of the ischium is lost, as well as the third head of PIFE (Hutchinson, 2001b; 2002).

The retention of the obturator process in *Piatnitzkysaurus*, *Condorraptor* and *Marshosaurus* (Figure 2.10), as well as in other non-avian theropods (e.g., Triassic *Coelophysis* – Bishop *et al*., 2021; and Cretaceous *Tyrannosaurus* – Carrano & Hutchinson, 2002) is indicative of the PIFE3 origin. However, variations in the size and shape of the theropod

puboischiadic plate throughout evolution indicate some variation in the size of the musculature associated with this region (Chapter 1). Although the PIFE3 origin's exact limits are undefined, it probably was located anteroventral to the ischial ridge on the posterior portion of the obturator process, similar to the position in Crocodylia and other theropod species, such as *Staurikosaurus* (Grillo & Azevedo, 2011) and *Coelophysis* (Bishop *et al*., 2021). In the right ischium of *Piatnitzkysaurus* MACN-Pv-CH 895, the probable origination site is more evident, being positioned between the ADD1 origin and the ischial ridge (level II) (Figure 2.11A–B). In the poorly preserved ischia of PVL 4073, as well as in *Condorraptor* and *Marshosaurus*, the PIFE3 boundaries are not possible to reliably estimate, but its general position is (level II) (Figure 2.11C–F). See above for details on the PIFE insertion (Figure 2.6, Figure 2.9).

M. ischiotrochantericus (ISTR). The ISTR in non-avian Reptilia including Crocodylia has a single head originating from the medial surface of the ischium (Gregory & Camp, 1918; Romer, 1923a; Hutchinson, 2001b; 2002; Otero *et al*., 2010; Suzuki *et al*., 2011). The ADD2 and FTI3 origins on the posterolateral margin of the ischium form the posterolateral boundary of the ISTR origin. In Aves, the homologous muscle (the large, fusiform *M. ischiofemoralis*, ISF; Hutchinson, 2001b) has shifted its origin to the lateral side of the ischium and ilioischiadic membrane (Romer, 1923a,b; Hudson *et al*., 1959; Hutchinson, 2002; Picasso, 2010; Suzuki *et al*., 2014).

Among the three piatnitzkysaurids studied here, the *Piatnitzkysaurus* right ischium of the MACN-Pv-CH 895 specimen is the best preserved proximally; followed by the *Marshosaurus* left ischium UMNH VP 6380, which has both, iliac and pubic peduncles, but lacks the ventral part of the obturator process (Madsen, 1976); and the *Condorraptor* left ischium MPEF-PV 1689, which although lacking most of the proximal articulation, preserves a partial, well-developed obturator process (Rauhut, 2005). None of the ischia of the three taxa presents evidence of the apomorphic condition of lateral origin of the ISTR muscle; in both *Piatnitzkysaurus* and *Marshosaurus* (Madsen, 1976), the medial surface of the ischium/obturator process is covered by fine striations. In *Condorraptor*, such striations are not discernible (there might be small ventral marks on the obturator process, if not taphonomic artifacts), but *Condorraptor* probably had the same origin. Therefore, the ISTR origin was on the medial surface of the ischium, including the entire area of the obturator process (level II for *Piatnitzkysaurus* and *Marshosaurus*, and level II' for *Condorraptor*).

In extant archosaurs, the ISTR insertion is by a tendinous attachment to the posteroproximal portion of the lateral femur, distal to the greater trochanter and PIFE1–3

insertions (Romer, 1923a; Hutchinson, 2001a; 2002; Otero *et al*., 2010; Suzuki *et al*., 2014; Clifton *et al*., 2018). In non-avian theropods (e.g., Carrano & Hutchinson, 2002; Grillo & Azevedo, 2011; Bishop *et al*., 2021; Smith, 2021; 2023), the insertion occurs between the greater and the fourth trochanter, onto the posterior portion of the trochanteric shelf (Hutchinson, 2001a).

The best-preserved femur of *Piatnitzkysaurus* (right femur PVL 4073) has a clear posteriorly projected structure proximal to the fourth trochanter and distal to the greater trochanter (Figure 2.9), similar in position and shape to other tetanurans (e.g., *Tyrannosaurus* – Carrano & Hutchinson, 2002). Although the bony surface is not well-preserved, this projection is preceded anteroposteriorly by a groove considered here as the insertion of ISTR (level I) (Figure 2.6, Figure 2.9). Due to the fragmentary nature of the proximal femur of *Condorraptor* MPEF-PV 1690 and the lack of femora for *Marshosaurus*, no inferences were made about the ISTR insertion for these taxa.

3.1.3.3 Mm. caudofemorales

M. caudofemoralis brevis (CFB). The CFB muscle in non-avian reptiles originates from the medial and partially the lateral surfaces of the ilium, in its postacetabular blade from a shallow fossa, as well as from the posterior sacral ribs (Romer, 1923a,b; Gatesy, 1990; Hutchinson, 2002; Otero *et al*., 2010). In Aves, the homologous (i.e., the large *M. caudofemoralis pars pelvica*, CFP; Hutchinson, 2001b) also has a single head, but it originates from the posteroventral surface of the lateral ilium (McKitrick, 1991; Hutchinson, 2002; Picasso, 2010; Clifton *et al*., 2018). Accordingly, following Hutchinson (2001b; 2002), in non-avian dinosaurs the CFB origin mainly was from the brevis fossa of the posteroventral ilium, a structure that was gradually reduced across the lineage to Aves as the CFB origin shifted laterally.

The posterior width of the brevis fossa varies in non-avian theropods (Carrano *et al*., 2012; Chapter 1). In megalosauroids, the brevis fossa is posteriorly wide in *Marshosaurus* (Figure 2.14) and some spinosaurids; whereas it is subequal in width in *Piatnitzkysaurus* and some megalosaurids (Chapter 1). The *Piatnitzkysaurus* ilium MACN-Pv-CH 895 has a large and relatively deep brevis fossa, and presumably the CFB in this taxon originated entirely in the fossa (level II), although the posterior edge of the postacetabular blade in this specimen is incomplete (Figure 2.14A). The postacetabular process of the ilium in *Condorraptor* MPEF-PV 1687 does not have the brevis fossa preserved, so although it almost certainly existed (level

II'), we do not infer details of it here. Regarding *Marshosaurus*, Madsen (1976) commented that the brevis fossa of the UMNH VP 6373 ilium has a shallow concavity and holds the CFB muscle; based on our studied specimen UMNH VP 6372, this shallow and posteriorly enlarged fossa is the osteological correlate of the CFB muscle origin (level II) (Figure 2.14B).

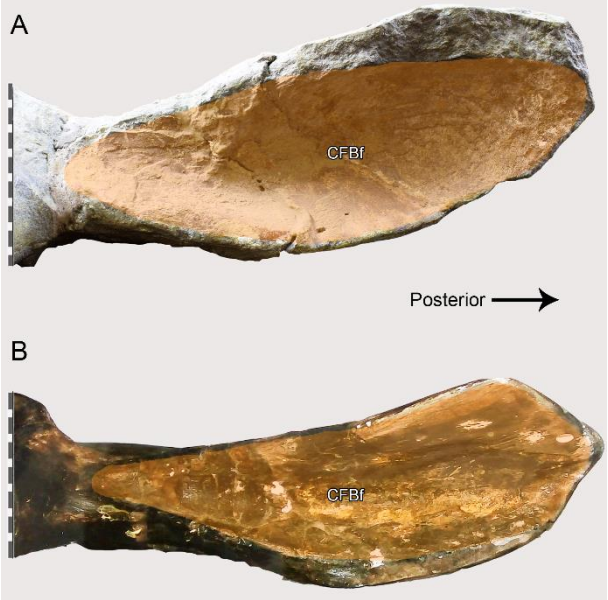

Figure 2.14. Brevis fossa in Piatnitzkysauridae. A, *Piatnitzkysaurus* (PVL 4073). B, *Marshosaurus* (UMNH VP 6372). Anatomical/muscular abbreviations: CFBf, *M. caudofemoralis brevis* fossa. Not to scale.

The CFB muscle of extant archosaurs inserts by a tendon on the posterolateral surface of the proximal region of the femur, positioned between the lip and the fourth trochanter (Hutchinson, 2001b; 2002; Otero *et al*., 2010; Picasso, 2010; Suzuki *et al*., 2014).

Among the femora of *Piatnitzkysaurus*, the better preserved fourth trochanter is on the right femur of PVL 4073 specimen, however, the surface between the fourth trochanter and the *lip* is not well-preserved and the insertion of CFB is not discernible based on scars, even though the well-developed fourth trochanter allows to infer the insertion of this muscle safely (level I) (Figure 2.6, Figure 2.9), based on that in extant and extinct archosaurs. The *Condorraptor* left femur MPEF-PV 1690 preserves a well-developed fourth trochanter. As noted by Rauhut (2005) it is a low but robust ridge, allowing to infer the position and extent of the CFB insertion (level I) (Figure 2.7).

M. caudofemoralis longus (CFL). In non-avian Reptilia, the CFL (= *M. caudofemoralis pars caudalis*, CFC in Aves; Gatesy, 1990; Hutchinson, 2001b) has a large fleshy origin from the caudal vertebrae, including the ventral surface of the transverse processes and haemal

arches, beginning around the 12th caudal vertebra (Gatesy, 1990; Hutchinson, 2002; Otero *et al*., 2010). In most Aves (where present), the CFC origin is restricted to the last free caudal vertebra and the uropygium (Hutchinson, 2001a; 2002; Suzuki *et al*., 2014; Clifton *et al*., 2018).

Although the tail in *Piatnitzkysaurus* and *Condorraptor* is poorly known, and any vertebral elements from *Marshosaurus* lack formal description, it is possible to reconstruct the CFL origin in the South American piatnitzkysaurids. Two caudal vertebrae are preserved in *Piatnitzkysaurus* PVL 4073 specimen, probably the 2nd and 4th (Bonaparte, 1986); both feature robust centra and transverse processes related to the CFL origin (level I). Three caudal vertebrae are known for *Condorraptor*; the proximalmost, MPEF-PV 1702, has a tall centrum with posterodorsal oval depression and a dorsolaterally, slightly posteriorly directed transverse process; the proximal mid-caudal vertebra, MPEF-PV 1682, has a more elongated centrum with a shallow depression and a prominent laterally/slightly dorsally and posteriorly directed transverse process; and the distal mid-caudal vertebra, MPEF-PV 1683, has a low and elongated centrum with no sign of a transverse process (Rauhut, 2005). These characteristics of the proximal most and the proximal mid-caudal vertebrae allow inferring part of the CFL origin (level I).

The CFL in non-avian Reptilia inserts onto the proximal femur, in the pit and on the medial surface of the fourth trochanter; a secondary tendon continues downwards to the fibula, contributing to the *M. gastrocnemius externus* (= *lateralis* of Aves) origin (Romer, 1923a; Gatesy, 1990; Hutchinson, 2001a; 2002; Otero *et al*., 2010). Once birds reduced their tail, the CFC muscle reduced as well as the fourth trochanter which reduced to a roughed area (Gatesy, 1990). Dinosauromorphs and theropods have a large crest-shaped fourth trochanter (e.g., Hutchinson, 2001a), this being the condition in both *Piatnitzkysaurus* and *Condorraptor*; thus, indicating the CFL insertion (level I) and exemplifying that it was a large muscle in early tetanurans (Figures 2.6, Figure 2.7). As proposed by Hutchinson (2001a) and Carrano & Hutchinson (2002), the secondary tendon of the CFL may have been lost in early theropods, as the fourth trochanter became less pendant than in many other archosaurs. Considering that the fourth trochanter of both studied taxa are well-developed but not pendant, this secondary tendon would probably be absent (level II').

3.1.4 Digital extensor Group

M. tibialis anterior (TA). The TA muscle (previous termed as *M. extensor digitorum longus* in non-avians reptiles; see Hattori & Tsuihiji, 2020) in Crocodylia (= *M. tibialis*

cranialis, TC in Aves) originates from a narrow tendon proximal to the lateral femoral condyle, lateral to the extensor groove and distal to the large *M. femorotibialis* origins (Hutchinson, 2002; Picasso, 2010; Suzuki *et al*., 2011; Hattori & Tsuihiji, 2020). In Aves, the homologous muscle originates from the distal extremity of the lateral femoral condyle, from the *fovea tendinis m. tibialis cranialis* (Baumel & Witmer, 1993); a second TC head also originates from the lateral and cranial cnemial crests of the tibia, proximal to the *M. extensor digitorum longus* origin (Hutchinson, 2002; Hattori & Tsuihiji, 2020).

Generally, reconstructions of the TA muscle origin in theropods consider both muscular heads, as aforementioned originating from the lateral condyle of the femur and the proximal tibia (e.g., Carrano & Hutchinson, 2002; Smith, 2021; 2023). In the femora of both *Piatnitzkysaurus* and *Condorraptor*, there is no evidence of the TA origin; the lateral condyles do not have the distally positioned *fovea tendinis m. tibialis cranialis* as in Aves (e.g., Baumel & Witmer, 1993; Picasso, 2010; Hattori & Tsuihiji, 2020) or proximal to the lateral condyle as in Crocodylia (e.g., Suzuki *et al*., 2011; Hattori & Tsuihiji, 2020). Therefore, the specific origin of this muscle head on the femur in both piatnitzkysaurids is ambiguous, but as the origin of this muscle is a conservative feature in Reptilia (Hattori & Tsuihiji, 2020), and probably present in theropods (Carrano & Hutchinson, 2002), we tentatively reconstruct this muscle on the anterior lateral condyle (level I') (Figure 2.6, Figure 2.7). Considering the second TA head, the tibiae of both *Piatnitzkysaurus* specimens, MACN-Pv-CH 895 and PVL 4073, distal to the insertion of the *triceps femoris* on the cnemial crest, have an elliptical and well demarcated depression (Figure 2.15). This depression is topologically equivalent to the TA reconstruction in early theropods such as *Coelophysis* (Bishop *et al*., 2021) and later coelurosaurs such as *Tyrannosaurus* (Carrano & Hutchinson, 2002), *Nothronychus* (Smith, 2021), as well as Aves (e.g., Hattori & Tsuihiji, 2020); thus, considered here as the second head of TA origin (level I) (Figure 2.4A–B, Figure 2.15). In *Condorraptor* tibia MPEF-PV 1672, this depression is not clearly noticeable (level I') (Figure 2.4C–D).

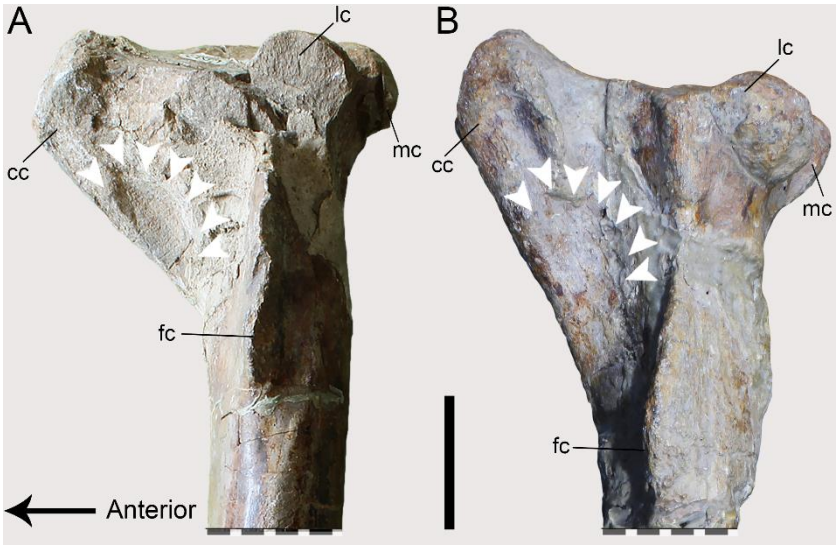

Figure 2.15. Proximal tibiae of *Piatnitzkysaurus* (left tibiae, lateral view). A, PVL 4073 specimen. B, MACN-Pv-CH 895 specimen. Anatomical/muscular abbreviations: cc, cnemial crest; fc, fibular crest; lc, lateral condyle, mc, medial condyle. Arrows indicates muscle scar. Scale bar = 50mm.

The TA in non-avian Reptilia inserts onto tubercles on the metatarsals, being distal in turtles and proximal in Lepidosauria and Crocodylia; in Aves this tendon splits and inserts onto the dorsal/anterior surface of the proximal tarsometatarsus on a tubercle (*tuberositas m. tibialis cranialis*) (Baumel & Witmer, 1993; Hutchinson, 2002; Suzuki *et al*., 2011; 2014; Hattori & Tsuihiji, 2020). These metatarsal tubercles or longitudinal crests (typically concentrated on metatarsal II but also III) are noted in other archosaurs and many dinosaur taxa (e.g., Carrano & Hutchinson, 2002; Hutchinson, 2002; Langer, 2003; Smith, 2021; 2023).

Similar to other dinosaurs (Dilkes, 2000; Carrano & Hutchinson, 2002; Langer, 2003; Smith, 2023), the anteroproximal metatarsal shafts in *Piatnitzkysaurus* specimen MACN-Pv-CH 895 have a longitudinal crest and a proximal excavation. We thus infer the proximal parts of metatarsals II–IV (mainly metatarsal II) as the TA insertions (level I). Only the left metatarsal IV (MPEF-PV 1692) is preserved in *Condorraptor*; although it does not have the evident ridge present in *Piatnitzkysaurus*, the proximal portion preserves an excavation, considered here a TA insertion (level I).

M. extensor digitorum longus (EDL). The EDL (previous termed as *M. tibialis cranialis* in non-avians reptiles; see Hattori & Tsuihiji, 2020) in extant Reptilia originates from the proximal shaft of the tibia; in Crocodylia from a rugose surface in the proximalmost portion and in Aves from a broad surface located between the cranial and the lateral cnemial crests and distal to the insertion of the *triceps femoris* tendon (Hutchinson, 2002; Suzuki *et al*., 2011; 2014; Hattori & Tsuihiji, 2020).

In the tibiae of *Piatnitzkysaurus* PVL 4073 and *Condorraptor* MPEF-PV 1672 a clear demarcation is visible on the anterolateral shaft, located in the sulcus intercnemialis. The proximal limits are not well-defined and may reach the cnemial crest (as in Aves – Suzuki *et al*., 2014; Hattori & Tsuihiji, 2020), but the anterior limits are bordered by a muscular line and the posterior limits proximally by the fibular crest and distally by a posterior muscular line. As noted for Aves (e.g., Hattori & Tsuihiji, 2020), the distal part of the EDL origin is tapered (level I) (Figure 2.4).

The EDL insertion in non-avian Reptilia is limited to a bulge(s) on the dorsal surface of metatarsals I–II (Hutchinson, 2002; Hattori & Tsuihiji, 2020), whereas in Aves this insertion is on the proximal processes of the distal pedal phalanges, in the hyperextensor fossae (Hutchinson, 2002; Picasso, 2010; Suzuki *et al*., 2014; Hattori & Tsuihiji, 2020). The EDL insertion in early dinosaurs is inferred as a distally positioned when compared to non-avian Reptilia, due to the presence of large extensor fossae and rugosities on the dorsal surfaces of the pedal phalanges (Hutchinson, 2002; Carrano & Hutchinson, 2002; Bishop *et al*., 2021; Smith, 2021). Although the condition in piatnitzkysaurids is probably the same as in other dinosaurs, this insertion has not been reconstructed as the specimens have no preserved phalanges (with the exception of an isolated ungual of *Condorraptor*).

M. extensor digitorum brevis (EDB). The EDB in Reptilia has its origin in the astragalus (or distal tarsal IV in Testudines), inserting onto the dorsal surface of the pedal phalanges; however, in Aves, this muscle is absent (Dilkes, 2000; Hutchinson, 2002; Hattori & Tsuihiji, 2020). The EDB is conjectured to have fused with the EDL in dinosaurs (Dilkes, 2000; Carrano & Hutchinson, 2002). We did not reconstruct this muscle following this hypothesis (a level II' reconstruction) and such elements are not preserved in piatnitzkysaurids.

M. extensor hallucis longus (EHL). The EHL (also termed *M. flexor* perforates digiti II) in non-avian Reptilia is conservative in position, being a small and short muscle originating from the distal shaft of the fibula in Aves (related to loss of the distal fibula), the EHL origin has moved distally to the anteromedial portion of the proximal tarsometatarsus (Patak & Baldwin, 1999; Hutchinson, 2002), or the EHL is absent in species that have lost the hallux (e.g., Suzuki *et al*., 2014).

In non-avian theropods (e.g., Carrano & Hutchinson, 2002; Bishop *et al*., 2021; Smith, 2023), including *Piatnitzkysaurus* specimen PVL 4073, the fibula is not distally reduced as in Aves and some other theropods (e.g., Smith, 2021) and thus represents the EHL origin, distal

to *Mm. fibulares longus et brevis* (FL, FB) (level I). *Condorraptor* and *Marshosaurus* do not have a fibula preserved.

The EHL muscle insertion is on the anterior portion of the hallucal phalanges in Reptilia; whereas in Aves it becomes more posterior due to changes in hallux position (Hutchinson, 2002). Reconstructions of this muscle in non-avian theropods consider this insertion as onto the anterior side of the hallucal ungual (Carrano & Hutchinson, 2002; Bishop *et al*., 2021; Smith, 2023). The lack of the well-preserved pes in piatnitzkysaurids precludes any inferences about this muscular insertion.

3.1.5 Digital flexor Group

M. gastrocnemius pars lateralis (GL). In Lepidosauria and extant archosaurs, the GL (variably named; = *M. gastrocnemius externus*, GE in Crocodylia) is a large and fusiform muscle with a fleshy origin from the posterodistal surface of the femur, distal to ADD2 (Romer, 1923a; McKitrick, 1991; Patak & Baldwin, 1998; Hutchinson, 2002; Otero *et al*., 2010; Picasso, 2010; Hattori & Tsuihiji, 2020). In Crocodylia and Aves, this muscle originates from a lateroventral distinct depression on the posterior portion of the distal femur. In Aves, it is delimited by a rough depression and has with deep and superficial layers; sometimes with an extra lateral head (e.g., Suzuki *et al*., 2011; Hattori & Tsuihiji, 2020).

Both femora of *Piatnitzkysaurus* PVL 4073 preserve a depression on the posterolateralmost part of the distal femoral shaft; right femur has some degree of rugosity on the lateral base of the tibiofibular crest. This posterolateral depression is topologically located in position similar to extant Reptilia; thus, interpreted here as the GL origin (level I) (Figure 2.6G–H). A depression similar in position and shape is present on the *Condorraptor* left femur MPEF-PV 1690, thus allowing reconstruction of the GL origin (level I) (Figure 2.7G–H).

In extant archosaurs, the GL and *M. gastrocnemius medialis* (GM) muscles and its homologous are inserted via a shared tendon (and aponeurosis/plantar fascia) to metatarsal V (plantar surface of pes) in Crocodylia, and medial and plantar margins of the hypotarsus of Aves (Romer, 1923a; McKitrick, 1991; Hutchinson, 2002; Otero *et al*., 2010; Picasso, 2010; Hattori & Tsuihiji, 2020). It is thought that the plantar aponeurosis was reduced in dinosaurs (see Hutchinson, 2002), yet with the GM+GL maintaining robust scars on the posterior metatarsal shafts (Dilkes, 2000; Carrano & Hutchinson, 2002; Hutchinson, 2002; Bishop *et al*., 2021; Smith, 2021).

The left metatarsals II–IV in the *Piatnitzkysaurus* MACN-Pv-CH 895 specimen are well-preserved. The metatarsal of *Piatnitzkysaurus* has a ridge on the posterior/plantar surface related to the insertion of GL + GM (level II) (Figure 2.16A–B), although not so prominent as in other theropods (e.g., *Tyrannosaurus* – Carrano & Hutchinson, 2002). The left metatarsal IV (MPEF-PV 1692) of *Condorraptor*, as previously noted by Rauhut (2005) has a posterolateral semilunate ridge on the posterior/plantar surface (Figure 2.16C–D), which is the insertion site of the GL + GM heads (level I), presumably also inserting onto metatarsals II and III; not preserved (level I').

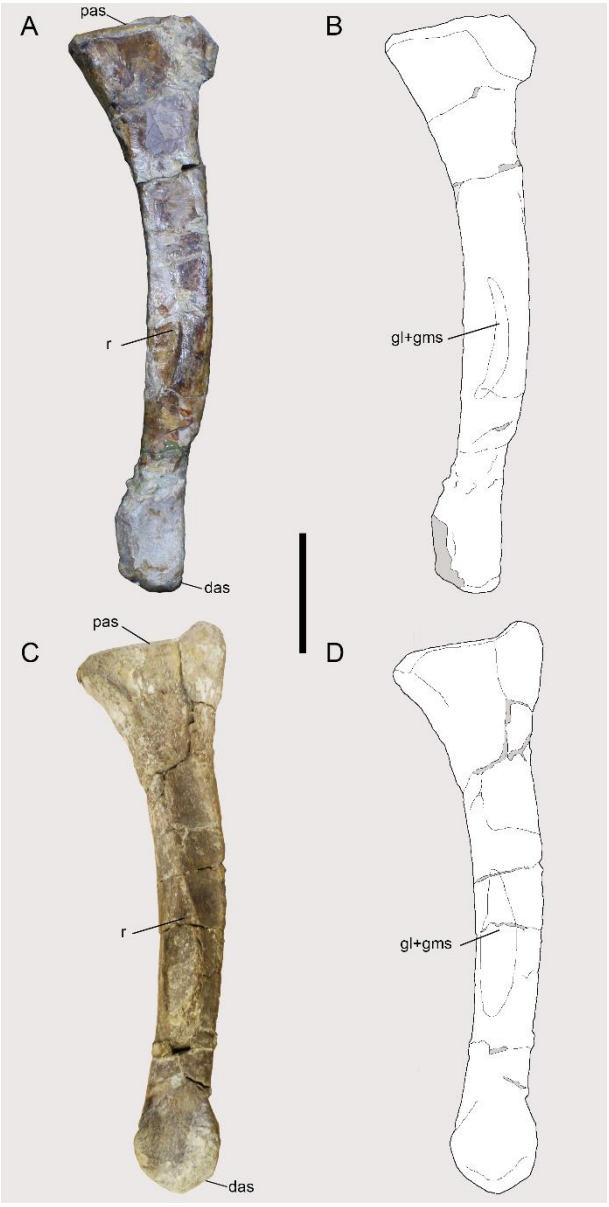

Figure 2.16. Metatarsal IV of Piatnitzkysauridae (left, posterior view). A–B, *Piatnitzkysaurus* (MACN-Pv-CH 895). C–D, *Condorraptor* (MPEF-PV 1692). Anatomical/muscular abbreviations: das, distal articular surface; gl+gms, *Mm. gastrocnemii* insertion scar; pas, proximal articular surface; r, ridge. Scale bar = 50mm.

M. gastrocnemius pars medialis (GM). In Reptilia, the GM muscle (= *M. gastrocnemius internus*, GI in Crocodylia) originates on the medial surface of the proximal tibia, occupying a large area on the cnemial crest in Aves (Romer, 1942; Patak & Baldwin, 1998; Hutchinson, 2002; Otero *et al*., 2010; Picasso, 2010; Suzuki *et al*., 2011; 2014; Hattori & Tsuihiji, 2020). Although *Mm. gastrocnemii* is composed of the lateral and medial head ancestrally in Reptilia, lepidosaurs and Aves evolved a third head independently (*M. gastrocnemius pars intermedia* in Aves), third head in lepidosaurs probably deriving from a subdivision of the lateral head and in Aves deriving from a subdivision of the medial head. At least in the lineage of Aves, the timing of the derivation of this extra head is difficult to determine (Hutchinson, 2002).

A large depression is on the medial surface of the proximal tibia on the tibiae of both *Piatnitzkysaurus* specimens, MACN-Pv-CH 895 and PVL 4073, covering almost the entire cnemial crest (except the anteroproximalmost part where the *triceps femoris* tendon should have attached) (Figure 2.12A–D). Although this broad depression exists in both specimens, in the PVL 4073 tibia, a ridge subdivides this depression into two subconcavities (Figure 2.12A–B). It is not clear whether these subdivisions signify an "extra head" of the GM (as already reported in Crocodylia, which originates from the *triceps femoris* tendon – Suzuki *et al*., 2011). Regardless, the origin of the GM muscle seems to have been in this position. The GM origin reconstructed here in *Piatnitzkysaurus* is the entire medial depression on the cnemial crest (level I), resembling the large area of GM origin in Aves (Figure 2.12A–D). Likewise, the medial side of the cnemial crest in the *Condorraptor* tibia MPEF-PV 1672 also has a broad and shallow depression, positioned distally in relation to the *triceps femoris* tendon, representing the GM origin (level I) (Fig. 12E–F). The insertion site of GL + GM was described above (Figure 2.16C–D).

Mm. fibulares longus et brevis (FL, FB). The FL and FB origins (also termed *M. peroneus longus et brevis* and *Mm. peronei anterior et posterior*) in Testudines and extant archosaurs is from the fibula, in some cases with contribution from the tibia (Dilkes, 2000; Hutchinson, 2002; Dick & Clemente, 2016; Hattori & Tsuihiji, 2020). Generally, the FL origin is on the lateral fibula, distal to the ILFB insertion; whereas the FB is more distally and anterolaterally positioned on the fibula (Hutchinson, 2002; Suzuki *et al*., 2011; 2014; Hattori & Tsuihiji, 2020). With the distal region of the fibula lost in early Aves, the origin of *Mm. fibulares* became superficial on the lateral sides of the proximal tibiotarsus and fibula (Patak & Baldwin, 1999; Hutchinson, 2002; Picasso, 2010).

Similar to other dinosauriform reconstructions (e.g., Dilkes, 2000; Carrano & Hutchinson, 2002; Piechowski & Tałanda, 2020; Bishop *et al*., 2021; Smith, 2021), the presence of a distally unreduced fibula suggests that the FL and FB origins in *Piatnitzkysaurus*, were mainly from the distal fibula. Although there is no clear demarcation or muscle scarring, we reconstructed these muscles (level I') based on the PVL 4073 fibula.

In general, ancestral Reptilia have the FL and FB insertions on the proximolateral tarsals, metatarsal V, and 5th digit aponeurosis; and near the proximal end of metatarsal V, respectively (Hutchinson, 2002; Hattori & Tsuihiji, 2020). Some modifications occurred in the avian lineage, especially the reduction/loss of the plantar aponeurosis and the 5th digit, concentrating these muscular insertions onto the lateroproximal side of the tarsometatarsus in Aves (Hutchinson, 2002; Hattori & Tsuihiji, 2020). Reconstruction of these insertions in Dinosauriformes usually are onto the tarsal/metatarsal elements, particularly metatarsal V (Dilkes, 2000; Carrano & Hutchinson, 2002; Piechowski & Tałanda, 2020; Bishop *et al*., 2021; Smith, 2021). The lack of preserved tarsals and metatarsal V in piatnitzkysaurids prevents reconstruction of the FL and FB insertions in detail, but presumably they were the same as in other non-avian Dinosauriformes.

3.2 Summary of muscle reconstructions

The muscle reconstructions inferred for *Piatnitzkysaurus*, *Condorraptor*, and *Marshosaurus* are summarised in Tables 2.2, 2.3 and 2.4, respectively. Figure 2.17 presents a 'muscle map' reconstruction for each of the studied species. Overall, we infer 29 muscles' origins for *Piatnitzkysaurus*, which is the best-preserved specimen; and among these 29 muscles, it was possible to infer the insertions of 25 (Figure 2.17A). In *Condorraptor*, 21 muscles were reconstructed; among these, 12 were inferred for both, origin and insertion (Figure 2.17B). *Marshosaurus* is the specimen with the fewest pelvic elements preserved, being possible to infer only 12 locomotor muscles (Figure 2.17C), but only the origins are inferred here, because no stylopodium and zeugopodium are known for this taxon.

Table 2.2. Pelvic and hindlimb musculature inferred for *Piatnitzkysaurus*, and required inference level based on the EPB. Refer to Table 2.1 or the main text results for muscle abbreviations.

Muscle	Origin	Insertion
IT1	Anterodorsal rim of the lateral ilium (I), in a rough and dorsoventrally delimited area	Tibial cnemial crest (I)
IT2	Dorsal rim of the ilium (I); anterior limits over the horizontal axis of the pubic peduncle, posterior limit over the horizontal axis of the posterior facet of the ischial peduncle	Tibial cnemial crest (I)
IT3	Posterodorsal rim of the ilium (I); posterior to the IT2, in the posterodorsal end of the postacetabular ilium	Tibial cnemial crest (I)
AMB	Pubic tubercle (I), on the lateral shaft of the pubis	Tibial cnemial crest (I)
FMTE	Lateral surface of the femoral shaft, delimited by the *lia* and *lip* (I)	Tibial cnemial crest (I)
FMTI	Anteromedial surface of the femoral shaft, delimited by *lia* and *la* (I)	Tibial cnemial crest (I)
ILFB	Shallow depression on the postacetabular surface of the ilium, ventral to IT3 (I)	Fibular tubercle (I)
IFE	Elliptical concavity on the dorsolateral surface of the ilium (I); posterior to ITC and ventral to IT2 (II)	Femoral trochanteric shelf (II)
ITC	Elliptical concavity on the lateral surface of the ilium (I), anterior to IFE (II)	Lesser trochanter (anterior) of the femur (II)
PIFI1	Preacetabular ventrolateral ‘cuppedicus’ fossa (I)	Anteromedial surface of the femur, distal to the lesser trochanter (I)
PIFI2	Centra of vertebrae anterior to ilium (I), and potentially near PIFI1 on ilium (I')	Anterolateral surface of the femur, distal to the lesser trochanter (‘accessory trochanter’) (I)
FTI1	Distal ischial tubercle (II)	Proximal posteromedial surface of the tibia in a broad depression (II)
FTI2	Equivocal (II'); not reconstructed (possible autapomorphy of Crocodylia)	Equivocal (II')
FTI3	Proximal ischial tuberosity (II)	Posteromedial surface of the proximal tibia (I)
FTI4	Equivocal (II'); not reconstructed (possible autapomorphy of Crocodylia)	Equivocal (II')
FTE	Postacetabular blade; posterior to the ILFB (I)	Posteromedial surface of the proximal tibia (I)
ADD1	Obturator process of the ischium (ischial apron) (I')	Posterior shaft of the femoral diaphysis (I')
ADD2	Depression on the posterodorsal ischial shaft, slightly distal to the ischial tuberosity (II)	Posterior shaft of the femoral diaphysis (I')
PIFE1	Anterior surface of the pubic apron (II)	Femoral greater trochanter (I)
PIFE2	Posterior surface of the pubic apron (II)	Femoral greater trochanter (I)
PIFE3	Obturator process of the ischium; between ADD1 and ADD2 (II)	Femoral greater trochanter (I)
ISTR	Medial surface of ischium/obturator process (II)	Posterolateral side of the proximal femur, between the greater and fourth trochanter (I)
CFB	Iliac brevis fossa (II)	Lateral surface of the fourth trochanter (I)
CFL	Centra and haemal arches of the caudal vertebrae (I), continuing distally until the transverse processes are strongly reduced/absent (I’)	Pit and crest of the medial to posterior surface of the fourth trochanter (I)
EDL	Anterolateral proximal shaft of the tibia (I)	?
EHL	Anterolateral surface of distal fibula (I)	?
GL	Depression on the posterolateral surface of the distal femoral shaft (I)	Posterior/plantar surface of metatarsals II–IV (I)
GM	Depression on the anteromedial proximal tibia (I)	Posterior/plantar surface of metatarsals II–IV (I)

Muscle	Origin	Insertion
TA	Anterolateral proximal side of femoral condyle (I') and/or depression distal to the cnemial crest of the tibia (I)	Anteroproximal metatarsals II–IV (I)
FL	Anterolateral fibula (I')	?
FB	Anterolateral fibula, distal to FL (I')	?

Table 2.3. Pelvic and hindlimb musculature inferred as present in *Condorraptor* and required inference level based on the EPB. Refer to Table 2.1 or the main text results for muscle abbreviations.

Muscle	Origin	Insertion
IT2	Dorsal rim of the ilium (I); anterior limits over the horizontal axis of the pubic peduncle	Tibial cnemial crest (I)
AMB	Pubic tubercle (I), on the lateral shaft of the pubis	Tibial cnemial crest (I)
FMTE	Lateral surface of the femoral shaft, delimited by the *lia* and *lip* (I)	Tibial cnemial crest (I)
FMTI	Anteromedial surface of the femoral shaft, delimited by *lia* and *la* (I)	Tibial cnemial crest (I)
ILFB	Shallow fragmentary depression on the postacetabular surface of the ilium (I)	?
IFE	Fragmentary concavity on the dorsolateral surface of the ilium (I); posterior to ITC and ventral to IT2 (II)	Femoral trochanteric shelf? (II)
ITC	Fragmentary concavity on the lateral surface of the ilium (I), anterior to IFE (II)	Lesser trochanter (anterior) of the femur? (II)
PIFI1	Preacetabular ventrolateral 'cuppedicus' fossa (I)	?
PIFI2	Centra of vertebrae anterior to ilium (I), and potentially near PIFI1 on ilium (I')	?
FTI3	Proximal ischial tuberosity? (II)	?
ADD1	Obturator process of the ischium (ischial apron) (I')	Posterior shaft of the femoral diaphysis (I')
ADD2	Depression on the posterodorsal ischial shaft, slightly distal to the ischial tuberosity (II)	Posterior shaft of the femoral diaphysis (I')
PIFE1	Anterior surface of the pubic apron (II)	?
PIFE2	Posterior surface of the pubic apron (II)	?
PIFE3	Obturator process of the ischium; between ADD1 and FTI3? + ADD2 (II)	?
ISTR	Medial surface of ischium/obturator process (II')	?
CFL	Centra and haemal arches of the caudal vertebrae (I), continuing distally until the transverse processes are strongly reduced/absent (I')	Pit and crest of the medial to posterior surface of the fourth trochanter (I)
EDL	Anterolateral proximal shaft of the tibia (I)	?
GL	Depression on the posterolateral surface of the distal femoral shaft (I)	Posterior/plantar surface of metatarsals II–IV (I)
GM	Depression on the anteromedial proximal tibia (I)	Posterior/plantar surface of metatarsals II–IV (I)
TA	Anterolateral proximal side of femoral condyle (II') and/or depression distal to the cnemial crest of the tibia (II)	Anteroproximal metatarsals II–IV (I)

Table 2.4. Pelvic and hindlimb musculature inferred as present in *Marshosaurus* and required inference level based on the EPB. Refer to Table 2.1 or the main text results for muscle abbreviations.

Muscle	Origin	Insertion
IT3	Posterodorsal rim of the ilium (I); posterior to the IT2, in the posterodorsal end of the postacetabular ilium	?
AMB	Pubic tubercle (I), on the lateral shaft of the pubis	?
ILFB	Shallow depression on the postacetabular surface of the ilium, ventral to IT3 (I)	?
PIFI1	Preacetabular ventrolateral 'cuppedicus' fossa (I)	?
FTI1	Distal ischial tubercle (II)	?
FTI2	Equivocal (II'); not reconstructed (possible autapomorphy of Crocodylia)	Equivocal (II')
FTI4	Equivocal (II'); not reconstructed (possible autapomorphy of Crocodylia)	Equivocal (II')
FTE	Postacetabular blade; posterior to the ILFB (I)	?
ADD1	Obturator process of the ischium (ischial apron) (I')	?
PIFE1	Anterior surface of the pubic apron (II)	?
PIFE2	Posterior surface of the pubic apron (II)	?
PIFE3	Obturator process of the ischium; between ADD1 and ADD2 (II)	?
ISTR	Medial surface of ischium/obturator process (II)	?
CFB	Iliac brevis fossa (II)	?

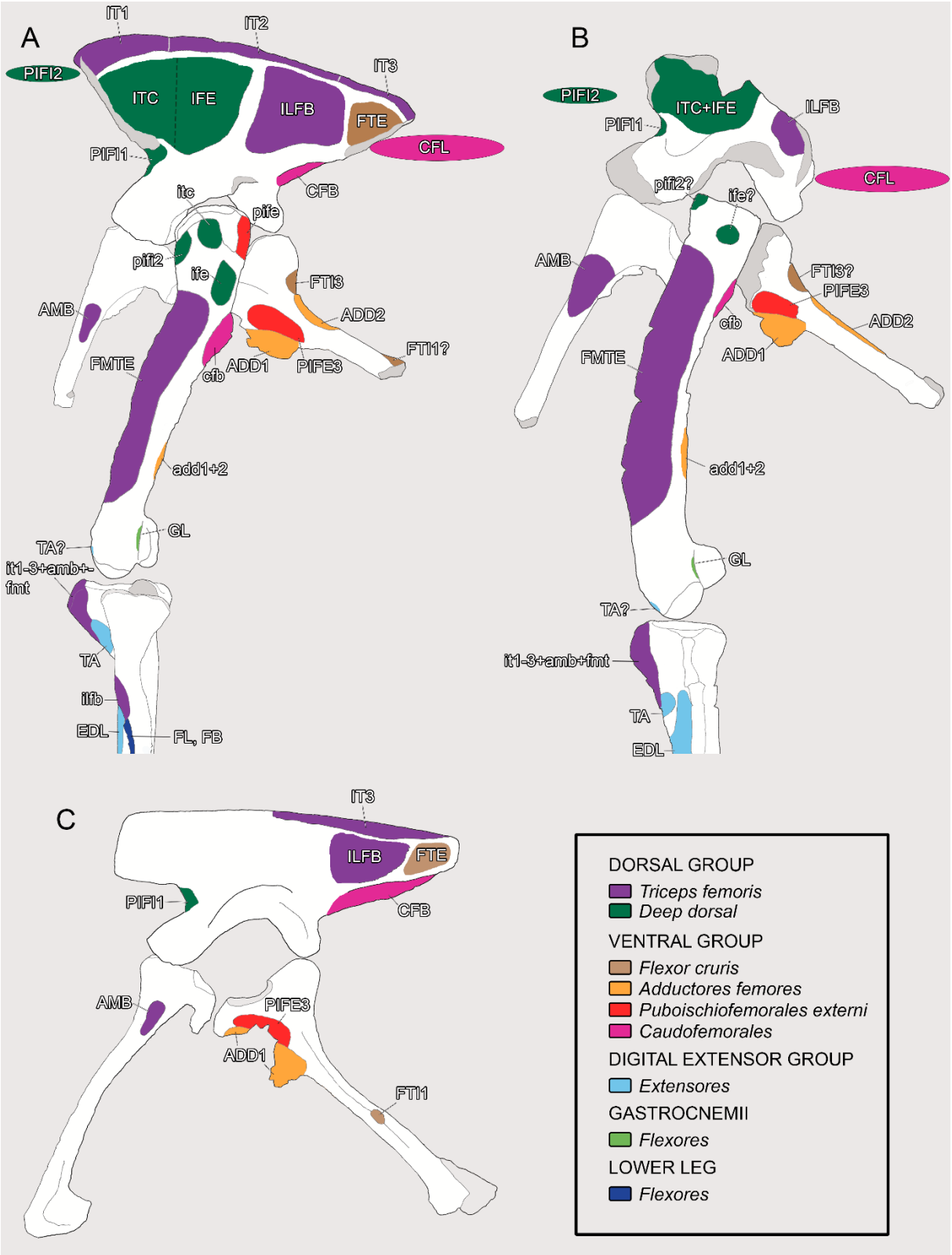

Figure 2.17. Pelvic and hindlimb 'muscle map' inferred for Piatnitzkysauridae (left lateral view). A, *Piatnitzkysaurus floresi*. B, *Condorraptor currumili*. C, *Marshosaurus bicentesimus*. Note that some muscles are not shown here, and some bones have been mirrored to illustrate the reconstructions of the three piatnitzkysaurid species. Muscle abbreviations are provided in Table 1; see text for inference levels and other comparisons. CFL and PIFI2 origins are much smaller than expected; simply shown for relative positions. Medial muscle origins (e.g., FMTI) and insertions (e.g., PIFI1) are not shown. Not to scale.

3.3 Ambiguous reconstructions and unknown character states in *Piatnitzkysaurus*

Table 2.5 summarizes the hypothesised character states for the most recent common ancestor of Tetanurae (i.e., Orionides + Coelurosauria; Gauthier, 1986; Carrano *et al*., 2012), based on maximum parsimony state reconstructions. The following characters have been mapped as unknown states (?) in *Piatnitzkysaurus*: 8–9, 11, 14, 24, 27, 30–34, 37–40, 42–46, 49, 64, 69–70, 72–79, 81–82, 85–100. This uncertainty was due to the lack of osteological correlates in this taxon that could clarify myological issues previously discussed in Hutchinson (2002) and Bishop *et al*. (2021).

On the other hand, the following muscles were inferred as absent is this taxon: (1) *M. puboischiotibialis* (PIT), which is present in non-avian Reptilia, arising from a muscle scar on the anterolateral ilium (Hutchinson, 2002; Otero *et al*., 2010; Suzuki *et al*., 2011) absent in Avialae (Hutchinson, 2002); and (2) *M. pubotibialis* (PUT), which originates from the pubis, near the pubic tubercle and puboischiadic ligament, in early Reptilia (Romer, 1942; Hutchinson, 2002) and was lost in Archosauria (Romer, 1923a; Dilkes, 2000; Hutchinson, 2002; Bishop *et al*., 2021). Other muscles such as FTI2 and 4, GIM and EDB (probably fused with EDL) are equivocal and were not reconstructed; thus their presence or absence were not inferred (see Table 2.2 for *Piatnitzkysaurus* reconstruction; and Hutchinson, 2002 and Bishop *et al*., 2021 for further discussions).

Table 2.5. Reconstruction of character states for the Tetanurae node after scoring *Piatnitzkysaurus floresi*. States 01 and 012 represent ambiguous reconstructions.

Character	**1**	**2**	**3**	**4**	**5**	**6**	**7**	**8**	**9**	**10**
State	*1*	*0*	*1*	*0*	*1*	*1*	*1*	*0*	*0*	*0*
Character	**11**	**12**	**13**	**14**	**15**	**16**	**17**	**18**	**19**	**20**
State	*1*	*0*	*1*	*0*	*1*	*0*	*1*	*2*	*4*	*1*
Character	**21**	**22**	**23**	**24**	**25**	**26**	**27**	**28**	**29**	**30**
State	*1*	*1*	*2*	*0*	*2*	*2*	*01*	*2*	*1*	*012*
Character	**31**	**32**	**33**	**34**	**35**	**36**	**37**	**38**	**39**	**40**
State	*012*	*2*	*01*	*23*	*0*	*0*	*1*	*2*	*2*	*01*
Character	**41**	**42**	**43**	**44**	**45**	**46**	**47**	**48**	**49**	**50**
State	*1*	*01*	*01*	*1*	*1*	*1*	*1*	*1*	*1*	*1*
Character	**51**	**52**	**53**	**54**	**55**	**56**	**57**	**58**	**59**	**60**
State	*1*	*1*	*1*	*0*	*2*	*0*	*0*	*2*	*2*	*1*
Character	**61**	**62**	**63**	**64**	**65**	**66**	**67**	**68**	**69**	**70**
State	*1*	*1*	*0*	*01*	*0*	*2*	*1*	*3*	*01*	*01*
Character	**71**	**72**	**73**	**74**	**75**	**76**	**77**	**78**	**79**	**80**
State	*1*	*01*	*2*	*3*	*0*	*0*	*1*	*01*	*1*	*0*
Character	**81**	**82**	**83**	**84**	**85**	**86**	**87**	**88**	**89**	**90**
State	*01*	*01*	*1*	*0*	*0*	*01*	*01*	*01*	*1*	*1*
Character	**91**	**92**	**93**	**94**	**95**	**96**	**97**	**98**	**99**	**100**
State	*1*	*01*	*1*	*2*	*2*	*2*	*2*	*3*	*1*	*01*

3.4 Myological comparisons among theropods

Here we have associated morphological structures with the myology of the locomotor apparatus in piatnitzkysaurids, combining our work with previous descriptions (Madsen, 1976; Bonaparte, 1979; 1986; Rauhut, 2005). This is the first myological study of the pelvic appendages in early Tetanurae, as far as we know. While the reconstructions we found are similar to others performed for different theropods, we present some key comparisons here.

Earlier reconstructions of theropod myology generally considered the superficial IT muscle as a single component of the thigh (e.g., Romer, 1923a; Russell, 1972; Tarsitano, 1983), whereas more recent reconstructions have considered three heads of this muscle (e.g., Carrano & Hutchinson, 2002; Grillo & Azevedo, 2011; Rhodes *et al*., 2021), which applies to our reconstruction based on *Piatnitzkysaurus* (Figure 2.17, Figure 2.19).

The division of the IF of non-avian Reptilia into the ITC + IFE of Aves is ubiquitous in recent pelvic musculature reconstructions of theropods (e.g., Hutchinson & Gatesy, 2000; Carrano & Hutchinson, 2002; Bates *et al*., 2012a; Bishop *et al*., 2021), based mainly on inferred insertions of these muscles, and we infer the same division in piatnitzkysaurids (mainly *Piatnitzkysaurus*; Figure 2.2, Figure 2.17). However, similar to *Staurikosaurus* (Grillo & Azevedo, 2011), it is not possible to distinguish the origins of these two muscles, except that, based on the EPB (Figure 2.1A), that the ITC was anteriorly positioned and IFE immediately posterior (see Hutchinson, 2002). This reconstruction, like others, differs from the *Falcarius* reconstruction (Smith, 2023), in which the IFE was positioned posteriorly on the ilium (between ILFB and FTE); a condition not known in Aves.

The insertion of ITC in *Piatnitzkysaurus*, similar to Ceratosauria, Allosauroidea, Tyrannosauroidea and Ornithomimosauria, occurs onto a large "blade-like" lesser trochanter of the femur (Figure 2.6, Figure 2.9), differing from other dinosauriformes and early theropods (e.g., Herrerasauridae and *Coelophysis*), in which the ITC insertion is onto a small "knob-like" lesser trochanter (Carrano & Hutchinson, 2002; Hutchinson, 2002; Grillo & Azevedo, 2011; Bishop *et al*., 2021; Chapter 1). Later theropods (e.g., Oviraptosauria) have this insertion on a more robust and proximally positioned lesser trochanter, whereas Aves have only a scar on the trochanteric crest (Hutchinson, 2002; Bishop *et al*., 2021), thus indicating a "transitional" position in *Piatnitzkysaurus* between early theropods and later coelurosaurians.

In early theropods such as *Staurikosaurus* (Grillo & Azevedo, 2011), *Coelophysis* (Bishop *et al*., 2021), the allosauroids *Allosaurus* and *Acrocanthosaurus* (Bates *et al*., 2012a), and later coelurosaurians such as *Tyrannosaurus* (Carrano & Hutchinson, 2002), *Nothronychus*

(Smith, 2021), and *Falcarius* (Smith, 2023), the AMB origin usually is reconstructed more anteroproximally on the pubis. However, in our reconstructions, based on the position of the pubic tubercle, the AMB origin in piatnitzkysaurids appears to have been more laterodistal (Figure 2.5, Figure 2.17). Similarly, a slightly more distal AMB is suggested for *Albertosaurus* (Rhodes *et al*., 2021) and even more distally in the dinosauriform *Silesaurus* (Piechowski & Tałanda, 2020).

Due to a well-developed accessory trochanter (Figure 2.9), our inferred insertion of PIFI2 on the proximal part of the femur in *Piatnitzkysaurus* is slightly more anteriorly positioned (Figure 2.6, Figure 2.9, Figure 2.17) than in *Tyrannosaurus* (Carrano & Hutchinson, 2002) and *Falcarius* (Smith, 2023), being more similar to the reconstructed insertion in early theropods (e.g., Bishop *et al*., 2021) and allosauroids (Bates *et al*., 2012a).

In early theropods such as *Staurikosaurus* (Grillo & Azevedo, 2011) and allosauroids (Bates *et al*., 2012a), the inferred ADD2 origin is restricted to the most posterior part of the ischial shaft, whereas in *Coelophysis* (Bishop *et al*., 2021), this muscle was reconstructed in a slightly more distal position. In our reconstruction of piatnitzkysaurids (mainly in *Condorraptor*; Figure 2.11, Figure 2.17), the ADD2 origin extends more distally, similar to Crocodylia (e.g., Suzuki *et al*., 2011) and reconstructions of some other theropods (e.g., Carrano & Hutchinson, 2002; Rhodes *et al*., 2021). Some of these differences might relate to subjective interpretations of the ADD2 scar location, but as Hutchinson (2001b) showed, this scar is fairly conservative and conspicuous in archosaurs.

As in Crocodylia (e.g., Romer, 1923b; Otero *et al*., 2010; Suzuki *et al*., 2011) as well as *Staurikosaurus* (Grillo & Azevedo, 2011) and *Coelophysis* (Bishop *et al*., 2021), we reconstructed the PIFE3 origin on the lateral aspect of the obturator process of the ischium, between the ADD1+2 (Figure 2.11, Figure 2.17). This origin extends more posteriorly in Crocodylia, but the anterior region lies between ADD1+2. In a *Tyrannosaurus* reconstruction (Carrano & Hutchinson, 2002), the PIFE3 originates slightly distal to ADD1, and is even more distally positioned in some maniraptoran reconstructions (Rhodes *et al*., 2021). These differences likely relate not only to subjective interpretations, but also to relative position of the ischial obturator process (Hutchinson, 2001b).

Our reconstruction of the ISTR origin differs from other myological models; in general, reconstructions in theropods consider the ISTR as dorsal and occupying a small medial part of the ischium (e.g., Carrano & Hutchinson, 2002; Grillo & Azevedo, 2011; Smith, 2021). However, here we consider the condition in Crocodylia and other non-avian Reptilia (e.g., Romer, 1923a; Suzuki *et al*., 2011) to be more plausible, reconstructing the ISTR originating

entirely on the medial surface of the ischium, probably occupying the entire area of the obturator process (similar to that hypothesized for *Coelophysis*; Bishop *et al*., 2021).

In theropod reconstructions, in general, the GM origin is on the medial portion of the proximal tibia. However, it variably is reconstructed somewhat distally, either more anteromedially (e.g., *Coelophysis*; Bishop *et al*., 2021), posteromedially (e.g., *Tyrannosaurus*; Carrano & Hutchinson, 2002), or anteriorly (e.g., *Falcarius*; Smith, 2023). Our reconstruction of the GM origin, based on the medial concavities on the cnemial crest (Figure 2.12), more closely resembles the condition in Aves, of a more anterior and proximal origin occupying the entire medial side of the cnemial crest, immediately distal to the *triceps femoris* tendon (e.g., Suzuki *et al*., 2014). This finding is cause to reinvestigate the GM origin in other theropods.

Overall, as in other recent studies of earlier (e.g., Grillo & Azevedo, 2011) and later (e.g., Carrano & Hutchinson, 2002) theropods, we infer that the myology of the pelvic appendage more resembled that of Aves than Crocodylia, thus characterising the evolution of locomotor musculature in the avian lineage (e.g., Hutchinson, 2001a,b; 2002). There seems to have been much conservatism across non-avian Theropoda until Maniraptora. For example, many theropods (and some other Dinosauriformes) are inferred to have had division of IF into IFE and ITC, an origin of PIFI1 (and possibly some of PIFI2) from the “cuppedicus fossa”, a CFB origin largely from the ‘brevis fossa’, a fused EDL and EDB, and the putative absence of some apomorphic muscles of Crocodylia such as FTI4 and a second AMB head; or loss of plesiomorphic muscles such as FTI2 and PIT. Some features inferred for piatnitzkysaurids, such as the tibial *triceps femoris* insertion, three IT heads and two FMT heads, ILFB insertion onto the fibular tubercle, two ADD heads, and insertions of the PIFI1+2, FTI3, FTE, ADD1+2, PIFEs, ISTR, CFB and CFL are plesiomorphic muscular conditions (for Archosauria, Reptilia or earlier) that are relatively conservative even through evolution to Aves. Others were lost or modified later in avian evolution, such loss of the FTI1 and PIFE3, and shifts of the PIFI1+2, CFB and ISTR origins from more medial to lateral. Lower limb muscle origins and insertions have more complex, and sometimes more ambiguous, evolutionary patterns, evident in piatnitzkysaurids.

3.5 Myological comparisons among piatnitzkysaurids

As a consequence of osteological similarities noted in the Introduction, the myology of the pelvic girdle in these taxa presents several similarities (Figure 2.17), although we highlight some five distinct differences here:

(1) Area of CFB origin in *Piatnitzkysaurus* and *Marshosaurus* – the posteriorly wider brevis fossa in *Marshosaurus* (Carrano *et al*., 2012; Chapter 1; Figure 2.4, Figure 2.12, Figure 2.17), may signal a larger CFB in *Marshosaurus* (likely greater force-generating potential; e.g., Cuff *et al*., 2023), and perhaps different CFB moment arms about the hip joint (e.g., Allen *et al*., 2021).

(2) Position and area of AMB origin among the three piatnitzkysaurids – the pubic tubercle is well-developed in piatnitzkysaurids; even more robust in *Condorraptor* (Rauhut, 2005). Thus, in our muscle reconstructions, the AMB origin appears to have occupied a larger area in *Condorraptor* (and perhaps greater force potential), followed by *Piatnitzkysaurus*, with the origin also more distally positioned in both (Figure 2.5, Figure 2.17), and consequently the AMB moment arms about the hip joint (e.g., Allen *et al*., 2021) should have varied among piatnitzkysaurids.

(3) Extent of ADD1 origin in *Piatnitzkysaurus* and *Condorraptor* – the shallow depression present on the ischium of both taxa (not observed in *Marshosaurus*), extends more distally in *Condorraptor* (Figure 2.11, Figure 2.17), and again these differences could change the maximal forces generated and moment arms about the hip joint (e.g., Allen *et al*., 2021).

(4) *Triceps femoris* tendon in *Piatnitzkysaurus* and *Condorraptor* – the cnemial crest in *Condorraptor* is only moderately developed (Figure 2.4B–C, Figure 2.12E–F), differing from *Piatnitzkysaurus*, which has a well-developed and nearly rectangular crest (Figure 2.4A–B, Figure 2.12A–D, Figure 2.15). Although this variation of the cnemial crest between these two species is an autapomophic feature in *Condorraptor* (Rauhut, 2005), it may have altered the size of the *triceps femoris* insertion (Figure 2.17).

(5) TA origin in *Piatnitzkysaurus* and *Condorraptor* – the second TA head (tibial) appears to have been more robust in *Piatnitzkysaurus* (Figure 2.5A–D, Figure 2.15); perhaps indicating greater force-generating capacity. However, considering that the Condorraptor specimen is a sub-adult individual (Rauhut, 2005), this difference might be an autapomorphic or ontogenetic feature.

3.6 Taphonomic limitations

The degree of preservation of the pelvic appendage varies in each of the three species studied here. *Piatnitzkysaurus* represents the best-preserved specimen. This better preservation led to the larger number of successful inferences noted above (Table 2.2; Figures 2.2–2.6, Figures 2.8–2.12, Figures 2.14–2.17). Furthermore, two individuals of *Piatnitzkysaurus* are known (Bonaparte, 1979; 1986), allowing comparisons between individuals to be performed (e.g., Figure 2.12, Figure 2.15), increasing the reliability in our reconstructions of this taxon. However, the absence of most of the pedal bones prevents the analysis of many lower limb muscles. An illustration of *Piatnitzkysaurus* in Figure 2.18 summarises the most superficial thigh muscles.

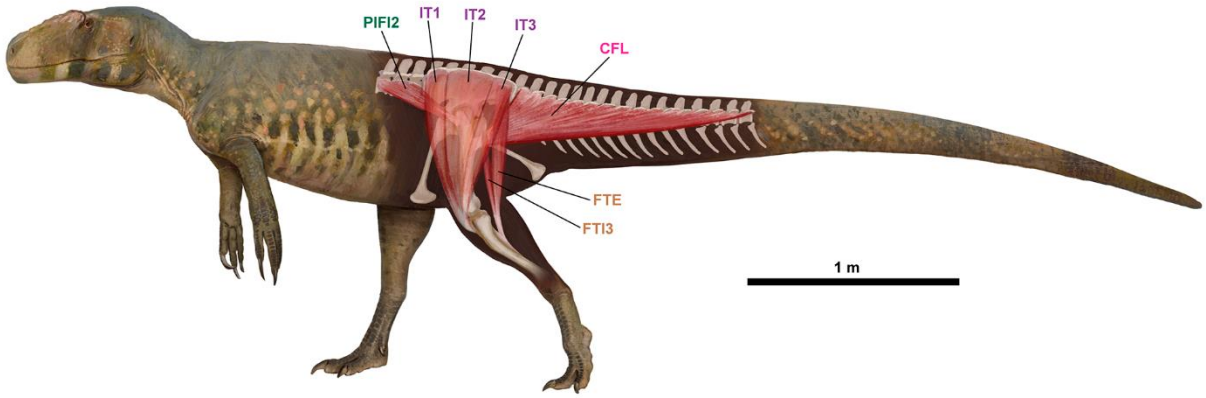

Figure 2.18. Restoration of pelvic and hindlimb muscles in *Piatnitzkysaurus floresi* (left lateral view). Artwork by Júlia d'Oliveira.

In taphonomic terms, *Condorraptor* has the second best-preserved piatnitzkysaurid pelvic appendages, although only one skeleton is known, probably from the same individual (Rauhut, 2005). The lack of many distal hindlimb elements such as the fibula and pes, as well as the fragmentary state of the femora of this taxon (compare Figure 2.6 and Figure 2.7) caused the weaker inferences (Table 2.3; Figure 2.2, Figures 2.4–2.5, Figure 2.7, Figures 2.11–2.13, Figures 2.16–2.17), especially for muscle insertions.

Although *Marshosaurus* is a better-known species in terms of the number of bones, which includes the cranium (Madsen, 1976; Carrano *et al*., 2012), has fewer preserved pelvic appendage elements than other piatnitzkysaurids, which prevents a more robust evaluation of the musculature in this species; only the muscle origins (Table 2.4; Figures 2.2–2.3, Figure 2.5, Figure 2.11, Figure 2.14, Figure 2.17). Description of new materials (e.g., Chure *et al*., 1997) should provide additional clues on its the locomotor musculature.

4. REFERENCES

Allen VR, Kilbourne BM, Hutchinson JR. 2021. The evolution of pelvic limb muscle moment arms in bird-line archosaurs. **Science Advances**, 7(12):eabe2778.

Barbi M, Bell PR, Fanti F, Dynes JJ, Kolsceke A, Buttigieg J, Coulson IM, Currie PJ. 2019. Integumentary structure and composition in an exceptionally well-preserved hadrosaur (Dinosauria: Ornithischia). **PeerJ**, 7:e7875.

Bates KT, Benson RB, Falkingham PL. 2012a. A computational analysis of locomotor anatomy and body mass evolution in Allosauroidea (Dinosauria: Theropoda). **Paleobiology**, 38(3):486–507.

Bates KT, Maidment SC, Allen V, Barrett, PM. 2012b. Computational modelling of locomotor muscle moment arms in the basal dinosaur *Lesothosaurus diagnosticus*: assessing convergence between birds and basal ornithischians. **Journal of Anatomy**, 220(3):212–232.

Bates KT, Falkingham PL. 2018. The importance of muscle architecture in biomechanical reconstructions of extinct animals: a case study using *Tyrannosaurus rex*. **Journal of Anatomy**, 233(5):625–635.

Baumel JJ, Witmer LM. 1993. Osteologia. *In* Baumel JJ, King AS, Breazile JE, Evans HE, Vanden Berge JC. (eds). Handbook of Avian Anatomy: Nomina Anatomica Avium. Second Edition. p. 45–132. Cambridge, Massachusetts: Publications of the Nutall Ornithological Club.

Benson, RBJ. 2010. A description of *Megalosaurus bucklandii* (Dinosauria: Theropoda) from the Bathonian of the UK and the relationships of Middle Jurassic theropods. **Zoological Journal of the Linnean Society**, 158:882–935.

Benson RBJ, Campione NE, Carrano MT, Mannion PD, Sullivan C, Upchurch P, Evans DC. 2014. Rates of dinosaur body mass evolution indicate 170 million years of sustained ecological innovation on the avian stem lineage. **PLoS Biology**, 12(5):e1001853.

Bishop PJ, Cuff AR, Hutchinson JR. 2021. How to build a dinosaur: Musculoskeletal modeling and simulation of locomotor biomechanics in extinct animals. **Paleobiology**, 47(1):1–38.

Bishop PJ, Hocknull SA, Clemente CJ, Hutchinson JR, Barret RS, Lloyd DG. 2018a. Cancellous bone and theropod dinosaur locomotion. Part II - a new approach to inferring posture and locomotor biomechanics in extinct tetrapod vertebrates. **PeerJ**, 6:e5779.

Bishop PJ, Hocknull SA, Clemente CJ, Hutchinson JR, Farke AA, Barret RS, Lloyd DG. 2018b. Cancellous bone and theropod dinosaur locomotion. Part III - Inferring posture and locomotor in extinct theropods, and its evolution on the line to birds. **PeerJ**, 6:e5777.

Bonaparte JF. 1979. Dinosaurs: A Jurassic Assemblage from Patagonia. **Science**, 205(4413):1377–1379.

Bonaparte JF. 1986. Les dinosaures (Carnosaures, Allosauridés, Sauropodes, Céto sauridés) du Jurassique Moyen de Cerro Cóndor (Chubut, Argentina). **Annales de Paléontologie (Vert.-Invert.)**, 72(3):247–289.

Carrano MT, Benson RBJ, Sampson SD. 2012. The phylogeny of Tetanurae (Dinosauria; Theropoda). **Journal of Systematic Palaeontology**, 10(2):211–300.

Carrano MT, Hutchinson JR. 2002. Pelvic and hindlimb musculature of *Tyrannosaurus rex* (Dinosauria: Theropoda). **Journal of Morphology**, 253:207–228.

Cau A, Serventi P. 2017. Origin attachments of the caudofemoralis longus muscle in the Jurassic dinosaur *Allosaurus*. **Acta Palaeontologica Polonica**, 62(2):273–277.

Chure DJ, Britt BB, Madsen JH. 1997. A new specimen of *Marshosaurus bicentesimus* (Theropoda) from the Morrison Formation (Late Jurassic) of Dinosaur National Monument. **Journal of Vertebrate Paleontology**, 17(3):38A.

Clifton GT, Carr JA, Biewener AA. 2018. Comparative hindlimb myology of foot-propelled swimming birds. **Journal of Anatomy**, 232(1):105–123.

Costa FR, Rocha-Barbosa O, Kellner AWA. 2014. Myological Reconstruction of the Pelvic Girdle of *Anhanguera piscator* (Pterosauria: Pterydactyloidea) Using Three-Dimensional Virtual Animation. **Revista Brasileira de Paleontologia**, 17:11–21.

Cuff AR, Demuth OE, Michel K, Otero A, Pintore R, Polet DT, Wiseman ALA, Hutchinson JR. 2023a. Walking—and Running and Jumping—with Dinosaurs and their Cousins, Viewed Through the Lens of Evolutionary Biomechanics. **Integrative and Comparative Biology**, 62(5):1281–1305.

Cuff AR, Wiseman AL, Bishop PJ, Michel KB, Gaignet R, Hutchinson JR. 2023b. Anatomically grounded estimation of hindlimb muscle sizes in Archosauria. **Journal of Anatomy**, 242(2):289–311.

Dai H, Benson R, Hu X, Ma Q, Tan C, Li N, Xiao M, Hu H, Zhou Y, Wei Z, Zhang F, Jiang S, Li D, Peng G, Xu X. 2020. A new possible megalosauroid theropod from the Middle Jurassic Xintiangou Formation of Chongqing, People's Republic of China and its implication for early tetanuran evolution. **Scientific Reports**, 10(1):139.

Dal Sasso, C, Signore, M. 1998. Exceptional soft-tissue preservation in a theropod dinosaur from Italy. **Nature**, 392(6674):383–387.

Dick TJ, Clemente CJ. 2016. How to build your dragon: scaling of muscle architecture from the world's smallest to the world's largest monitor lizard. **Frontiers in Zoology**, 13(1):1–17.

Dilkes DW. 2000. Appendicular myology of the hadrosaurian dinosaur *Maiasaura peeblesorum* from the Late Cretaceous (Campanian) of Montana. **Transactions of the Royal Society of Edinburgh: Earth Sciences**, 90:87–125.

Farlow JO, Gatesy SM, Holtz Jr TR, Hutchinson JR, Robinson JM. 2000. Theropod locomotion. **American Zoologist**, 40(4):640–663.

Farlow JO, Smith MB, Robinson JM. 1995. Body mass, bone "strength indicator," and cursorial potential of *Tyrannosaurus rex*. **Journal of Vertebrate Paleontology**, 15(4):713–725.

Foster J. 2020. Jurassic West: the dinosaurs of the Morrison Formation and their world. Indiana University Press.

Gatesy SM. 1990. Caudofemoral musculature and the evolution of theropod locomotion. **Paleobiology**, 16:170–186.

Gatesy SM, Middleton KM. 1997. Bipedalism, flight, and the evolution of theropod locomotor diversity. **Journal of Vertebrate Paleontology**, 17(2):308–329.

Gauthier J. 1986. Saurischian monophyly and the origin of birds. **Memoirs of the Californian Academy of Sciences**, 8:1–55.

Gregory WK, Camp CL. 1918. Studies in comparative myology and osteology. No. 3. **Bulletin of the American Museum of Natural History**, 38:15.

Griffin CT. 2018. Developmental patterns and variation among early theropods. **Journal of Anatomy**, 232(4):604–640.

Grillo ON, Azevedo SAK. 2011. Pelvic and hind limb musculature of *Staurikosaurus pricei* (Dinosauria: Saurischia). **Anais da Academia Brasileira de Ciências**, 83(1):73–98.

Hattori S, Tsuihiji T. 2021. Homology and osteological correlates of pedal muscles among extant sauropsids. **Journal of Anatomy**, 238(2):365–399.

Hendrickx C, Hartman SA, Mateus O. 2015. An overview of non-avian theropod discoveries and classification. **Palarch's Journal of Vertebrate Palaeontology**, 12(1):1–73.

Holtz TR, Molnar RE, Currie PJ. 2004. Basal Tetanurae. *In* Weishampel DB, Dodson P, Osmólska H. (eds.). The Dinosauria. pp. 71–110. University of California Press, Berkeley, Florida

Hudson GE, Lanzillotti PJ, Edwards GD. 1959. Muscles of the pelvic limb in galliform birds. **The American Midland Naturalist**, 61(1):1–67.

Hutchinson JR. 2001a. The evolution of femoral osteology and soft tissues on the line to extant birds (Neornithes). **Zoological Journal of the Linnean Society**, 131(2):169–197.

Hutchinson JR. 2001b. The evolution of pelvic osteology and soft tissues on the line to extant birds (Neornithes). **Zoological Journal of the Linnean Society**, 131(2):123–168.

Hutchinson JR. 2002. The evolution of hindlimb tendons and muscles on the line to crown-group birds. **Comparative Biochemistry and Physiology Part A: Molecular & Integrative Physiology**, 133(4):1051–1086.

Hutchinson JR. 2004a. Biomechanical Modeling and Sensitivity Analysis of Bipedal Running Ability. I. Extant taxa. **Journal of Morphology**, 262(1):421–440.

Hutchinson JR. 2004b. Biomechanical Modeling and Sensitivity Analysis of Bipedal Running Ability. II. Extinct taxa. **Journal of Morphology**, 262(1):441–461.

Hutchinson JR. 2012. On the inference of function from structure using biomechanical modelling and simulation of extinct organisms. **Biology letters**, 8(1):115–118.

Hutchinson JR, Allen V. 2009. The evolutionary continuum of limb function from early theropods to birds. **Naturwissenschaften**, 96(4): 423–448.

Hutchinson JR, Anderson FC, Blemker SS, Delp SL. 2005. Analysis of hindlimb muscle moment arms in *Tyrannosaurus rex* using a three-dimensional musculoskeletal computer model: implications for stance, gait, and speed. **Paleobiology**, 31:676–701.

Hutchinson JR, Garcia M. 2002. *Tyrannosaurus* was not a fast runner. **Nature**, 415(6875):1018–1021.

Hutchinson JR, Gatesy SM. 2000. Adductors, abductors, and the evolution of archosaur locomotion. **Paleobiology**, 26(4):734–751.

Hutchinson JR, Miller C, Fritsch G, Hildebrandt T. 2008. The anatomical foundation for multidisciplinary studies of animal limb function: examples from dinosaur and elephant limb imaging studies. *In* **Anatomical Imaging**. Springer, Tokyo. 23–28 p.

Jones KE, Dickson BV, Angielczyk KD, Pierce SE. 2021. Adaptive landscapes challenge the "lateral-to-sagittal" paradigm for mammalian vertebral evolution. **Current Biology**, 31(9):1883–1892.

Kellner, AWA. 1996. Fossilized theropod soft tissue. **Nature**, 379(6560):32–32.

Lacerda MBS, Bittencourt JS, Hutchinson JR. 2023. Reconstruction of the pelvic girdle and hindlimb musculature of the early tetanurans Piatnitzkysauridae (Theropoda, Megalosauroidea). figshare. Dataset. (https://figshare.com/s/4cded3bafca1932a7c0b)

Langer MC. 2003. The pelvic and hind limb anatomy of the stem-sauropodomorph *Saturnalia tupiniquim* (Late Triassic, Brazil). **PaleoBios**, 23:1–40.

Liparini A, Schultz CL. 2013. A reconstruction of the thigh musculature of the extinct pseudosuchian *Prestosuchus chiniquensis* from the Dinodontosaurus Assemblage Zone (Middle Triassic Epoch), Santa Maria 1 Sequence, southern Brazil. *In* Nesbitt SJ, Desojo JB, Irmis RB. (eds.). *Anatomy, Phylogeny and Palaeobiology of Early Archosaurs and their Kin*. Geological Society of London, Special Publications, 379.

Maddison WP, Maddison DR. 2015. Mesquite: a modular system for evolutionary analysis. Version 3.61. Available in http://www.mesquiteproject.org.

Madsen JH. 1976. A second new theropod dinosaur from the Late Jurassic of east central Utah. **Utah Geology**, 3:51–60.

Maidment SC, Barrett PM. 2011. The locomotor musculature of basal ornithischian dinosaurs. **Journal of Vertebrate Paleontology**, 31(6):1265–1291.

Mallison H. 2010. The Digital *Plateosaurus* I: Body Mass, Mass Distribution and Posture Assessed Using CAD and CAE on a Digitally Mounted Complete Skeleton. **Palaeontologia Electronica**, 13(2):8A.

McKitrick MC. 1991. Phylogenetic analysis of avian hindlimb musculature. **Miscellaneous Publications Museum of Zoology, University of Michigan**, 179:1–85.

Molnar JL, Diogo R, Hutchinson JR, Pierce SE. 2018. Reconstructing pectoral appendicular muscle anatomy in fossil fish and tetrapods over the fins-to-limbs transition. **Biological Reviews**, 93:1077–1107.

Müller RT, Garcia MS. 2023. A new silesaurid from Carnian beds of Brazil fills a gap in the radiation of avian line archosaurs. **Scientific Reports**, 13(1):4981.

Novas FE. 1996. Dinosaur monophyly. **Journal of vertebrate Paleontology**, 16(4):723–741.

Otero A, Gallina PA, Herrera Y. 2010. Pelvic musculature and function of *Caiman latirostris*. **The Herpetological Journal**, 20(3):173–184.

Patak AE, Baldwin J. 1998. Pelvic limb musculature in the emu *Dromaius novaehollandiae* (Aves: Struthioniformes: Dromaiidae): Adaptations to high-speed running. **Journal of Morphology**, 238(1):23–37.

Paul GS. 1988. Predatory Dinosaurs of the World. Simon & Schuster Press.

Paul GS. 2016. The Princeton Field Guide to Dinosaurs. Princeton University Press.

Paulina-Carabajal A. 2015. Guía para el estudio de la neuroanatomía de dinosaurios Saurischia, con énfasis en formas sudamericanas. *In* Fernández M, Herrera Y. (eds.). Reptiles Extintos – Volumen en Homenaje a Zulma Gasparini. **Publicación Electrónica de la Asociación Paleontológica Argentina**, 15(1):108–142.

Persons IV WS, Currie PJ. 2011. Dinosaur speed demon: the caudal musculature of *Carnotaurus sastrei* and implications for the evolution of South American abelisaurids. **PloS one**, 6(10):e25763.

Picasso MBJ. 2010. The hindlimb muscles of *Rhea americana* (Aves, Palaeognathae, Rheidae). **Anatomia, histologia, embryologia**, 39(5):462–472.

Piechowski R, Tałanda M. 2020. The locomotor musculature and posture of the early dinosauriform *Silesaurus opolensis* provides a new look into the evolution of Dinosauromorpha. **Journal of Anatomy**, 236(6):1044–1100.

Rauhut OWM. 2003. The Interrelationships and Evolution of Basal Theropod Dinosaurs. **Special Papers in Palaeontology**, 69:213 pp.

Rauhut OWM. 2004. Braincase structure of the Middle Jurassic theropod dinosaur *Piatnitzkysaurus*. **Canadian Journal of Earth Sciences**, 41(9):1109–1122.

Rauhut OWM. 2005. Osteology and relationships of a new theropod dinosaur from the Middle Jurassic of Patagonia. **Palaeontology**, 48(1):87–110.

Rauhut OWM. 2007. A fragmentary theropod skull from the Middle Jurassic of Patagonia. **Ameghiniana**, 44(2):479–483.

Rauhut OWM, Hübner T, Lanser KP. 2016. A new megalosaurid theropod dinosaur from the late Middle Jurassic (Callovian) of north-western Germany: Implications for theropod evolution and faunal turnover in the Jurassic. **Palaeontologia Electronica**, 19(2):1–65.

Rhodes MM, Henderson DM, Currie PJ. 2021. Maniraptoran pelvic musculature highlights evolutionary patterns in theropod locomotion on the line to birds. **PeerJ**, 9:e10855.

Romer AS. 1923a. Crocodilian pelvic muscles and their avian and reptilian homologues. **Bulletin of the American Museum of Natural History**, 48:533–552.

Romer AS. 1923b. The pelvic musculature of saurischian dinosaurs. **Bulletin of the American Museum of Natural History**, 48:605–617.

Romer AS. 1923c. The ilium in dinosaurs and birds. **Bulletin of the American Museum of Natural History**, 48:141–145.

Romer AS. 1927. The pelvic musculature of ornithischian dinosaurs. **Acta Zoologica**, 8(2-3):225–275.

Romer AS. 1942. The development of tetrapod limb musculature – the thigh of Lacerta. **Journal of Morphology**, 71:251–298.

Rowe T. 1986. Homology and evolution of the deep dorsal thigh musculature in birds and other Reptilia. **Journal of Morphology**, 189(3):327–346.

Russell DA. 1972. Ostrich dinosaurs from the Late Cretaceous of western Canada. **Canadian Journal of Earth Sciences**, 9(4):375–402.

Russell DA. 1984. A check list of the families and genera of North American dinosaurs. **Syllogeus**, 53:1–35.

Schachner ER, Manning PL, Dodson P. 2011. Pelvic and hindlimb myology of the basal archosaur *Poposaurus gracilis* (Archosauria: Poposauroidea). **Journal of Morphology**, 272(12):1464–1491.

Sereno PC. 1999. The evolution of dinosaurs. **Science**, 284(5423):2137–2147.

Smith DK. 2021. Hind limb muscle reconstruction in the incipiently opisthopubic large therizinosaur *Nothronychus* (Theropoda; Maniraptora). **Journal of Anatomy**, 238(6): 1404–1424.

Smith DK. 2023. Hindlimb Musculature of the Lower Cretaceous (Barremian) Therizinosaur *Falcarius utahensis* (Maniraptora, Theropoda) with Implications for Evolution, Stance, and Stride. **Cretaceous Research**, 149:105557.

Surmik D, Słowiak-Morkovina J, Szczygielski T, Wojtyniak M, Środek D, Dulski M, Balin K, Krzykawski T, Pawlicki R. 2023. The first record of fossilized soft parts in ossified tendons and implications for the understanding of tendon mineralization. **Zoological Journal of the Linnean Society**, 198(3):747–766.

Suzuki D, Chiba K, Tanaka Y, Hayashi, S. 2011. Myology of crocodiles III: pelvic girdle and hindlimb. **Fossils The Palaeontological Society of Japan**, 90:37–60.

Suzuki D, Chiba K, Vanburen CS, Ohashi T. 2014. The appendicular anatomy of the elegant crested *Tinamou* (Eudromia elegans). **Bulletin of the Kitakyushu Museum of Natural History and Human History, Series A (Natural History)**, 12:1–48.

Tarsitano S. 1983. Stance and gait in theropod dinosaurs. **Acta Palaeontologica Polonica**, 28:251–264.

Witmer LM. 1995. The extant phylogenetic bracket and the importance of reconstructing soft tissues in fossils. *In* Thomason JJ. (eds.), **Functional morphology in vertebrate paleontology**, Cambridge University Press, p.19–33.

Zinoviev AV. 2011. Notes on the hindlimb myology and syndesmology of the Mesozoic toothed bird *Hesperornis regalis* (Aves: Hesperornithiformes). **Journal of Systematic Palaeontology**, 9(1):65–84.

APPENDIX A - List of characters scored and mapped onto a simplified Reptilia phylogeny

For the original and updated version of the taxon-character matrix refer to Hutchinson (2001a,b; 2002) and Bishop et al. (2021).

1. *M. iliotibialis* (IT), number of heads: one or two, weakly subdivided (0); three [three separate regions of muscle scarring] (1).

2. IT, origin: dorsolateral ilium, superficial to other iliac muscles [rugose dorsal rim of ilium] (0).

3. IT, insertion (common "triceps" extensor tendon): tibial tuberosity (0); cnemial crest (1); cranial and cnemial crests (2). Ordered.

4. Patella, ossified sesamoid in extensor tendon: absent (0); present [patellar sulcus presents on femur as proximal extension of intercondylar sulcus] (1).

5. *M. femorotibialis* (FMT), number of heads: one, weak subdivision (0); two [anterior and posterior intermuscular lines] (1); three [medial intermuscular line] (2). Ordered.

6. FMT, origin: proximal half of femoral shaft (0); bulk of femoral shaft [strong intermuscular lines] (1).

7. FMT, distal subdivision of lateral head: absent (0); present [anteromedial muscle scar on distal femoral shaft] (1).

8. FMT, insertion: with IT + AMB extensor tendon (0).

9. *M. ambiens* (AMB), number of heads: one (0); two (1).

10. AMB, origin(s): pubic tubercle; proximally adjacent to *M. pubotibialis*, PUT (if present) (0); anterior preacetabular cartilage and medial proximal pubis (1).

11. AMB, insertion: with IT + FMT extensor tendon (0); additional secondary tendon perforating extensor tendon, to origins of digital flexors (and GL) (1).

12. *M. iliofibularis* (ILFB), origin: dorsal postacetabular ilium, between IF and FTE [scarred region] (0).

13. ILFB, insertion: anterolateral proximal fibula [rugosity] (0); anterolateral proximal fibula [tubercle] (1); lateral proximal fibula [tubercle] (2); posterior proximal fibula [tubercle] (3). Ordered.

14. ILFB, secondary tendon: absent (0); present to GL aponeurosis (1).

15. ILFB, insertion induces fibular crest on tibia: absent (0); present (1).

16: ILFB, ansa: absent (0); present [tubercles on lateral femoral condyle near GL origin] (1).

17. *M. iliofemoralis* (IF), number of heads: one, IF (0); two, IFE and ITC [separate insertions evident] (1).

18. IF, origin: small, above acetabulum (0); large, expanded preacetabularly with ilium (1); divided into IFE and ITC portions (2).

19. IF (or IFE), insertion: posterolateral [internal trochanter] (0); anterolateral [greater trochanter] (1); posterolateral femoral shaft between FMT origins [flat shelf; proximal knob] (2); IFE on prominent trochanteric shelf or lateral ridge; ITC separate (3); IFE on reduced scar-like trochanteric shelf; ITC separate (4).

20. IF (or ITC+IFE), insertion type: fleshy [flat surface or internal trochanter] (0); tendinous [bladelike trochanters or fibrous scars] (1).

21. IFE, origin: absent; not divided from ITC (0); above acetabulum on lateral surface of ilium (1); reduced to dorsolateral tubercle [processus supratrochantericus] (2).

22. ITC, origin: absent; not divided from IFE (0); anterior to IFE on lateral iliac surface (1); expanded into preacetabular concavity (2). Ordered.

23. ITC, insertion: absent; not divided from IFE (0); small distal knob-like lesser trochanter (1); large blade-like lesser trochanter (2); robust lesser trochanter; proximally positioned and closely appressed to greater trochanter (3); scar on cranial rim of proximal trochanteric crest [greater and lesser trochanters fused] (4). Ordered.

24. *M. puboischiofemoralis internus* (PIFI) 1 + 2, number of heads: one; PIFI1 + 2 (PIFI1 of Crocodylia or *M. iliofemoralis internus*, IFI of Neornithes) (0); two; PIFI1 and PIFI2 (weakly subdivided in Squamata) (1).

25. PIFI1 + 2, origin: anteromedial puboischiadic plate and epipubic cartilage (0); medial ilium and proximal ischium [puboischiadic plate reduced] (1); ventrolateral ilium [preacetabular "cuppedicus" fossa] (2); lateral ilium [preacetabular fossa reduced] (3); lateral pubic peduncle of ilium [preacetabular fossa "lost"] (4).

26. PIFI1 + 2, insertion: anteromedial femoral shaft [scar] (0); anteromedial proximal femur; with PIFI3 [lesser trochanter] (1); medial proximal femoral shaft [scar] (2).

27. PIFI3, number of heads: one; PIFI2 or PIFI3 (Crocodylia) [one insertion scar] (0); two; *Mm. iliotrochanterici cranialis* (ITCR) *et medius* (ITM) of Neornithes [two distinct scars] (1).

28. PIFI3 (PIFI2 of Crocodylia or ITCR+ITM of Neornithes), origin: anteromedial pubes and part of medial ilium [puboischiadic plate] (0); lumbar vertebrae [puboischiadic plate reduced] (1); ilium [no lumbar vertebrae; preacetabular "cuppedicus" fossa] (2); lateral preacetabular ilium [preacetabular fossa lost] (3).

29. PIFI3 (PIFI2 or ITCR+ITM), insertion: anterolateral proximal femur [scars] (0); accessory trochanter (1); anterior and lateral trochanteric crest [two scars] (2); lesser trochanter, with PIFI1 + 2 (3).

30. *M. puboischiotibialis* (PIT), number of heads; most superficial of flexor cruris: one, PIT1–3; weakly subdivided (0); two, PIT1 + 2 and PIT3 (PIT and FTI2 of Crocodylia) (1); none; absent (2).

31. PIT1 + 2, origin: anteroventral puboischiadic ligament and pubic tubercle; near PUT (0); anteroproximal ischium (PIT of Crocodylia) [reduced ligament; scar; PUT lost] (1); none; absent (2).

32. PIT3, origin: posterior end of puboischiadic ligament and pelvic symphyses (0); anterolateral ilium (FTI2 of Crocodylia); posteroventral to FTE, dorsal to CFB [ligament reduced] (1); none; absent or not separate from PIT1 + 2 (same origin) (2).

33. PIT1–3, insertion: medial proximal tibia; with or proximal to FTI1 (0); none; absent (1).

34. *M. flexor tibialis internus* (FTI), number of heads: two; FTI1 and FTI2 (0); three; FTI1 and FTI2a/b (FTI2a/b = superficial/deep=FTI4/3 of Crocodylia) (1); one; *M. flexor cruris medialis* (FCM of Neornithes; equivalent to FTI2b of FTI3 of Crocodylia); FTI1 and FTI4 absent (2).

35. FTI1, origin; posterodorsal to FTI2 and ISTR, near *M. ischiocaudalis* origin: ilioischiadic ligament or fascia on posterolateral side of distal ischium (0); last sacral and proximal caudal vertebrae, fascia (1); none; absent (2).

36. FTI1, insertion: posteromedial proximal tibia; with or distal to PIT (0); Unites distally with FTI2, to GM origin at posteromedial proximal tibia (1); none; absent (2).

37. FTI2, origin: anterior end of ilioischiadic ligament/fascia, near or on ischial tuberosity and distal ischium (0); scar on ischial tuberosity, and ilioischiadic fascia (FTI3 + 4 of Crocodylia) (1); proximal dorsal process of ischium, and ilioischiadic fascia [ischial tuberosity expanded as process] (2); posterolateral distal ischium, and ilioischiadic membrane (FCM of Neornithes) [proximal dorsal process lost] (3).

38. FTI2; insertion of tendon of superficial part (FTI2a or FTI4): splits distally into two tendons, inserting on medial and lateral proximal tibia around GM origin (0); unites distally with FTE and deeper part (FTI2b; FTI3 of Crocodylia) (1); none; muscle absent or not separate (2).

39. FTI; insertion of deep part (FTI2b or FTI3 or FCM): posterior proximal tibia; distal to PUT (0); not distinct from superficial part (FTI2a), unites distally with FTI1 (1); unites distally with FTE (= M. flexor cruris lateralis pars pelvica; FCLP of Neornithes) tendon (and FTI4, if present) (2).

40. FTI2 (FTI3 + 4 of Crocodylia); secondary tendon to GL: absent (0); present (1).

41. *M. flexor tibialis externus* (FTE) (= FCLP); origin, most posterodorsal of flexor cruris: ilioischiadic ligament/fascia around posteroventral ilium and posterodorsal ischium (0); posterolateral surface of ilium [muscle scar] (1).

42. FTE; insertion, shared tendon inserts between heads of *Mm. gastrocnemii*: tendon splits distally; medial tendon to posteromedial proximal tibia near GM; lateral tendon to posterolateral proximal tibia near GL and digital flexors, contributing to plantar aponeurosis (0); medial proximal tibia (FCLP of Neornithes), with FCM, between GM + GIM (1).

43. FCL pars accessoria head (FCLA): absent (0); present, originating from FCLP raphe and inserting in popliteal fossa of femur (1).

44. *M. pubotibialis* (PUT): present (0); absent (1).

45. PUT, origin; most anterior of flexor cruris and distally adjacent to AMB: pubes, proximal to or onto pubic tubercle and puboischiadic ligament (0); none; absent (1).

46. PUT, insertion: posterolateral proximal tibia; between GM and GL; proximal to other flexor cruris parts (0); none; absent (1).

47. *M. adductor femoris* (ADD), number of heads: one (0); two; ADD1 and ADD 2 of Crocodylia, or Mm. puboischiofemorales medialis (PIFM) et lateralis (PIFL) of Neornithes [two insertion scars] (1).

48. ADD, origin: puboischiadic ligament, anterior and deep to flexor cruris (0); anterior and posterior edges of ischium, separated by PIFE3 [scars; PIFE3 present] (1); anterolateral edge of ischium, puboischiadic membrane, and posterolateral pubis [PIFE3 absent] (2).

49. ADD, insertion: posterior distal femoral shaft, one scar on adductor ridge (0); posterior distal femoral shaft, medial and lateral scars (1); adductor ridge or crista supra condylaris medialis connecting to medial condyle (2).

50. *M. puboischiofemoralis externus* (PIFE), number of heads: one; PIFE1–3; weakly subdivided [nearly continuous puboischiadic plate] (0); three; PIFE1–3 [expanded and separated pubic and ischial aprons; obturator process] (1); two; Mm. obturatorii lateralis (OL) et medialis (OM) of Neornithes, equivalent to PIFE1 and PIFE2; PIFE3 lost [obturator process lost] (2).

51. PIFE1, origin: thyroid fenestra and puboischiadic plate (0); anteromedial surface of pubic apron and epipubic cartilage (1); proximal lateral pubis; OL of Neornithes [pubic apron lost] (2).

52. PIFE2, origin: anterior to PIFE1; not separated (0); posterior surface of pubic apron (1); medial puboischiadic membrane; OM of Neornithes [pubic apron lost] (2).

53. PIFE3, origin: posterior to PIFE1 + 2; not separated (0); lateral ischium, remnant of puboischiadic plate [or obturator process] (1); absent [obturator process lost] (2).
54. PIFE1 + 2, pubic retroversion: pubic shaft oriented anteriorly (0); pubic shaft near vertical (1); pubic shaft oriented posteriorly (2); ilia, pubes, and ischial lie nearly parallel (3). Ordered.
55. PIFE insertion: anterolateral internal trochanter, posterior ridge, and intertrochanteric fossa (0); tip of trochanter minor and intertrochanteric fossa (1); posterolateral proximal femur [greater trochanter] (2); lateral proximal femur [greater trochanter rotated laterally] (3); groove and pit on posterolateral side of trochanteric crest [greater and lesser trochanters fused] (4).
56. PIFE2 (OM of Neornithes), obturator tuberosity of ischium for tendon: absent (0); present (1).
57. *M. ischiotrochantericus* (ISTR) (*M. ischiofemoralis*; ISF of Neornithes), origin: medial surface of posterior ischium [ischial symphysis] (0); lateral surface of posterior ischium and ilioischiadic membrane [ischial symphysis lost] (1).
58. ISTR, insertion: posterolateral proximal femur [scar] (0); groove proximal to trochanteric shelf (1); lateral proximal femur near trochanteric shelf [reduced trochanteric shelf] (2); proximal to large posterior trochanter (3); posterolateral trochanteric crest [scar; reduced posterior trochanter] (4).
59. *M. caudofemoralis brevis* (CFB) (*M. caudofemoralis pars pelvica*; CFP of Neornithes), origin: proximal caudal vertebrae and fascia (0); proximal caudals, lasta sacrals, and medioventral ilium [small shelf] (1); posteroventral ilium [brevis fossa] (2); ventrolateral ilium [brevis fossa reduced onto lateral ilium] (3); posterolateral ilium [brevis fossa lost] (4).
60. CFB, insertion: weakly differentiated from CFL; near internal trochanter (0); proximal and lateral to CFL, if separate [fourth trochanter or scar present] (1); posterolateral proximal femur [greater trochanter] (2).
61. *M. caudofemoralis longus* (CFL) (*M. caudofemoralis pars caudalis*; CFC of Neornithes), origin: ventral centra and transverse processes of caudal vertebrae [no transition zone in caudals] (0); restricted to proximal half of tail [“transition zone”] (1); restricted to proximal caudals [tail shortened to 15–30 vertebrae] (2); anteroventral pygostyle (3); none; absent (4). Ordered.
62. CFL, insertion: posterior femoral shaft and internal trochanter (0); prominent fourth trochanter and medial pit (1); small fourth trochanter (2); fourth trochanter reduced to a scar (3); none; absent (4).

63. CFL, secondary tendon to lateral knee region (and GL): absent [loss of pendant trochanter or CFL absent] (0); from distal to CFL (1); from crest-like fourth trochanter (2); from tip of pendant fourth trochanter (3).

64. *Mm. gastrocnemii*, number of heads: two; Mm. gastrocnemii lateralis (GL) et medialis (GM; "femorotibial gastrocnemius" of Lepidosauria) (0); three; GM divided into GM and M. gastrocnemius pars intermedia (GIM; Neornithes) or GL divided into superficial and deep heads of "femoral gastrocnemius" (Lepidosauria) (1).

65. GL, origin: posterolateral distal femur near lateral condyle [tubercle or scar] (0).

66. GL, insertion: plantar aponeurosis to metatarsal V and tarsal, then to digits 2–4 (0); plantar aponeurosis to metatarsal V, process on distal tarsal 4, and calcaneal tuber, then to digits 2–4 [calcaneal tuber present] (1); reduced plantar aponeurosis to posterior surface of metatarsals II–V [scars; calcaneal tuber and distal tarsal 4 process lost] (2); forms lateral part of "Achilles tendon" onto small flat hypotarsus, then vestigial plantar aponeurosis to posterior surface of tarsometatarsus (3); forms lateral part of "Achilles tendon" onto large grooved hypotarsus, then vestigial plantar aponeurosis to posterior surface of tarsometatarsus (4).

67. GM, origin; medial to TA: medial proximal tibia (0); medial side of lateral cnemial crest (1).

68. GM, insertion: plantar aponeurosis to metatarsal V, calcaneum, then to digit 5 (0); plantar aponeurosis to metatarsal V, calcaneal tuber, then to digit 5 [calcaneal tuber present] (1); plantar aponeurosis to metatarsal V and calcaneal tuber [digit 5 phalanges lost] (2); plantar aponeurosis to metatarsal V [calcaneal tuber lost] (3); forms medial part of "Achilles tendon" onto small flat hypotarsus, then vestigial plantar aponeurosis to posterior surface of tarsometatarsus [metatarsal V lost] (4); forms medial part of "Achilles tendon" onto large grooved hypotarsus, then vestigial plantar aponeurosis to caudal surface of tarsometatarsus (5).

69. GIM, origin: absent; not divided (0); posterior side of distal femur, near medial femoral condyle; at distal end of PIFM, PIFL, and FCLA insertions (1).

70. GIM, insertion: absent; not divided (0); joins GM, then forms posterior part of "Achilles tendon" onto hypotarsus and posterior tarsometatarsus (1).

71. GM and GL, relative size: GL larger than GM [no large cnemial crest] (0); GM larger than GL (including GIM, if present) [expanded cnemial crest] (1).

78. *M. extensor digitorum longus* (EDL), origin: anteromedial proximal tibia; distal to tibial tuberosity and deep to TA origin (0); anterior proximal tibia; distal, medial and deep to TA origin (1). Modified after Hattori & Tsuihiji (2020).

79. EDL, insertion: anterolateral proximal metatarsals I–IV; especially metatarsal I (0); dorsal surfaces of phalanges, digits 2–4 [through extensor sulci to scars and pits] (1). Modified after Hattori & Tsuihiji (2020).

80. EDL, extensor canal on cranial side of distal tibiotarsus: absent (0); present; shallow groove (1); present; deep groove enclosed anteriorly by an ossified supratendinal bridge (2). Ordered.

81. TA, number of heads: one (0); two (femoral and tibial heads of *M. tibialis cranialis* of Neornithes; TC) [fossa on anterolateral distal femur for femoral origin] (1).

82. TA, origin: anterior surface of distal lateral femoral condyle; superficial to EDL origin (0); femoral fossa and anterior surfaces of cnemial crests; proximal and superficial to EDL origin [fossa on femur and two cnemial crests presents]. Modified after Hattori & Tsuihiji (2020).

83. TA, insertion: anterior surfaces of proximal metatarsals II–IV (0); tubercles on anterior proximal metatarsals II–IV [metatarsal I shifted distally] (1); *tuberositas m. tibialis cranialis*, on cranial proximal metatarsal II (2). Modified after Hattori & Tsuihiji (2020).

84. *M. extensor hallucis longus* (EHL), origin: anterolateral distalmost fibula (0); anteromedial proximal tarsometatarsus [distal fibular shaft lost] (1).

85. EHL, insertion: anterior surfaces of digit 1 phalanges [hallux not retroverted] (0); posterior surfaces of digit 1 phalanges [hallux retroverted] (1).

86. *M. extensor digitorum brevis* (EDB): present (0); absent; presumably fused to distal EDL (1).

87. EDB, origin: anterior surfaces of proximal tarsals (0); absent (1).

88. EDB, insertion: dorsal surfaces of distal phalanges (0); absent (1).

97. *M. fibularis longus* (FL), origin: lateral fibular shaft; distal to IFLB; between FB and FDL (0); lateral side of lateral femoral condyle (1); lateral proximal fibular shaft and nearby cnemial crests [distal fibular shaft lost]; proximal to ILFB (2).

98. FL, insertion: lateral side of metatarsal V; distal to FB; and slight tendon to dorsal surfaces of digit V phalanges (0); lateral side of metatarsal V; distal to FB; and calcaneal tuber and slight tendon to dorsal surfaces of digit 5 phalanges [calcaneal tuber present] (1); lateral side of metatarsal V, calcaneal tuber, and flexor tendon [digit 5 phalanges lost] (2); lateral side of metatarsal V and flexor tendon [calcaneal tuber lost] (3); tibial cartilage and through sulcus m. fibularis longi on tarsometatarsus o tendon of *M. flexor* perforates digitorium III [metatarsal V lost] (4).

99. *M. fibularis brevis* (FB), origin: anterolateral distal fibula (and tibia); anterolateral and distal to FL (0); anterolateral distal tibial shaft [distal fibular shaft lost] (1).

100. FB, insertion: anterolateral side of metatarsal V (and IV); proximal to FL (0); anterolateral proximal metatarsal IV [metatarsal V lost; *Tuberculum m. fibularis brevis* present] (1)

FINAL REMARKS

After nearly a century and a half of research with theropods, and on the eve of the 200th anniversary of the description of *Megalosaurus*, the first theropod species to be described; this thesis focused on contributing by providing the analysis of morphofunctional characteristics of the pelvis and hindlimb appendage of early theropods highlighting the medium to large-sized bipedal predators of the Megalosauroidea clade.

The first chapter presented a phylogenetic tree recovering piatnitzkysaurids as the first clade to diverge among megalosauroids, then a succession of taxa represented by a polytomy among megalosaurids and a monophyletic Spinosauridae. The analyses revealed key morphological transitions within/at Megalosauroidea during the evolution, allowing inferences to be drawn about the associated musculature and other morphofunctional aspects. Furthermore, it was characterized how pelvic and hindlimb characters occupy different (or similar) regions of morphospace in Theropoda, highlighting possible homoplasy and phylogenetic signal.

The second chapter hypothesizes and develops a myological model of the pelvis and hindlimb of Piatnitzkysauridae, considering 32 muscles, for *Piatnitzkysaurus*, the attachments of 29 could be inferred based on the osteological correlates; Meanwhile, in *Condorraptor* and *Marshosaurus*, was inferred 21 and 12 muscles, respectively. A great anatomical similarity within Piatnitzkysauridae was found, but differences such as the origin of AMB and size of CFB are present. Similarities were evident with Aves, such as the division of the IFE and ITC and the broad depression of origin of GM in the cnemial crest.

The results obtained here with the analyses in a macroevolutionary context combined with the musculoskeletal models constructed here, allow us to better understand the evolutionary palaeobiology of megalosauroids, providing the first accurate models of the locomotor muscles in these dinosaurs in which the musculature is unknown.

REFERENCES

Benson RB. 2018. Dinosaur macroevolution and macroecology. **Annual Review of Ecology, Evolution, and Systematics**, 49:379–408.

Buckland W. 1824. XXI.—Notice on the *Megalosaurus* or great Fossil Lizard of Stonesfield. **Transactions of the Geological Society of London**, 1(2):390–396.

Carrano MT, Benson RBJ, Sampson SD. 2012. The phylogeny of Tetanurae (Dinosauria; Theropoda). **Journal of Systematic Palaeontology**, 10(2):211–300.

Carrano MT, Hutchinson JR. 2002. Pelvic and hindlimb musculature of *Tyrannosaurus rex* (Dinosauria: Theropoda). **Journal of Morphology**, 253:207–228.

Holtz Jr TR, Molnar RE, Currie PJ. 2004. Basal Tetanurae. In The Dinosauria (eds DB Weishampel, P Dodson, H Osmólska), pp. 71–110. University of California Press, Berkeley, Florida.

Hutchinson JR, Gatesy SM. 2000. Adductors, abductors, and the evolution of archosaur locomotion. **Paleobiology**, 26(4):734–751.

Iijima M, Kobayashi Y. 2014. Convergences and trends in the evolution of the archosaur pelvis. **Paleobiology**, 40(4):608–624.

Marsh OC. 1881. Principal characters of American Jurassic dinosaurs. Part V. **American Journal of Science (Series 3)**, 21:417–423.

GENERAL APPENDIX - List of articles/book chapter published during the doctorate

Lacerda MBS, Souza LG, Lobo LS, Schaefer CEGR, Romano PSR. 2020. New outcrop with vertebrate remains from Solimões Formation (Eocene-Pliocene), Southern Solimões Basin, Acre State, Northern Brazil. **Journal of South American Earth Sciences**, 101, 102588. (https://doi.org/10.1016/j.jsames.2020.102588)

Pinto CB, **Lacerda MBS**, Rodrigues BL, Mussel WN, Romano PSR. 2020. Geochemical characterization of fossil turtles from Tartaruguito outcrop (Upper Cretaceous, Bauru Basin, Presidente Prudente Formation), São Paulo state, southeastern Brazil. **Journal of South American Earth Sciences**, 104, 102843. (https://doi.org/10.1016/j.jsames.2020.102843)

Souza-Filho JP, Guilherme E, Toledo PM, Carvalho IS, Negri FR, Maciente AAR, Cidade GM, **Lacerda MBS**, Souza LG. 2020. On a new *Melanosuchus* species (Alligatoroidea: Caimaninae) from Solimões Formation (Eocene-Pliocene), Northern Brazil, and evolution of Caimaninae. **Zootaxa**, 4894(4), 561–593. (https://doi.org/10.11646/zootaxa.4894.4.5)

Lacerda MBS, Romano PSR, Bandeira KN, Souza LG. 2021. Georeferencing fossiliferous localities from Solimões and Acre Basins (Brazil) - what we know so far about Solimões Formation and future perspectives. **Annals of the Brazilian Academy of Sciences**, 93(2), 20201642. (https://doi.org/10.1590/0001-3765202120201642)

Lacerda MBS, Grillo ON, Romano PSR. 2022. Rostral morphology of Spinosauridae (Theropoda, Megalosauroidea): premaxilla shape variation and a new phylogenetic inference. **Historical Biology**, 34(11), 2089–2109. (https://doi.org/10.1080/08912963.2021.2000974)

Lacerda MBS, Andrade MB, Sales MAF, Aragão PRL, Vieira FS, Bittencourt JS, Liparini A. 2023. The vertebrate fossil record from the Feliz Deserto Formation (Lower Cretaceous), Sergipe, NE Brazil: paleoecological, taphonomic, and paleobiogeographic implications. **Cretaceous Research**, 147, 105463. (https://doi.org/10.1016/j.cretres.2022.105463)

Lacerda MBS, Aragão PRL, Vieira FS, Sales MAF, Liparini A. 2023. On the first Baryonychinae (Theropoda, Spinosauridae) teeth from South America. **Zootaxa**, 5264(4), 526–544. (https://doi.org/10.11646/zootaxa.5264.4.4)

Souza LG, Pêgas RV, **Lacerda MBS**, Riff D. 2023. Tales of long faces: piscivorous Archosauriformes and the evolutionary ways to form a fisher. In RULING REPTILES: Crocodylian Biology and Archosaur Paleobiology (eds H.N. Woodward, J.O. Farlow). Bloomington: Indiana University Press, Indiana. p. 215–239. (https://doi.org/10.2307/jj.6047951.13)

Lacerda MBS, Bittencourt JS, Hutchinson JR. 2023. Macroevolutionary patterns in the pelvis, stylopodium and zeugopodium of megalosauroid theropod dinosaurs and their importance for locomotor function. **Royal Society Open Science**, 10(8), 230481. (https://doi.org/10.1098/rsos.230481)